ANTICANCER ACTIVITY OF MODIFIED SOMATOSTATIN ANALOGS

ASTRID CAPELLO

The described research in the present thesis was performed at the Department of Nuclear Medicine at the Erasmus University Rotterdam.

ISBN: 90-8559-041-8

Printed by: Optima Grafische Communicatie, Rotterdam, The Netherlands

ANTICANCER ACTIVITY OF MODIFIED SOMATOSTATIN ANALOGS

ANTITUMOR ACTIVITEIT VAN GEMODIFICEERDE SOMATOSTATINE ANALOGEN

PROEFSCHRIFT

ter verkrijging van de graad van doctor aan de
Erasmus Universiteit Rotterdam
op gezag van de rector magnificus

Prof.dr. S.W.J. Lamberts
en volgens besluit van het College voor Promoties.

De openbare verdediging zal plaatsvinden op
woensdag 6 april 2005 om 15:45 uur

door

Astrid Capello

geboren te Gouda

Promotiecommissie

Promotor:	Prof.dr. E.P. Krenning
Overige leden:	Prof.dr.ir. T.J. Visser
	Prof.dr. S. Pauwels
	Prof.dr. P.C. Levendag
Copromotor:	Dr.ir. M. de Jong

aan mijn ouders

aan Jeroen

CONTENTS

CHAPTER 1

GENERAL INTRODUCTION

Peptide receptor radionuclide therapy; preclinical findings

Astrid Capello, Eric Krenning, Wout Breeman and Marion de Jong.

In:
Radionuclide Peptide Cancer Therapy; preclinical findings. Ed: Chinol and Paganelli. Marcell Dekker, 2005, in press.

RADIONUCLIDE THERAPY

The use of radionuclides for therapeutic applications began more than 50 years ago. The agents available for therapy have long been limited to iodine-131 (^{131}I) for differentiated thyroid cancer and phosphorus-32 (^{32}P) for the treatment of painful bone metastases [1]. In the past decades, however, the interest on the use of radiolabeled peptides for diagnosis and therapy, especially in the areas of oncology, endocrinology and rheumatology, grew enormously. This heightened interest can be ascribed partly to an increasing number of radionuclides for therapy, in conjunction with simplified methods of purification, characterization and optimization have resulted in a growing number of possible tumor seeking agents [2].

Radionuclides

Peptides are used for diagnosis and/or therapy by the coupling of radionuclides. The choice of the radionuclide depends on the application of the radiolabel: tumor detection, treatment, or treatment planning. Important characteristics of the radionuclide that have to be taken in account are half-life, particle type and the intensity, and energy emitted by the radionuclide [3]. Besides that, also the chemical properties play a role, e.g. the mode of labeling needed and its fate after conjugation in vivo. Some radionuclides are rapidly released from the cell after internalization and catabolism, while others are known to be retained intracellularly and are thus called residualizing radionuclides [4]. Other practical considerations for selecting a radionuclide are availability in high radionuclide purity as well as high specific activity and production logistics. Radionuclides with potential for therapy fall into three main categories by their mode of decay; (I) alpha (α-), (II) beta (β-) emitting radionuclides, and (III) electron capture and internal conversion decaying radionuclides.

α-Emitting radionuclides. Alpha-particles are high-energy helium nuclei (^{4}He) with high (about 100 keV/μm) linear energy transfer (LET) [3]. Alpha-particles deposit their energy in a very short range, the typical path-length of α-particles is in the order of 60 μm, reducing the non-specific irradiation to normal tissue around the target cell. Furthermore, cells have limited ability to repair the damage to DNA from α-particle irradiation, which makes α-particles extremely cytotoxic. To date only a few α-emitting radionuclides have been considered for radionuclide therapy. Astatine-211 (^{211}At), bismuth-212 (^{212}Bi), bismuth-213 (^{213}Bi) and more recent actinium-225 (^{225}Ac) are radionuclides which have been indicated to be suitable [5-7]. Most α-emitters have a very short half-life which makes them less suitable for therapy. Nevertheless ^{213}Bi-labeled MAb have been used in clinical trials with leukaemia [8] and prostate cancer [9].

β-Emitting radionuclides. For radionuclide therapy β-emitters have been most extensively studied (Table 1). β-Particles are negatively charged electrons emitted from the nucleus with a continuous spectrum. The average energy of a β-particle is about one-third of its maximum energy [3]. β-Emitters can be subdivided into 3 categories: low, medium and high energy according to β-particle energy and hence range [1, 3]. The range of β-particles is, generally, much greater than α-particles, which permits crossfire in a heterogeneous distribution of the radionuclide. Dependent on its energy and corresponding particle range, each β-emitting radionuclide is associated with a certain optimal tumor size for curability [10].

^{131}I is the most studied radionuclide for clinical use. Iodine-131 is readily availably, inexpensive, emits a medium-energy β-particle and can be directly linked to carbon atoms in molecules by a single covalent bond [11]. A major disadvantage of ^{131}I is its high γ-emission, which implies that extensive safety measures are needed to limit the radiation dose to medical personnel and relatives.

New developments in radionuclide production and labeling techniques have facilitated the use of other therapeutic radionuclides as well. This is particularly true for ^{90}Y. Its high β-energy and particle range of up to 12 mm makes ^{90}Y more suitable for irradiation of larger tumors (centimeter size [10]). Since it is a residualizing label, i.e. it has a long residence time in the tumor after internalization, ^{90}Y can deliver a relatively large radiation dose to the tumor [12]. The absence of γ-emission minimizes external radiation exposure, however it also makes imaging of the *in vivo* distribution of the ^{90}Y-labeled radiopharmaceutical virtually impossible.

Other β-particle-emitting radionuclides for therapy include ^{177}Lu and ^{67}Cu. ^{177}Lu is similar to ^{90}Y in stable binding to the chelator DOTA, but has a longer half-life and a considerable shorter maximum particle range of 1.5 mm, making it more suitable for treatment of smaller tumors. Rhenium isotopes (^{186}Re and ^{188}Re) have also been used for radionuclide therapy and have sufficient γ-energies for external scintigraphy, similar to ^{131}I [12].

A non-homogeneous distribution of radioactivity in the tumors is a recognized problem, especially for monoclonal antibodies, and its effect on dosimetry has been investigated [13, 14]. Howell et al. [13] concluded that high-energy β-emitters (e.g., ^{90}Y, ^{188}Re) are most effective in treating large tumors (diameter, d greater than approximately 1 cm), whereas for small tumors (millimeter size), medium energy beta emitters (e.g. ^{67}Cu, ^{186}Re, ^{177}Lu, ^{131}I) are better suited. Humm [14] has investigated the effect of various sizes of "cold regions" within a tumor and concludes that as the size of the cold region increases, higher β-energy emitters are advantageous in providing a more uniform dose throughout the tumor [11]. The approach for effective radionuclide therapy is to relate the choice of the radionuclide to the physical properties of the tumor [14].

TABLE 1. *Main characteristics of β-emitting radionuclides for radionuclide therapy.*

Radionuclide	Half-life (h)	Main β-energies (keV)[a]	(%)	Main γ-energies (keV)	(%)	Maximum particle range (mm)
Iodine-131	192	333	7	364	82	2.0
		606	89			
Yttrium-90	64	2284	100			12.0
Rhenium-186	89	939	21	137	10	5.0
		1077	71			
Rhenium-188	17	1965	25	155	15	11.0
		2120	71			
Copper-67	62	390	57	93	16	1.8
		482	22	185	49	
		575	20			
Lutetium-177	161	176	12	113	7	1.5
		384	9	208	11	
		497	79			

[a]Maximum β-energy

Electron capture and internal conversion decaying radionuclides. In both electron capture and internal conversion, an inner shell electron vacancy is created within the atom which is filled from an outer shell with the release of Auger electrons or low energy X-rays [1]. Due to the very short path length of Auger electrons (≤ cell diameter) the therapeutic application is limited to situations where the radiopharmaceutical localizes in, or very close, to the cell nucleus. Auger electron are capable of delivering a large radiation dose to the small volume surrounding the radionuclide decay site [15]. Incorporation of Auger electron within the nucleus of the cell produces high radiotoxicity [16]. This is the result of the deposition of these electrons with a shower of energies ranging from only a few to several hundred electron volts into an extremely small volume within the nuclear DNA [11].

Radiolabeling

Initially radiolabeling methods were focused on direct labeling because of its simplicity, which was relatively successful for the iodine radioisotopes ^{123}I, ^{125}I, and ^{131}I. But for stable coupling to the radionuclides ^{111}In, ^{90}Y, and ^{177}Lu indirect labeling methods with bi-functional chelators are mandatory. Bi-functional chelators are compounds that are able to form a stable complex with the radionuclide while containing a reactive group that can be used for coupling to the peptide or monoclonal antibody.

One of the first chelators used successfully for the coupling of ^{111}In was diethylenetriamenepentaacetic acid (DTPA). Examples of ^{111}In-labeled pharmaceuticals are the commercially available imaging agents OncoScint® (monoclonal antibody) and OctreoScan® (peptide). More recently, the macrocyclic chelator 1,4,7,10-tetraaza-cyclododecane-*N,N',N'',N'''*-tetraacetic acid (DOTA) was developed, which can form stable complexes with ^{90}Y and ^{177}Lu.

SOMATOSTATIN RECEPTOR TARGETED RADIONUCLIDE THERAPY

Somatostatin is a cyclopeptide that has a broad inhibitory effect on the secretion of hormones such as growth hormone, glucagon and insulin. The finding that somatostatin inhibits hormone secretion of various glands led to the application of somatostatin in the treatment of diseases based on for instance overproduction of hormones by tumors. The native peptide somatostatin itself is unsuitable for routine treatment, as after intravenous administration it has a very short half-life due to rapid enzymatic degradation. Therefore, somatostatin analogs that are more resistant to enzymatic degradation were synthesized; the molecule was modified in various ways with preservation of the biological activity of the original molecule. Introduction of D-amino acids, an amino-alcohol Thr-ol at the C-terminus and shortening of the molecule resulted e.g. in the 8 amino acids-containing somatostatin analog octreotide, having a long and therapeutically useful plasma half-life. The diagnostic radiolabeled peptide ^{111}In-DTPA-octreotide (OctreoScan®, ^{111}In-pentetreotide) was approved by the FDA on June 2, 1994 for scintigraphy of patients with neuroendocrine tumors. Nowadays somatostatin analogs are widely used in the treatment of symptoms due to neuroendocrine-active tumors, such as growth hormone-producing pituitary adenomas and gastroenteropancreatic tumors [17-20]. Recently, improvement of quality of life has been demonstrated with long acting depot formulations.

Somatostatin effects are mediated by high-affinity G-protein coupled membrane receptors, integral membrane glycoproteins. Five different human somatostatin receptor subtypes have been cloned [21-23]. Somatostatin binds to all subtypes with high affinity, while the affinity of the different somatostatin analogs for these subtypes differ considerably. Octreotide e.g. binds with high affinity to the somatostatin receptor subtype 2 (sst_2), and with lower affinities to sst_5 and sst_3. It shows no binding to sst_1 and sst_4 [22] (Table 2).

TABLE 2. *Affinity profiles (IC_{50}, nM) for human sst_2, sst_3 and sst_5 (based on [24] and [25]).*

Peptide	sst_2	sst_3	sst_5
SS-28	2.7	7.7	4.0
In-DTPA-octreotide	22	182	237
Y-DOTA-Tyr^3-octreotide (DOTATOC)	11	389	114
Y-DOTA-lanreotide (DOTALAN)	23	290	16
Y-DOTA-Tyr^3-octreotate (DOTATATE)	1.6	>1,000	187
Y-DOTA- 1-Nal^3-octreotide	3.3	26	10

Octreotide

The molecular basis of the use of radiolabeled octreotide in scintigraphy and radionuclide therapy is receptor-mediated internalization and cellular retention of the radionuclide. Internalization of radiolabeled DTPA-octreotide in somatostatin receptor-positive tumors and tumor cell lines has been investigated [26-28], it appeared that this process is receptor-specific and temperature dependent. Receptor-mediated internalization of ^{111}In-DTPA-octreotide results in degradation to the final radiolabeled metabolite ^{111}In-DTPA-D-Phe in the lysosomes [29]. This metabolite is not capable of passing the lysosomal and/or other cell membrane(s), and will therefore stay in the lysosomes, causing the long retention time of ^{111}In in sst_2-positive (tumor) cells.

Internalization of ^{111}In-DTPA-octreotide is especially important for radionuclide therapy of tumors when radionuclides emitting therapeutical particles with very short path lengths are used, like those emitting Auger electrons (e.g. ^{111}In). These electrons are only effective in a short distance of only a few nm up to μm from their target, the nuclear DNA.
Recently, Hornick et al. [30] and Wang et al. [31] described in vitro cellular internalization, nuclear translocation, and DNA binding of radiolabeled somatostatin analogs, which significantly increased after prolonged exposure.

However, the response of the tumor cells to peptide receptor radionuclide therapy (PRRT) is dependent on the cell's radiosensitivity. Therefore, we measured the radiosensitivity of the CA20948 tumor cells by using clonogenic survival assays after high-dose-rate external-beam radiotherapy (XRT) in vitro. It can be expected that results of high-dose-rate XRT are not representative for those after low-dose-rate radionuclide therapy (RT), such as PRRT. Therefore, we compared clonogenic survival in vitro in CA20948 tumor cells after increasing doses of XRT or RT, the latter using ^{131}I (Chapter 2).

Since ^{111}In emits both Auger and internal conversion electrons the question arose which electrons were responsible for the antiproliferative effects of ^{111}In-DTPA-octreotide. Therefore, in a clonogenic assay in vitro the therapeutic potential of ^{111}In-DTPA-octreotide was investigated in the CA20948 rat pancreatic cell line [32] (Chapter 3.1). In this in vitro system ^{111}In-DTPA-octreotide could completely control tumor growth, the effects were dependent on incubation time, radiation dose and specific activity used. Similar concentrations of ^{111}In-DTPA, which unlike ^{111}In-DTPA-octreotide is not internalized into sst_2-positive tumor cells, did not influence tumor survival.

In our preclinical radionuclide therapy studies in vivo, we used the rat pancreatic CA20948 tumor as a model for receptor-targeted scintigraphy and therapy using radiolabeled somatostatin analogs. This tumor is transplantable in Lewis rats, not only subcutaneously in the flank, but also metastasized to the liver. The latter is achieved by inoculation of tumor cells in the portal vein of the liver. The CA20948 tumor has been shown to be somatostatin receptor-positive, being an excellent model to study receptor-targeted scintigraphy and therapy in rats using radiolabeled somatostatin analogs [33].

We investigated the therapeutic effects of the ^{111}In-labeled somatostatin analog octreotide in various tumor sizes in a CA20948 flank tumor model (Chapter 3.2). After therapy with multiple doses of ^{111}In-labeled octreotide we found various responses. Complete responses were only found in the smaller tumors. As ^{111}In emits Auger electrons with mean particle ranges of up to one cell diameter, radiation emitted from a receptor-positive tumor cell will not kill neighboring receptor-negative cells. Therefore the receptor density/expression of somatostatin receptor on the tumors before and after radionuclide therapy was investigated. After a single dose treatment of 185 MBq ^{111}In-DOTA-Tyr^3-octreotate a clear sst_2 receptor expression in the control as well as the treated tumor was found.

We also performed radionuclide therapy using ^{111}In-DTPA-octreotide in the CA20948 liver metastases model [34]. Therapy with administrations of 370 MBq (coupled to 0.5 μg octreotide) ^{111}In-DTPA-octreotide after intraportal CA20948 tumor cell inoculation induced a significant decrease in the number of hepatic metastases at day 21. Co-injection with 1 mg unlabeled octreotide resulted in inhibition of the tumor response to radionuclide therapy, pointing to a receptor-dependent therapeutic effect. Also dose dependent effects of therapy by injection of 370, 37 or 3.7 MBq ^{111}In-DTPA-octreotide one day after tumor inoculation were investigated [34]. The 370 MBq dosage had significantly more therapeutic effects and inhibited the increase of liver weight due to tumor growth more than the 37 or 3.7 MBq doses. These findings hold promise for application of therapy with ^{111}In-labeled peptides in an adjuvant, micrometastatic setting, e.g. after surgery to eradicate occult metastases.

So, ^{111}In-labeled peptides are therefore suitable for both scintigraphy and radionuclide therapy, all the more so as the decay of Auger electron emitter has recently been shown to lead to a "bystander effect", an in vivo, dose-independent inhibition or retardation of tumor growth in non-radiotargeted cells by a signal produced in Auger electron-labeled cells [35].

In clinical studies an anti-tumor response of high doses of ^{111}In-DTPA-octreotide was found, however, the radiopeptide was not very effective in end-stage patients and in patients with large tumors [36-41]. Consequently, various research groups aimed to develop somatostatin analogs that can be linked via a chelator to a radionuclide, which emits β-particles with longer particle ranges, such as ^{90}Y and ^{177}Lu. In addition, new somatostatin analogs were synthesized to improve receptor affinity.

Octreotide analogs

Various chelator-peptide constructs have been synthesized and evaluated concerning their receptor affinity, internalization capacities, and biodistribution in vivo [42] (Table 2). The analogs tested included DTPA-Tyr^3-octreotide and DTPA-Tyr^3-octreotate (in octreotate the C-terminal threoninol has been replaced with the native amino acid threonine) in comparison to DTPA-octreotide. Phe^3-residues were replaced with Tyr to increase the hydrophylicity of the peptides. Octreotate was synthesized to investigate the effects of an additional negative charge on clearance and cellular uptake. We concluded that radiolabeled DTPA-Tyr^3-octreotate and second best DTPA-Tyr^3-octreotide, and also their DOTA-coupled counterparts, were most promising for scintigraphy and therapy of octreotide receptor-positive tumors in humans [42].

DOTA is a universal chelator capable of formation of stable complexes with metals like ^{111}In, ^{67}Ga, ^{68}Ga, ^{86}Y and ^{64}Cu for imaging as well as with ^{90}Y (high energy β-particle emitter) and with radiolanthanides like e.g. ^{177}Lu (low energy β-particle and gamma emitter) for receptor-mediated radionuclide therapy. Reubi et al. [24] evaluated the in vitro binding characteristics of labeled (indium, yttrium, gallium) and unlabeled DOTA-Tyr^3-octreotide, DOTA-octreotide, DOTA-lanreotide, DOTA-vapreotide (RC-160), DTPA-Tyr^3-octreotate and DOTA-Tyr^3-octreotate using cell lines transfected with the human somatostatin receptor subtypes sst_1, sst_2, sst_3, sst_4 and sst_5 (Table 2). They found that small structural modifications, chelator substitution or metal replacement considerably affected the receptor binding affinity. A marked improvement of sst_2 affinity was e.g. found for Ga-DOTA-Tyr^3-octreotide (IC_{50} 2.5 nM) compared with the Y-labeled compound and In-DTPA-octreotide. An excellent binding affinity for sst_2 in the same range was also found for In-DTPA-Tyr^3-octreotate (IC_{50} 1.3 nM) and for Y-DOTA-Tyr^3-octreotate (IC_{50} 1.6 nM). Of ^{111}In-, ^{88}Y- and ^{177}Lu-labeled DOTA-Tyr^3-octreotate, biodistribution and tumor uptake were compared in CA20948 tumor-bearing rats [43]. In vivo, for all 3 radiolabeled analogs a rapid clearance from the blood and very high, specific uptake in sst_2-positive organs and tumor were found. For tumor and sst_2-positive organs it was found that uptake of ^{111}In- ≈ ^{88}Y- < ^{177}Lu-DOTA-Tyr^3-octreotate, making the latter analog most promising for radionuclide therapy. Schmitt et al. [44] investigated ^{177}Lu-DOTA-Tyr^3-octreotate in nude mice with human small cell lung cancer and concluded that the tumor had a higher activity concentration compared to all measured normal tissues at all time points tested, pointing to the therapeutic potential of ^{177}Lu-DOTA-Tyr^3-octreotate for small cell lung cancer.

To provide insight in the tumoricidal effects of Tyr^3-octreotide and Tyr^3-octreotate labeled with either ^{177}Lu or ^{90}Y a therapeutic comparison was performed in vitro, in a colony-forming assay using the rat pancreatic tumor cell line CA20948 [45] (Chapter 4). Both Tyr^3-octreotide and Tyr^3-octreotate labeled with either ^{177}Lu or ^{90}Y, were able to control tumor growth in a dose dependent manner. In all concentrations used radiolabeled Tyr^3-octreotate had a higher tumor kill capacity compared to radiolabeled Tyr^3-octreotide, labeled with ^{177}Lu (Figure 1) or ^{90}Y.

A comparison between radiolabeled octreotide and octreotate analogs was also performed in rats using ^{64}Cu-labeled analogs, reaching the same conclusion, that because of its high tumor uptake in comparison to that of the other analogs tested, Tyr^3-octreotate was selected for future PET imaging and targeted radiotherapy studies. New stable analogs of somatostatin with high affinity for different somatostatin receptors are currently being developed. An interesting example is DOTA-1-Nal^3-octreotide, which has high affinity for sst_2, sst_3 and sst_5 [25, 46]. This compound may allow PRRT of tumors, which do not bind octreotide and octreotate with high affinity, i.e. sst_3- and sst_5-positive tumors.

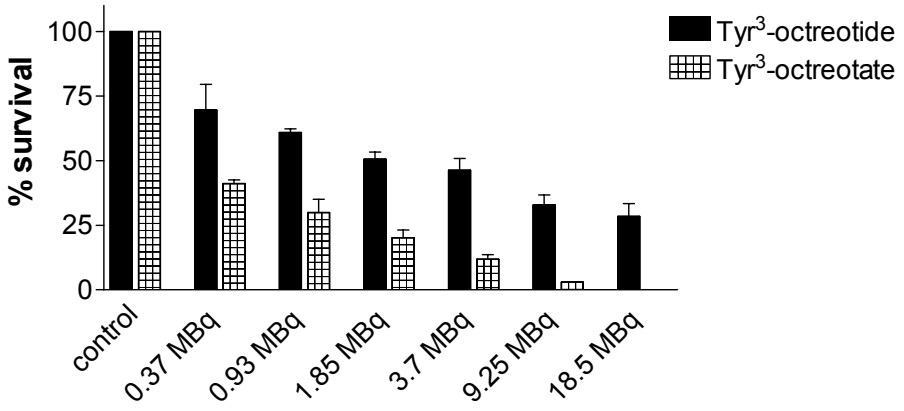

FIGURE 1. *Inhibitory effect of ^{177}Lu coupled to either octreotide or octreotate on the tumor cell survival of the CA20948 cell line. Cells were incubated for 1 hour at 37°C with increasing amounts of ^{177}Lu-octreotate or ^{177}Lu-octreotide. Data are expressed as mean ± SEM.*

A problem during radionuclide therapy may be caused by the high uptake of radioactivity in the kidneys; small peptides in the blood plasma are filtered through the glomerular capillaries in the kidneys and subsequently reabsorbed by and retained in the proximal tubular cells, thereby reducing the scintigraphic sensitivity for detection of small tumors in the perirenal region and the possibilities for radionuclide-therapy. The renal uptake of radiolabeled octreotide in rats could be reduced by positively charged amino acids, e.g. with about 50 % by single intravenous administration of 400 mg/kg L- or D-lysine [47, 48]. Therefore, during PRRT an infusion containing the positively charged amino acids L-lysine and L-arginine (in patients e.g. 25 g lysine and 25 g arginine infused in 4 h) can be given during and after the infusion of the radiopharmaceutical, in order to reduce the kidney uptake [49, 50].

After ^{111}In, the next radionuclide investigated was ^{90}Y, emitting β-particles with a high maximum energy (2.27 MeV) and a long maximum particle range (>10 mm). The first somatostatin analog radiolabeled with ^{90}Y and applied for PRRT in animals and patients was ^{90}Y-DOTA-Tyr^3-octreotide, in which, in comparison with octreotide, the phenylalanine residue at position 3 has been replaced with tyrosine; this makes the compound more hydrophilic and increases the affinity for sst_2, leading to higher uptake in sst_2-positive tumors both in preclinical studies and in patients [27, 34].

We compared the radiotherapeutic effect of different doses ^{90}Y-DOTA-Tyr^3-octreotide in rats bearing pancreatic CA20948 tumors of different size in the flank [43]. After the highest dose, i.e. 370 MBq ^{90}Y-DOTA-Tyr^3-octreotide, 50% complete response was reached for the small tumors (< 1 cm^2), whereas only growth delay was found in the very large tumors (> 12 cm^2). Medium sized tumors (about 8 cm^2), however, showed 100% cure after this same dose of ^{90}Y-DOTA-Tyr^3-octreotide. So, in this study a difference is found in the

radiotherapeutic effects in CA20948 tumors of different size. In larger tumors more clonogenic, presumably hypoxic, cells will be present, thereby limiting radiocurability. The small tumors on the other hand, will not absorb all energy emitted by ^{90}Y, thereby decreasing tumor curability.

Significant tumor growth delay was also found in rats bearing small CA20948 tumors after radionuclide therapy with up to 3 x 740 MBq ^{64}Cu-TETA,Tyr^3-octreotide or ^{64}Cu-TETA-Tyr^3-octreotate [34, 51], the first compound given either fractionated or as a single dose. Dose fractionation in 2 doses induced significantly increased tumor-growth inhibition compared with rats given a single dose. However, in this study the single 555 MBq dose was bound to twice the amount of peptide compared to the two 278 MBq doses. So, partial saturation of the receptors using the single high dose and therefore relatively lower uptake of radioactivity in the tumor may have contributed to these findings.

Tumor growth inhibition in the same model was also found after treatment of CA20948 tumor-bearing rats with ^{90}Y-DTPA-benzyl-acetamido-Tyr^3-octreotide [52]. Using 370 MBq/kg of ^{90}Y-DOTA-Tyr^3-octreotide the same group observed even complete tumor reduction in 5 out of 7 rats [53].

Clinical studies to determine the therapeutic efficacy of ^{90}Y-DOTA-Tyr^3-octreotide in cancer patients are ongoing at various institutions in Basel, Milano, Brussels and Rotterdam [50, 54-64]. The most promising rate of complete plus partial responses seen in the various ^{90}Y-DOTA-Tyr^3-octreotide studies consistently surpasses that obtained with ^{111}In-DTPA-octreotide.

The next analog investigated in preclinical radionuclide therapy studies was ^{177}Lu-DOTA-Tyr^3-octreotate. ^{177}Lu emits gamma radiation with a suitable energy for imaging and therapeutic β-particles with low to medium energy (maximum 0.50 MeV), so the same complex can be used for both imaging and dosimetry and radionuclide therapy, thus obviating the need for a pre-therapeutic diagnostic study. The approximate range of the β-particles is 20 cell diameters, whereas the range of those emitted by ^{90}Y is 150 cell diameters. Less "cross-fire" induced radiation damage in the renal glomeruli can therefore be expected with ^{177}Lu. Also, in comparison with ^{90}Y, a higher percentage of the ^{177}Lu radiation energy will be absorbed in very small tumors and (micro)metastases.

We investigated the anti-tumor effects of ^{177}Lu-DOTA-Tyr^3-octreotate in various models, including a rat liver micrometastatic model, mimicking disseminated disease, and a solid tumor model. ^{177}Lu-DOTA-Tyr^3-octreotate showed anti-tumoral effects in the rat liver tumor metastases model leading to significant better survival in the treated rats [63].

In studies using ^{177}Lu-labeled octreotate for therapy of solid tumors, 100% cure was found in the groups of rats bearing small (≤ 1 cm^2) CA20948 tumors after two repeated doses of 277.5 MBq or after a single dose of 555 MBq (estimated tumor dose 60 Gy) [43]. After therapy with the same doses of ^{177}Lu-DOTA-Tyr^3-octreotide, that has a lower tumor uptake than the octreotate analog, these data were 50% and 60% cure in rats bearing small tumors. In rats bearing larger (≥ 1 cm^2, range 1.4 – 10 cm^2) tumors, 40 and 50% cure were found in the groups that received one or two 277.5 MBq injections of ^{177}Lu-DOTA-Tyr^3-octreotate, respectively (estimated tumor dose is 30 Gy and 60 Gy respectively) [43]. However, in another study in a

different rat pancreatic tumor model (AR42J), in which a more favorable tumor dose was reached after 555 MBq ^{177}Lu-DOTA-Tyr^3-octreotate (140 Gy), all rats but one were cured irrespective the size of their tumor (unpublished result). So, ^{177}Lu-DOTA-Tyr^3-octreotate therapy showed excellent therapeutic results in the rats bearing small to big tumors (especially when the tumor dose is high), the findings for the small tumors were in accordance with those of an earlier study [64]. Patients treated with ^{177}Lu-DOTA-Tyr^3-octreotate showed complete or partial remissions in an impressive 30% of the patients, and a minor response in 12 % [55].

In a different set of preclinical experiments the combination of ^{177}Lu-DOTA-Tyr^3-octreotate and ^{90}Y-DOTA-Tyr^3-octreotide (at a constant total dose) was studied in rats that each had a small (0.1 cm^2) and a large tumor (8 cm^2), to mimic the clinical situation, in which large tumors and small metastases are usually present in the same patient. The rats treated with the combination of 50% ^{177}Lu-DOTA-Tyr^3-octreotate plus 50% ^{90}Y-DOTA-Tyr^3-octreotide/or -octreotate showed a longer survival than those treated with 100% ^{90}Y-DOTA-Tyr^3-octreotide/ -octreotate or ^{177}Lu-DOTA-Tyr^3-octreotate [65]. This underscores the great promise of ^{177}Lu- and ^{90}Y-labeled peptides for radionuclide therapy and the potential of the combination of these radionuclides with different β-energies and particle ranges to achieve higher cure rates in the presence of tumors of different size.

We conclude that ^{177}Lu-DOTA-Tyr^3-octreotate is a very promising somatostatin analog for radionuclide therapy in patients suffering from sst_2-expressing tumors. In patients with tumors of different size, including small metastases, also combinations of radionuclides are of interest, e.g. ^{90}Y and ^{177}Lu, to obtain the widest range of tumor curability.

Apart from the combination of analogs labeled with different radionuclides, future directions to improve this therapy may also include efforts to increase the somatostatin receptor expression on the tumors, as well as studies to the effects of the use of radiosensitizers.

Lanreotide

Virgolini et al. developed an ^{111}In- / ^{90}Y- labeled somatostatin analog, DOTA-lanreotide, for tumor diagnosis and therapy [66-68]. They described that ^{111}In-/ ^{90}Y-labeled DOTA-lanreotide bound with high affinity to a number of human tumors. ^{111}In-DOTA-lanreotide bound with high affinity to $hsst_2$, $hsst_3$, $hsst_4$, and $hsst_5$ and with lower affinity to $hsst_1$ expressed on COS7 cells, suggesting it is a universal receptor binder [68]. In Sprague Dawley rats, ^{90}Y-DOTA-lanreotide was rapidly cleared from the circulation and concentrated in somatostatin receptor-positive tissues, such as pancreas and pituitary. It was indeed concluded that this radiolabeled peptide can be used for somatostatin receptor-mediated diagnosis as well as systemic radiotherapy of human tumors.

However, Reubi et al. found in vitro in cell lines transfected with the different somatostatin receptor subtypes that whereas Y-DOTA-lanreotide had a good affinity for the sst_5, it had a low affinity for sst_3 (IC_{50} 290 nM) and sst_4 (IC_{50} > 10000 nM) [24]. Thereby, they challenged the concept that lanreotide is a universal binder to the different somatostatin receptors. Froidevaux et al. [69] concluded from their comparison study of among other things DOTA-Tyr^3-octreotide and DOTA-lanreotide in rats that radiolabeled DOTA-Tyr^3-octreotide has more potential for clinical application than DOTA-lanreotide.

Lanreotide was the second analog labeled with ^{90}Y and used for clinical PRRT studies. Virgolini et al. [67] reported on the biodistribution, safety and radiation absorbed dose of ^{111}In-DOTA-lanreotide. ^{90}Y-DOTA-lanreotide treatment was further studied at different centers in the MAURITIUS (Multicenter Analysis of a Universal Receptor Imaging and Treatment Initiative, a European Study) trial [66]. Overall treatment results in 70 patients indicated stable tumor disease in 35% of patients and regressive tumor disease in 10% of tumor patients with different tumor entities expressing hSSTR. In two-thirds of patients with neuroendocrine tumor lesions, ^{90}Y-DOTA-Tyr^3-octreotide showed a higher tumor uptake than ^{90}Y-DOTA-lanreotide, which can be explained by the lower affinity of ^{90}Y-DOTA-lanreotide for sst_2.

RC-160

Several reports have been published on the in vitro receptor binding to somatostatin receptors of another somatostatin analog, the octapeptide RC-160 (vapreotide). It has been reported that RC-160 has a higher affinity than octreotide for the somatostatin receptors in human breast, ovarian, exocrine pancreatic, prostatic and colonic cancer, explained by the much higher affinity of RC-160 for sst_4 [70, 71]. Therefore, the possible binding of RC-160 to a somatostatin receptor subtype (sst_4) that does not bind octreotide, should offer a potential advantage for RC-160 over octreotide. However, different experiments showed that ^{111}In-DTPA-RC-160 does not seem to have advantages over ^{111}In-DTPA-octreotide as a radiopharmaceutical for somatostatin receptor scintigraphy, despite the fact that ^{111}In-DTPA-RC-160 shows specific high-affinity binding to somatostatin receptor-positive organs [72-74]. This is in accordance with the findings of Reubi et al. [24], showing that the affinities of DOTA-RC-160 and ^{90}Y-DOTA-RC-160 for the human sst_2 and sst_3 are in the same range as that of ^{111}In-DTPA-octreotide. The affinities (IC_{50}) of the RC-160 analogs for the sst_4, however, were found to be low, around 700 nM (for ^{111}In-DTPA-octreotide the IC_{50} for the sst_4 was > 1000 nM), in contrast to the above-mentioned findings of non-chelated RC160. Furthermore, unlike (radioiodinated) RC-160 that passes the blood-brain barrier, it was also shown that ^{111}In-DTPA-RC-160 and ^{111}In-DTPA-octreotide do not pass the blood-brain barrier organs [72-74]. Also Froidevaux et al. [69] concluded from biodistribution studies in experimental animals comparing DOTA-RC-160 and other DOTA-coupled somatostatin analogs (lanreotide, octreotide, Tyr^3-octreotide) and from clinical data that DOTA-Tyr^3-octreotide has a better potential in the clinic than chelated RC-160.

Rhenium-188 coupled to the analog RC-160 has also been used to establish the feasibility of treating tumors with radiolabeled peptides [75, 76]. In different experimental tumor models in nude mice, treatment resulted in significant reduction or elimination of tumor burden. Long-term studies with ^{188}Re-RC-160 demonstrated a protracted reduction of tumor volume and a positive effect on animal survival. Neither RC-160 by itself nor an ^{188}Re-labeled peptide unrelated to somatostatin demonstrated the reduction in tumor mass observed with ^{188}Re-RC-160.

RGD-(DTPA-)octreotate

As described above a large variety of radiolabeled somatostatin derivatives have been prepared for targeted radionuclide therapy purposes. They are in various stages of investigation. Cell matrix interactions are also fundamental to tumor invasion and formation of metastases as well as to tumor-induced angiogenesis. Integrins, heterodimeric transmembrane glycoproteins, composed of an alpha- and beta-subunit, play a key role in these interactions. One of these integrins, the $\alpha_v\beta_3$ receptor, is able to bind a number of extracellular matrix proteins via an Arg-Gly-Asp (RGD) sequence [77]. This receptor is expressed on various malignant human tumors and upregulated in proliferating endothelial cells. Based on the RGD sequence, several compounds have been designed as $\alpha_v\beta_3$ antagonists. In tumor models using the $\alpha_v\beta_3$ antagonists not only blocked tumor-angiogenesis but in some cases also resulted in tumor regression [78, 79].

In addition, several procaspases also contain potential RGD-binding motifs near the site necessary for activation to the mature caspase. Caspases are proteases that are critical in programmed cell death [80]. Buckley et al. demonstrated that RGD peptides are able to directly activate caspase-3 and thereby inducing apoptosis [81]. Other work has shown that molecules specific for GPIIb/IIIa integrins can also stimulate caspase-3 activity [82]. Since caspase-3 is one of the key executioners proteases [83] in the apoptosis pathway, it seems likely that this enzyme will be an important site of action for targeted therapeutics that are designed to selectively induce cell death.

To further enhance the therapeutic potential of the somatostatin analogs we hypothesized that the synergistic effects of an apoptosis-inducing factor, such an Arg-Gly-Asp (RGD) motif, can increase the radiotherapeutic efficacy of these peptides. We combined the characteristics of the somatostatin analog Tyr^3-octreotate and RGD in one compound by synthesizing the hybrid peptide RGD-DTPA-octreotate [c(Arg-Gly-Asp-D-Tyr-Asp)-Lys(DTPA)-Phe-c(Cys-Tyr-D-Trp-Lys-Thr-Cys)-Thr] (Figure 2) [84] (Chapter 5).

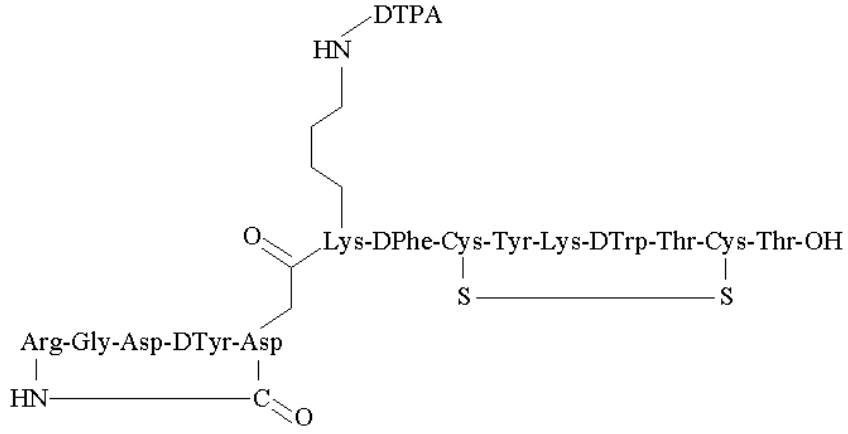

FIGURE 2. *Structure of RGD-DTPA-octreotate [c(Arg-Gly-Asp-D-Tyr-Asp)-Lys(DTPA)-Phe-c(Cys-Tyr-D-Trp-Lys-Thr-Cys)-Thr].*

In biodistribution studies in rats we showed that there is a high receptor-specific uptake in sst_2-positive tissues and tumors of RGD-^{111}In-DTPA-octreotate (Figure 3), comparable to the uptake of ^{111}In-DOTA-Tyr^3-octreotate in sst_2-positive tissues and tumors. A decreased uptake in sst_2-positive tissues and tumors was found after co-injection of RGD-^{111}In-DTPA-octreotate with 500 μg unlabeled octreotide. A drawback of the new hybrid compound was the high renal uptake and retention of radioactivity, limiting the therapeutic radioactivity dose that can be administered, as the kidneys are critical organs in radionuclide therapy using somatostatin analogs. D-lysine injection resulted in 40% reduction of the renal uptake.

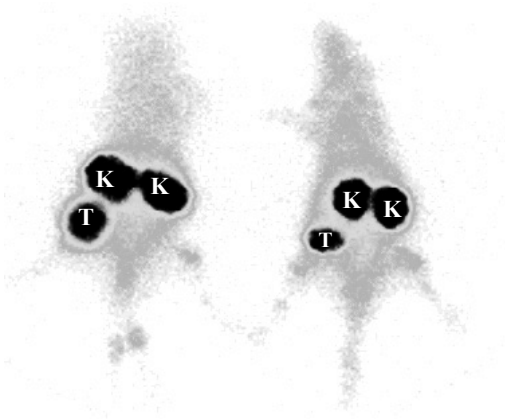

FIGURE 3. *Scan of two rats bearing a CA20948 tumor on their right hind leg, 24 h post injection of RGD-^{111}In-DTPA-Tyr^3-octreotate. K=kidney, T=tumor.*

In an in vitro study the tumoricidal effects of the ^{111}In-labeled peptide RGD-DTPA-octreotate in comparison with ^{111}In-labeled RGD and Tyr^3-octreotate were evaluated using a colony-forming assay [85]. CA20948 tumor cell survival after incubation with 9.25 MBq for 1h with ^{111}In-labeled RGD, Tyr^3-octreotate and RGD-DTPA-octreotate was; 81%, 68% and 43% respectively, showing that the radiolabeled RGD-DTPA-octreotate has a more pronounced tumoricidal effect than ^{111}In-DTPA-RGD and ^{111}In-DTPA-Tyr^3-octreotate. The superior tumoricidal effect is probably the result of increased apoptosis, as is shown by an increased caspase-3 activity after incubation with ^{111}In-labeled RGD-DTPA-octreotate.

These results show that the ^{111}In-labeled peptide RGD-DTPA-octreotate promotes apoptosis in comparison with the two monopeptides RGD and Tyr^3-octreotate, via an increase in caspase-3 levels. The ^{111}In-labeled hybrid peptide can therefore significantly enhance the therapeutic efficacy of somatostatin-based agents. Because of the high renal uptake of this hybrid peptide it is also very interesting to use the unlabeled peptide RGD-DTPA-octreotate for (adjuvant) therapy (Chapter 5.3). The unlabeled hybrid peptide, RGD-DTPA-octreotate induced a significant increase in caspase-3 levels in comparison with RGD and Tyr^3-octreotate. In order to change the elimination route from the body (from renal clearance to more hepatic clearance), the biodistribution of iodinated RGD-octreotate, without the

presence of the chelator DTPA, was examined. ^{125}I-RGD-octreotate showed indeed a much lower renal uptake in comparison with RGD-^{111}In-DTPA-octreotate. Furthermore, the affinity of RGD-octreotate increased in comparison with RGD-DTPA-octreotate (IC_{50} values of $1.4x10^{-8}$M vs $9.4x10^{-8}$M respectively).

So, this concept of targeting somatostatin receptor-expressing tumors using peptide receptor radionuclide therapy might also apply for the use of somatostatin analogs coupled to chemotherapeutic compounds, which is further described in Chapter 5.4. The development of hybrid molecules that combine targeting and an effector function, such as apoptosis, can be a new approach in the treatment of cancer.

CONCLUSIONS

This overview shows that therapy with radiolabeled somatostatin analogs is a most promising new treatment modality for patients with sst_2-positive tumors.

A variety of other peptide-based radioligands, like derivatives of bombesin, gastrin/cholecystokinin and neurotensin, which receptors are expressed on different major cancers, and RGD peptides, which can be targeted to many major tumors because of either binding to receptors expressed on newly formed blood vessels and induction of apoptosis, is currently under development.

In conclusion, radiolabeled peptides have opened a new era in nuclear oncology, not only for localization but also for radionuclide therapy.

REFERENCES

1. Clarke SE. Radionuclide therapy in oncology. *Cancer Treat Rev* 1994;20:51-71.
2. Weiner RE, Thakur ML. Radiolabeled peptides in the diagnosis and therapy of oncological diseases. *Appl Radiat Isot* 2002;57:749-763.
3. Zweit J. Radionuclides and carrier molecules for therapy. *Phys Med Biol* 1996;41:1905-1914.
4. Press OW, Shan D, Howell-Clark J, Eary J, Appelbaum FR, Matthews D, King DJ, Haines AM, Hamann P, Hinman L, Shochat D, Bernstein ID. Comparative metabolism and retention of iodine-125, yttrium-90, and indium-111 radioimmunoconjugates by cancer cells. *Cancer Res* 1996;56:2123-2129.
5. McDevitt MR, Sgouros G, Finn RD, Humm JL, Jurcic JG, Larson SM, Scheinberg DA. Radioimmunotherapy with alpha-emitting nuclides. *Eur J Nucl Med* 1998;25:1341-1351.
6. Andersson H, Palm S, Lindegren S, Back T, Jacobsson L, Leser G, Horvath G. Comparison of the therapeutic efficacy of 211At- and 131I-labelled monoclonal antibody MOv18 in nude mice with intraperitoneal growth of human ovarian cancer. *Anticancer Res* 2001;21:409-412.
7. McDevitt MR, Ma D, Lai LT, Simon J, Borchardt P, Frank RK, Wu K, Pellegrini V, Curcio MJ, Miederer M, Bander NH, Scheinberg DA. Tumor therapy with targeted atomic nanogenerators. *Science* 2001;294:1537-1540.
8. Sgouros G, Ballangrud AM, Jurcic JG, McDevitt MR, Humm JL, Erdi YE, Mehta BM, Finn RD, Larson SM, Scheinberg DA. Pharmacokinetics and dosimetry of an alpha-particle emitter labeled antibody: 213Bi-HuM195 (anti-CD33) in patients with leukemia. *J Nucl Med* 1999;40:1935-1946.
9. McDevitt MR, Barendswaard E, Ma D, Lai L, Curcio MJ, Sgouros G, Ballangrud AM, Yang WH, Finn RD, Pellegrini V, Geerlings MW, Jr., Lee M, Brechbiel MW, Bander NH, Cordon-Cardo C, Scheinberg DA. An alpha-particle emitting antibody ([213Bi]J591) for radioimmunotherapy of prostate cancer. *Cancer Res* 2000;60:6095-6100.
10. O'Donoghue JA, Bardies M, Wheldon TE. Relationships between tumor size and curability for uniformly targeted therapy with beta-emitting radionuclides. *J Nucl Med* 1995;36:1902-1909
11. Volkert WA, Goeckeler WF, Ehrhardt GJ, Ketring AR. Therapeutic radionuclides: production and decay property considerations. *J Nucl Med* 1991;32:174-185.
12. Goldenberg DM. Targeted therapy of cancer with radiolabeled antibodies. *J Nucl Med* 2002;43:693-713.
13. Howell RW, Rao DV, Sastry KS. Macroscopic dosimetry for radioimmunotherapy: nonuniform activity distributions in solid tumors. *Med Phys* 1989;16:66-74.
14. Humm JL. Dosimetric aspects of radiolabeled antibodies for tumor therapy. *J Nucl Med* 1986;27:1490-1497.
15. McLean JR, Blakey DH, Douglas GR, Bayley J. The Auger electron dosimetry of indium-111 in mammalian cells in vitro. *Radiat Res* 1989;119:205-218.
16. Adelstein SJ, Kassis AI. Radiobiologic implications of the microscopic distribution of energy from radionuclides. *Int J Rad Appl Instrum B* 1987;14:165-169.
17. Kvols LK, Moertel CG, O'Connell MJ, Schutt AJ, Rubin J, Hahn RG. Treatment of the malignant carcinoid syndrome. Evaluation of a long- acting somatostatin analogue. *N Engl J Med* 1986;315:663-666.
18. Eriksson B, Oberg K. Summing up 15 years of somatostatin analog therapy in neuroendocrine tumors: future outlook. *Ann Oncol* 1999;10:S31-38.

19. Lamberts SW, Krenning EP, Reubi JC. The role of somatostatin and its analogs in the diagnosis and treatment of tumors. *Endocr Rev* 1991;12:450-482.
20. Lamberts SW, Reubi JC, Krenning EP. Somatostatin analogs in the treatment of acromegaly. *Endocrinol Metab Clin North Am* 1992;21:737-752
21. Patel YC, Greenwood MT, Panetta R, Demchyshyn L, Niznik H, Srikant CB. The somatostatin receptor family. *Life Sci* 1995;57:1249-1265.
22. Patel YC. Somatostatin and its receptor family. *Front Neuroendocrinol* 1999;20:157-198
23. Schonbrunn A. Somatostatin receptors present knowledge and future directions. *Ann Oncol* 1999;10:S17-21.
24. Reubi JC, Schar JC, Waser B, Wenger S, Heppeler A, Schmitt JS, Macke HR. Affinity profiles for human somatostatin receptor subtypes SST1-SST5 of somatostatin radiotracers selected for scintigraphic and radiotherapeutic use. *Eur J Nucl Med* 2000;27:273-282.
25. Wild D, Schmitt JS, Ginj M, Macke HR, Bernard BF, Krenning E, De Jong M, Wenger S, Reubi JC. DOTA-NOC, a high-affinity ligand of somatostatin receptor subtypes 2, 3 and 5 for labelling with various radiometals. *Eur J Nucl Med Mol Imaging* 2003;30:1338-1347.
26. Andersson P, Forssell-Aronsson E, Johanson V, Wangberg B, Nilsson O, Fjalling M, Ahlman H. Internalization of indium-111 into human neuroendocrine tumor cells after incubation with indium-111-DTPA-D-Phe1-octreotide. *J Nucl Med* 1996;37:2002-2006.
27. De Jong M, Bernard BF, De Bruin E, Van Gameren A, Bakker WH, Visser TJ, Macke HR, Krenning EP. Internalization of radiolabelled [DTPA0]octreotide and [DOTA0,Tyr3]octreotide: peptides for somatostatin receptor-targeted scintigraphy and radionuclide therapy. *Nucl Med Commun* 1998;19:283-288.
28. Hofland LJ, van Koetsveld PM, Waaijers M, Lamberts SW. Internalisation of isotope-coupled somatostatin analogues. *Digestion* 1996;57:2-6.
29. Duncan JR, Stephenson MT, Wu HP, Anderson CJ. Indium-111-diethylenetriaminepentaacetic acid-octreotide is delivered in vivo to pancreatic, tumor cell, renal, and hepatocyte lysosomes. *Cancer Res* 1997;57:659-671.
30. Hornick CA, Anthony CT, Hughey S, Gebhardt BM, Espenan GD, Woltering EA. Progressive nuclear translocation of somatostatin analogs. *J Nucl Med* 2000;41:1256-1263.
31. Wang M, Caruano AL, Lewis MR, Meyer LA, VanderWaal RP, Anderson CJ. Subcellular localization of radiolabeled somatostatin analogues: implications for targeted radiotherapy of cancer. *Cancer Res* 2003;63:6864-6869.
32. Capello A, Krenning EP, Breeman WA, Bernard BF, de Jong M. Peptide receptor radionuclide therapy in vitro using [111In-DTPA0]octreotide. *J Nucl Med* 2003;44:98-104.
33. Bernard BF, Krenning E, Breeman WA, Visser TJ, Bakker WH, Srinivasan A, de Jong M. Use of the rat pancreatic CA20948 cell line for the comparison of radiolabelled peptides for receptor-targeted scintigraphy and radionuclide therapy. *Nucl Med Commun* 2000;21:1079-1085.
34. De Jong M, Breeman WA, Bernard HF, Kooij PP, Slooter GD, Van Eijck CH, Kwekkeboom DJ, Valkema R, Macke HR, Krenning EP. Therapy of neuroendocrine tumors with radiolabeled somatostatin- analogues. *Q J Nucl Med* 1999;43:356-366.
35. Xue LY, Butler NJ, Makrigiorgos GM, Adelstein SJ, Kassis AI. Bystander effect produced by radiolabeled tumor cells in vivo. *Proc Natl Acad Sci U S A* 2002;99:13765-13770.
36. Valkema R, De Jong M, Bakker WH, Breeman WA, Kooij PP, Lugtenburg PJ, De Jong FH, Christiansen A, Kam BL, De Herder WW, Stridsberg M, Lindemans J, Ensing G, Krenning

EP. Phase I study of peptide receptor radionuclide therapy with [In- DTPA]octreotide: the Rotterdam experience. *Semin Nucl Med* 2002;32:110-122.

37. Krenning EP, de Jong M, Kooij PP, Breeman WA, Bakker WH, de Herder WW, van Eijck CH, Kwekkeboom DJ, Jamar F, Pauwels S, Valkema R. Radiolabelled somatostatin analogue(s) for peptide receptor scintigraphy and radionuclide therapy. *Ann Oncol* 1999;10:S23-29.
38. Fjalling M, Andersson P, Forssell-Aronsson E, Gretarsdottir J, Johansson V, Tisell LE, Wangberg B, Nilsson O, Berg G, Michanek A, Lindstedt G, Ahlman H. Systemic radionuclide therapy using indium-111-DTPA-D-Phe1-octreotide in midgut carcinoid syndrome. *J Nucl Med* 1996;37:1519-1521.
39. Anthony LB, Woltering EA, Espenan GD, Cronin MD, Maloney TJ, McCarthy KE. Indium-111-pentetreotide prolongs survival in gastroenteropancreatic malignancies. *Semin Nucl Med* 2002;32:123-132.
40. McCarthy KE, Woltering EA, Espenan GD, Cronin M, Maloney TJ, Anthony LB. In situ radiotherapy with 111In-pentetreotide: initial observations and future directions. *Cancer J Sci Am* 1998;4:94-102.
41. McCarthy KE, Woltering EA, Anthony LB. In situ radiotherapy with 111In-pentetreotide. State of the art and perspectives. *Q J Nucl Med* 2000;44:88-95.
42. de Jong M, Breeman WA, Bakker WH, Kooij PP, Bernard BF, Hofland LJ, Visser TJ, Srinivasan A, Schmidt MA, Erion JL, Bugaj JE, Macke HR, Krenning EP. Comparison of (111)In-labeled somatostatin analogues for tumor scintigraphy and radionuclide therapy. *Cancer Res* 1998;58:437-441.
43. de Jong M, Breeman WA, Bernard BF, Bakker WH, Schaar M, van Gameren A, Bugaj JE, Erion J, Schmidt M, Srinivasan A, Krenning EP. [177Lu-DOTA(0),Tyr3] octreotate for somatostatin receptor-targeted radionuclide therapy. *Int J Cancer* 2001;92:628-633.
44. Schmitt A, Bernhardt P, Nilsson O, Ahlman H, Kolby L, Schmitt J, Forssel-Aronsson E. Biodistribution and dosimetry of 177Lu-labeled [DOTA0,Tyr3]octreotate in male nude mice with human small cell lung cancer. *Cancer Biother Radiopharm* 2003;18:593-599.
45. Capello A, Krenning EP, Breeman WA, Bernard BF, Konijnenberg MW, de Jong M. Tyr3-octreotide and Tyr3-octreotate radiolabeled with 177Lu or 90Y: peptide receptor radionuclide therapy results in vitro. *Cancer Biother Radiopharm* 2003;18:761-768.
46. Schmitt JS, Wild D, Ginj M, Reubi JC, Waser B, De Jong M, Bernard HF, Krenning EP, Maecke HR. DOTA-NOC, a high affinity ligand of the somatostatin receptor subtypes 2,3 and 5 for radiotherapy. *J Labelled Cpd Radiopharm* 2001;44:s697-s699.
47. de Jong M, Rolleman EJ, Bernard BF, Visser TJ, Bakker WH, Breeman WA, Krenning EP. Inhibition of renal uptake of indium-111-DTPA-octreotide in vivo. *J Nucl Med* 1996;37:1388-1392
48. Bernard BF, Krenning EP, Breeman WA, Rolleman EJ, Bakker WH, Visser TJ, Macke H, de Jong M. D-lysine reduction of indium-111 octreotide and yttrium-90 octreotide renal uptake. *J Nucl Med* 1997;38:1929-1933.
49. Rolleman EJ, Valkema R, de Jong M, Kooij PP, Krenning EP. Safe and effective inhibition of renal uptake of radiolabelled octreotide by a combination of lysine and arginine. *Eur J Nucl Med Mol Imaging* 2003;30:9-15.
50. Bodei L, Cremonesi M, Zoboli S, Grana C, Bartolomei M, Rocca P, Caracciolo M, Macke HR, Chinol M, Paganelli G. Receptor-mediated radionuclide therapy with 90Y-DOTATOC in

association with amino acid infusion: a phase I study. *Eur J Nucl Med Mol Imaging* 2003;30:207-216.

51. Anderson CJ, Jones LA, Bass LA, Sherman EL, McCarthy DW, Cutler PD, Lanahan MV, Cristel ME, Lewis JS, Schwarz SW. Radiotherapy, toxicity and dosimetry of copper-64-TETA-octreotide in tumor-bearing rats. *J Nucl Med* 1998;39:1944-1951.
52. Stolz B, Smith-Jones P, Albert R, Tolcsvai L, Briner U, Ruser G, Macke H, Weckbecker G, Bruns C. Somatostatin analogues for somatostatin-receptor-mediated radiotherapy of cancer. *Digestion* 1996;57:17-21.
53. Stolz B, Weckbecker G, Smith-Jones PM, Albert R, Raulf F, Bruns C. The somatostatin receptor-targeted radiotherapeutic [90Y-DOTA-DPhe1, Tyr3]octreotide (90Y-SMT 487) eradicates experimental rat pancreatic CA 20948 tumours. *Eur J Nucl Med* 1998;25:668-674.
54. de Jong M, Krenning E. New advances in peptide receptor radionuclide therapy. *J Nucl Med* 2002;43:617-620.
55. De Jong M, Kwekkeboom D, Valkema R, Krenning EP. Radiolabelled peptides for tumour therapy: current status and future directionsPlenary lecture at the EANM 2002. *Eur J Nucl Med Mol Imaging* 2003;30:463-469.
56. De Jong M, Valkema R, Jamar F, Kvols LK, Kwekkeboom DJ, Breeman WA, Bakker WH, Smith C, Pauwels S, Krenning EP. Somatostatin receptor-targeted radionuclide therapy of tumors: preclinical and clinical findings. *Semin Nucl Med* 2002;32:133-140.
57. Otte A, Mueller-Brand J, Dellas S, Nitzsche EU, Herrmann R, Maecke HR. Yttrium-90-labelled somatostatin-analogue for cancer treatment [letter]. *Lancet* 1998;351:417-418.
58. Otte A, Herrmann R, Heppeler A, Behe M, Jermann E, Powell P, Maecke HR, Muller J. Yttrium-90 DOTATOC: first clinical results. *Eur J Nucl Med* 1999;26:1439-1447.
59. Paganelli G, Bodei L, Chinol M, Zoboli S, Cremonesi M, Gatti M, Bartolomei M, Grana C, Maecke H. Receptor mediated radiotherapy with ^{90}Y-DOTATOC: results of a phase I study. *J Nucl Med* 2001;42:36P.
60. Waldherr C, Pless M, Maecke HR, Haldemann A, Mueller-Brand J. The clinical value of [90Y-DOTA]-D-Phe1-Tyr3-octreotide (90Y-DOTATOC) in the treatment of neuroendocrine tumours: a clinical phase II study. *Ann Oncol* 2001;12:941-945.
61. Waldherr C, Pless M, Maecke HR, Schumacher T, Crazzolara A, Nitzsche EU, Haldemann A, Mueller-Brand J. Tumor response and clinical benefit in neuroendocrine tumors after 7.4 GBq (90)Y-DOTATOC. *J Nucl Med* 2002;43:610-616.
62. Bushnell D, O'Dorisio T, Menda Y, Carlisle T, Zehr P, Connolly M, Karwal M, Miller S, Parker S, Bouterfa H. Evaluating the clinical effectiveness of 90Y-SMT 487 in patients with neuroendocrine tumors. *J Nucl Med* 2003;44:1556-1560.
63. Breeman WA, Mearadji A, Capello A, Bernard BF, van Eijck CH, Krenning EP, de Jong M. Anti-tumor effect and increased survival after treatment with [177Lu-DOTA0,Tyr3]octreotate in a rat liver micrometastases model. *Int J Cancer* 2003;104:376-379.
64. Erion JL, Bugaj JE, Schmidt MA, Wilhelm RR, Srinivasan A. High radiotherapeutic efficacy of [Lu-177]-DOTA-Y3-octreotate in a rat tumor model. *J Nucl Med* 1999;40:223p.
65. De Jong M, Bernard HF, Breeman WAP, van Gameren A, Krenning EP. Combination of ^{90}Y- and ^{177}Lu-labeled somatostatin analogs is superior for radionuclide therapy compared to ^{90}Y- or ^{177}Lu-labeled analogs only. *J Nucl Med* 2005;in press.
66. Virgolini I, Britton K, Buscombe J, Moncayo R, Paganelli G, Riva P. In- and Y-DOTA-lanreotide: results and implications of the MAURITIUS trial. *Semin Nucl Med* 2002;32:148-155.

67. Virgolini I, Szilvasi I, Kurtaran A, Angelberger P, Raderer M, Havlik E, Vorbeck F, Bischof C, Leimer M, Dorner G, Kletter K, Niederle B, Scheithauer W, Smith-Jones P. Indium-111-DOTA-lanreotide: biodistribution, safety and radiation absorbed dose in tumor patients. *J Nucl Med* 1998;39:1928-1936.
68. Smith-Jones PM, Bischof C, Leimer M, Gludovacz D, Angelberger P, Pangerl T, Peck-Radosavljevic M, Hamilton G, Kaserer K, Kofler A, Schlangbauer-Wadl H, Traub T, Virgolini I. DOTA-lanreotide: a novel somatostatin analog for tumor diagnosis and therapy. *Endocrinology* 1999;140:5136-5148.
69. Froidevaux S, Heppeler A, Eberle AN, Meier AM, Hausler M, Beglinger C, Behe M, Powell P, Macke HR. Preclinical comparison in AR4-2J tumor-bearing mice of four radiolabeled 1,4,7,10-tetraazacyclododecane-1,4,7,10-tetraacetic acid- somatostatin analogs for tumor diagnosis and internal radiotherapy. *Endocrinology* 2000;141:3304-3312.
70. Srkalovic G, Cai RZ, Schally AV. Evaluation of receptors for somatostatin in various tumors using different analogs. *J Clin Endocrinol Metab* 1990;70:661-669.
71. Liebow C, Reilly C, Serrano M, Schally AV. Somatostatin analogues inhibit growth of pancreatic cancer by stimulating tyrosine phosphatase. *Proc Natl Acad Sci U S A* 1989;86:2003-2007.
72. Breeman WA, Hofland LJ, Bakker WH, van der Pluijm M, van Koetsveld PM, de Jong M, Setyono-Han B, Kwekkeboom DJ, Visser TJ, Lamberts SW, et al. Radioiodinated somatostatin analogue RC-160: preparation, biological activity, in vivo application in rats and comparison with [123I- Tyr3]octreotide. *Eur J Nucl Med* 1993;20:1089-1094.
73. Breeman WA, Hofland LJ, van der Pluijm M, van Koetsveld PM, de Jong M, Setyono-Han B, Bakker WH, Kwekkeboom DJ, Visser TJ, Lamberts SW. A new radiolabelled somatostatin analogue [111In-DTPA-D-Phe1]RC-160: preparation, biological activity, receptor scintigraphy in rats and comparison with [111In-DTPA-D-Phe1]octreotide. *Eur J Nucl Med* 1994;21:328-335.
74. Breeman WAP, van Hagen PM, Kwekkeboom DJ, Visser TJ, Krenning EP. Somatostatin receptor scintigraphy using [111In-DTPA0]RC-160 in humans: a comparison with [111In-DTPA0]octreotide. *Eur J Nucl Med* 1998;25:182-186.
75. Zamora PO, Bender H, Gulhke S, Marek MJ, Knapp FF, Jr., Rhodes BA, Biersack HJ. Pre-clinical experience with Re-188-RC-160, a radiolabeled somatostatin analog for use in peptide-targeted radiotherapy. *Anticancer Res* 1997;17:1803-1808.
76. Zamora PO, Gulhke S, Bender H, Diekmann D, Rhodes BA, Biersack HJ, Knapp FF, Jr. Experimental radiotherapy of receptor-positive human prostate adenocarcinoma with 188Re-RC-160, a directly-radiolabeled somatostatin analogue. *Int J Cancer* 1996;65:214-220.
77. Varner JA. The role of vascular cell integrins alpha v beta 3 and alpha v beta 5 in angiogenesis. *Exs* 1997;79:361-390.
78. Brooks PC, Montgomery AM, Rosenfeld M, Reisfeld RA, Hu T, Klier G, Cheresh DA. Integrin alpha v beta 3 antagonists promote tumor regression by inducing apoptosis of angiogenic blood vessels. *Cell* 1994;79:1157-1164.
79. Brooks PC, Stromblad S, Klemke R, Visscher D, Sarkar FH, Cheresh DA. Antiintegrin alpha v beta 3 blocks human breast cancer growth and angiogenesis in human skin. *J Clin Invest* 1995;96:1815-1822.
80. Salvesen GS, Dixit VM. Caspases: intracellular signaling by proteolysis. *Cell* 1997;91:443-446.

81. Buckley CD, Pilling D, Henriquez NV, Parsonage G, Threlfall K, Scheel-Toellner D, Simmons DL, Akbar AN, Lord JM, Salmon M. RGD peptides induce apoptosis by direct caspase-3 activation. *Nature* 1999;397:534-539.
82. Adderley SR, Fitzgerald DJ. Glycoprotein IIb/IIIa antagonists induce apoptosis in rat cardiomyocytes by caspase-3 activation. *J Biol Chem* 2000;275:5760-5766.
83. Wolf BB, Green DR. Suicidal tendencies: apoptotic cell death by caspase family proteinases. *J Biol Chem* 1999;274:20049-20052.
84. Bernard BF, Capello A, van Hagen PM, Breeman WA, Srinivasan A, Schmidt MA, Erion JL, van Gameren A, Krenning EP, de Jong M. Radiolabeled RGD-DTPA-Tyr^3-octreotate for receptor-targeted radionuclide therapy. *Cancer Biother Radiopharm* 2004;19:273-280.
85. Capello A, Krenning EP, Bernard BF, Breeman WA, van Hagen MP, de Jong M. Increased cell death after therapy with an arg-gly-asp-linked somatostatin analog. *J Nucl Med* 2004;45:1716-1720.

CHAPTER 2

RADIOSENSITIVITY

Low-dose-rate irradiation by ^{131}I versus high-dose-rate external-beam irradiation in the rat pancreatic tumor cell line CA20948.

Suzanne Verwijnen, Astrid Capello, Bert Bernard, Gerard van den Aardweg, Mark Konijnenberg, Wout Breeman, Eric Krenning and Marion de Jong.

Cancer Biotherapy and Radiopharmaceuticals, 2004, 19 (3): 285-292.

ABSTRACT

Aim: the rat pancreatic CA20948 tumor cell line is widely used in receptor-targeted preclinical studies because many different peptide receptors are expressed on the cell membrane. The response of the tumor cells to peptide radionuclide therapy, however, is dependent on the cell line's radiosensitivity. Therefore, we measured the radiosensitivity of the CA20948 tumor cells by using clonogenic survival assays after high-energy external-beam radiotherapy (XRT) in vitro. It can, however, be expected that results of high-dose-rate XRT are not representative for those after low-dose-rate radionuclide therapy (RT), such as peptide-receptor radionuclide therapy. Therefore, we compared clonogenic survival in vitro in CA20948 tumor cells after increasing doses of XRT or RT, the latter using ^{131}I. **Methods:** Survival of CA20948 cells was investigated using a clonogenic survival assay after RT by incubation with increasing amounts of ^{131}I, leading to doses of 1-10 Gy after 12 days of incubation (maximum dose rate, 0.92 mGy/min), or with doses of 1-110 Gy using an X-ray machine (dose rate, 0.66 Gy/min). Colonies were scored after a 12-day-incubation period. Also, the doubling time of this cell line was calculated. **Results:** We observed a dose-dependent reduction in tumor-cell survival, which, at low doses, was similar for XRT and RT. For high-dose-rate XRT, the quadratic over linear component ratio (α/β) for CA20948 was 8.3 Gy, whereas that ratio for low-dose-rate RT was calculated to be 86.5 Gy. The calculated doubling time of CA20948 cells was 22 hours. **Conclusions:** Despite the huge differences in dose rate, RT tumor cell-killing effects were approximately as effective as those of XRT at doses of 1 and 2 Gy, the latter being the common daily dose given in fractionated external-beam therapies. At higher doses, RT was less effective than XRT.

INTRODUCTION

Receptor-targeting peptides have been developed into a new generation of therapeutic radiopharmaceuticals. Peptide receptor radionuclide therapy (PRRT) can be performed using these peptide analogs radiolabeled with therapeutic radionuclides, such as low linear energy transfer (LET) beta-particle emitters ^{177}Lu and ^{90}Y [1]. This new application of peptide analogs—somatostatin analogs being the most commonly used—have shown to be most promising in preclinical studies [2] and in clinical patient treatment [3, 4].

However, until now, the emphasis of PRRT has been on efficacy in clinical and preclinical studies, and less consideration has been placed of radioactivity at the cellular level and to radiobiology in radionuclide therapy. Extrapolations have most often been made from external beam radiation effects, despite differences in the nature of the radiation—especially in the dose rate and irradiation period. These factors, as well as cell-growth kinetics, are important determinants of tumor-cell survival. They emphasize the need for further research on the effects, at the cellular level, of low-dose-rate irradiation over long periods delivered. We wanted to make a comparison between radionuclide therapy (RT) (without peptides) and external-beam radiotherapy (XRT) in CA20948 cells to establish the intrinsic radiosensitivity. The authors and other colleagues have shown that the rat pancreatic tumor cell line CA20948 can be used as *in vitro* and *in vivo* models for research of different radiolabeled peptides for imaging and therapy [1, 5-13]. This cell line expresses different kinds of high-affinity peptide receptors, such as somatostatin receptors, and also CCK/gastrin, NK1, gastrin-releasing peptide (GRP) and $\alpha_v\beta_3$ receptors [5-9, 12-19]. Therefore, this cell line is very interesting for testing newly developed analogs and the effects of PRRT using these analogs.

For radiation-based therapy, tumor cure depends on several factors, such as the radiation dose absorbed in the tumor including the pattern of delivery (dose rate, fractionation), the number of clonogenic tumor cells that have to be sterilized in order to kill the tumor and the response of the tumor cells to radiation, dependent on radiosensitivity and proliferation rate. We wanted to establish the intrinsic radiosensitivity of the CA20948 to interpret our in vitro and in vivo PRRT results. Therefore, we performed XRT therapy in a clonogenic survival assay to obtain radiation dose-survival curves, where clonogenicity is the ability of a tumor cell to undergo viable division and to proliferate. For many cell lines and for low LET irradiation, the logarithmic function of the survival fraction is characterized by an initial low-dose region starting with shallow slope followed by a shoulder region, and then an exponential survival decrease. This can be approximated by a linear-quadratic function of the dose, which is described in the linear-quadratic model [20]; the cellular survival (S) is in relation to the dose (D) as: $\text{Ln } S = -(\alpha D+\beta D^2)$. In this equation, the α and β parameters refer to different categories of lesions, namely lethal (α) versus repairable sublethal damage (β). The linear character of the model stems form the idea that a single hit can cause a lethal event. The α-component is indicative for the intrinsic radiosensitivity of the cells. The quadratic components stem form the idea that two hits on single target are required for cell death. Close proximity of these two lesions can cause lethality, while further apart the lesions remain

sublethal and repairable. The β-component is an estimate for the capacity of repairable damage. The α/β ratio is the dose where cell death is caused equally by irreparable and reparable lesions. For RT in our cell line, a different curve is expected than for XRT because of the difference in dose rate compared to XRT.

The aim of our experiments was to further characterize the CA20948 rat pancreatic tumor cell line by comparing clonogenic survival and radiosensitivity in vitro using XRT and RT.

MATERIALS AND METHODS

Cell Culture

The rat pancreatic CA20948 tumor cells, which attach to a cell culture plate, were grown in Dulbecco's modified Eagle's medium (DMEM, Gibco, Life Technologies, Breda, The Netherlands) supplemented with 10% heat-inactivated fetal bovine serum (FBS), 2 mmol/L of glutamine, 50 IU/mL penicillin/streptomycin (Gibco, Life Technologies, Breda, The Netherlands), 1 mmol/L sodium pyruvate and 0.1 mg/L fungizone. The medium was changed twice or three times per week. Cells were cultured in a 37ºC incubator with a gas mixture of 95% air and 5% CO_2.

Cellular Uptake Characteristics of ^{131}I

These experiments were performed to investigate whether or not ^{131}I (Mallinckrodt, Petten, The Netherlands) added to the medium would stick to the cells or the plastic of a 6-wells plate. We also determined whether the ^{131}I would stay homogeneously distributed in the medium. In these experiments, 400 and 800 cells were plated in 6-wells plates. After two days, these cells were incubated with 0.26 MBq ^{131}I in the medium. After an incubation time of 1, 2, 3, 20, 22, 23.5, 92, 94, 96, 98 and 116 hours, 10 different 10 µL samples were taken from the medium and counted in an LKB-1282-Compugammasystem (PerkinElmer, Oosterhout, The Netherlands) to determine possible disappearance from the medium. Thereafter, the cells were lysed with 0.1 M NaOH and also counted in the LKB-gammasystem to exclude cellular uptake.

Calculations with a Monte Carlo model

The well-plate was modeled with the Monte Carlo code MCNP4C [21] to calculate the absorbed dose to the cells attached to the bottom on each well. The polyethylene well plate (density ρ = 0.92 g/cm^3) has a thickness of 4.118 mm, and each of the 6-wells has a surface area of 9.62 cm^2 and a depth of 3.118 mm, resulting in a volume of 3 cm^3, evenly spaced over the whole plate. The well-plate cavities were filled with water (ρ = 1 g/cm^3) and only one cavity was assumed to be filled with a radioactivity source. The self-dose and cross-doses to the other wells could thereby be determined.

The radiation characteristics of ^{131}I ($T_{1/2}$ = 8.04 d) were taken from the ICRP38 database [22]. Three separate calculations were performed for the beta emission (E_{max} = 806.9 keV), the gamma and X-rays (main γ line: 365.5 keV (81.2%/decay)) and the internal conversion and Auger electrons. The source distributions were modeled with a homogeneous distribution of the activity in the well. The thickness of the well cavity is too small to achieve electron equilibrium in the lateral direction. In the radial direction there is electron equilibrium apart from a small region on the outer rim of the plate. To gain insight to the dose distribution in the lateral direction, scoring of the radiation dose in the bottom half of the well was done in 4 regions of 25 μm, 1 region of 59 μm and, consecutively, 14 regions of 100 μm. The top half of the well was not subdivided into scoring regions.

The Monte Carlo calculations were performed with 1 million starting particles, thus obtaining statistical variance in the scoring regions below 1%. Both the electron and photon minimum energy threshold was set at 1 keV. The deposited energy (in MeV) per starting particle was scored in all geometry elements.

For an *in vitro* experiment with the ^{131}I activity (of A MBq) load lasting T days the cumulated activity (in MBq.d) is given by:

$$\widetilde{A} = \int_0^T A\, e^{-\frac{\ln 2\, t}{T_{1/2}}}\, dt = \frac{A \times T_{1/2}}{\ln 2}\left(1 - e^{-\frac{\ln 2\, T}{T_{1/2}}}\right)$$

In vitro clonogenic survival assay

Single-cell suspensions of CA20948 cells were plated in 6-wells plates at 400 and 800 cells/well, with each concentration in triplicate and incubated for 24 hours. Cells were irradiated with either 200 kV X-rays (XRT) or with ^{131}I added to the medium (RT).

External X-irradiation was carried out at a dose rate of 0.66 Gy/min and with the machine operating at 20 mA. The X-ray machine contained a 1 mm Cu-filter resulting in a half-value layer (HVL) of 1.6 mm Cu [23]. Delivered doses were checked with thermoluminescent dosimetry (TLD), which indicated < 3% dose variation over the entire irradiation field. After irradiation, the cells were allowed to form colonies for 12 days in the above-mentioned incubator at 37ºC.

The cells irradiated with ^{131}I solutions were incubated with ^{131}I free in 3 mL of medium for 12 days in the 37ºC incubator, leading to a dose of 1 to 10 Gray (Gy) with a maximum dose rate of 0.92 mGy/minute. ^{131}I was added as a sterile ^{131}I chloride solution, specific activity: 1-1.5 mCi/mL. The ^{131}I solutions were made according to Table 1 (range: 0.17 to 1.75 MBq/well).

After the colony-forming period, the cell colonies were fixated for 15 minutes with methanol:glacial acid (3:1), and then stained for 15 minutes with heamatoxylin. Colonies that contained ≥ 50 cells were counted and used to calculate the surviving fraction [19].

TABLE 1. *Amount of ^{131}I activity in DMEM solutions, leading to a dose of 1 to 10 Gy in the clonogenic survival assay.*

MBq/well	D (Gy)	MBq/well	D (Gy)
0.000	0		
0.174	1	1.050	6
0.351	2	1.224	7
0.525	3	1.398	8
0.699	4	1.572	9
0.873	5	1.746	10

Data analysis

For each dose point, the number of colonies —as obtained from 3 wells with identical cell concentrations— was averaged and used to calculate the surviving fraction. Standard deviations were used as weighing factor. Based on these surviving fractions a cell-survival curve was computer-fitted to the LQ-model using a Curve Expert 3.1 program.

Sulforhodamine B (SRB) assay

The cell-doubling time was determined with the SRB-assay [24]. This assay was adapted for *in vitro* cell cultures (Van den Aardweg, in progress). In short, cells were grown at 37°C in 96-well plates with lanes of 8 wells containing cell concentrations of 100, 250, 500, 1000, 2500, 5000 cells/mL and 200 µL medium per well. At intervals of 24 hours up to 6 days after plating, the cells were fixed with 10% trichloroacetic acid solution for 1 hour at 4°C using 200 µL per well. After drying the plates, the cells were stained for 2 hours adding 50 µL per well of a 0.4% SRB solution in 1% acetic acid. Plates were washed and 150 µL Tris ([hydroxymethyl]aminomethane, 10 mM, Sigma-Aldrich, Zwijndrecht, The Netherlands) was added. The following day, the optical density was measured for each well at 540 nm using a spectrophotometer (Biorad, Veenendaal, The Netherlands). For each cell concentration, the logarithmic values for the mean optical densities plotted as a function of time gave straight lines, the cell-doubling time was calculated.

RESULTS

Binding and Cellular uptake of ^{131}I

The results of these experiments are shown in Table 2. These results show that ^{131}I did not disappear from the medium, and did not bind to the cells plated in the 6-wells plate, but stayed homogeneously distributed in the medium.

Monte Carlo Calculations

The results for the dosimetry calculations inside the well with ^{131}I homogeneously distributed are given in Table 3 as a function of the distance from the bottom of the well. The tumor cells are situated in the bottom layer of the well, and the dose is 5.51E-03 mGy/MBq.s. For a total activity load time of 12 days, the dose-per-unit activity is 3.56 Gy/MBq. The cross doses from the β- and γ-emissions from ^{131}I in neighboring wells are maximally 0.4 and 7 mGy/MBq, respectively, and are, therefore, neglected.

TABLE 2. *Percentage of the activity of ^{131}I in the medium and uptake of ^{131}I in CA20948 cells.*

Hours	Activity in 400 cells %A ± SD	Activity in 800 cells %A ± SD	Mean activity in 400 and 800 cells %A ± SD
1	0.017 ± 0.005	0.009 ± 0.000	0.013 ± 0.005
2	0.009 ± 0.003	0.012 ± 0.001	0.010 ± 0.003
3	0.016 ± 0.012	0.007 ± 0.001	0.011 ± 0.012
20	0.006 ± 0.001	0.005 ± 0.001	0.006 ± 0.001
22	0.009 ± 0.003	0.007 ± 0.001	0.008 ± 0.003
24	0.007 ± 0.001	0.010 ± 0.008	0.009 ± 0.008
92	0.007 ± 0.000	0.005 ± 0.001	0.006 ± 0.001
94	0.006 ± 0.001	0.005 ± 0.000	0.005 ± 0.001
96	0.013 ± 0.004	0.005 ± 0.001	0.009 ± 0.004
98	0.010 ± 0.004	0.005 ± 0.001	0.007 ± 0.004
116	0.008 ± 0.002	0.007 ± 0.001	0.008 ± 0.002

SD, standard deviation

Clonogenic survival assay

We investigated the effects of two cell densities—400 and 800 cells/well—on cellular survival after incubation with ^{131}I (data not shown). The radiobiological parameters were calculated from the two curves, which showed that the α- and β-component were in the same range for the two different cell densities. Therefore, for other experiments we have used the cell density of 400 cells/well.

Fig. 1 shows the effects of external-beam therapy (XRT) and radionuclide therapy (RT) on clonogenic survival of CA20948 cells. XRT was delivered in a single fraction by an X-ray machine in less than 30 minutes, while RT was delivered by using ^{131}I over a period of 12 days. For both therapies, we observed a dose-dependent reduction of tumor cell survival. At low doses, the surviving fraction was almost identical for XRT and RT. The XRT curves exhibited a more rapid exponential decrease at higher doses. The radiobiological parameters were calculated and are presented in Table 4. The α/β ratios for the CA20948 cell line was higher for RT than for XRT. These results indicate that the survival curve of the RT-irradiated

cells have a relatively flat slope at higher doses, compared to that after XRT. Therefore, RT resulted in less cell killing than XRT for both cell lines at higher doses. The surviving fraction at 2 Gy (SF_2) was approximately 0.47 for CA20948 cells; this parameter was similar for both RT as XRT.

TABLE 3. *Dose distribution in the 9.62 cm^2 well plate with ^{131}I distributed homogeneously inside the 3 mL well plate.*

	z_{min}- z_{max}		Absorbed dose per cum. act. (mGy/MBq.s)			
Region	(μm)	Mass (g)	β-ray (E-03)	γ-ray (E-04)	IC+Auger (E-04)	Total (E-03)
1	0 - 25	0.0241	5.22	2.08	0.815	5.51
2	25 - 50	0.0241	5.92	2.20	0.948	6.24
3	50 - 75	0.0241	6.40	2.22	0.973	6.72
4	75 -100	0.0241	6.80	2.25	0.978	7.12
5	100 - 159	0.0568	7.26	2.23	1.02	7.58
6	159 - 259	0.0962	7.95	2.45	1.06	8.30
7	259 - 359	0.0962	8.58	2.63	1.10	8.96
8	359 - 459	0.0962	8.89	2.56	1.12	9.26
9	459 - 559	0.0962	9.11	2.62	1.15	9.48
10	559 - 659	0.0962	9.34	2.69	1.15	9.72
11	659 - 759	0.0962	9.45	2.76	1.18	9.85
12	759 - 859	0.0962	9.43	2.83	1.17	9.83
13	859 - 959	0.0962	9.52	2.89	1.17	9.93
14	959 - 1059	0.0962	9.54	2.91	1.19	9.94
15	1059 - 1159	0.0962	9.59	3.05	1.17	10.0
16	1159 - 1259	0.0962	9.61	2.91	1.17	10.0
17	1259 - 1359	0.0962	9.56	2.79	1.19	9.96
18	1359 - 1459	0.0962	9.60	2.76	1.18	9.99
19	1459 - 1559	0.0962	9.67	2.85	1.18	10.1
20	1559 - 3118	1.500	8.92	2.66	1.13	9.29
Total	0 - 3118	3.000	8.95	2.68	1.13	9.34

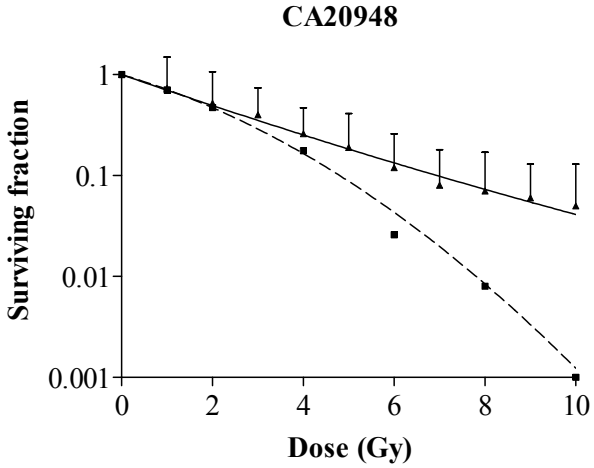

FIGURE 1. *Clonogenic survival curve for CA20948 cells using two methods: (1) external-beam therapy (dashed line) and (2) radionuclide therapy (solid line). Data are expressed as the mean ± standard deviation of at least three independent experiments.*

TABLE 4. *The radiobiological parameters α, β, α/β ratio and surviving fraction at 2 Gy (SF_2) calculated for CA20948.*

	CA20948	
Parameter	XRT	RT
α	0.304	0.351
β	0.0366	0.0031
α/β ratio (Gy)	8.3	102
SF_2	0.47	0.52

XRT, external-beam therapy;
RT, radionuclide therapy

SRB Assay

Figure 2 shows the results of the SRB assay for the CA20948 cells, and a doubling time of 22 ± 1 hours was calculated.

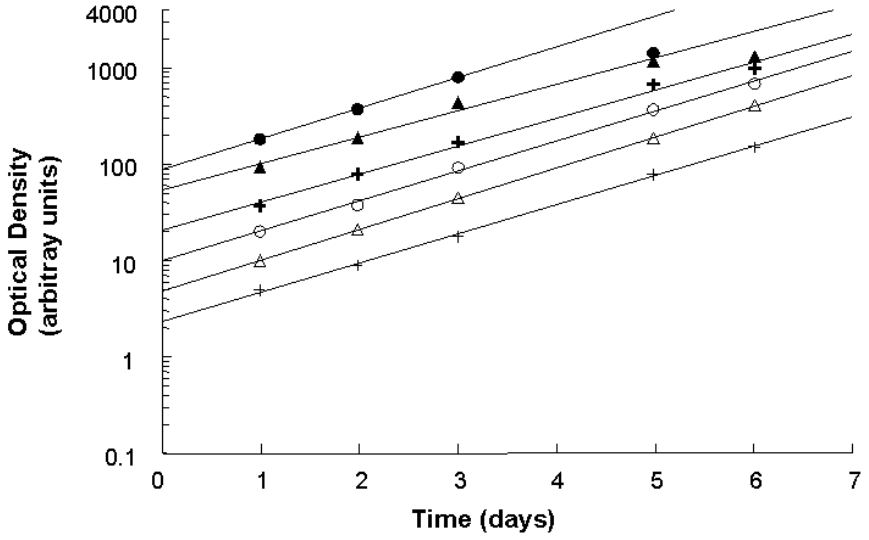

FIGURE 2. *Growth curves for CA20498 cells obtained with the SRB assay. The slope of the curves is an estimate for the cell-doubling time. Increasing cell concentrations of 100 cells/mL (gray +), 250 cells/mL (△), 500 cells/mL (○), 1000 cells/ml (black +), 2500 cells/ml (▲), and 5000 cells/ml (●) were used.*

DISCUSSION

In this study, we compared the survival curves of the CA20948 cell line *in vitro* using both high-dose-rate XRT or exponentially decreasing low-dose-rate RT. The CA20948 cell line is widely used for radiolabeled peptide studies performed *in vitro* and *in vivo* in tumor-bearing rats [1, 2, 5-9, 12, 13, 19, 25-27]. We performed *in vitro* clonogenic survival assays using high-energy XRT to determine the radiation sensitivity. However, it can be expected that the results of XRT are not representative for the results of RT, because of the difference in, for instance, dose rate. RT has a continuously decreasing dose rate because of radionuclide decay, whereas XRT is given at a constant dose rate for a short period of time. Therefore, we also performed survival assays using ^{131}I free in culture medium. Damage to the cells is caused by the crossfire effect of ^{131}I. The radionuclide was not coupled to a peptide analogue, because we wanted to exclude the effects of receptor affinity, as well as the internalization and externalization rate of the radiolabeled analogue, which will influence the results.

To be able to compare the effects of RT and XRT, we shall describe here the development and validation of a RT clonogenic survival assay using incubation with the radionuclide ^{131}I present in its free form in a culture medium. The physical characteristics of this radionuclide are in the same range as those of ^{177}Lu, which is used in our PRRT studies using ^{177}-DOTA-Tyr^3-octreoatate. The half-life of ^{177}Lu is 6.7 days, compared to 8.0 days for ^{131}I. Furthermore, the maximum range in water or tissue is approximately 2-3 mm.

Several studies have been performed comparing XRT and radioimmunotherapy (RIT) in cell lines, such as the human colon carcinoma cell lines LS174T and WiDr [28-30]. Experiments [28, 29]

have shown that the LS174T human colon carcinoma cell line showed a comparable response to RIT and XRT. However, compared to XRT, RIT was less effective in radioresistent cell lines, such as the human colon carcinoma cell line WiDr. A possible explanation would be a greater DNA-repair capacity of WiDr versus LS174T [28, 29]. These studies conclude that the effectiveness of cell killing with RIT was lower than with XRT because of the dose-rate effect and dose heterogeneity in the tumor [28, 29].

The shape of any survival curve is dependent on different aspects, such as the type of cells, the kind of radiation, and the dose rate of the radiation used. In CA20948, RT caused a more linear than exponential decrease of cell survival. This can be explained by the lower dose rate of RT than of XRT; therefore, less damage occurs and there is more time to repair. We can, therefore, conclude from these results that a Gy of RT is not the same as a Gy of XRT. Table 4 also shows higher α/β ratios for RT compared to XRT for the CA20948, showing that this cell line is less sensitive to RT than to XRT at higher doses. Studies by Joiner et al. [31, 32] described a higher sensitivity in the radiation survival response of mammalian cells at doses below 0.5 Gy with low dose rates (2 cGy - 1 Gy h^{-1}), the so-called hyper-radiosensitivity. We did not find this phenomenon on our studies with CA2948, because we did not use these low doses. In our further studies, possible hyper-radiosensitivity effects in our cell lines will be further investigated.

Cellular survival after exposure to radiation is a function of the detection and successful repair of double-stranded DNA breaks [33]. A larger α than β component in the radiation survival curves, which was seen in our RT curves, suggests that the cell lines were more capable of repairing sublethal damage in RT than in XRT [34, 35]. This was also seen in other studies, where the authors concluded that the differences between continuous low-dose-rate and acute high-dose-rate irradiation are caused by differences in the repair of sublethal and potentially lethal damage [36].

Low-dose-rate irradiation (such as in RIT and also PRRT) has earlier been described to be less effective in cell killing than high-dose-rate irradiation (such as XRT) [35, 37]. However, because in (PR)RT, and also in RIT, radiation is delivered selectively to the tumor(s) and metastases, the radiation dose to the tumor can be much higher than with XRT. This, however, is dependent on factors as affinity of the peptide to its receptor and homogeneity of receptor distribution throughout the tumor. These factors have been excluded from this study.

The possible explanations for the differences in effectiveness of RT versus XRT are dose rate and irradiation period. In RT, the damage to the cells will be lower because of the lower dose rate and irradiation period. In RT, the damage to the cells will be lower because of the lower dose rate, and more repair time is allowed [28, 29, 36, 38]. Despite the fact that RT is less efficient at higher doses than XRT, our PRRT results were very promising. When using ^{177}Lu-DOTA-Tyr^3-octreotate in CA20948 tumor-bearing rats a 100% cure rate could be achieved [1]. Also in patients, this radiolabeled compound is very successful, because the effects of therapy showed that 3% and 35% of the patients had a compete or partial response, respectively [39]. This success of ^{177}Lu-octreotate can be explained by a high-receptor density on tumor cells and a very high affinity of the radiolabeled peptide to the receptor.

Deacon et al. [34] published a report in which they compared the surviving fraction at 2 Gy (SF_2) of 51 human tumor cell lines. The mean SF_2 was calculated to discriminate between radioresistant and radiosensitive tumor cell lines. The cell lines were classified in category A-E, according to their clinical radioresponsiveness—with category A being radiosensitive with a mean SF_2 of 0.187 and category E being radioresistant with a mean SF_2 of 0.518 [34]. The latter SF_2 is similar to that calculated for the CA20948. Therefore, we can conclude that the CA20948 cell line we use in our *in vivo* PRRT studies was not radiosensitive. Also, Deacon t al. concluded that a positive correlation exists between the steepness of the initial portion of the cell-survival curve after XRT *in vitro* and the clinical radioresponsiveness of the tumor.

CONCLUSION

In conclusion, we have shown that the CA20948 cell line is relatively radioresistant, and is more sensitive to XRT than to RT at high doses of 3-10 Gy in an *in vitro* clonogenic survival assay. However, RT and XRT are approximately equally toxic at lower doses.

REFERENCES

1. de Jong M, Breeman WA, Bernard BF, Bakker WH, Schaar M, van Gameren A, Bugaj JE, Erion J, Schmidt M, Srinivasan A, Krenning EP. [177Lu-DOTA(0),Tyr3] octreotate for somatostatin receptor-targeted radionuclide therapy. *Int J Cancer* 2001;92:628-633.
2. de Jong M, Breeman WA, Bernard BF, van Gameren A, de Bruin E, Bakker WH, van der Pluijm ME, Visser TJ, Macke HR, Krenning EP. Tumour uptake of the radiolabelled somatostatin analogue [DOTA0, TYR3]octreotide is dependent on the peptide amount. *Eur J Nucl Med* 1999;26:693-698.
3. De Jong M, Valkema R, Jamar F, Kvols LK, Kwekkeboom DJ, Breeman WA, Bakker WH, Smith C, Pauwels S, Krenning EP. Somatostatin receptor-targeted radionuclide therapy of tumors: preclinical and clinical findings. *Semin Nucl Med* 2002;32:133-140.
4. Kwekkeboom D, Krenning EP, de Jong M. Peptide receptor imaging and therapy. *J Nucl Med* 2000;41:1704-1713.
5. Achilefu S, Dorshow RB, Bugaj JE, Rajagopalan R. Novel receptor-targeted fluorescent contrast agents for in vivo tumor imaging. *Invest Radiol* 2000;35:479-485.
6. Bernard BF, Krenning E, Breeman WA, Visser TJ, Bakker WH, Srinivasan A, de Jong M. Use of the rat pancreatic CA20948 cell line for the comparison of radiolabelled peptides for receptor-targeted scintigraphy and radionuclide therapy. *Nucl Med Commun* 2000;21:1079-1085.
7. Bugaj JE, Erion JL, Johnson MA, Schmidt MA, Srinivasan A. Radiotherapeutic efficacy of (153)Sm-CMDTPA-Tyr(3)-octreotate in tumor-bearing rats. *Nucl Med Biol* 2001;28:327-334.
8. de Jong M, Breeman WA, Bernard BF, Bakker WH, Visser TJ, Kooij PP, van Gameren A, Krenning EP. Tumor response after [(90)Y-DOTA(0),Tyr(3)] octreotide radionuclide therapy in a transplantable rat tumor model is dependent on tumor size. *J Nucl Med* 2001;42:1841-1846.
9. Lewis JS, Laforest R, Lewis MR, Anderson CJ. Comparative dosimetry of copper-64 and yttrium-90-labeled somatostatin analogs in a tumor-bearing rat model. *Cancer Biother Radiopharm* 2000;15:593-604.
10. Lewis JS, Wang M, Laforest R, Wang F, Erion JL, Bugaj JE, Srinivasan A, Anderson CJ. Toxicity and dosimetry of (177)Lu-DOTA-Y3-octreotate in a rat model. *Int J Cancer* 2001;94:873-877.
11. Vallabhajosula S, Moyer BR, Lister-James J, McBride BJ, Lipszyc H, Lee H, Bastidas D, Dean RT. Preclinical evaluation of technetium-99m-labeled somatostatin receptor-binding peptides. *J Nucl Med* 1996;37:1016-1022.
12. van Hagen PM, Breeman WA, Bernard HF, Schaar M, Mooij CM, Srinivasan A, Schmidt MA, Krenning EP, de Jong M. Evaluation of a radiolabelled cyclic DTPA-RGD analogue for tumour imaging and radionuclide therapy. *Int J Cancer* 2000;90:186-198.
13. Breeman WA, Hofland LJ, de Jong M, Bernard BF, Srinivasan A, Kwekkeboom DJ, Visser TJ, Krenning EP. Evaluation of radiolabelled bombesin analogues for receptor-targeted scintigraphy and radiotherapy. *Int J Cancer* 1999;81:658-665.
14. Behr TM, Behe MP. Cholecystokinin-B/Gastrin receptor-targeting peptides for staging and therapy of medullary thyroid cancer and other cholecystokinin-B receptor-expressing malignancies. *Semin Nucl Med* 2002;32:97-109.
15. Markwalder R, Reubi JC. Gastrin-releasing peptide receptors in the human prostate: relation to neoplastic transformation. *Cancer Res* 1999;59:1152-1159.

16. Mantyh CR, Gates TS, Zimmerman RP, Welton ML, Passaro EP, Jr., Vigna SR, Maggio JE, Kruger L, Mantyh PW. Receptor binding sites for substance P, but not substance K or neuromedin K, are expressed in high concentrations by arterioles, venules, and lymph nodules in surgical specimens obtained from patients with ulcerative colitis and Crohn disease. *Proc Natl Acad Sci U S A* 1988;85:3235-3239.
17. Haubner R, Wester HJ, Burkhart F, Senekowitsch-Schmidtke R, Weber W, Goodman SL, Kessler H, Schwaiger M. Glycosylated RGD-containing peptides: tracer for tumor targeting and angiogenesis imaging with improved biokinetics. *J Nucl Med* 2001;42:326-336.
18. DeNardo SJ, Burke PA, Leigh BR, O'Donnell RT, Miers LA, Kroger LA, Goodman SL, Matzku S, Jonczyk A, Lamborn KR, DeNardo GL. Neovascular targeting with cyclic RGD peptide (cRGDf-ACHA) to enhance delivery of radioimmunotherapy. *Cancer Biother Radiopharm* 2000;15:71-79.
19. Capello A, Krenning EP, Breeman WA, Bernard BF, de Jong M. Peptide receptor radionuclide therapy in vitro using [111In- DTPA0]octreotide. *J Nucl Med* 2003;44:98-104.
20. Hall EJ. radiobiology for the radiologist, 5th ed.. Philadelphia: Lippincot Williams & Wilkins. 2000;478.
21. Briestmeister JF. MCNP-A genral Monte Carlo N-particle transport code, version 4C. 2000.
22. Eckerman KF, Westfall RJ, Ryman JC, Cristy M. Availability of nuclear decay data in electronic form, including beta spectra not previously published. *Health Phys* 1994;67:338-345.
23. van den Aardweg GJ, Naus NC, Verhoeven AC, de Klein A, Luyten GP. Cellular radiosensitivity of primary and metastatic human uveal melanoma cell lines. *Invest Ophthalmol Vis Sci* 2002;43:2561-2565.
24. Skehan P, Storeng R, Scudiero D, Monks A, McMahon J, Vistica D, Warren JT, Bokesch H, Kenney S, Boyd MR. New colorimetric cytotoxicity assay for anticancer-drug screening. *J Natl Cancer Inst* 1990;82:1107-1112.
25. Breeman WA, Hofland LJ, van der Pluijm M, van Koetsveld PM, de Jong M, Setyono-Han B, Bakker WH, Kwekkeboom DJ, Visser TJ, Lamberts SW. A new radiolabelled somatostatin analogue [111In-DTPA-D-Phe1]RC-160: preparation, biological activity, receptor scintigraphy in rats and comparison with [111In-DTPA-D-Phe1]octreotide. *Eur J Nucl Med* 1994;21:328-335.
26. de Jong M, Bakker WH, Bernard BF, Valkema R, Kwekkeboom DJ, Reubi JC, Srinivasan A, Schmidt M, Krenning EP. Preclinical and initial clinical evaluation of 111In-labeled nonsulfated CCK8 analog: a peptide for CCK-B receptor-targeted scintigraphy and radionuclide therapy. *J Nucl Med* 1999;40:2081-2087.
27. Lewis JS, Lewis MR, Srinivasan A, Schmidt MA, Wang J, Anderson CJ. Comparison of four 64Cu-labeled somatostatin analogues in vitro and in a tumor-bearing rat model: evaluation of new derivatives for positron emission tomography imaging and targeted radiotherapy. *J Med Chem* 1999;42:1341-1347.
28. Langmuir VK, Fowler JF, Knox SJ, Wessels BW, Sutherland RM, Wong JY. Radiobiology of radiolabeled antibody therapy as applied to tumor dosimetry. *Med Phys* 1993;20:601-610.
29. Buras RR, Wong JY, Kuhn JA, Beatty BG, Williams LE, Wanek PM, Beatty JD. Comparison of radioimmunotherapy and external beam radiotherapy in colon cancer xenografts. *Int J Radiat Oncol Biol Phys* 1993;25:473-479.

30. Roberson PL, Buchsbaum DJ. Reconciliation of tumor dose response to external beam radiotherapy versus radioimmunotherapy with 131iodine-labeled antibody for a colon cancer model. *Cancer Res* 1995;55:5811s-5816s.
31. Joiner MC, Marples B, Lambin P, Short SC, Turesson I. Low-dose hypersensitivity: current status and possible mechanisms. *Int J Radiat Oncol Biol Phys* 2001;49:379-389.
32. Mitchell CR, Folkard M, Joiner MC. Effects of exposure to low-dose-rate (60)co gamma rays on human tumor cells in vitro. *Radiat Res* 2002;158:311-318.
33. Collis SJ, Sangar VK, Tighe A, Roberts SA, Clarke NW, Hendry JH, Margison GP. Development of a novel rapid assay to assess the fidelity of DNA double-strand-break repair in human tumour cells. *Nucleic Acids Res* 2002;30:E1.
34. Deacon J, Peckham MJ, Steel GG. The radioresponsiveness of human tumours and the initial slope of the cell survival curve. *Radiother Oncol* 1984;2:317-323.
35. Ning S, Trisler K, Wessels BW, Knox SJ. Radiobiologic studies of radioimmunotherapy and external beam radiotherapy in vitro and in vivo in human renal cell carcinoma xenografts. *Cancer* 1997;80:2519-2528.
36. Morton J, Yabuki H, Porter EA, Rockwell S, Nath R. Relative biological effectiveness of 241Am relative to 192Ir for continuous low-dose-rate irradiation of BA1112 rat sarcomas. *Radiat Res* 1989;119:478-488.
37. Fowler JF. Radiobiological aspects of low dose rates in radioimmunotherapy. *Int J Radiat Oncol Biol Phys* 1990;18:1261-1269.
38. Dale RG. Dose-rate effects in targeted radiotherapy. *Phys Med Biol* 1996;41:1871-1884.
39. Kwekkeboom DJ, Bakker WH, Kam BL, Teunissen JJ, Kooij PP, de Herder WW, Feelders RA, van Eijck CH, de Jong M, Srinivasan A, Erion JL, Krenning EP. Treatment of patients with gastro-entero-pancreatic (GEP) tumours with the novel radiolabelled somatostatin analogue [177Lu-DOTA(0),Tyr3]octreotate. *Eur J Nucl Med Mol Imaging* 2003;30:417-422.

CHAPTER 3

RADIONUCLIDE THERAPY WITH ^{111}In-LABELED PEPTIDES

3.1 Peptide Receptor Radionuclide Therapy in vitro using ^{111}In-DTPA-octreotide

Astrid Capello, Eric Krenning, Wout Breeman, Bert Bernard, and Marion de Jong.

Journal of Nuclear Medicine, 2003, 44 (1): 98-104.

ABSTRACT

Peptide receptor radionuclide therapy (PRRT) using ^{111}In-DTPA-octreotide (where DTPA is diethylene-triamine-penta-acetic acid) is feasible because, besides γ-radiation, ^{111}In emits both therapeutic Auger and internal conversion electrons having a tissue penetration of 0.02-10 μm and 200-500 μm, respectively. The aim of this study was to investigate the therapeutic effects of ^{111}In-DTPA-octreotide in a single-cell model including the effects of incubation time, radiation dose, and specific activity of ^{111}In-DTPA-octreotide. Finally, we discriminated between the effects of the Auger electrons and internal conversion electrons in PRRT. **Methods:** An in vitro, colony-forming assay to study cell survival after PRRT using the sst subtype 2-positive rat pancreatic tumor cell line CA20948 was developed. **Results:** In this in vitro system ^{111}In-DTPA-octreotide can control tumor growth to 0% survival, and the effects were dependent on incubation time, radiation dose, and specific activity used. Similar concentrations of ^{111}In-DTPA, which is not internalized into sst-positive tumor cells like ^{111}In-DTPA-octreotide, did not influence tumor survival. Excess unlabeled octreotide (10^{-6} M) could decrease tumor cell survival to 60% of control; the addition of radiolabeled peptide (^{111}In-DTPA-octreotide [10^{-9} M] + 10^{-6} M octreotide) did not further decrease survival. **Conclusion:** These in vitro studies show that the therapeutic effect of ^{111}In is dependent on internalization, enabling the Auger electrons with their very short particle range to reach the nucleus. Our results also indicate that the PRRT-effects were receptor-mediated.

INTRODUCTION

Somatostatin receptors are present in normal tissues, such as pancreas, anterior pituitary and brain. Many tumors, such as endocrine pancreatic tumors, carcinoids, paragangliomas, pheochromocytomas, small cell lung cancer, brain tumors, and breast cancer, express an increased number of somatostatin receptors [1]. At present, 5 somatostatin receptor subtypes (sst_1-sst_5) have been identified. All somatostatin receptors are G-protein coupled and belong to the 7-transmembrane receptor family [2]. All subtypes bind somatostatin with high affinity, whereas the affinity of the more stable somatostatin analogs, such as octreotide, differs considerably. Octreotide binds with high affinity to the sst_2, whereas this analogue has a moderate affinity for sst_3 and sst_5 and shows no binding to sst_1 and sst_4 [2-5]. Peptide receptor scintigraphy with the radioactive somatostatin analogue ^{111}In-DTPA-octreotide (where DTPA is diethylene-triamine-penta-acetic acid) is widely used to visualize sst_2-positive tumors in vivo. The method has now been accepted as an important tool for staging and localization of neuroendocrine tumors [6]. Octreotide scintigraphy is therefore based on the visualization of octreotide-binding somatostatin receptor(s), most probably the sst_2.

A new and fascinating application of radiolabeled somatostatin analogs, such as ^{111}In-DTPA-octreotide is their use in peptide receptor radionuclide therapy (PRRT). ^{111}In not only emits γ-rays, which can be visualized, but also therapeutic Auger and internal conversion electrons with a medium-to-short tissue penetration (0.02-10 and 200-550 μm, respectively). The success of this therapeutic strategy relies on the concentration of the radioligand within tumor cells, which will depend on, for example, the rates of internalization, degradation and recycling of both ligand and receptor. Binding of several peptide hormones to specific surface receptors is generally followed by internalization of the ligand-receptor complex via invagination of the plasma membrane [7]. We have studied internalization of radiolabeled ^{111}In-DTPA-octreotide in somatostatin receptor-positive rat pancreatic tumor cell lines and detected internalization of the radiopharmaceutical in vitro [8], in accordance with Andersson et al. [9], and found that this process was receptor specific and temperature dependent. The resulting intracellular vesicles, termed endosomes, rapidly acidify, thus causing dissociation of the ligand from the receptor. Subsequently, the radiopharmaceutical ^{111}In-DTPA-octreotide is degraded in the lysosomes to the radiolabeled metabolite ^{111}In-DTPA-D-Phe [10]. This metabolite is not capable of passing the lysosomal or other cell membrane(s), and will therefore stay in the lysosomes, causing the long retention time of ^{111}In in sst_2-positive (tumor) cells. Receptor-mediated endocytosis of radiolabeled somatostatin analogs is especially important when radionuclide therapy is considered using radionuclides emitting therapeutical particles with very short pathlengths, such as those emitting Auger electrons (e.g., ^{111}In) [11, 12]. These electrons are only effective in a short distance of a few nanometers up to micrometers form their target, DNA.

^{111}In-DTPA-octreotide has been used for radionuclide therapy in preclinical studies where it effectively inhibited tumor growth in a flank and liver tumor model [13, 14]. Peptide receptor radionuclide therapy with ^{111}In-DTPA-octreotide has also been performed in patients with somatostatin receptor-positive tumors and showed a tendency towards better results in patients whose tumors had a higher accumulation of the radioligand [15-18].

Given the fact that ^{111}In emits both therapeutic Auger and internal conversion electrons we investigated, in this study we investigated which electrons are responsible for the described antiproliferative effects. Most Auger electrons have an energy of <30 keV and a very short pathlength (0.02-10 μm) in tissues. Thus, Auger electrons can exert their radiotoxic effects on cells only when internalized into the cytoplasm and particularly when they are near the cell nucleus [19]. High doses of radiation delivered to the cell nucleus from internalized Auger electrons are able to cause cell death [20]. Conversion electrons have a tissue penetration of 200-500 μm, so they do not have to be internalized into the cell to reach the cell nucleus. To investigate the therapeutic effects of ^{111}In-DTPA-octreotide and to discriminate between the effects of the short-range Auger electrons and longer-range internal conversion electrons we developed an in vitro colony-forming assay to study cell survival after PRRT using the rat pancreatic tumor cell line CA20948. The effects of incubation time, radiation dose and, specific activity were investigated in this system. CA20948 cells were incubated with ^{111}In-DTPA-octreotide (internalized) versus ^{111}In-DTPA (not internalized) to discriminate between the effects of the short-range Auger electrons and longer-range internal conversion electrons.

MATERIALS AND METHODS

Radiolabeled peptides

DTPA-octreotide and $^{111}InCl_3$ (DRN 4901, 370 MBq/mL in HCl, pH = 1.5 - 1.9) were obtained from Mallinckrodt Medical BV (Petten, The Netherlands). DTPA-octreotide was labeled with $^{111}InCl_3$ as described [21].

Cell culture

CA20948 rat pancreatic tumor cells were grown in Dulbecco's modified Eagle's medium (DMEM) (Gibco BRL, Grand Island, NY). Medium was supplemented with 10% fetal calf serum, 2 mM glutamine, 1 mM sodium pyruvate, 0.1 mg/L fungizone and 50 IU/mL penicillin/streptomycin.

Internalization studies

One day before the experiment cells were transferred to 6 well plates. Different cell concentrations (200-10,000 cells per well) were used. The cells were washed with 2 mL phosphate-buffered saline (PBS) (37°C) and incubated in 1 mL incubation medium (RPMI-1640 medium [Gibco BRL] supplemented with 1% bovine serum albumin and 20 mM Hepes) with 40 kBq/mL radiotracer for 1 hour at 37°C. Peptide concentrations were between 10^{-10} M and 10^{-8} M. To determine nonspecific internalization, cells were incubated with an excess of

unlabeled peptide (10^{-6}M octreotide). Cellular uptake was stopped by removing medium from the cells, followed by washing twice with 2 mL PBS. To discriminate between internalized and not internalized (surface bound) radiopharmaceutical, intact cells were incubated with 1 mL 20 mM sodium acetate (pH=5), as described [8].

Internalization of ^{111}In-DTPA-octreotide versus ^{111}In-DTPA. CA20948 cells were incubated for 1 hour with 40 kBq/mL ^{111}In-DTPA-octreotide (5×10^{-10} M) or 40 kBq/mL ^{111}In-DTPA. To determine nonspecific internalization, cells were incubated with 5×10^{-10} M ^{111}In-DTPA-octreotide plus 10^{-6} M unlabeled octreotide.

Determination of internalized ^{111}In-DTPA-octreotide in increasing cell concentrations directly after 1 hour and after culturing for 72 hours. CA20948 cells (200-10,000 cells per well) were incubated with ^{111}In-DTPA-octreotide for 1 h; thereafter, the amount of internalized and membrane-bound radioactivity was determined in some wells. Other wells were washed with PBS followed by cultured for another 72 h in growth medium. After these 72 h, the amount of internalized and membrane-bound radioactivity was determined.

PRRT in vitro with ^{111}In-DTPA-octreotide

One day before the experiment cells were transferred to 6 well plates in a density of 200 cells per well. Cells were washed with PBS (37°C) and incubated for at least 1 h in 1 mL incubation medium (RPMI-1640 medium without fetal calf serum but with 1% bovine serum albumin and 20 mM HEPES) containing ^{111}In-DTPA-octreotide. Control cells received only incubation medium for 1 h. Thereafter, cells were thoroughly washed with PBS and allowed to form colonies during 10 d in growth medium (based on the method of Puck and Marcus [22, 23]). The medium was refreshed once after 72 h.

After the 10-d recovery the cells were fixated with 1 mL methanol:glacial acid (3:1) for 15 minutes. Subsequently the cells were stained with haematoxylin. Colonies that contained >50 cells per colony were scored as survivors.

PRRT using ^{111}In-DTPA-octreotide, effects of incubation time, concentration, and specific activity. CA20948 cells were incubated for 1, 3 and 5 h with ^{111}In-DTPA-octreotide. In this experiment 2 different specific activities were used.

Effects of ^{111}In-DTPA and low amounts of octreotide. CA20948 cells were incubated for 1 h with 0.5 µg octreotide and 370 MBq ^{111}In-DTPA and compared with cells incubated with (0.5 µg) 370 MBq ^{111}In-DTPA-octreotide. The amount of ^{111}In that is normally attached to the cells after 1-h incubation with ^{111}In-DTPA-octreotide (internalization experiment) was added to the medium after the 1-h incubation. This amount of ^{111}In-DTPA was also added when the medium was refreshed after 3 days.

PRRT with ^{111}In-DTPA-octreotide plus excess amount of unlabeled octreotide. CA20948 cells were incubated with ^{111}In-DTPA-octreotide for 1 h as described. In the medium 10^{-6} M octreotide was added. Control cells were also incubated with 10^{-6} M octreotide.

RESULTS

Internalization studies

Figure 1 shows the internalization of ^{111}In-DTPA-octreotide and ^{111}In-DTPA after 1-h incubation. Cells were also incubated with an excess of octreotide (10^{-6} M) to determine nonspecific internalization. The percentage of the dose that is internalized is approximately 0.06; the noninternalized radioactivity represented <10% of the total cellular uptake. Figure 1 shows that ^{111}In-DTPA is much less internalized into the cells compared with that of ^{111}In-DTPA-octreotide.

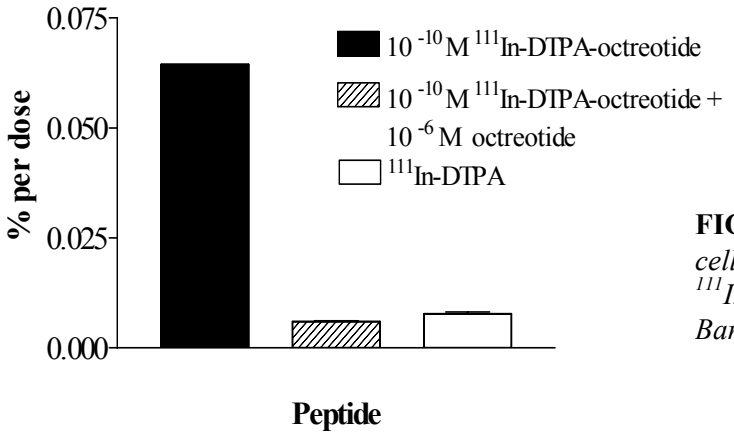

FIGURE 1. *Internalization in CA20948 cells after 1-h incubation at 37°C with ^{111}In-DTPA-octreotide and ^{111}In-DTPA. Bars represent mean ± SEM.*

To investigate the PRRT effects of the internalized radioactivity, and not of radioactivity in the medium, a short incubation time in the medium and a low number of cells per well were necessary, the latter to rule out the option of crossfire between cells. In our PRRT studies with ^{111}In-DTPA-octreotide in vitro, we incubated 200 cells per well for 1 h. In this way the distance between the cells is 1.2 mm (the surface of a well in a 6-well plate is 9.62 cm^2; 962 mm^2/200 = 4.81 mm^2 per cell; $\pi r^2 = 4.81$; $r^2 = 1.5$ mm; r = 1.2 mm), this is longer than the maximum pathlength of conversion electrons, which is 200-500 μm, which rules out the option of crossfire between the cells when distributed equally in the well.

The cells were incubated for 1 h with ^{111}In-DTPA-octreotide and after 3 d the medium was refreshed. We determined how much radioactivity is internalized in the cells directly after 1-h incubation and also after 72 h in growth medium to be able to mimic the PRRT experiments with ^{111}In-DTPA-octreotide with a similar amount of ^{111}In-DTPA in the medium.

To determine whether internalization of ^{111}In-DTPA-octreotide is dependent on the cell number in the wells we performed experiments using an increasing cell concentration (range, 200-10,000 cells/well). Figure 2A shows the amount of internalized counts per minute after 72 h with an increasing amount of ^{111}In-DTPA-octreotide (specific activity is kept constant). Figure 2A also demonstrates that when more cells are used, at constant radioactivity, more radioactivity is internalized. It also shows that when more radioactivity is used, at constant cell concentration, more radioactivity is internalized into the cells. In figure 2B the amount of ^{111}In-DTPA-octreotide that is internalized into the cells is expressed as

percentage of the dose. This shows that more or less the same percentage of the dose is internalized into the cells, which is for 200 cells/well approximately 0.003% of the dose for 200 cells per well. Directly after the 1-h incubation this percentage is higher—namely, 0.03 % of the dose.

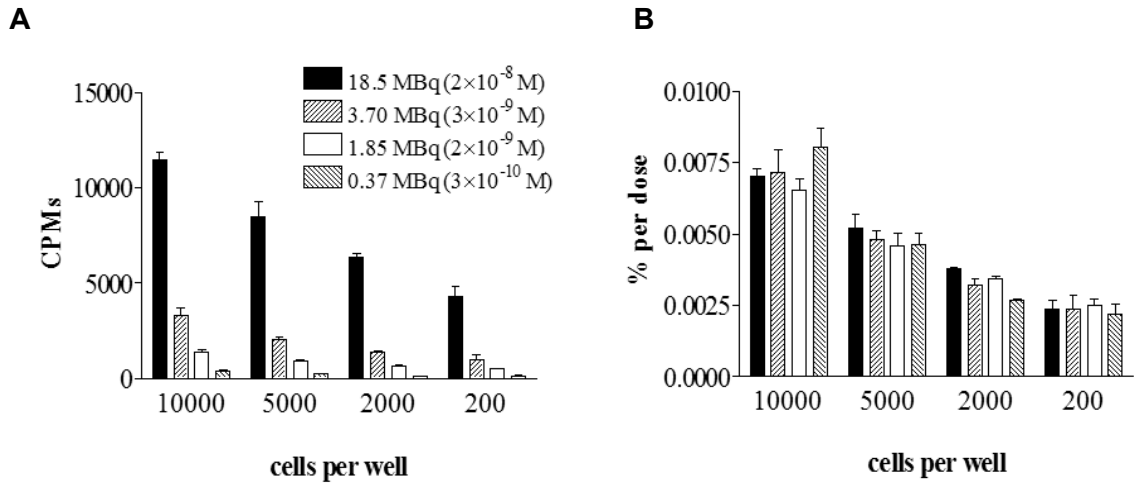

FIGURE 2. *Amount of internalized ^{111}In-DTPA-octreotide after 72 h in growth medium with 200-10,000 cells per well. Cells were incubated for 1 h at 37°C with increasing concentrations of ^{111}In-DTPA-octreotide. Amount of internalized ^{111}In-DTPA-octreotide was determined after 72 h. (A) Amount of internalized counts per minute. (B) Internalized amount presented as percentage of given dose. Bars represent mean ± SEM.*

PRRT in vitro with ^{111}In-DTPA-octreotide

Figure 3 shows the percentage of tumor cell survival of the CA20948 cell line after treatment with 3.7 MBq/10^{-8} M (Fig. 3A), 3.7 MBq/10^{-7} M (Fig. 3B) and 37 MBq/10^{-7} M (Fig. 3C) ^{111}In-DTPA-octreotide for 1, 3 and 5 h. Survival values are shown as percentage survival compared with that of the control cells (no peptide added). Figures 3A and 3B share the same amount of radioactivity, but the latter one has a 10 times higher peptide amount, so a lower specific activity. Figure 3B and 3C share the same amount of peptide, but the latter has a 10 times higher radioactivity, so a higher specific activity. Figures 3A and 3C share the same specific activity. When the tumor cell survival of Figures 3A and 3B is compared, Figure 3B shows a higher tumor cell survival than that of Figure 3A, despite the same amount of radioactivity that is used. Figure 3 also shows a time- and dose-dependent inhibition of the colony growth: When cells were incubated for 5 h with the highest concentration used, survival is virtually zero. Because the 1-h incubation time already shows a clear inhibition of the clonogenic cell survival we continued with a 1-h incubation time.

The same experiment was performed with a higher specific activity of ^{111}In-DTPA-octreotide, 370 MBq/0.5 µg. As is shown in Figure 4 CA20948 cells were incubated for 1 h with 18.5, 3.7, 1.85 and 0.37 MBq ^{111}In-DTPA-octreotide. The control cells received incubation medium without ^{111}In-DTPA-octreotide for 1 h. Figure 4 shows less tumor cell survival when a higher concentration of ^{111}In-DTPA-octreotide is used, indicating a clear dose-dependent relation.

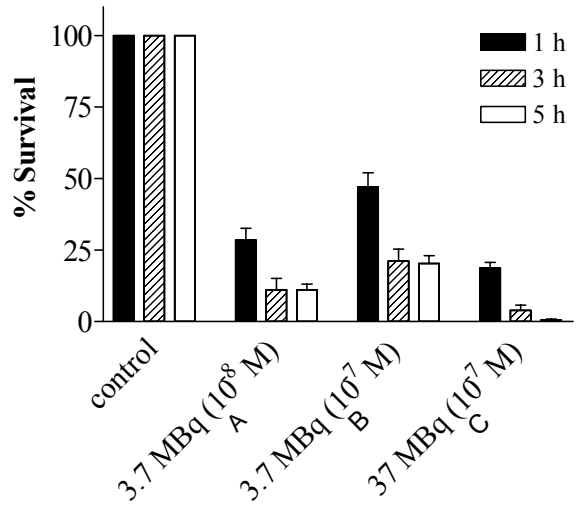

FIGURE 3. *Effects of incubation time, concentration, and specific activity of ^{111}In-DTPA-octreotide on cell survival of CA20948 cells after PRRT. Cells were incubated for 1, 3 and 5 h with 0.37 or 3.7 MBq ^{111}In-DTPA-octreotide at 37°C using two different specific activities (specific activity of B is different from that of A and C). Bars represent mean ± SEM.*

Effects of ^{111}In-DTPA and low amounts of octreotide. To investigate whether Auger or conversion electrons emitted by ^{111}In-DTPA-octreotide were responsible for the inhibitory effect, CA20948 cells were exposed to increasing concentrations of ^{111}In-DTPA for 1 h, the same concentrations as used for ^{111}In-DTPA-octreotide (Fig. 4). Because ^{111}In-DTPA is internalized (Fig. 1) to a much lesser extent than ^{111}In-DTPA-octreotide, the amount of radioactivity from ^{111}In-DTPA-octreotide that is normally internalized into the cells is added to the medium as ^{111}In-DTPA after the 1-h incubation and also after 3 d, when the medium is normally refreshed (Fig. 2). Figure 5A clearly shows that there is no difference in tumor cell survival compared to the control, when CA20948 cells are incubated with an increasing amount of ^{111}In-DTPA. Thus, ^{111}In-DTPA does not have an effect on the tumor cell survival. Because it is known that octreotide alone can have an inhibitory effect on the cell survival we also incubated the CA20948 cells with octreotide, again the same concentration that is used with ^{111}In-DTPA-octreotide (Fig. 4). Figure 3B shows that when CA20948 cells are incubated with low amounts of octreotide (10^{-10} M to 10^{-8} M) for 1 h there might be a slight inhibition of the tumor cell survival (≈5%).

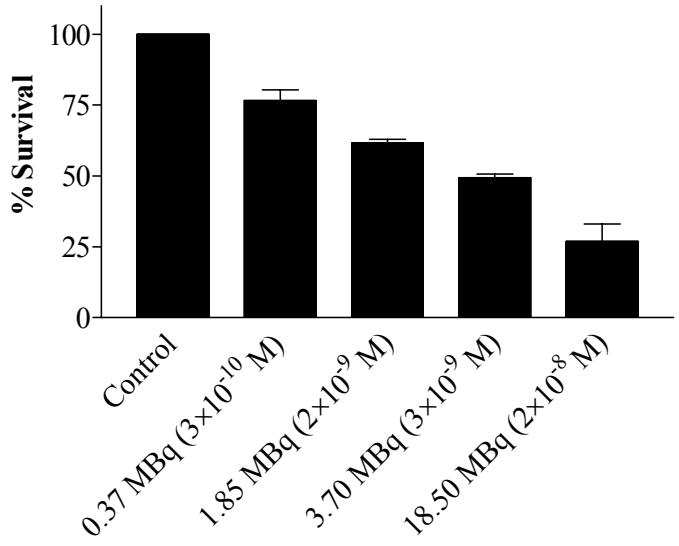

FIGURE 4. *Inhibitory effect of ^{111}In-DTPA-octreotide on clonogenic cell survival of rat pancreatic tumor cell line CA20948. Cells were incubated for 1h at 37°C with increasing amount of ^{111}In-DTPA-octreotide. Bars represent mean ± SEM.*

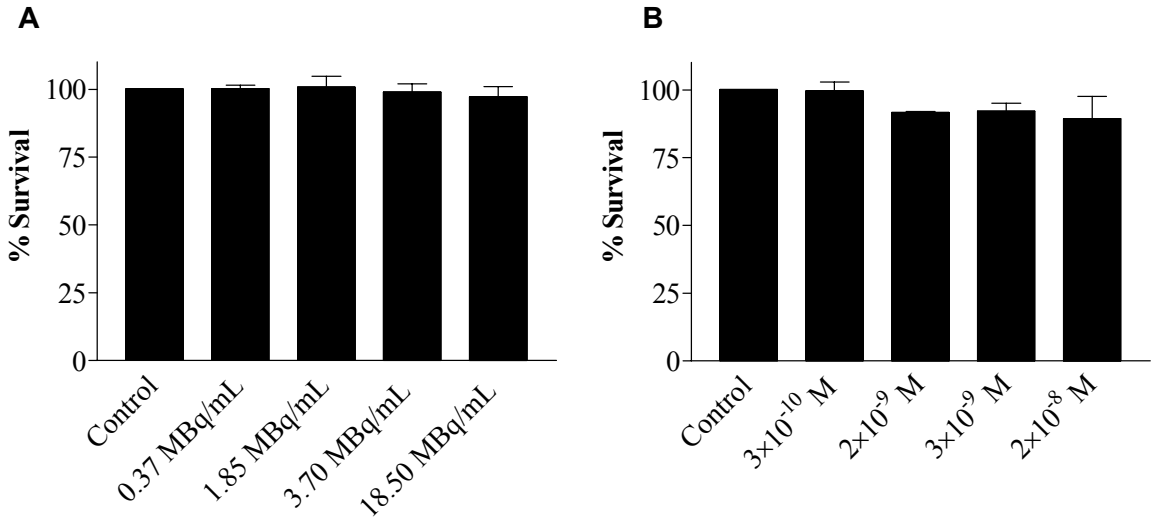

FIGURE 5. *Effect of ^{111}In-DTPA (A) and octreotide (B) on clonogenic cell survival of CA20948 cells. The cells were incubated for 1 h in increasing amount of ^{111}In-DTPA (the same was given as was used with ^{111}In-DTPA-octreotide [Fig. 4]). Amount of radioactivity that is normally attached to the cells was added to medium after 1-h incubation time. ^{111}In-DTPA was also added when medium was refreshed after 3 d. Bars represent mean ± SEM.*

PRRT with ^{111}In-DTPA-octreotide plus excess amount of unlabeled octreotide. Figure 6 shows the effect of ^{111}In-DTPA-octreotide incubated together with an excess (10^{-6} M) of unlabeled octreotide. The cells were incubated with the same amount of ^{111}In-DTPA-octreotide as used previously. In this way the receptors are occupied with octreotide and ^{111}In-DTPA-octreotide is not internalized into the cells. Figure 6 shows that a high amount of octreotide alone gives an inhibition of ≈30% on the tumor cell survival. When cells were incubated with 10^{-6} M octreotide together with ^{111}In-DTPA-octreotide there is no further reduction seen of the tumor cell survival compared with only 10^{-6} M octreotide.

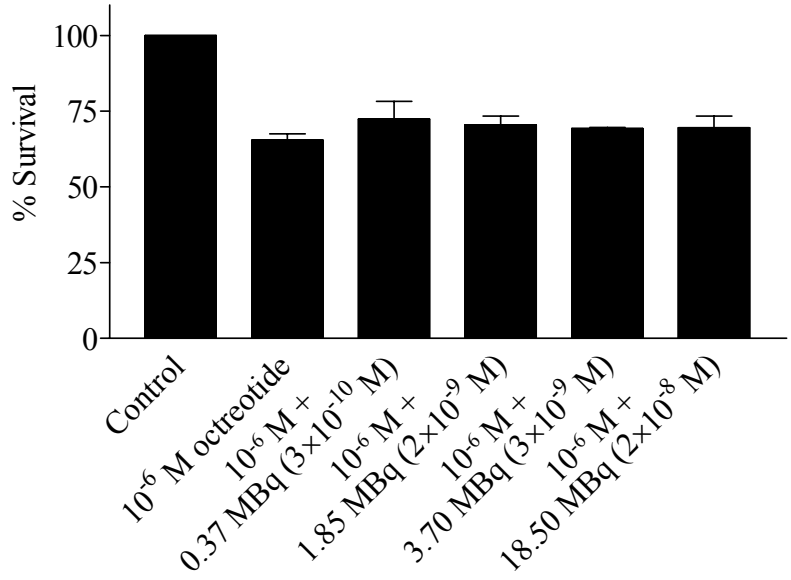

FIGURE 6. *Inhibitory effect of octreotide on tumor cell survival of CA20948 cell line. Cells were incubated for 1 h at 37°C with 10^{-6} M octreotide (second bar from left) and cells were incubated with 10^{-6} M octreotide plus increasing amount of ^{111}In-DTPA-octreotide (third to fifth bars from left). Bars represent mean ± SEM.*

DISCUSSION

Peptide receptor scintigraphy with the radioactive somatostatin analogue ^{111}In-DTPA-octreotide is widely used to visualize sst-positive tumors in vivo. Besides γ-radiation, ^{111}In emits also both therapeutic Auger and internal conversion electrons; therefore, a new application of ^{111}In-DTPA-octreotide is PRRT.

In preclinical studies on rats, different experiments with ^{111}In-DTPA-octreotide were performed by determining the response of a solid octreotide receptor-positive tumor (CA20948) inoculated in the flank [13]. For ^{111}In-DTPA-octreotide a dose-response was found, leading in rats bearing small tumors (<1 cm^2) to 50% cure after the highest dose (3 injections of 370 MBq, given with an interval of 1 wk), whereas in rats bearing large tumors (>10 cm^2) only a partial response could be achieved. In larger tumors, more clonogenic, presumably

hypoxic, cells will be present, thereby limiting radiocurability. So, ^{111}In is more suitable for smaller rather than large tumors. This is in agreement with the antiproliferative effects of ^{111}In-DTPA-octreotide found in a rat liver tumor metastases model [14]. Administration of 370 MBq ^{111}In-DTPA-octreotide on day 1 or day 8 after intraportal CA20948 tumor cell inoculation induced a significant decrease in the number hepatic metastases at day 21. These findings show that, after radionuclide therapy, reduction of tumor volume can be obtained because of the radiotherapeutic effect of ^{111}In-octreotide. These findings hold promise for the application of radionuclide therapy with ^{111}In-octreotide in an adjuvant, micrometastatic setting and are consistent with the findings in this study. We showed that ^{111}In-DTPA-octreotide is able to control tumor growth in our single-cell in vitro system of CA20948 cells. Apart from uptake, tumor response is also dependent on radiosensitivity. To determine the radiosensitivity of these tumor cells, we performed external beam radiation experiments. It appeared that CA20948 cells are relative radioresistant, making our results the more interesting.

In this in vitro system we also demonstrated that the Auger electrons emitted by ^{111}In are responsible for the tumor response, not the conversion electrons. Because we use only 200 cells per well in our in vitro system the distance between the cells is 1.2 mm, which rules out the option of crossfire between the cells because the cells are approximately equally distributed in the well.

No tumor cell survival was found after a 5-h incubation time with 37 MBq (coupled to 0.15 μg peptide) ^{111}In-DTPA-octreotide, while we found almost 50% survival with 3.7 MBq (coupled to 0.15 μg peptide) ^{111}In-DTPA-octreotide with a 1-h incubation. When a higher specific activity was used there was less tumor cell survival (Fig. 3). With a higher specific activity more radioactivity is internalized into the cells, leading to a lower tumor cell survival [24]. Thus, the differences in tumor cell survival are dependent on the radiation dose, incubation time, and the specific activity that is used. Because we found a clear effect of ^{111}In-DTPA-octreotide on the tumor cell survival after 1-h incubation, we continued with this short incubation time to investigate the effects of the internalized radioactivity, not of the radioactivity in the medium.

Because ^{111}In emits both Auger and conversion electrons we discriminated between the effects of both electrons by comparing internalized (^{111}In-DTPA-octreotide) versus noninternalized (^{111}In-DTPA) ^{111}In. The effects of the conversion electrons were investigated using ^{111}In-DTPA in the medium; with a tissue penetration of 200-500 μm they could reach the nucleus without being internalized. The results showed a 100% survival in the number of colonies after incubation for 1 h with 18.5 MBq with ^{111}In-DTPA (Fig. 5A) compared with a 30% survival with 18.5 MBq ^{111}In-DTPA-octreotide (Fig 4). McLean and Wilkinson [25] determined the radiation dose to cells in vitro from intracellular ^{111}In. In these experiments, the radiation dose to the cell from the intranuclear decay of ^{111}In was determined from cell survival studies to be 3.5 mGy per decay, using ^{60}Co as a reference radiation. The average dose to the cells from extracellular ^{111}In was calculated to be much lower—that is, 5.8

pGy/decay. So from ^{111}In that remains extracellular, Auger electrons, with their short pathlengths, would have little biological effect. For intracellular ^{111}In, however, the release of Auger electrons into the nucleus or the DNA would have the potential to cause extensive biological damage.

CA20948 cells were incubated with an excess of octreotide (10^{-6} M) together with an increasing amount of ^{111}In-DTPA-octreotide in 1 experiment. The excess of octreotide was used to inhibit the internalization of ^{111}In-DTPA-octreotide. The results show that the excess of octreotide inhibited cell survival with 30%; addition of radiolabeled peptide (^{111}In-DTPA-octreotide [10^{-10} M] + 10^{-6}M octreotide) did not further decrease survival, showing that PRRT effects were sst receptor mediated.

A phase I study using this radioligand on patients with neuroendocrine tumor has started in our center. Fifty patients with somatostatin receptor-positive tumors were treated with multiple doses of ^{111}In-DTPA-octreotide [26]. Forty patients were evaluable after cumulative doses of at least 20 GBq up to 160 GBq. Therapeutic effects were seen in 21 patients: partial remission in 1 patient, minor remissions in 6 patients, and stabilization of previously progressive tumors in 14 patients. All the patients in this study had advanced tumor, and many were end-stage patients with a large tumor burden.

Anthony et al. [27] published a phase II trial on patients with gastroenteropancreatic tumors in which 2 doses (6.66 GBq each) of ^{111}In-DTPA-octreotide were given. It improved symptoms in 62% of the patients, decreased hormonal markers with 81%, decreased Hounsfield units on CT scans in 27% of patients, with 8% partial radiographic responses and increased expected survival in gastroenteropancreatic cancer patients with somatostatin receptor-expressing tumors, showing the promise of this compound in patients with neuroendocrine tumors.

PRRT with β-emitting radionuclides, such as ^{90}Y and ^{177}Lu, can be even more effective because higher tumor radiation doses can be achieved and the longer range of the β-particles, typically 1-10 mm, may cause irradiation of neighboring receptor-negative tumor cells by crossfire. We are currently performing experiments with ^{90}Y- and ^{177}Lu-labeled somatostatin analogs in this in vitro system. In micrometastases or even single tumor cells the absorbed fraction of the radiation energy will be very low especially for ^{90}Y. Recently Bernhardt et al. [28] have calculated with a mathematical model the tumor-to-normal tissue mean absorbed dose ratios (TNDs) for different tumor sizes. The results show that radionuclides suitable for therapy should emit few photons, emit many electrons with moderate energy, and have a rather long half-live (>2 d). In these calculations ^{161}Tb and ^{177}Lu obtained the highest TNDs values. We had promising results with biodistribution studies in rats after administration of ^{161}Tb-DTPA-octreotide [29]. Both of these radionuclides will be of interest for somatostatin receptor-based therapy in the future.

However, in very small lesions PRRT with Auger electron-emitting radiopharmaceuticals may be the best choice. Recently, it was shown that after internalization ^{111}In is translocated to the perinuclear area and into the nucleus [30]; it was also shown that prolonged exposure to radiolabeled somatostatin analogs significantly increases their cellular internalization, nuclear translocation, and DNA binding [31]. Behr et al. [32] demonstrated a

therapeutic advantage of the Auger electron-emitting ^{111}In over the β-emitter ^{90}Y. It was shown that internalizing antibodies labeled with Auger electron-emitting radionuclides, such as ^{125}I and ^{111}In, have encouraging therapeutic results. They cause biological effects similar to those of typical high linear-energy-transfer (LET) radiation, such as α-emitters. Auger electron emitters decaying in the neighborhood of the DNA produce similar amounts of reactive chemical radical species as do α-emitters, which are regarded as the classical form of high LET radiation [32]. So it is conceivable to use ^{111}In-DTPA-octreotide, or other low-energy emitters like ^{161}Tb, ^{58m}Co, ^{103m}Rh, ^{119}Sb and ^{189m}Os, in cocktails combined with β-emitting radionuclides as a neo-adjuvant therapy.

CONCLUSIONS

^{111}In-DTPA-octreotide is able to control tumor growth in this in vitro system; the effects were dependent on radiation dose, incubation time, and specific activity used. An excess of unlabeled octreotide decreased survival to 60% of the control; addition of radiolabeled peptide did not further decrease survival, showing that PRRT was receptor mediated. ^{111}In-DTPA, which is not internalized into sst_2-positive tumor cells like ^{111}In-DTPA-octreotide, did not influence survival, showing that the therapeutic effect of ^{111}In is dependent on internalization, enabling the Auger electrons with their very short particle range, to reach the nucleus.

REFERENCES

1. Reubi JC, Laissue J, Krenning E, Lamberts SW. Somatostatin receptors in human cancer: incidence, characteristics, functional correlates and clinical implications. *J Steroid Biochem Mol Biol* 1992;43:27-35.
2. Patel YC. Somatostatin and its receptor family. *Front Neuroendocrinol* 1999;20:157-198.
3. Patel YC, Greenwood M, Panetta R, Hukovic N, Grigorakis S, Robertson LA, Srikant CB. Molecular biology of somatostatin receptor subtypes. *Metabolism* 1996;45:31-38.
4. Bell GI, Reisine T. Molecular biology of somatostatin receptors. *Trends Neurosci* 1993;16:34-38.
5. Reisine T, Bell GI. Molecular properties of somatostatin receptors. *Neuroscience* 1995;67:777-790.
6. Krenning EP, Kwekkeboom DJ, Pauwels S, Kvols LK, Reubi JC. Somatostain receptor scintigraphy. *Nucl Med Ann* 1995;1:1-50.
7. Schwartz AL, Fridovich SE, Lodish HF. Kinetics of internalization and recycling of the asialoglycoprotein receptor in a hepatoma cell line. *J Biol Chem* 1982;257:4230-4237.
8. De Jong M, Bernard BF, De Bruin E, Van Gameren A, Bakker WH, Visser TJ, Macke HR, Krenning EP. Internalization of radiolabeled [DTPA0]octreotide and [DOTA0,Tyr3]octreotide: peptides for somatostatin receptor-targeted scintigraphy and radionuclide therapy. *Nucl Med Commun* 1998;19:283-288.
9. Andersson P, Forssell-Aronsson E, Johanson V, Wangberg B, Nilsson O, Fjalling M, Ahlman H. Internalization of indium-111 into human neuroendocrine tumor cells after incubation with indium-111-DTPA-D-Phe1-octreotide. *J Nucl Med* 1996;37:2002-2006.
10. Duncan JR, Stephenson MT, Wu HP, Anderson CJ. Indium-111-diethylenetriaminepentaacetic acid-octreotide is delivered in vivo to pancreatic, tumor cell, renal, and hepatocyte lysosomes. *Cancer Res* 1997;57:659-671.
11. Adelstein SJ. Merrill C. Sosman Lecture. The Auger process: a therapeutic promise? *AJR Am J Roentgenol* 1993;160:707-713.
12. McLean JR, Blakey DH, Douglas GR, Bayley J. The Auger electron dosimetry of indium-111 in mammalian cells in vitro. *Radiat Res* 1989;119:205-218.
13. De Jong M, Breeman WA, Bernard HF, Kooij PP, Slooter GD, Van Eijck CH, Kwekkeboom DJ, Valkema R, Macke HR, Krenning EP. Therapy of neuroendocrine tumors with radiolabeled somatostatin- analogues. *Q J Nucl Med* 1999;43:356-366.
14. Slooter GD, Breeman WA, Marquet RL, Krenning EP, van Eijck CH. Anti-proliferative effect of radiolabelled octreotide in a metastases model in rat liver. *Int J Cancer* 1999;81:767-771.
15. Krenning EP, Valkema R, Kooij PP, Breeman WA, Bakker WH, deHerder WW, vanEijck CH, Kwekkeboom DJ, deJong M, Pauwels S. Scintigraphy and radionuclide therapy with [indium-111-labelled-diethyl triamine penta-acetic acid-D-Phe1]-octreotide. *Ital J Gastroenterol Hepatol* 1999;31 Suppl 2:S219-223.
16. Meyers MO, Anthony LB, McCarthy KE, Drouant G, Maloney TJ, Espanan GD, Woltering EA. High-dose indium 111In pentetreotide radiotherapy for metastatic atypical carcinoid tumor. *South Med J* 2000;93:809-811.
17. McCarthy KE, Woltering EA, Anthony LB. In situ radiotherapy with 111In-pentetreotide. State of the art and perspectives. *Q J Nucl Med* 2000;44:88-95.
18. Oberg K. Established clinical use of octreotide and lanreotide in oncology. *Chemotherapy* 2001;47:40-53.

19. Hofer KG, Harris CR, Smith JM. Radiotoxicity of intracellular 67Ga, 125I and 3H. Nuclear versus cytoplasmic radiation effects in murine L1210 leukaemia. *Int J Radiat Biol Relat Stud Phys Chem Med* 1975;28:225-241.
20. Martin RF, Bradley TR, Hodgson GS. Cytotoxicity of an 125I-labeled DNA-binding compound that induces double-stranded DNA breaks. *Cancer Res* 1979;39:3244-3247.
21. Bakker WH, Krenning EP, Reubi JC, Breeman WA, Setyono-Han B, de Jong M, Kooij PP, Bruns C, van Hagen PM, Marbach P, et al. In vivo application of [111In-DTPA-D-Phe1]-octreotide for detection of somatostatin receptor-positive tumors in rats. *Life Sci* 1991;49:1593-1601.
22. Puck TT, Marcus PI. A rapid method for viable cell titration and clone production with HeLa cells in tissue culture: the use of X-irradiated cells to supply conditioning factors. *Proc Nat Acad Sci* 1955;41:432-437.
23. Puck TT, Marcus PI, Cieciura SJ. Clonal growth of mammalian cells in vitro, growth characteristics of colonies from single HeLa cells with and without a "feeder" layer. *J Exp Med* 1955;103:273-289.
24. Breeman WA, Kwekkeboom DJ, Kooij PP, Bakker WH, Hofland LJ, Visser TJ, Ensing GJ, Lamberts SW, Krenning EP. Effect of dose and specific activity on tissue distribution of indium- 111-pentetreotide in rats. *J Nucl Med* 1995;36:623-627.
25. McLean JR, Wilkinson D. The radiation dose to cells in vitro from intracellular indium-111. *Biochem Cell Biol* 1989;67:661-665.
26. Valkema R, De Jong M, Bakker WH, Breeman WA, Kooij PP, Lugtenburg PJ, De Jong FH, Christiansen A, Kam BL, De Herder WW, Stridsberg M, Lindemans J, Ensing G, Krenning EP. Phase I study of peptide receptor radionuclide therapy with [In- DTPA]octreotide: the Rotterdam experience. *Semin Nucl Med* 2002;32:110-122.
27. Anthony LB, Woltering EA, Espenan GD, Cronin MD, Maloney TJ, McCarthy KE. Indium-111-pentetreotide prolongs survival in gastroenteropancreatic malignancies. *Semin Nucl Med* 2002;32:123-132.
28. Bernhardt P, Forssell-Aronsson E, Jacobsson L, Skarnemark G. Low-energy electron emitters for targeted radiotherapy of small tumours. *Acta Oncol* 2001;40:602-608.
29. de Jong M, Breeman WA, Bernard BF, Rolleman EJ, Hofland LJ, Visser TJ, Setyono-Han B, Bakker WH, van der Pluijm ME, Krenning EP. Evaluation in vitro and in rats of 161Tb-DTPA-octreotide, a somatostatin analogue with potential for intraoperative scanning and radiotherapy. *Eur J Nucl Med* 1995;22:608-616.
30. Janson ET, Westlin JE, Ohrvall U, Oberg K, Lukinius A. Nuclear localization of 111In after intravenous injection of [111In- DTPA-D-Phe1]-octreotide in patients with neuroendocrine tumors. *J Nucl Med* 2000;41:1514-1518.
31. Hornick CA, Anthony CT, Hughey S, Gebhardt BM, Espenan GD, Woltering EA. Progressive nuclear translocation of somatostatin analogs. *J Nucl Med* 2000;41:1256-1263.
32. Behr TM, Behe M, Lohr M, Sgouros G, Angerstein C, Wehrmann E, Nebendahl K, Becker W. Therapeutic advantages of Auger electron- over beta-emitting radiometals or radioiodine when conjugated to internalizing antibodies. *Eur J Nucl Med* 2000;27:753-765.

CHAPTER 3

RADIONUCLIDE THERAPY WITH ^{111}In LABELED PEPTIDES

3.2 Effect of peptide receptor radionuclide therapy (PRRT) using ^{111}In-labeled somatostatin analogs in a rat tumor model: relation to somatostatin receptor expression

Astrid Capello, Eric Krenning, Bert Bernard, Jean-Claude Reubi, Wout Breeman and Marion de Jong

Submitted for publication

ABSTRACT

Peptide receptor scintigraphy with the radioactive somatostatin analog ^{111}In-DTPA-octreotide is a sensitive and specific technique to show in vivo the presence of somatostatin receptors on various tumors. Since ^{111}In emits not only gamma-rays, but also therapeutic Auger and internal conversion electrons with a medium to short tissue penetration (0.02-10 μm and 200-550 μm, respectively), ^{111}In-DTPA-octreotide is also being used for peptide receptor radionuclide therapy (PRRT).

In this study we investigated the therapeutic effects of ^{111}In-DTPA-octreotide in tumors of various sizes. Re-grow of a tumor despite PRRT with ^{111}In-DTPA-octreotide can be due to the lack of crossfire of ^{111}In, whereby any possible receptor-negative tumor cell can multiply. We therefore also investigated the somatostatin receptor status on the tumor before and after PRRT.

Therapy (low and high doses) in small and large tumors with ^{111}In-DTPA-octeotide. We investigated the radiotherapeutic effects of different doses of ^{111}In-DTPA-octreotide in vivo in Lewis rats bearing small (≤ 1 cm^2) or larger (≥ 8 cm^2) somatostatin receptor-positive rat pancreatic CA20948 tumors expressing the sst_2 (somatostatin receptor subtype 2). The results show impressive radiotherapeutic effects of ^{111}In-labeled octreotide in this rat tumor model. Complete responses (up to 50%) were found in the animals bearing small (≤ 1 cm^2) tumors after at least three injections of 111 MBq or a single injection of 370 MBq ^{111}In-DTPA-octreotide, leading to a dose of 6.3 – 7.8 mGy/MBq (1 – 10 g tumor). In the rats bearing the larger (≥ 8 cm^2) tumors the effects were much less pronounced and only partial responses were reached in these groups.

Low dose therapy to determine receptor expression. The somatostatin receptor density on the tumor after injection with a therapeutic labeled somatostatin analog was investigated when the tumor was either declining in size or when the tumor re-grew after initial size decline. To initiate a partial response of the tumor (so that re-growth would follow) and not a complete response a relatively low dose was administered. A clear sst_2 expression was found in the control as well as in the treated tumors. In fact, a significantly higher tumor receptor density ($p < 0.001$) was found when the tumors re-grew after an initial decline in size after low dose PRRT in comparison with the untreated tumors.

Conclusion: Therapy with ^{111}In-labeled somatostatin analogs is feasible but should preferably start as early as possible during tumor development. One might also consider the use of radiolabeled somatostatin analogs in an adjuvant setting after surgery of somatostatin receptor-positive tumors to eradicate occult metastases. Finally we showed that PRRT led to an increase in receptor density of somatostatin receptors when the tumors re-grew after an initial decline in size because of PRRT. The upregulation of the somatostatin receptor will lead to a higher uptake of the radiolabeled peptides in therapeutic applications, making repetitions of radiolabeled peptides interesting.

INTRODUCTION

A variety of receptor proteins with high affinity for regulatory peptides, including somatostatin, are expressed on the cellular membranes of cells. Somatostatin receptors are integral membrane glycoproteins, of which at present five somatostatin receptor subtypes (sst_{1-5}) have been cloned. All subtypes bind somatostatin with high affinity, while the more stable analog octreotide binds with high affinity to the somatostatin receptor subtype 2 (sst_2) and with lower affinity to sst_3 and sst_5. It shows no binding to sst_1 and sst_4 [1-5]. Continuing research resulted in the development of the somatostatin analogs Tyr^3-octreotide and Tyr^3-octreotate, in the latter the alcohol Thr(ol) at the C-terminus as used in octreotide is replaced with the natural amino acid Thr. This analog was found to have a very high affinity for the somatostatin receptor subtype 2 (sst_2) and showed the highest uptake in the rat pancreatic CA20948 tumor in a biodistribution study in rats using different ^{111}In-labeled somatostatin analogs [6].

Many tumors, particularly of neuroendocrine origin, express an increased number of somatostatin receptors, which can be visualized by imaging techniques. These somatostatin receptor-positive tumors can be visualized with e.g. ^{111}In-DTPA-octreotide. ^{111}In-DTPA-octreotide is nowadays recognized to be the imaging technique for the localization and staging of somatostatin receptor-positive neuroendocine tumors [7, 8].

Another application is the use of this ^{111}In-labeled somatostatin analog for peptide receptor radionuclide therapy (PRRT). Since ^{111}In emits not only gamma-rays, which are visualized during scintigraphy, but also Auger and conversion electrons, an effect on tumor cell proliferation could be expected. These electrons have a tissue penetration of 0.02 to 10 μm and 200 to 500 μm respectively, so especially the radiotoxicity of Auger electrons is very high if the DNA of the cell is within their particle range [9, 10]. In a previous study we showed that ^{111}In-DTPA-octreotide is able to control tumor growth in a single cell in vitro system [11]. In this in vitro system it was demonstrated that the Auger electrons emitted by ^{111}In are responsible for the anti-tumor response and not the conversion electrons [11].

We reported a biological half-life for ^{111}In of >700 hours in tumor tissue in vivo in patients [7, 8], therefore ^{111}In-labeled DTPA-octreotide has an appropriate distribution profile in humans for scintigraphy and radionuclide therapy. In clinical studies evidence of tumor response to treatment was indeed demonstrated [12-14]. We also reported in an animal model [15] that high radioactive doses of ^{111}In-DTPA-octreotide could inhibit the growth of somatostatin receptor-positive liver metastases; the therapeutic effect was dependent on the presence of somatostatin receptors.

The aim of this study was to investigate the therapeutic effects of the ^{111}In labeled somatostatin analog octreotide in tumors of various sizes. A tumor can relapse after peptide receptor radionuclide therapy (PRRT) with ^{111}In-DTPA-octreotide by for instance the lack of crossfire. A possible explanation can be that in larger tumors probably a higher amount of tumor heterogeneity occurs, which can be explained by dedifferentiation of the tumor. A possible consequence could be that certain tumor cells loose the expression of the somatostatin receptor, leading to a heterogeneous receptor distribution in larger tumors. This may result in a reduced anti-tumor effect to PRRT due to the lack of crossfire from ^{111}In. Therefore it is especially

important to know the effect of radionuclide therapy on the receptor expression of the tumor in various stages of tumor development. We therefore investigated the sst_2 expression in tumors after therapy with an In-111 labeled somatostatin analog. The sst_2 expression was determined when tumors were either declining in size or at re-growth after low dose PRRT (see Fig. 3). The receptor expression was compared with tumors in control animals, not receiving PRRT.

MATERIALS AND METHODS

Labeled peptides

DTPA-octreotide (DTPA = diethylenetriaminepentaacetic acid) and $^{111}InCl_3$ (DRN 4901, 370 MBq/ml in HCl, pH = 1.5 - 1.9) were obtained from Mallinckrodt Medical BV (Petten, The Netherlands). DTPA-octreotide was labeled with $^{111}InCl_3$ as has been described previously [16]. DOTA-Tyr^3-octreotate (DOTA= tetraazacyclododecanetetraacetic acid) was labeled with $^{111}InCl_3$ as described previously [6].

Radionuclide therapy experiments using radiolabeled somatostatin-analogs

Tumor model: CA20948 pancreatic tumors were grown in the flank of male Lewis rats (Harlan, The Netherlands; 250-300 g). These rats were injected subcutaneously into the flank, with 500 µl of a cell suspension of CA20948 tumor, prepared from 5 g crude tumor tissue in 100 ml saline.

Tumor growth, animal condition and body weight was determined regularly. Loss of more than 10% of original body weight and tumor growth beyond about 15 cm^2 were indications to sacrifice the animal.

Responses were recorded according to the criteria of the South-West Oncology Group with some modifications. Partial response (PR) was defined as at least 50% reduction of the product of the 2 largest perpendicular tumor diameters measured at onset of therapy, whereas complete response (CR) was defined as 100% reduction of this product and at least lasting for 150 days.

(A) Therapy (low and high doses) in small and large tumors with ^{111}In-DTPA-octreotide: At the start of therapy, about 10 days after inoculation, 50% of the rats, all bearing tumors ≤ 1 cm^2, were anaesthetized and the radiolabeled peptides were injected into the dorsal vein of the penis. The therapeutic groups received either a single intravenous injection or three injections (one week apart) with indicated amounts of ^{111}In-DTPA-octreotide. Specific activity of ^{111}In-DTPA-octreotide was 370 MBq/0.5 µg peptide. Groups were 6-9 rats, a typical group having 8 rats. The control group did not receive radiolabeled peptide. One week later, in the remaining 50% of the rats, bearing ≥ 8 cm^2 tumors, therapy was started using the same doses of radiolabeled peptides as used in the first group.

(B) Low dose therapy to determine receptor expression: The somatostatin receptor density in CA20948 tumors was determined after injection with 185 MBq (4 µg) ^{111}In-DOTA-Tyr^3-octreotate in tumor-bearing rats. Therapy started 15 days after inoculation. This relatively low dose was administered to initiate a partial response of the tumor (decline in size, regression) followed by tumor re-growth. The somatostatin receptor status on the tumors was determined

after therapy at 2 time points: 1) in some animals when tumor size was declining in size (at least 50%), and 2) in other animals when the tumor escaped after the initial tumor size decline. Receptor status using autoradiography with DOTA-^{125}I-Tyr^3-octreotate was determined after isolation of the tumor (described below). Only the "vital" parts of the tumor were taken in account for receptor status determination, "vital" parts were discriminated from "necrotic" parts in histological sections.

Statistical analysis

GraphPad Prism (PraphPad Prism Software, Inc; San Diego, USA) was used to design and comparing survival curves for the different groups and to calculate the median survival, being the time at which half the rats from a therapeutic group had been sacrificed. For comparison of survival curves the logrank test (Mantel-Haenszel test) was used.

Autoradiography

The receptor density in CA20948 tumors was determined using autoradiography after therapy with 185 MBq ^{111}In-Tyr^3-octretate in tumor-bearing rats. The radioactivity due to the consequence of PRRT with ^{111}In was decayed by the time of receptor determination by autoradiography. The tumors of the treated groups together with the controls were embedded in TissueTek (Saqura, Zoeterwoude, The Netherlands) after isolation and quickly frozen. Tissue sections (10 μm) were mounted on glass slides and stored at –20 °C for at least 1 day to improve adhesion of the tissue to the slide. Several slides were used for autoradiography, whereas adjacent sections were haematoxylin-eosin (HE) stained. Sections were air-dried, pre-incubated in 170 mM Tris-HCl buffer, pH 7.6, for 10 min at room temperature (RT) and then incubated for 60 min at RT with 10^{-10}M DOTA-^{125}I-Tyr^3-octreotate. In order to determine non-specific binding of the radiopharmaceutical, adjacent slides were co-incubated with 10^{-6}M octreotide. The incubation solution was 170 mM Tris-HCl buffer, pH 7.6, containing 1% (w/v) BSA, 1 mg bacitricin and 5 mM $MgCl_2$. After incubation, the sections were washed twice for 5 min in cold incubation buffer including 0.25% BSA, subsequently in buffer alone and once with cold MilliQ, finally the sections were dried quickly. The sections were exposed to phosphor imaging screens (Packard Instruments Co., Meriden, USA) in X-ray cassettes. The screens were analyzed using a Cyclone phosphor imager and a computer-assisted OptiQuant 03.00 image processing system (Packard Instruments Co, Groningen, The Netherlands). OptiQuant was used for quantification of the receptor density expressed in % density light units (DLU) per mm^2 relative to the control. Dependent on the size of the tumor slide, different regions of interest were drawn.

Dosimetry

Estimation of tumor dose was based on biodistribution studies in this rat model as published earlier [6]. The dose to the rat tumors in Gy was calculated assuming uniform distribution of radioactivity in a spherical mass. Tumor-to-tumor dose was taken into account only and S-values (mean absorbed dose per unit cumulated activity) for ^{111}In in spheres of 1 and 10 g were used as described [17, 18].

RESULTS

(A) Therapy (low and high doses) in small and large tumors with ^{111}In-DTPA-octreotide

The tumors of the rats in the control group grew excessively; spontaneous growth inhibition was not observed. Survival curves for the control and therapeutic groups are shown in Figure 1. The treatment with a single dose of 111 MBq ^{111}In-DTPA-octreotide, leading to a dose of 0.70 – 0.87 Gy in the tumor (for the relative biological effectiveness (RBE) of the Auger electrons a factor of 1 was used), did not induce significant differences between the survival curves of the animals bearing the smaller versus larger tumors, as in both groups the onset of sacrifice of the first rats was at the same time. For the groups that received the fractionated dose, i.e. 3 injections of 37 MBq, the survival curves of animals bearing smaller versus larger tumors were significantly different (Fig. 1). In this 3 × 37 MBq dose-group 100% PR was found for the smaller tumor-bearing animals, whereas this was 25% PR for the smaller tumors in the single 111 MBq dose-group (Fig. 2).

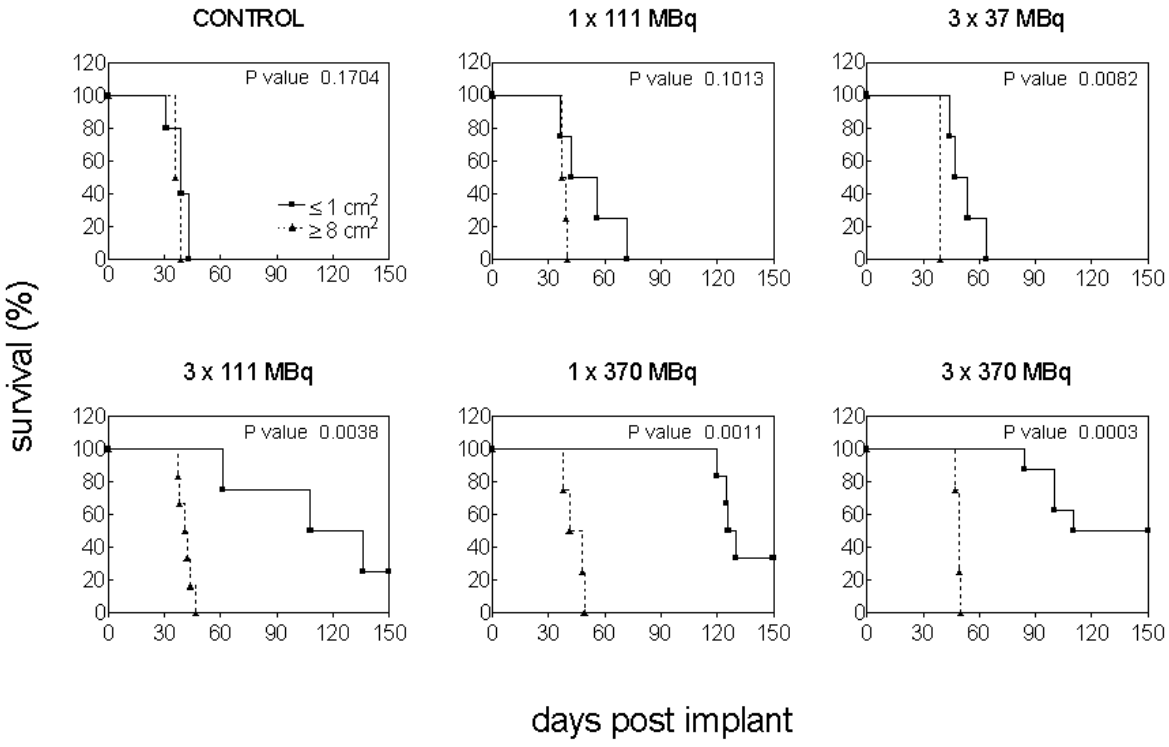

FIGURE 1. *Survival curves of groups of rats bearing either smaller (solid line) versus larger (dashed line) CA20948 tumors after indicated doses of ^{111}In-DTPA-octreotide.*

With increased doses of ^{111}In-labeled octreotide, median survival, the time at which half the rats from a group had been sacrificed, increased as well (Table 1), both for the rats bearing smaller and larger tumors. The effects however, were far more pronounced for the smaller tumors, also shown by the increased ratio between the median survival data for smaller and larger tumor-bearing rats with increasing doses as shown in Table 1. For all doses but 111 MBq, a significant difference was found with regard to survival between rats bearing smaller versus larger tumors (Fig. 1).

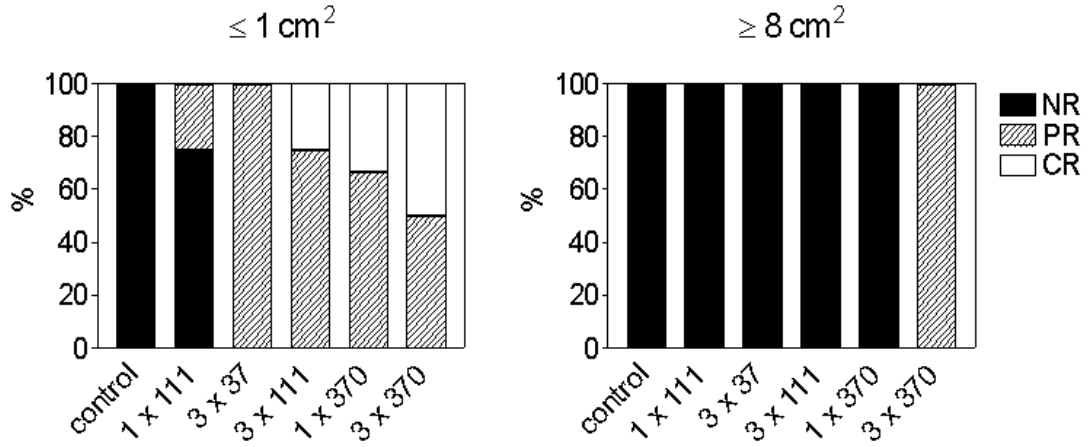

FIGURE 2. *Tumor responses found in groups of rats bearing either smaller (≤ 1 cm^2) versus larger (≥ 8 cm^2) CA20948 tumors after indicated doses of ^{111}In-DTPA-octreotide. NR = no response, PR = partial response, CR = complete response.*

TABLE 1. *Median survival data for groups of rats bearing either smaller (≤ 1 cm^2) or larger (≥ 8 cm^2) CA20948 tumors after indicated doses of ^{111}In-DTPA-octreotide and the ratio between the median survival of the smaller and larger tumor-bearing rats.*

MBq	≤ 1 cm^2	≥ 8 cm^2	ratio
0	39	38	1.04
1 × 111	49	38	1.29
3 × 37	51	39	1.30
3 × 111	122	42	2.94
1 × 370	128	45	2.88
3 × 370	130	49	2.65

Figure 2 shows that after administration of at least 3 × 111 MBq (2.1 – 2.6 Gy) or the equivalent single dose, CR is found in different groups, increasing to 50% in the group that received the highest dose: 3 × 370 MBq (7.0 – 8.7 Gy). This held only true in animals bearing smaller tumors. When therapy was initiated at a later stage (≥ 8 cm^2 tumors), results were much less pronounced. No CR, but only PR was reached, the latter after administration of the highest dose (Fig. 2).

(B) Low dose therapy to determine receptor expression

The radiation dose of 185 MBq ^{111}In-labeled somatostatin analog Tyr^3-octreotate led to a tumor dose of 3.3 – 4.1 Gy (tumor size of 1 – 10 g, for the RBE of the Auger electrons a factor of 1 was used). As was intended with this dose most tumors indeed initially responded to the given therapy, but after a certain time all tumors re-grew, as was expected. Figure 3 shows the tumor growth of the rats treated with a single dose of 185 MBq ^{111}In-labeled somatostatin analog. At two time points the tumor receptor expression was determined using in vitro autoradiography. First when the CA20948 tumors were declining in size and secondly when re-growth occurred (as indicated in Fig. 3B and 3C). With autoradiography a clear receptor expression was found in both control tumors and ^{111}In-treated tumors; when an excess of octreotide (1 μM) was co-incubated a clear decrease in radioactivity was found (Fig. 4A). Quantification showed a higher receptor density, only taking into account the "vital" parts of the tumor (Fig. 4A&C), when the tumors re-grew ($p < 0.001$) (Fig. 4B). No significant difference was found when the tumors were in regression.

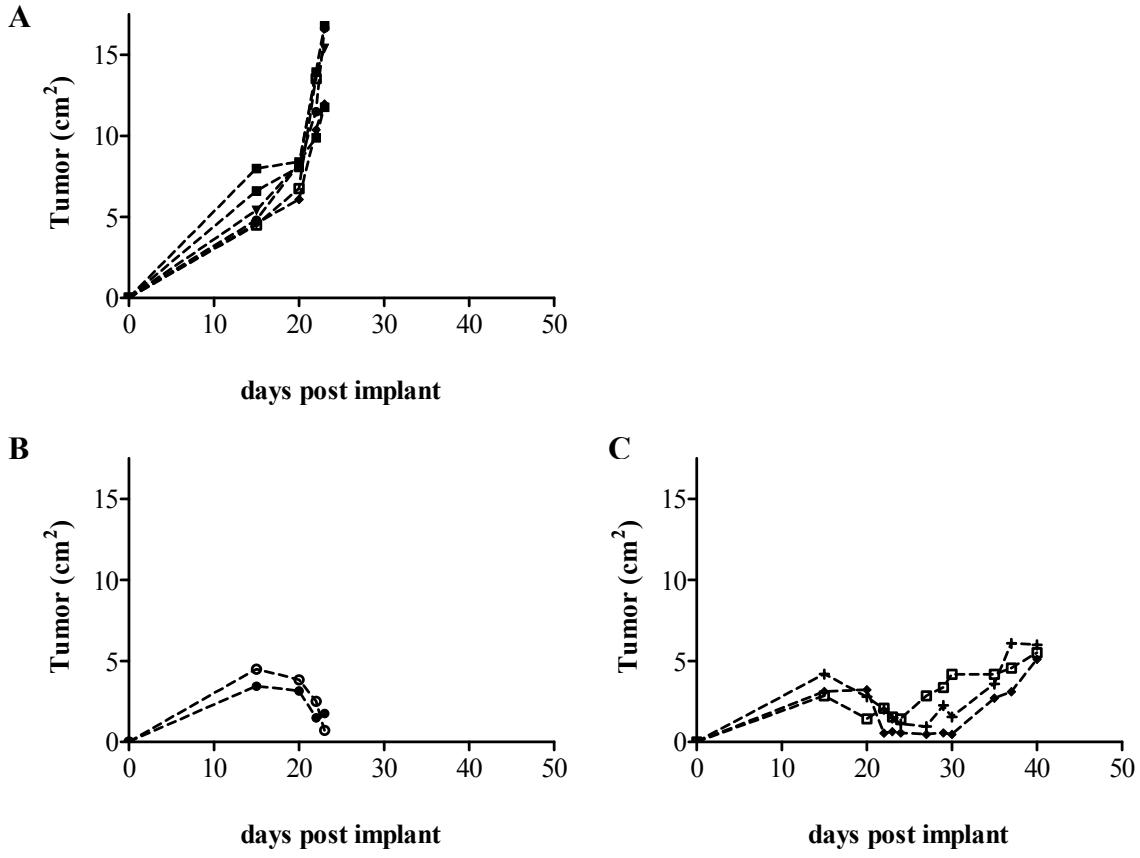

FIGURE 3. *Tumor growth of groups of rats bearing CA20948 tumors treated with 185 MBq ^{111}In-DOTA-Tyr^3-octreotate. (A) Tumor growth the control group. (B) Tumor growth of rats treated with 185 MBq ^{111}In-DOTA-Tyr^3-octreotate, sacrificed when the tumor was declining in size. (C) Tumor growth of rats treated with 185 MBq ^{111}In-DOTA-Tyr^3-octreotate, sacrificed after re-growth of the tumor after initial tumor shrinkage.*

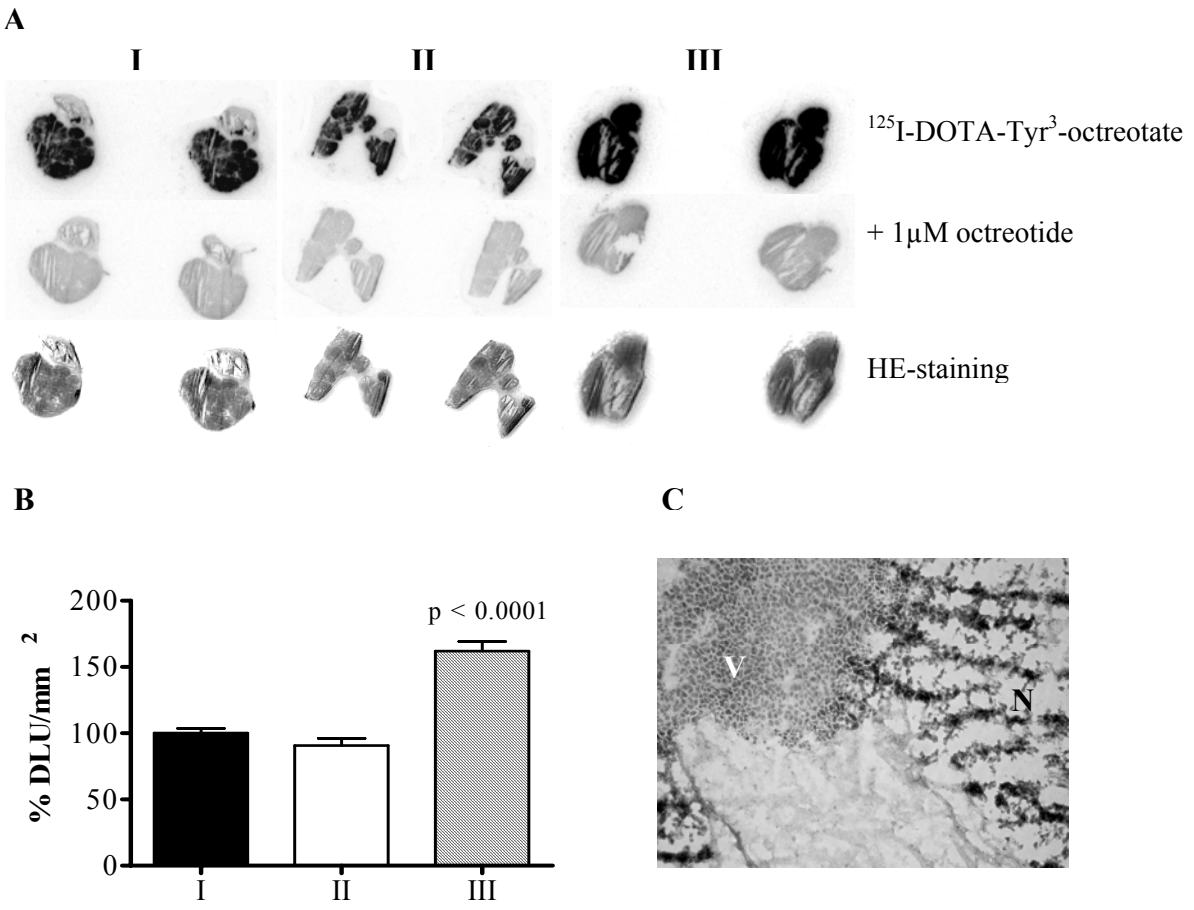

FIGURE 4. *(A) Autoradiography with 10^{-10} M DOTA-^{125}I-Tyr^3-octreotate of CA20948 tumors treated with saline (control) (I) or 185 MBq ^{111}In-DOTA-Tyr^3-octreotate (II&III) to determine the density of the somatostatin receptors when the tumor was declining in size (II) or when re-growth occurred after the initial tumor shrinkage (III). For determination of receptor specificity of the radiopharmaceutical, adjacent slides were co-incubated with 10^{-6}M octreotide (middle row). Histology was determined using HE-staining (third row). (B) Quantification of the somatostatin receptor density using autoradiography of treated and control tumors. This was determined when the tumor was declining (in regression) or at re-growth after initial size decline. The receptor density is expressed in % Density Light Units (DLU) per mm^2 relative to control. (C) A 200 magnification of a HE-tumor section presenting vital (V) and necrotic tissue (N).*

DISCUSSION

Our results show impressive radiotherapeutic effects of ^{111}In-labeled somatostatin-analogs in this rat tumor model. Complete responses (up to 50%) were only measured in the animals bearing small, but palpable tumors after at least 3 × 111 MBq/370 MBq ^{111}In-DTPA-octreotide.

The success of the therapeutic strategy depends on the amount of radioligand that can be concentrated within tumor cells, and the rates of internalization of both ligand and receptor will among other things determine this. We studied internalization of radiolabeled DTPA-octreotide in tumor cells, in accordance with the findings of Andersson et al. [19] this process appeared to be receptor-specific and temperature dependent [20]. Receptor-mediated internalization of ^{111}In-DTPA-octreotide will most probably result in degradation to ^{111}In-DTPA-D-Phe, this metabolite is not capable of passing the lysosomal membrane [21], thereby contributing to the long residence time of radioactivity in the target cells (see below). Furthermore, the amount of radioligand taken up in the tumor may depend on the specific activity of the radiolabeled peptide used, as we have shown that tumor uptake of radiolabeled peptides is dependent on the unlabeled peptide amount that is co-injected with the radiolabel [22].

The rat pancreatic CA20948 flank tumor has been shown to be a good model for therapy using radiolabeled somatostatin analogs. This is in agreement with the antiproliferative effects of ^{111}In-DTPA-octreotide found in a rat liver tumor metastases model [15]. Administration of 370 MBq ^{111}In-DTPA-octreotide on day 1 and/or day 8 after intraportal CA20948 tumor cell inoculation induced a significant decrease in the number hepatic metastases at day 21. These findings show that after radionuclide therapy reduction of tumor volume can be obtained because of the radiotherapeutic effect of ^{111}In-labeled octreotide. Recently we reported an in vitro colony-forming assay in which we studied the therapeutic effects of ^{111}In-DTPA-octreotide using the rat pancreatic tumor cell line CA20948 [11]. In this in vitro system we showed that ^{111}In-DTPA-octreotide can control tumor growth, the effects were dependent on incubation time, radiation dose and specific activity used. Similar concentrations of ^{111}In-DTPA, which is not internalized into sst-positive tumor cells like ^{111}In-DTPA-octreotide, did not influence tumor survival, showing that the therapeutic effect of ^{111}In is dependent on internalization, enabling the Auger electrons with their very short particle range to reach the nucleus. These findings hold promise for the application of therapy with ^{111}In-labeled octreotide in an adjuvant, micrometastatic setting and are consistent with the findings in this study.

After therapy with multiple doses of ^{111}In-labeled octreotide we found various responses. CRs were only found in the smaller tumors. Cure (up to 50%) was found in the animals bearing small ($\leq$ 1 cm^2) tumors after at least three injections of 111 MBq or a single injection of 370 MBq ^{111}In-DTPA-octreotide, leading to a dose of 6.3 – 7.8 mGy/MBq (1 – 10 g tumor, for the RBE of the Auger electrons a factor of 1 was used). In the rats bearing the larger ($\geq$ 8 cm^2) tumors the effects were much less pronounced and only partial responses were reached in these groups.

Preclinical PRRT studies in vivo with the β-emitting radionuclides ^{177}Lu and ^{90}Y showed very promising results [23, 24]. The cure rate of the rats was however also dependent on the tumor size. Based on a mathematical model the tumor curability in relation to the tumor size was examined [25]. It was calculated that the optimal tumor diameter for ^{90}Y was 34.0 mm and for ^{177}Lu 2.0 mm. Tumors smaller than the optimal size will not absorb all the energy of the β-emitting radionuclide. In larger tumors more clonogenic, presumably hypoxic, cells will be

present, thereby limiting radiocurability. Another possible explanation can be that in larger tumors probably a higher amount of tumor receptor heterogeneity occurs, which can be explained by dedifferentiation of the tumor. A possible consequence could be that certain tumor cells loose the expression of the somatostatin receptor, leading to a heterogeneous receptor distribution in larger tumors. This may result in a reduced anti-tumor effect to PRRT due to the lack of crossfire from this ^{111}In. So, it is important to know after PRRT the receptor expression of the tumor in various stages of tumor development. Since 50% of the tumors escaped after 3 × 370 MBq ^{111}In-DTPA-octreotide we investigated the sst_2 expression in tumors after ^{111}In-therapy. The sst_2 expression was determined when tumors were either declining in size or when re-growth occurred after an initial decline in size. The receptor expression was compared with control tumors, which did not receive PRRT.

We therefore investigated whether the somatostatin receptors were still present after therapy with 185 MBq ^{111}In-labeled somatostatin analog. After this relatively low tumor dose of 3.3 – 4.1 Gy (for a tumor size of 1 – 10 g, for the RBE of the Auger electrons a factor of 1 was used) initially a partial response of the tumor (decline in size, regression) followed by tumor re-growth (escape, post-regression) was expected. We showed that a single dose of 185 MBq ^{111}In-DOTA-Tyr^3-octreotate gave a clear decline in tumor size but all tumors re-grew. In this study we found an sst_2 receptor expression in the control tumors as well as in the tumors treated with ^{111}In. In fact, a significant ($p < 0.001$) higher receptor density after re-growth in comparison with the control tumors was found. However, the histology of the tumors should be taken into account as well, to investigate differences in terms of cell size, shape or cellularity of the two tumors types (control vs. re-growth). To further investigate the effects of PRRT on the receptor expression studies including these items are ongoing.

Recently Béhé et al. [26, 27] also found an increase in receptor density after irradiation. AR42J cells were irradiated with a dose of 4, 8 and 16 Gy (external beam irradiation). Subsequent binding assays showed a time-dependent upregulation of somatostatin and gastrin receptors for all doses. Also the tumoral uptake in vivo was increased, indicating that fractionation of radiolabeled peptides is feasible.

The results found here with regard to radiotherapeutic effects in smaller and larger tumors may be highly clinically significant. They hold promise for application of radionuclide therapy with ^{111}In-labeled octreotide (as well as ^{177}Lu), in an adjuvant, micrometastatic setting, e.g. after surgery to eradicate occult metastases. This is in accordance with our earlier findings that high radioactive doses of ^{111}In-DTPA-octreotide inhibited the growth of somatostatin receptor-positive micro-metastases in a rat liver tumor model [15]. Furthermore the data observed here point to the importance of early onset of radionuclide therapy during tumor development, whereas in the phase I studies performed in our hospital using ^{111}In-DTPA-octreotide only end-stage patients with often a large tumor load were included.

Finally we showed that PRRT leads to an increase in receptor density of the somatostatin receptor. This upregulation of the somatostatin receptor leads to a possible higher uptake of the radiolabeled peptides in therapeutic applications, probably making repeated injections of radiolabeled peptides more effective.

REFERENCES

1. Bell GI, Reisine T. Molecular biology of somatostatin receptors. *Trends Neurosci* 1993;16:34-38.
2. Yamada Y, Kagimoto S, Kubota A, Yasuda K, Masuda K, Someya Y, Ihara Y, Li Q, Imura H, Seino S, et al. Cloning, functional expression and pharmacological characterization of a fourth (hSSTR4) and a fifth (hSSTR5) human somatostatin receptor subtype. *Biochem Biophys Res Commun* 1993;195:844-852.
3. Kubota A, Yamada Y, Kagimoto S, Shimatsu A, Imamura M, Tsuda K, Imura H, Seino S, Seino Y. Identification of somatostatin receptor subtypes and an implication for the efficacy of somatostatin analogue SMS 201-995 in treatment of human endocrine tumors. *J Clin Invest* 1994;93:1321-1325.
4. Reisine T, Bell GI. Molecular properties of somatostatin receptors. *Neuroscience* 1995;67:777-790.
5. Patel YC, Greenwood M, Panetta R, Hukovic N, Grigorakis S, Robertson LA, Srikant CB. Molecular biology of somatostatin receptor subtypes. *Metabolism* 1996;45:31-38.
6. de Jong M, Breeman WA, Bakker WH, Kooij PP, Bernard BF, Hofland LJ, Visser TJ, Srinivasan A, Schmidt MA, Erion JL, Bugaj JE, Macke HR, Krenning EP. Comparison of (111)In-labeled somatostatin analogues for tumor scintigraphy and radionuclide therapy. *Cancer Res* 1998;58:437-441.
7. Krenning EP, Kwekkeboom DJ, Bakker WH, Breeman WA, Kooij PP, Oei HY, van Hagen M, Postema PT, de Jong M, Reubi JC, et al. Somatostatin receptor scintigraphy with [111In-DTPA-D-Phe1]- and [123I- Tyr3]-octreotide: the Rotterdam experience with more than 1000 patients. *Eur J Nucl Med* 1993;20:716-731.
8. Krenning EP, Kwekkeboom DJ, Pauwels S, Kvols LK, Reubi JC. Somatostatin receptor scintigraphy. *In: Freeman LM (ed) Nuclear Medicine Annual. Raven Press, New York* 1995;1-50.
9. Hofer KG, Harris CR, Smith JM. Radiotoxicity of intracellular 67Ga, 125I and 3H. Nuclear versus cytoplasmic radiation effects in murine L1210 leukaemia. *Int J Radiat Biol Relat Stud Phys Chem Med* 1975;28:225-241.
10. Martin RF, Bradley TR, Hodgson GS. Cytotoxicity of an 125I-labeled DNA-binding compound that induces double-stranded DNA breaks. *Cancer Res* 1979;39:3244-3247.
11. Capello A, Krenning EP, Breeman WA, Bernard BF, de Jong M. Peptide receptor radionuclide therapy in vitro using [111In-DTPA0]octreotide. *J Nucl Med* 2003;44:98-104.
12. Fjalling M, Andersson P, Forssell-Aronsson E, Gretarsdottir J, Johansson V, Tisell LE, Wangberg B, Nilsson O, Berg G, Michanek A, Lindstedt G, Ahlman H. Systemic radionuclide therapy using indium-111-DTPA-D-Phe1-octreotide in midgut carcinoid syndrome. *J Nucl Med* 1996;37:1519-1521.
13. McCarthy KE, Lemen L, Espenan G, Woltering EA, Nelson J, Cronin M, Maloney T, Anthony LB. Dose-escalation of indium-111 pentetreotide (Somatother^{TM}): toxicity and clinical response. *Clin Nucl Med* 1999;24:213.
14. Valkema R, De Jong M, Bakker WH, Breeman WA, Kooij PP, Lugtenburg PJ, De Jong FH, Christiansen A, Kam BL, De Herder WW, Stridsberg M, Lindemans J, Ensing G, Krenning EP. Phase I study of peptide receptor radionuclide therapy with [In- DTPA]octreotide: the Rotterdam experience. *Semin Nucl Med* 2002;32:110-122.

15. Slooter GD, Breeman WA, Marquet RL, Krenning EP, van Eijck CH. Anti-proliferative effect of radiolabelled octreotide in a metastases model in rat liver. *Int J Cancer* 1999;81:767-771.
16. Bakker WH, Krenning EP, Reubi JC, Breeman WA, Setyono-Han B, de Jong M, Kooij PP, Bruns C, van Hagen PM, Marbach P, et al. In vivo application of [111In-DTPA-D-Phe1]-octreotide for detection of somatostatin receptor-positive tumors in rats. *Life Sci* 1991;49:1593-1601.
17. Stabin MG, Konijnenberg MW. Re-evaluation of absorbed fractions for photons and electrons in spheres of various sizes. *J Nucl Med* 2000;41:149-160
18. Konijnenberg MW, Bijster M, Krenning EP, De Jong M. A stylized computational model of the rat for organ dosimetry in support of preclinical evaluations of peptide receptor radionuclide therapy with (90)Y, (111)In, or (177)Lu. *J Nucl Med* 2004;45:1260-1269.
19. Andersson P, Forssell-Aronsson E, Johanson V, Wangberg B, Nilsson O, Fjalling M, Ahlman H. Internalization of indium-111 into human neuroendocrine tumor cells after incubation with indium-111-DTPA-D-Phe1-octreotide. *J Nucl Med* 1996;37:2002-2006.
20. De Jong M, Bernard BF, De Bruin E, Van Gameren A, Bakker WH, Visser TJ, Macke HR, Krenning EP. Internalization of radiolabelled [DTPA0]octreotide and [DOTA0,Tyr3]octreotide: peptides for somatostatin receptor-targeted scintigraphy and radionuclide therapy. *Nucl Med Commun* 1998;19:283-288.
21. Duncan JR, Stephenson MT, Wu HP, Anderson CJ. Indium-111-diethylenetriaminepentaacetic acid-octreotide is delivered in vivo to pancreatic, tumor cell, renal, and hepatocyte lysosomes. *Cancer Res* 1997;57:659-671.
22. de Jong M, Breeman WA, Bernard BF, van Gameren A, de Bruin E, Bakker WH, van der Pluijm ME, Visser TJ, Macke HR, Krenning EP. Tumour uptake of the radiolabelled somatostatin analogue [DOTA0, TYR3]octreotide is dependent on the peptide amount. *Eur J Nucl Med* 1999;26:693-698.
23. de Jong M, Breeman WA, Bernard BF, Bakker WH, Schaar M, van Gameren A, Bugaj JE, Erion J, Schmidt M, Srinivasan A, Krenning EP. [177Lu-DOTA(0),Tyr3] octreotate for somatostatin receptor-targeted radionuclide therapy. *Int J Cancer* 2001;92:628-633.
24. de Jong M, Breeman WA, Bernard BF, Bakker WH, Visser TJ, Kooij PP, van Gameren A, Krenning EP. Tumor response after [(90)Y-DOTA(0),Tyr(3)]octreotide radionuclide therapy in a transplantable rat tumor model is dependent on tumor size. *J Nucl Med* 2001;42:1841-1846.
25. O'Donoghue JA, Bardies M, Wheldon TE. Relationships between tumor size and curability for uniformly targeted therapy with beta-emitting radionuclide. *J Nucl Med* 1995;36:1902-1909.
26. Behe M, Püsken M, Henzel M, Gross M, Reitz I, Engelhart-Cabillic E, Behr TM. Upregulation of gastrin and somatostatin receptor after irradiation. *Eur J Nucl Med Mol Imaging* 2003;30:S218.
27. Behe M, Koller S, Püsken M, Gross M, Alfke H, Keil B, Henzel M, Neidel HO, Schramm N, Gotthardt M, Behr TM, Engelhart-Cabillic E. Irradiation-induced upregulation of somatostatin and gastrin receptors in vitro and in vivo. *Eur J Nucl Med Mol Imaging* 2004;31:S237-238.

CHAPTER 4

RADIONUCLIDE THERAPY WITH ^{177}Lu OR ^{90}Y LABELED PEPTIDES

4.1 Tyr^3-octreotide and Tyr^3-octreotate radiolabeled with ^{177}Lu or ^{90}Y: Peptide Receptor Radionuclide Therapy results in vitro.

Astrid Capello, Eric Krenning, Wout Breeman, Bert Bernard, Marc Konijnenberg and Marion de Jong.

Cancer Biotherapy and Radiopharmaceuticals, 2003, 18 (5):761-768.

ABSTRACT

Somatostatin analogs promising for Peptide Receptor Scintigraphy (PRS) and Peptide Receptor Radionuclide Therapy (PRRT) are D-Phe-c(Cys-Tyr-D-Trp-Lys-Thr-Cys)-Thr(ol) (Tyr^3-octreotide) and D-Phe-c(Cys-Tyr-D-Trp-Lys-Thr-Cys)-Thr (Tyr^3-octreotate). For radiotherapeutic applications these peptides are being labeled with the β^- particle emitters ^{177}Lu or ^{90}Y. We evaluated the therapeutic effects of these analogs chelated with tetra-azacyclododecanetetra-acetic acid (DOTA) and labeled with ^{90}Y or ^{177}Lu in an *in vitro* colony-forming assay using the rat pancreatic tumor cell line CA20948. Furthermore, we investigated the effects of incubation time, radiation dose, and specific activity of ^{177}Lu-DOTA-D-Phe^1-c(Cys-Tyr-D-Trp-Lys-Thr-Cys)-Thr (^{177}Lu-octreotate). ^{177}Lu-octreotate could reduce tumor growth to 100% cell kill and effects were dependent on radiation dose, incubation time, and specific activity used. Similar concentrations of ^{177}Lu-DOTA, which is not bound to the cells, had a less pronounced effect on the tumor cell survival. Both Tyr^3-octreotide and Tyr^3-octreotate labeled with either ^{177}Lu or ^{90}Y, using DOTA as chelator, were able to control tumor growth in a dose-dependent manner. In all concentrations used radiolabeled Tyr^3-octreotate had a higher tumor kill compared to radiolabeled Tyr^3-octreotide, labeled with ^{177}Lu or ^{90}Y. This is in accordance with the higher affinity of Tyr^3-octreotate for the somatostatin subtype 2 (sst_2)-receptor compared to Tyr^3-octreotide, leading to a higher amount of cell-associated radioactivity, resulting in a significantly higher tumor radiation dose. In conclusion, Tyr^3-octreotate labeled with ^{177}Lu or ^{90}Y is the most promising analog for PRRT.

INTRODUCTION

Somatostatin receptors are integral membrane glycoproteins that are distributed in a variety of tissues throughout the body. At present five somatostatin receptor subtypes (sst_{1-5}) have been identified [1, 2]. Somatostatin binds to all subtypes with high affinity, while the affinity of the different somatostatin analogs for these subtypes differ considerably. For example, octreotide binds with high affinity to the somatostatin receptor subtype 2 (sst_2) and with lower affinity to sst_3 and sst_5. It shows no binding to sst_1 and sst_4 [3-6].

Many tumors, such as endocrine pancreatic tumors, carcinoids, paragangliomas, pheochromocytomas, small cell lung cancer as well as certain brain tumors and breast cancer, express an increased number of somatostatin receptors [7]. These somatostatin receptor-positive tumors can be visualized with ^{111}In-DTPA-octreotide in which DTPA is diethylene-triamine-penta-acetic acid. ^{111}In-DTPA-octreotide is nowadays recognized to be the imaging technique for the localization and staging of somatostatin receptor-positive tumors. ^{111}In-DTPA-octreotide has also been used for radionuclide therapy in preclinical studies in rats, where it effectively reduced or inhibited tumor growth in a flank and liver tumor model. Peptide Receptor Radionuclide Therapy (PRRT) with ^{111}In-DTPA-octreotide has been shown to induce therapeutic responses in patients with neuroendocrine tumors [8-14].

Promising somatostatin analogs are Tyr^3-octreotide and Tyr^3-octreotate; in the latter the alcohol Thr(ol) at the C-terminus (as used in octreotide) is replaced with the natural amino acid Thr. This analog was found to have a very high affinity for sst_2 and showed the highest uptake in the rat pancreatic CA20948 tumor in a biodistribution study in rats using different ^{111}In-labeled somatostatin analogs [15]. Lewis et al. also reported that the somatostatin analog ^{64}Cu-TETA-Tyr^3-octreotate has a higher tumor uptake than ^{64}Cu-TETA-octreotide (TETA is 1,4,8,11-tetraazacycloetradecane-N,N',N'',N'''-tetraacetic acid) both *in vitro* and *in vivo* [16, 17]. In patients, radiolabeled octreotate appeared to have a three to four times higher tumor uptake than ^{111}In-labeled octreotide [18].

For radiotherapeutic applications, Tyr^3-octreotide and Tyr^3-octreotate have been derivatised with the chelator tetra-azacyclododecanetetra-acetic acid (DOTA), enabling stable radiolabeling with ^{90}Y and ^{177}Lu. ^{90}Y is a high-energy β^- particle emitter with a maximum β^- energy of 2.3 MeV and a half-life of 64 hours. ^{177}Lu is a low-energy β^- particle emitter (479 keV, 78%) with a half-life of 6.7 days. ^{177}Lu also emits gamma radiation (208 keV, 11%), which allows scintigraphy and subsequent dosimetry using the same compound. Currently, various phase I and II studies are being performed with ^{90}Y-octreotide and ^{177}Lu-octreotate with most favorable results regarding tumor growth [8, 19-26].

Earlier we reported an *in vitro* colony-forming assay in which we studied the therapeutic effects of ^{111}In-DTPA-octreotide using the rat pancreatic tumor cell line CA20948 [27]. In this study we expanded these ^{111}In-DTPA-octreotide experiments and compared the different therapeutic effects of Tyr^3-octreotide and Tyr^3-octreotate labeled with ^{90}Y or ^{177}Lu in the colony-forming assay. To provide insight into the tumoricidal effects of ^{177}Lu-octreotate we investigated the effects of incubation time, radiation dose, and specific activity used.

MATERIALS AND METHODS

Compounds

$^{177}LuCl_3$ was from IDB Holland (Baarle Nassau, The Netherlands). $^{90}YCl_3$ was obtained from Perkin Elmer (Boston, MA). ^{90}Y and ^{177}Lu labeling of DOTA-Tyr^3-octreotide and DOTA-Tyr^3-octreotate was performed as described previously [28-31].

Cell culture

CA20948 rat pancreatic tumor cells were grown in Dulbecco's modified Eagle's medium (DMEM) (Gibco BRL, Grand Island, NY). Medium was supplemented with 10% fetal calf serum, 2 mM glutamine, 1 mM sodium pyruvate, 0.1 mg/L fungizone and 50 IU/mL penicillin/streptomycin.

Internalization studies

Determination of internalized ^{177}Lu-octreotate in increasing cell concentrations with therapeutic doses. Cells (200-10,000 cells/well) were washed with 2 mL phosphate-buffered saline (PBS) and incubated in 1 mL incubation medium (RPMI-1640 supplemented with 1% bovine serum albumin and 20 mM Hepes) with 0.37-3.7 MBq/mL ^{177}Lu-octreotate for 1 hour at 37°C. Peptide concentrations were between 8×10^{-9}M – 8×10^{-8}M. Cellular uptake was stopped by removing medium from the cells, followed by washing twice with 2 mL PBS. In some wells the amount of internalized and membrane bound radioactivity was determined directly after the 1 hour incubation period. Other wells were washed with PBS after the 1 hour incubation step to remove the radiolabeled peptide from the medium, and cultured for another 72 hours in growth medium. After these 72 hours the amount of internalized and membrane bound radioactivity was also determined.

Peptide receptor radionuclide therapy *in vitro*

One day before the experiment cells were transferred to six-well plates in a density of 200 cells per well. Cells were washed with PBS (37°C) and incubated for 1 hour in 1 mL incubation medium (RPMI-1640 medium with 1% bovine serum albumin and 20 mmol HEPES, also called N-[2-hydroxyethyl]piperazine-N'-[Z-ethanesulfonic acid]) containing

^{177}Lu-octreotate. Control cells received only incubation medium. Thereafter, cells were thoroughly washed with PBS and cultivated for 10 days in growth medium to form colonies (as described previously) [27]. The medium was refreshed once after 72 hours.
After 10 days the cells were fixated with 1 mL methanol:glacial acid (3:1) for 15 minutes. Subsequently the cells were colored with haematoxylin. Colonies that contained more than 50 cells per colony were scored as survivors.

PRRT using ^{177}Lu-octreotate, effects of incubation time, concentration, and specific activity. CA20948 cells were incubated for 1 or 3 hours with ^{177}Lu-octreotate. In this experiment two different specific activities were used; 1.85 MBq/0.15 µg (10^{-7}M), 18.5 MBq/1.50 µg (10^{-6}M) compared with 1.85 MBq/1.50 µg (10^{-6}M).

The effects of ^{177}Lu-DOTA and equimolar amounts of octreotate in comparison with ^{177}Lu-octreotate. CA20948 cells were incubated for 1 hour with 0.85 µg octreotate and 37 MBq ^{177}Lu-DOTA and compared to (0.85 µg) 37 MBq ^{177}Lu-octreotate.

Comparison of Tyr^3-octreotide versus Tyr^3-octreotate labeled with ^{177}Lu or ^{90}Y. CA20948 cells were incubated for 1 hour with increasing concentrations of ^{177}Lu-octreotide versus ^{177}Lu-octreotate and ^{90}Y-octreotide versus ^{90}Y-octreotate.

Statistical analysis

Statistical analysis of the data, for the comparison of octreotide versus octreotate, was carried out by comparing means using the independent *t* test, SPSS (SPSS, Inc., Chicago, IL). Statistical significance was defined as $p < 0.05$.

Total number of decays per cell

The total number of decays per cell was calculated by integration of an assumed cell bound fraction of activity of 0.1% after the incubation period over the whole *in vitro* therapy time. It is assumed that the bound fraction of activity is evenly distributed over the initial number of cells. No redistribution occurs of the radioactivity over newly formed cells during the therapy period. The clearance of radioactivity from the cells is assumed to be just by physical decay. For a cell culture of N cells with incubation time T_i with activity A of a nuclide with decay constant λ_p, leading to relative bound activity u, after therapy time T the number of decays per cell $\tilde{A}_{cell}$ is:

$$\tilde{A}_{cell} = \frac{uA}{N}\int_{T_i}^{T} e^{-\lambda_p t}\,dt = \frac{uA}{\lambda_p N}\left(e^{-\lambda_p T_i} - e^{-\lambda_p T}\right).$$

RESULTS

Internalization studies

Determination of internalized ^{177}Lu-octreotate in increasing cell concentrations with therapeutic doses. We determined how much radioactivity was internalized in the cells when we use therapeutic doses of ^{177}Lu-octreotate. We performed the experiments using an increasing cell concentration (range 200-10,000 cells/well). Figure 1A shows the internalized CPM after 1 hour incubation with an increasing amount of ^{177}Lu-octreotate (specific activity is kept constant) and 72 hours further culture in growth medium. The noninternalized radioactivity represented less than 10% of the total cellular uptake. Figure 1A demonstrates that when more cells are plated per well, and incubated with a constant amount of radioactivity, more radioactivity was internalized. Hence, internalization is dependent on cell number. It also shows that when more radioactivity is added, at constant cell concentration, more radioactivity is internalized into the cells.

In figure 1B the amount of ^{177}Lu-octreotate that is internalized into the cells is expressed as percentage of the dose. This figure shows that with the lowest amount of radioactivity, 0.37 MBq ^{177}Lu-octreotate (which has the lowest peptide concentration; 8×10^{-8}M), the highest percentage of the dose is internalized into the cells.

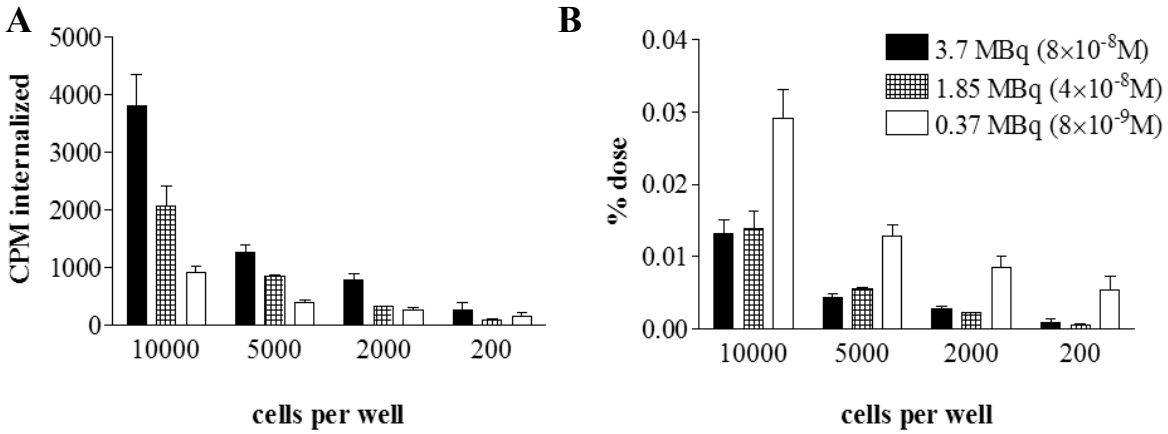

FIGURE 1. *The amount of internalized ^{177}Lu-octreotate after 1-hour incubation with increasing concentrations of ^{177}Lu-octreotate and 72 hours further culture in growth medium with 200-10,000 cells/well. Part **A** shows the amount of internalized counts per minute (CPM) and part **B** shows the internalized amount presented as the percentage of the given dose. Data are expressed as mean ± standard error of the mean from 2 independent experiments performed in triplicate.*

Peptide receptor radionuclide therapy *in vitro*

PRRT using ^{177}Lu-octreotate, effects of incubation time, concentration, and specific activity. Figure 2 shows the percentage of tumor cell survival of the CA20948 cell line after treatment with 1.85 MBq/10^{-7}M (A); 1.85 MBq/10^{-6}M (B); and 18.5 MBq/10^{-6}M (C) ^{177}Lu-octreotate for 1 and 3 hours. Survival values are shown as percentage survival compared to that of the control cells, the plating efficiency was 70% ± 10%. A and B share the same amount of radioactivity only the latter one has a 10-times higher peptide amount, so a lower specific activity. B and C share the same amount of peptide, but the latter has a 10-times higher amount of radioactivity, so a higher specific activity. A and C share the same specific activity. When the tumoricidal effect of A and B are compared, Figure 2 clearly shows that B has a higher tumor cell survival than A, despite the same amount of radioactivity that is used. Figure 2 also shows a time- and dose-dependent inhibition of the colony growth. When the cells were incubated with 1.85 MBq/10^{-7}M for 1 hour the percentage survival is approximately 15% of control; survival is further reduced to approximately 8% when incubated for 3 hours. When the cells are incubated with 18.5 MBq the tumor cell survival reaches zero. Because the 1-hour incubation shows clear tumoricidal effects, we continued with this incubation time.

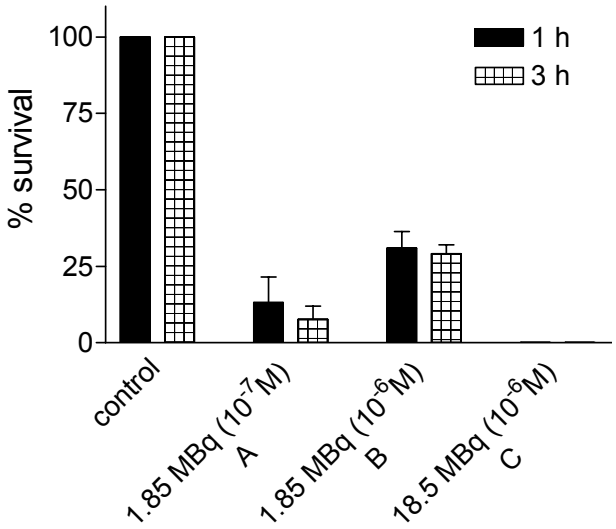

FIGURE 2. *Effects of incubation time, concentration, and specific activity of ^{177}Lu-octreotate on the cell survival of CA20948 cells after peptide receptor radionuclide therapy. Cells were incubated for 1 and 3 hours with 1.85 or 18.5 MBq ^{177}Lu-octreotate at 37°C using two different specific activities (B versus (A&C)). Data are expressed as mean ± standard error of the mean from 2 independent experiments performed in triplicate.*

The effects of ^{177}Lu-DOTA and equimolar amounts of octreotate in comparison with ^{177}Lu-octreotate. The same experiment as described above was performed with a higher specific activity of ^{177}Lu-octreotate, 37 MBq/0.85 μg (6×10^{-7}M). As is shown in figure 3, CA20948 cells were incubated for 1 hour with 1.85, 3.7 and 18.5 MBq ^{177}Lu-octreotate. To investigate the effects of the 1-hour incubation with ^{177}Lu-octreotate in the medium, cells were incubated during 1 hour with the same concentration of ^{177}Lu-DOTA and equimolar

amounts of Tyr^3-octreotate in comparison with ^{177}Lu-octreotate. Figure 3 shows that ^{177}Lu-octreotate induces a dose-dependent inhibition of the tumor cell survival; higher concentrations of ^{177}Lu-octreotate result in a higher percentage tumor kill. This effect reaches its maximum when the cells were incubated for 1 hour with 18.5 MBq; at this radioactivity level the tumor cell survival is zero. To investigate the effects of the medium radioactivity during the 1-hour incubation period on the CA20948 cells, cells were incubated for 1 hour, with ^{177}Lu-DOTA, which is noncell bound and noninternalized radioactivity, in the same concentration that is used with ^{177}Lu-octreotate. Figure 3 shows that there is a dose-dependent inhibition of tumor cell survival when the cells were incubated with high amounts of ^{177}Lu-DOTA, with 1.85, 3.7 and 18.5 MBq there is a tumor cell survival of respectively 65%, 60% and 45%. ^{177}Lu-octreotate, on the other hand, results after internalization in a further cell-killing effect to 30%, 9% and 0% survival with these amounts of radioactivity (see Fig. 3). When the cells were incubated with octreotate (range $3 \times 10^{-8} - 3 \times 10^{-7}$M) in the same concentration that is used with ^{177}Lu-octreotate, there is only a slight reduction of tumor cell survival (5% to 10%, Fig. 3).

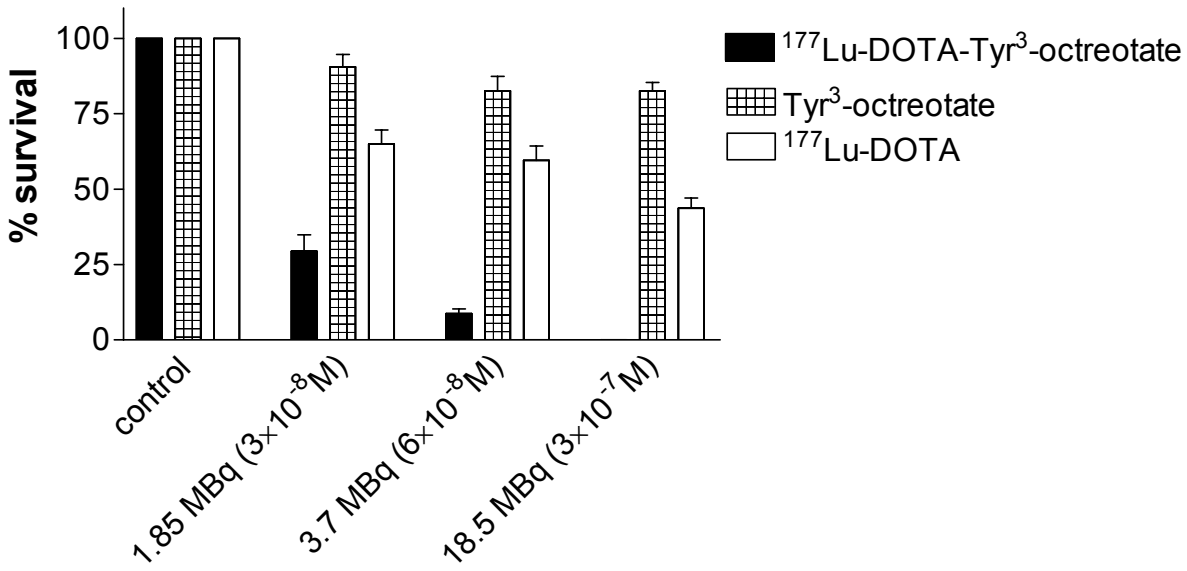

FIGURE 3. *Tumoricidal effect of ^{177}Lu-octreotate, octreotate and ^{177}Lu-DOTA on the clonogenic cell survival on the rat pancreatic tumor cell line CA20948. Cells were incubated for 1 hour at 37°C with increasing amounts of ^{177}Lu-octreotate, octreotate and ^{177}Lu-DOTA. Data are expressed as mean ± standard error of the mean from 2 independent experiments performed in triplicate.*

Comparison of octreotide versus octreotate labeled with ^{177}Lu or ^{90}Y. To compare the tumoricidal effects of the two peptides, Tyr^3-octreotide versus Tyr^3- octreotate, the peptides were labeled with either ^{177}Lu or ^{90}Y. Figure 4 shows the tumoricidal effect of the two peptides Tyr^3-octreotate and Tyr^3-octreotide labeled with the radiolanthanide ^{177}Lu, to compare their tumoricidal effect. The peptides were labeled with the same specific activity, 18.5 MBq to 0.6 μg peptide. The cells were incubated for 1 hour with the radiolabeled peptides and survival values are shown as percentage survival compared to control. Figure 4 shows that both peptides Tyr^3-octreotide and Tyr^3-octreotate labeled with ^{177}Lu control tumor growth in a dose-dependent manner. The peptide Tyr^3-octreotate has a higher tumoricidal effect compared with Tyr^3-octreotide at each concentration that was used ($p < 0.05$). The calculated number of decays per cell assuming 0.1% uptake after 1 hour incubation with 0.37 MBq ^{177}Lu-peptide was 4.9×10^5 decays per cell.

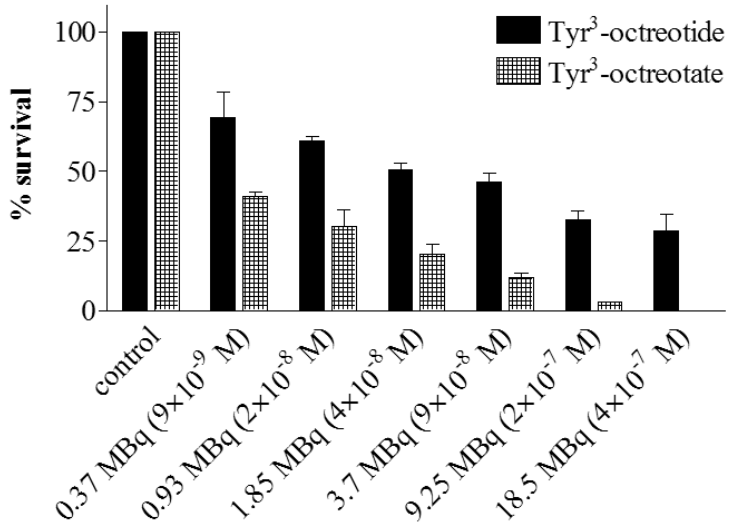

FIGURE 4. *Inhibitory effect of ^{177}Lu coupled to either octreotide or octreotate on the tumor cell survival of the CA20948 cell line. Cells were incubated for 1 hour at 37°C with increasing amounts of ^{177}Lu-octreotate or ^{177}Lu-octreotide. Data are expressed as mean ± standard error of the mean from 2 independent experiments performed in triplicate.*

Figure 5 shows the tumoricidal effect of ^{90}Y labeled with Tyr^3-octreotate or Tyr^3-octreotide on the CA20948 cell line after an incubation of 1 hour. Survival values are shown as percentage survival compared with that of the control cells. Figure 5 shows that both peptides Tyr^3-octreotide and Tyr^3-octreotate labeled with ^{90}Y are also able to control tumor growth in a dose-dependent manner. When the tumoricidal effects of the two peptides Tyr^3-octreotate and Tyr^3-octreotide are compared, Figure 5 also shows that the tumoricidal effect of Tyr^3-octreotate is superior to that of Tyr^3-octreotide ($p < 0.002$). The calculated number of decays per cell, assuming 0.1% uptake after 1 hour incubation with 0.37 MBq ^{90}Y-peptide was 2.81×10^5 decays per cell.

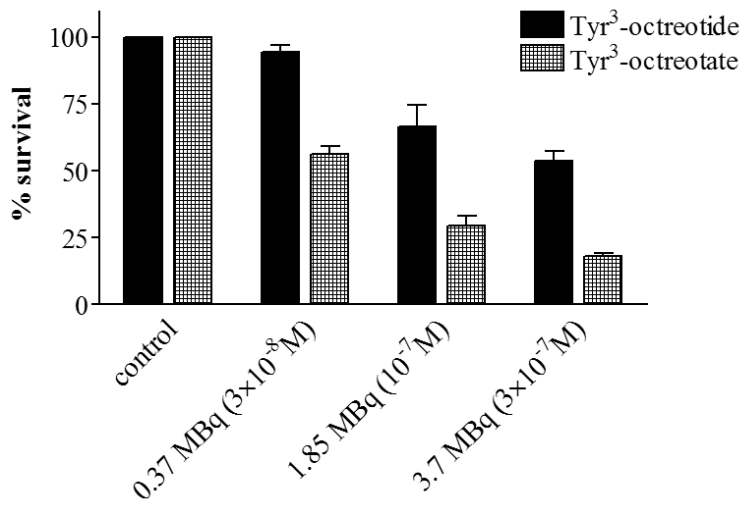

FIGURE 5. *Inhibitory effect of ^{90}Y coupled to either octreotide or octreotate on the tumor cell survival of the CA20948 cell line. Cells were incubated for 1 hour at 37°C with increasing amounts of ^{90}Y-octreotate or ^{90}Y-octreotide. Data are expressed as mean ± standard error of the mean from 2 independent experiments performed in triplicate.*

DISCUSSION

Despite promising results with the ^{111}In-labeled peptides targeting somatostatin receptors, there have been several reports describing alternative somatostatin radioligands [20, 28, 32-35]. Using cell lines transfected with somatostatin receptor subtypes sst_1, sst_2, sst_3, sst_4 or sst_5, Reubi et al. [36] evaluated the *in vitro* characteristics of labeled (indium, yttrium, gallium) and unlabeled DOTA-Tyr^3-octreotide, DOTA-octreotide, DOTA-lantreotide, DOTA-vapreotide, DTPA-Tyr^3-octreotate and DOTA-Tyr^3-octreotide. They found that small structural modifications, chelator substitution or metal replacement were shown to considerably affect the binding affinity. For example, a marked improvement of sst_2 affinity was found for ^{67}Ga-DOTA-Tyr^3-octreotide (IC_{50} 2.5 nM) compared with the ^{90}Y-labeled compound and ^{111}In-DTPA-octreotide. A binding affinity for sst_2 in the same range was also found for ^{111}In-DTPA-Tyr^3-octreotate (IC_{50} 1.3 nM) and for ^{90}Y-DOTA-Tyr^3-octreotate (IC_{50} 1.6 nM). In our preclinical PRRT studies the rat pancreatic CA20948 tumor cell line is used. In this model the analog Tyr^3-octreotate gives the highest uptake of 4 different ^{111}In-labeled DTPA-chelated somatostatin analogs in tumor bearing rats [15]. In patients, radiolabeled octreotate appeared to have a higher tumor uptake than ^{111}In-labeled octreotide as well [18].

In this study we investigated the tumoricidal effects of Tyr^3-octreotide and Tyr^3-octreotate labeled with either ^{177}Lu or ^{90}Y in an *in vitro* colony-forming assay. We first investigated the uptake and internalization characteristics of ^{177}Lu-octreotate in this *in vitro* system. The amount of internalized radioactivity was dependent on the amount of cells and on the dose of radioactivity that was added to them. Figure 1B also shows that the amount of

peptide affects the percentage radioactivity that is internalized into the cells. The lowest amount of radioactivity combined with the lowest amount of peptide revealed the highest percentage internalized radioactivity. This is consistent with the findings that the percentage internalized radioactivity is dependent on the amount of peptide that is added [37, 38]. The percentage cell-bound radioactivity is also dependent on the specific activity used; at a high specific activity there is less unlabeled peptide present and therefore there will be less competition between labeled and unlabeled peptide for the receptor, and a higher percentage of the dose is internalized compared with a lower specific activity. The highest concentration of ^{177}Lu-octreotate that is used, shown in Figure 1 (3.7 MBq), also has the highest peptide amount, which is approximately 8×10^{-8} M, and the lowest percentage of the dose internalized. This peptide concentration is rather high; the lower percentage of the dose that is internalized is probably due to partial saturation of the sst_2.

We further showed that ^{177}Lu-octreotate (Fig. 2) had a considerable tumoricidal effect in this single cell *in vitro* system. With a higher specific activity used, a higher tumoricidal effect was observed (see Fig. 2); also a lower tumor survival was found with a longer incubation period. So, the differences in tumor cell survival were dependent on the radiation dose, incubation time and, the specific activity used.

The tumoricidal effects of ^{177}Lu-octreotate, ^{177}Lu-DOTA and Tyr^3-octreotate were compared. One-hour incubation with ^{177}Lu-DOTA had already a pronounced effect on the tumor cell survival. As only a small fraction of radioactivity under these low cell density conditions will be internalized after incubation with ^{177}Lu-octreotate, a considerable percentage of tumor kill is already started during the 1-hour incubation period, most probably due to crossfire.

We finally compared the tumoricidal effects of the two peptides Tyr^3-octreotide versus Tyr^3-octreotate. Both compounds, radiolabeled with either ^{177}Lu or ^{90}Y, were capable of controlling tumor growth in a dose-dependent manner. Our results illustrates that Tyr^3-octreotate caused a higher tumor kill compared to Tyr^3-octreotide at all concentrations studied. This is in accordance with the finding that the radiolabeled octreotate analogs have a higher affinity for the sst_2-receptor compared with the corresponding octreotide analogs, which leads to a higher amount of internalized radioactivity, thereby resulting in a significantly higher tumor radiation dose in radionuclide therapy studies [15].

It is difficult to compare the effects of ^{177}Lu versus ^{90}Y in this in vitro system. ^{90}Y has higher energy compared with ^{177}Lu, leading to a higher dose to the cell, but the absorbed fraction of energy per cell is smaller for ^{90}Y than for ^{177}Lu, resulting in a lower *S* value (mGy/MBq/s^{-1}) of ^{90}Y (6.00×10^{-5} mGy/MBq/s^{-1}) in a single cell of 10 μm compared to ^{177}Lu (2.11×10^{-4} mGy/MBq/s^{-1}). We calculated the number of decays per cell per 0.1% uptake of ^{177}Lu- or ^{90}Y-peptide after 1-hour incubation with 0.37 MBq, resulting in 4.95×10^5 decays per cell for ^{177}Lu, and 2.81×10^5 decays per cell for ^{90}Y. So, ^{177}Lu is more effective in this

single cell system compared to ^{90}Y. On the other hand, crossfire in our system is much more pronounced with ^{90}Y than with ^{177}Lu, due to the longer particle range of the ^{90}Y β-particles versus ^{177}Lu-particles (maximum 12 mm versus 2 mm, respectively).

In preclinical PRRT studies *in vivo* [29] we also had promising results: a 100% cure rate in rats bearing small (≤1 cm^2) CA20948 tumors after 2 doses of 277.5 MBq or after a single dose of 555 MBq ^{177}Lu-octreotate. After PRRT with two doses of 277.5 MBq ^{177}Lu-DOTA-Tyr^3-octreotide, which has a lower tumor uptake compared with ^{177}Lu-octreotate, a cure rate of 60% was found. In rats bearing larger tumors (≥1 cm^2), 40% and 50% cure rates were found in groups that received 1 or 2 injections of 277.5 MBq ^{177}Lu-octreotate, respectively.
Currently, various phase I and II studies are being performed with ^{90}Y-octreotide [8, 19-25]. In these different studies partial and complete remissions were found in approximately 24% of the patients. Also studies with ^{177}Lu-octreotate have been started recently [26]. The effects of ^{177}Lu-octreotate therapy have been reported in 35 patients with neuroendocrine gastro-entero-pancreatic (GEP) tumors. Patients were treated with dosages of 3700, 5500 or 7400 MBq ^{177}Lu-octreotate, to a final cumulative dose of 22.2-29.6 GBq with treatment intervals of 6-9 weeks. Three months after the final administration, complete or partial remissions were found in 38% of the patients, showing the great potential of ^{177}Lu-octreotate for PRRT.

REFERENCES

1. Yamada Y, Kagimoto S, Kubota A, Yasuda K, Masuda K, Someya Y, Ihara Y, Li Q, Imura H, Seino S, et al. Cloning, functional expression and pharmacological characterization of a fourth (hSSTR4) and a fifth (hSSTR5) human somatostatin receptor subtype. *Biochem Biophys Res Commun* 1993;195:844-852.
2. Kubota A, Yamada Y, Kagimoto S, Shimatsu A, Imamura M, Tsuda K, Imura H, Seino S, Seino Y. Identification of somatostatin receptor subtypes and an implication for the efficacy of somatostatin analogue SMS 201-995 in treatment of human endocrine tumors. *J Clin Invest* 1994;93:1321-1325.
3. Patel YC. Somatostatin and its receptor family. *Front Neuroendocrinol* 1999;20:157-198.
4. Patel YC, Greenwood M, Panetta R, Hukovic N, Grigorakis S, Robertson LA, Srikant CB. Molecular biology of somatostatin receptor subtypes. *Metabolism* 1996;45:31-38.
5. Bell GI, Reisine T. Molecular biology of somatostatin receptors. *Trends Neurosci* 1993;16:34-38.
6. Reisine T, Bell GI. Molecular properties of somatostatin receptors. *Neuroscience* 1995;67:777-790.
7. Reubi JC, Laissue J, Krenning E, Lamberts SW. Somatostatin receptors in human cancer: incidence, characteristics, functional correlates and clinical implications. *J Steroid Biochem Mol Biol* 1992;43:27-35.
8. De Jong M, Breeman WA, Bernard HF, Kooij PP, Slooter GD, Van Eijck CH, Kwekkeboom DJ, Valkema R, Macke HR, Krenning EP. Therapy of neuroendocrine tumors with radiolabeled somatostatin- analogues. *Q J Nucl Med* 1999;43:356-366.
9. Krenning EP, Valkema R, Kooij PP, Breeman WA, Bakker WH, deHerder WW, vanEijck CH, Kwekkeboom DJ, deJong M, Pauwels S. Scintigraphy and radionuclide therapy with [indium-111-labelled-diethyl triamine penta-acetic acid-D-Phe1]-octreotide. *Ital J Gastroenterol Hepatol* 1999;31 Suppl 2:S219-223.
10. McCarthy KE, Woltering EA, Anthony LB. In situ radiotherapy with 111In-pentetreotide. State of the art and perspectives. *Q J Nucl Med* 2000;44:88-95.
11. Anthony LB, Woltering EA, Espenan GD, Cronin MD, Maloney TJ, McCarthy KE. Indium-111-pentetreotide prolongs survival in gastroenteropancreatic malignancies. *Semin Nucl Med* 2002;32:123-132.
12. Valkema R, De Jong M, Bakker WH, Breeman WA, Kooij PP, Lugtenburg PJ, De Jong FH, Christiansen A, Kam BL, De Herder WW, Stridsberg M, Lindemans J, Ensing G, Krenning EP. Phase I study of peptide receptor radionuclide therapy with [In- DTPA]octreotide: the Rotterdam experience. *Semin Nucl Med* 2002;32:110-122.
13. Krenning EP, de Jong M, Kooij PP, Breeman WA, Bakker WH, de Herder WW, van Eijck CH, Kwekkeboom DJ, Jamar F, Pauwels S, Valkema R. Radiolabelled somatostatin analogue(s) for peptide receptor scintigraphy and radionuclide therapy. *Ann Oncol* 1999;10:S23-29.
14. Kwekkeboom D, Krenning EP, de Jong M. Peptide receptor imaging and therapy. *J Nucl Med* 2000;41:1704-1713.

15. de Jong M, Breeman WA, Bakker WH, Kooij PP, Bernard BF, Hofland LJ, Visser TJ, Srinivasan A, Schmidt MA, Erion JL, Bugaj JE, Macke HR, Krenning EP. Comparison of (111)In-labeled somatostatin analogues for tumor scintigraphy and radionuclide therapy. *Cancer Res* 1998;58:437-441.
16. Lewis JS, Srinivasan A, Schmidt MA, Anderson CJ. In vitro and in vivo evaluation of 64Cu-TETA-Tyr3-octreotate. A new somatostatin analog with improved target tissue uptake. *Nucl Med Biol* 1999;26:267-273.
17. Lewis JS, Lewis MR, Cutler PD, Srinivasan A, Schmidt MA, Schwarz SW, Morris MM, Miller JP, Anderson CJ. Radiotherapy and dosimetry of 64Cu-TETA-Tyr3-octreotate in a somatostatin receptor-positive, tumor-bearing rat model. *Clin Cancer Res* 1999;5:3608-3616.
18. Kwekkeboom DJ, Bakker WH, Kooij PP, Konijnenberg MW, Srinivasan A, Erion JL, Schmidt MA, Bugaj JL, de Jong M, Krenning EP. [177Lu-DOTAOTyr3]octreotate: comparison with [111In-DTPAo]octreotide in patients. *Eur J Nucl Med* 2001;28:1319-1325.
19. Otte A, Herrmann R, Heppeler A, Behe M, Jermann E, Powell P, Maecke HR, Muller J. Yttrium-90 DOTATOC: first clinical results. *Eur J Nucl Med* 1999;26:1439-1447.
20. Otte A, Jermann E, Behe M, Goetze M, Bucher HC, Roser HW, Heppeler A, Mueller-Brand J, Maecke HR. DOTATOC: a powerful new tool for receptor-mediated radionuclide therapy. *Eur J Nucl Med* 1997;24:792-795.
21. Paganelli G, Bodei L, Chinol M, Zoboli S, Cremonesi M, Gatti M, Bartolomei M, Grana C, Maecke H. Receptor mediated radiotherapy with ^{90}Y-DOTATOC: results of a phase I study. *J Nucl Med* 2001;42:36P.
22. Valkema R, Jamar F, Bakker WH, Norenberg J, Smith C, Stolz B, Kvols L, Pauwels S, Krenning EP. Safety and efficacy of [Y-90-DOTA,Tyr(3)]octreotide (Y-90-SMT487; OCTREOTHER ™) peptide receptor radionuclide therapy (PRRT). Preliminary results of a phase-1 study. *Eur J Nucl Med* 2001;28:1025P.
23. Waldherr C, Pless M, Maecke HR, Haldemann A, Mueller-Brand J. The clinical value of [90Y-DOTA]-D-Phe1-Tyr3-octreotide (90Y-DOTATOC) in the treatment of neuroendocrine tumours: a clinical phase II study. *Ann Oncol* 2001;12:941-945.
24. Waldherr C, Pless M, Maecke HR, Schumacher T, Crazzolara A, Nitzsche EU, Haldemann A, Mueller-Brand J. Tumor response and clinical benefit in neuroendocrine tumors after 7.4 GBq (90)Y-DOTATOC. *J Nucl Med* 2002;43:610-616.
25. Paganelli G, Zoboli S, Cremonesi M, Bodei L, Ferrari M, Grana C, Bartolomei M, Orsi F, De Cicco C, Macke HR, Chinol M, de Braud F. Receptor-mediated radiotherapy with 90Y-DOTA-D-Phe1-Tyr3-octreotide. *Eur J Nucl Med* 2001;28:426-434.
26. De Jong M, Kwekkeboom D, Valkema R, Krenning EP. Radiolabelled peptides for tumour therapy: current status and future directionsPlenary lecture at the EANM 2002. *Eur J Nucl Med Mol Imaging* 2003;5:5
27. Capello A, Krenning EP, Breeman WA, Bernard BF, de Jong M. Peptide receptor radionuclide therapy in vitro using [111In- DTPA0]octreotide. *J Nucl Med* 2003;44:98-104.
28. De Jong M, Bakker WH, Breeman WA, Bernard BF, Hofland LJ, Visser TJ, Srinivasan A, Schmidt M, Behe M, Macke HR, Krenning EP. Pre-clinical comparison of [DTPA0] octreotide, [DTPA0,Tyr3] octreotide and [DOTA0,Tyr3] octreotide as carriers for

somatostatin receptor- targeted scintigraphy and radionuclide therapy. *Int J Cancer* 1998;75:406-411.

29. de Jong M, Breeman WA, Bernard BF, Bakker WH, Schaar M, van Gameren A, Bugaj JE, Erion J, Schmidt M, Srinivasan A, Krenning EP. [177Lu-DOTA(0),Tyr3] octreotate for somatostatin receptor-targeted radionuclide therapy. *Int J Cancer* 2001;92:628-633.
30. de Jong M, Breeman WA, Bernard BF, Bakker WH, Visser TJ, Kooij PP, van Gameren A, Krenning EP. Tumor response after [(90)Y-DOTA(0),Tyr(3)]octreotide radionuclide therapy in a transplantable rat tumor model is dependent on tumor size. *J Nucl Med* 2001;42:1841-1846.
31. Erion JL, Bugaj JE, Schmidt MA, Wilhelm RR, Srinivasan A. High radiotherapeutic efficacy of [Lu-177]-DOTA-Y3-octreotate in a rat tumor model [abstract]. *J Nucl Med* 1999;40:223p.
32. Virgolini I, Szilvasi I, Kurtaran A, Angelberger P, Raderer M, Havlik E, Vorbeck F, Bischof C, Leimer M, Dorner G, Kletter K, Niederle B, Scheithauer W, Smith-Jones P. Indium-111-DOTA-lanreotide: biodistribution, safety and radiation absorbed dose in tumor patients. *J Nucl Med* 1998;39:1928-1936.
33. Breeman WAP, van Hagen PM, Kwekkeboom DJ, Visser TJ, Krenning EP. Somatostatin receptor scintigraphy using [111In-DTPA0]RC-160 in humans: a comparison with [111In-DTPA0]octreotide. *Eur J Nucl Med* 1998;25:182-186.
34. Zamora PO, Gulhke S, Bender H, Diekmann D, Rhodes BA, Biersack HJ, Knapp FF, Jr. Experimental radiotherapy of receptor-positive human prostate adenocarcinoma with 188Re-RC-160, a directly-radiolabeled somatostatin analogue. *Int J Cancer* 1996;65:214-220.
35. De Jong M, Bernard BF, De Bruin E, Van Gameren A, Bakker WH, Visser TJ, Macke HR, Krenning EP. Internalization of radiolabelled [DTPA0]octreotide and [DOTA0,Tyr3]octreotide: peptides for somatostatin receptor-targeted scintigraphy and radionuclide therapy. *Nucl Med Commun* 1998;19:283-288.
36. Reubi JC, Schar JC, Waser B, Wenger S, Heppeler A, Schmitt JS, Macke HR. Affinity profiles for human somatostatin receptor subtypes SST1-SST5 of somatostatin radiotracers selected for scintigraphic and radiotherapeutic use. *Eur J Nucl Med* 2000;27:273-282.
37. Breeman WA, Kwekkeboom DJ, Kooij PP, Bakker WH, Hofland LJ, Visser TJ, Ensing GJ, Lamberts SW, Krenning EP. Effect of dose and specific activity on tissue distribution of indium- 111-pentetreotide in rats. *J Nucl Med* 1995;36:623-627.
38. de Jong M, Breeman WA, Bernard BF, van Gameren A, de Bruin E, Bakker WH, van der Pluijm ME, Visser TJ, Macke HR, Krenning EP. Tumour uptake of the radiolabelled somatostatin analogue [DOTA0, TYR3]octreotide is dependent on the peptide amount. *Eur J Nucl Med* 1999;26:693-698.

CHAPTER 4

RADIONUCLIDE THERAPY WITH ^{177}Lu OR ^{90}Y LABELED PEPTIDES

4.2 Anti-tumor effect and increased survival after treatment with ^{177}Lu-DOTA-Tyr^3-octreotate in a rat liver micrometastases model

Wout Breeman, Amir Mearadji, Astrid Capello, Bert Bernard, Casper van Eijck, Eric Krenning and Marion de Jong.

International Journal of Cancer, 2003, 104: 376-379.

ABSTRACT

Peptide receptor scintigraphy with ^{111}In-DTPA-octreotide (a stabilized radiolabeled somatostatin (SS) analog, OctreoScan®) is widely used for the visualization and staging of somatostatin receptor-positive tumors. The application of likewise somatostatin analogs as vehicle for the deliverance of radionuclides to somatostatin receptor-positive targets are now in use for peptide receptor-targeted radionuclide therapy (PRRT). Currently preclinical and clinical investigation are ongoing trying to find the optimal combination of radionuclide and ligand. The anti-tumoral effects of such combinations, like ^{90}Y-DOTA-Tyr^3-octreotide and ^{177}Lu-DOTA-Tyr^3-octreotate, on SSR-positive solid tumors have been reported. In this study we present the anti-tumor effects of ^{177}Lu-DOTA-tate on: a) a single SSR-positive cell model and b) on a SSR-positive tumor in a rat liver micrometastatic model, mimicking disseminated disease. ^{177}Lu-DOTA-tate showed anti-tumoral effects in both cases and significant survival in the PRRT-treated rats. ^{177}Lu-DOTA-tate is a very promising new treatment modality for SSR-positive tumors, including disseminated disease.

INTRODUCTION

Somatostatin receptors (SSRs) have been demonstrated on a variety of human tumors [1]. At least 5 different human subtypes (SSR Subtype 1–5) have been cloned [2]. All subtypes bind somatostatin with high affinity, whereas octreotide, a somatostatin analog, binds with high affinity to SSR2, and with decreasing affinity for SSR5 and SSR3 [3]. The vast majority of human SSR-positive tumors express SSR Subtype 2 [3, 4]. SSR-positive tumors, like carcinoids, breast cancer and various neuroendocrine tumors, can be visualized with ^{111}In-DTPA-octreotide (OctreoScan®). OctreoScan is nowadays recognized to be the imaging technique for the detection and staging of SSR-positive tumors. Peptide receptor radionuclide therapy (PRRT) with high dosages of ^{111}In-DTPA-octreotide showed anti-tumor effects in a rat liver micrometastases model [5] and in patients with neuroendocrine tumors [6-9]. The disadvantage of ^{111}In for PRRT is the short particle range and consequently small tissue penetration [10]. Therefore, other radionuclides, like ^{90}Y and ^{177}Lu, were coupled to DOTA-conjugated somatostatin analogs, such as DOTA-Tyr^3-octreotide (DOTATOC) and DOTA-Tyr^3-octreotate [3]. These radionuclides emit high-energy beta particles (2.27 and 0.5 MeV, respectively) with accordingly larger particle range of 10 and 2 mm, respectively [3].

Various studies have shown favorable results of ^{90}Y-DOTATOC and ^{177}Lu-DOTA-tate use in patients with neuroendocrine tumors [11-14]. PRRT with radionuclides emitting higher energy beta-particles (*e.g.*, ^{90}Y) are in theory and in practice advantageous for larger tumors (>1g), but not for smaller tumors (<1g). For uniform activity distribution in these larger tumors, almost all energy of the emitted electrons will be deposited in the target. For the smaller tumors, however, only a small energy fraction from the emitted electrons will be deposited within the tumor [15-18]. We recently presented successful PRRT with ^{177}Lu-DOTA-tate of SSR-positive solid tumors in rats [17] and also in patients [14]. The question still remains whether ^{177}Lu has anti-tumor effects on SSR-positive micrometastases. We describe a PRRT study with ^{177}Lu-DOTA-tate of SSR-positive tumor cells in an *in vitro* model and in a rat liver micrometastatic model.

MATERIALS AND METHODS

Animals

Male inbred Lewis rats, 10–14 weeks old with a body weight of 250–275 g, were obtained from Harlan-CPB (Horst, The Netherlands). Animals were kept under standard laboratory conditions (12 hr light/12 hr dark) and given a standard laboratory diet (Hope Farms, Woerden, The Netherlands) and water *ad lib*. The experimental protocol adhered to the rules of the Dutch Animal Experimental Act and was approved by the Committee on Animal Research of the Erasmus University.

Tumor

CC531 is a SSR-negative, moderately differentiated rat colon carcinoma, induced by 1,2-dimethylhydrazine, and is transplantable in syngeneic WAG/Rij rats [5]. The tumor is maintained in tissue culture as a monolayer in RPMI 1640 medium (Gibco, Paisley, UK) supplemented with 5% FCS. Cells were harvested from stationary cultures by gentle trypsinization (Boehringer, Mannheim, Germany).

CA20948 is a SSR-positive, pancreatic tumor of acinar origin that was originally induced by azaserine and is transplantable in syngeneic Lewis rats [16]. The tumor is maintained in tissue culture as a monolayer in RPMI 1640 medium (Gibco, Paisley, UK) supplemented with 10% FCS. For the *in vitro* experiments, cells were harvested from stationary cultures by gentle trypsinisation (Boehringer). To produce artificial liver metastases for the *in vivo* experiments, tumors were excised from donor rat livers, cleaned from normal liver tissue and pressed through sieves with decreasing mesh size. The resulting suspension was washed twice in RPMI 1640. Viability was measured with trypan-blue exclusion (0.3% in a 0.9% NaCl solution). A suspension of 2.5 x 10^6 living cells per 5 ml was used for direct injection into the portal vein [5, 19].

Radiolabeling and quality control of the radioligand

Reactor-produced ^{177}Lu from 70% enriched ^{176}Lu-target was obtained from IDB Holland Baarle Nassau, The Netherlands). DOTA-tate was obtained from Mallinckrodt (St. Louis, MO). ^{177}Lu-labeling of DOTA-tate was carried out as described previously [17, 18, 20]. Measurement of the incorporation of the radionuclide was carried out in the presence of 4 mM DTPA pH 4 on ITLC-SG with 0.1 M Na-citrate as eluents [17, 18]. The labeling yield always exceeded 99% and the radiochemical purity was higher than 90%. Post radiolabeling and before the administration of the radioligand-containing solution 4 mM DTPA pH 4 was added to a final mol/mol ratio (DTPA over DOTA-tate) of 30.

In vitro PRRT

One day before the experiment CC531 and CA20948 tumor cells were transferred to 6-well plates in a density of 200 and 400 cells per well. Cells were washed with PBS (37°C) and incubated for at least 1 hr in 1 ml incubation medium (RPMI-1640 medium without FCS but with 1% bovine serum albumin and 20 mmol HEPES) containing ^{177}Lu-DOTA-tate. Control cells received only incubation medium for 1 hr. Thereafter, cells were thoroughly washed with PBS and allowed to form colonies during 2 days in growth medium. The medium was once refreshed after 3 days. At Day 12 the cells were fixated with 1 ml methanol:glacial acid (3:1) for 15 min. Subsequently the cells were colored with haematoxylin (Dako, Glostrup, Denmark). Colonies that contained more than 50 cells per colony were scored as survivors.

In vivo PRRT

Under ether anesthesia, the abdomen was opened through a 2.5 cm midline incision. 0.25 x 10^6 viable CA20948 cells in 0.5 ml RPMI 1640 were injected slowly into the portal vein through a 0.4 x 12 mm needle. The abdominal wall was closed in one layer by a continuous

silk suture. The day after the operation, rats were randomized in an experimental and control group. Each group consisted of 12 rats. Rats of the experimental group were treated with 185 (1.9 µg) or 370 MBq (3.8 µg) ^{177}Lu-DOTA-Tyr^3-octreotate i.v. on Day 8. Rats in the control group did not receive treatment. Body weight and animal condition (*i.e.*, lethargy, scruffy coat and diarrhea) were determined at regular intervals at least twice a week.

To evaluate anti-tumor effects, half of the rats were sacrificed 21 days after inoculation of tumor cells. Livers were removed, washed and immersed in PBS. Livers were weighed and 2 independent investigators counted the number of metastases on the surface of the liver lobes (up to 100) while blinded for treatment modality determined tumor growth. The number of metastases was subdivided in a semi-quantitative tumor score, with concordant ranking from 0 (no metastases) up to 5 (> 100 tumor colonies, with >50% of liver affected) as presented in Table I.

The remaining rats were used for a survival experiment. The experiment was ended 150 days post inoculation of the tumor; 150 days is the generally accepted equivalent of 5 years human survival. Body weight and animal condition was determined at regular intervals at least twice a week. When loss of body weight was more than 10% of original body weight, rats were sacrificed and livers examined.

Statistical analysis

Statistical analysis of the data was carried out using one-way analysis of variance. When significant effects were obtained by analysis of variance, multiple comparison were made by the Newman-Keuls test. Statistical significance was defined as $p < 0.05$. Data are expressed as mean ± SD. GraphPad Prism (GraphPad Prism Software, San Diego, CA) was used to plot survival curves for the different groups.

RESULTS

In vitro PRRT

Figure 1 shows the % survival of CA20948 and CC531 cells after *in vitro* PRRT with various amounts of ^{177}Lu-DOTA-tate. No differences were found between the experiments with 200 and 400 cells (data not shown).

In vivo PRRT

The results of PRRT with 185 MBq (1.9 µg) or 370 MBq (3.8 µg) ^{177}Lu-DOTA-tate on Day 8 on the growth of CA20948 liver metastases compared to rats of the control group are summarized in Table I. Both 185 MBq and 370 MBq ^{177}Lu-DOTA-tate had an anti-tumor effect on CA20948 liver metastases compared to controls. Mean tumor scores were 2.0 ± 1.3, 1.3 ± 0.8 and 5.0 ± 0.0, respectively ($p < 0.001$ *vs.* controls). Liver weight was significantly less in PRRT treated rats compared to controls: mean liver weights (in g) were 8.9 ± 0.9, 9.3 ± 0.7 and 19.2 ± 2.0, respectively ($p < 0.001$ *vs*. controls; Fig. 2).

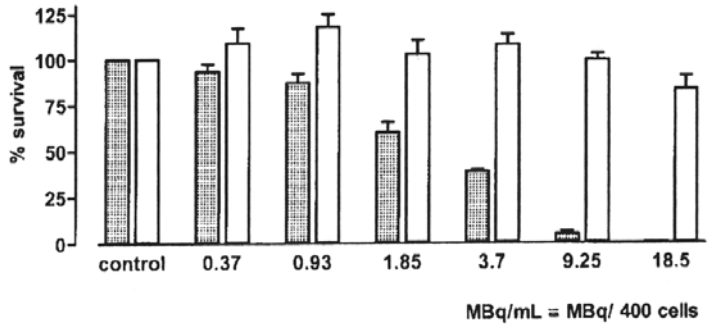

FIGURE 1. *The percentage survival of CA20948 and CC531 cells (open bar) after in vitro PRRT with various amounts of ^{177}Lu-DOTA-tate.*

TABLE 1. *Effect of 185 or 370 MBq ^{177}Lu-DOTA-octreotatate on CA20948 liver metastases*[1]

	0	1-20	21-50	51-100	>100[2]	>100[3]
Rank	0	1	2	3	4	5
Controls	-	-	-	-	-	6
185 MBq	1	1	1	3	-	-
370 MBq	2	-	4	-	-	-

[1]Number of animals with given range of metastases, 21 days after direct injection of CA20948 tumor cells into the portal vein. Treated rats (185 or 370 MBq ^{177}Lu-DOTA-tate) with CA20948 liver metastases had significantly fewer liver metastases compared with control rats ($p < 0.001$). [2]More than 100 tumor colonies, but <50% of liver is affected. [3]More than 100 tumor colonies, and >50% of liver is affected.

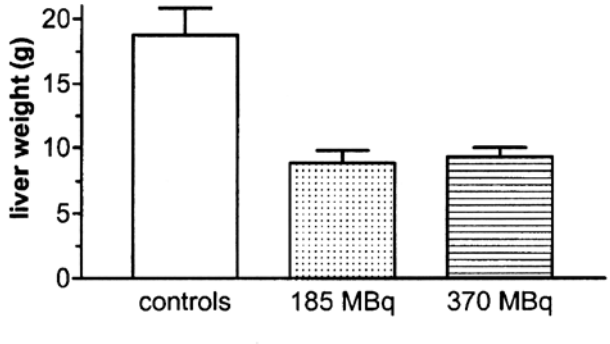

FIGURE 2. *Liver weight of groups of rats with CA20948 liver metastases after indicated doses (expressed as mean ± SD, n equals; 6). Mean liver weights of rats treated with 185 or 370 MBq ^{177}Lu-DOTA-tate are both less significant than control rats ($p < 0.001$).*

Survival curves for the control and therapeutic groups are shown in Figure 3. Tumors of the rats in the control group grew excessively and no survival at 150 days was found. Treatment with a single dose of 185 MBq ^{177}Lu-DOTA-tate resulted in a significant increase of the survival of the rats of this group. In all sacrificed rats livers were full of metastases. At 150 days after tumor inoculation, 2 of the 6 rats (33%) in this group were still alive and autopsy showed no visible liver metastases in these 2 rats ($p < 0.05$). Animals that received a single injection of 370 MBq ^{177}Lu-DOTA-tate also showed a significant increase in survival compared to controls, however, no animals survived 150 days ($p < 0.05$).

In the *in vivo* experiments no overt signs of toxicity such as weight loss, scruffy coat, lethargy or diarrhea were observed.

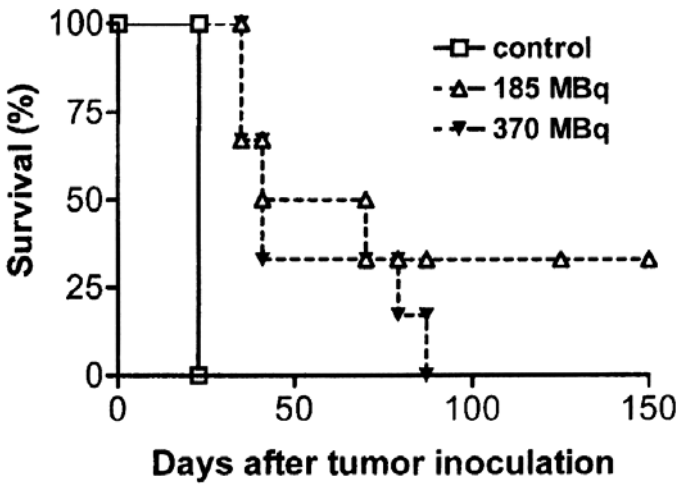

FIGURE 3. *Survival curves of groups of rats with CA20948 liver metastases after indicated doses (n = 6 per group). Both groups of rats treated with 185 and 370 MBq ^{177}Lu-DOTA-tate showed a significant increase in survival compared to controls (p < 0.05). Two of the 6 rats treated with 185 MBq ^{177}Lu-DOTA-tate survived 150 days and had no visible liver metastases after sacrifice.*

DISCUSSION

Peptide receptor scintigraphy with ^{111}In-DTPA-octreotide is widely used for the visualization and staging of SSR-positive tumors. The application of likewise ligands as vehicle for the deliverance of radionuclides to SSR-positive targets is now also in use for PRRT. Preclinical and clinical investigation is currently ongoing in an attempt to find the optimal combination of radionuclide and ligand (with both their specific characteristics) for several parameters, including tumor volume. The anti-tumoral effects of such a combination, ^{177}Lu-DOTA-tate, on SSR-positive solid tumors have been reported [14, 17].

We present the anti-tumor effects of ^{177}Lu-DOTA-tate *in vitro* in a single SSR-positive cell model, and on a SSR-positive tumor in a rat liver micrometastatic model, mimicking disseminated disease.

As shown in Figure 1, SSR-positive CA20948 tumor cell survival decreases with increasing doses of ^{177}Lu-DOTA-tate, and this in contrast to SSR-negative CC531 tumor cells in a parallel experiment. We reported earlier on experiments carried out to study internalization of radiolabeled somatostatin analogs such as ^{111}In-DTPA-octreotide and ^{90}Y-DOTATOC in rat pancreatic tumor cells [21, 22]. This process was found to be receptor-specific and temperature-dependent [22, 23]. Furthermore, the amount of radioligand taken up in the tumor depends on the total amount of unlabeled peptide present and thus on changes in specific activity of the radiolabeled peptide [24, 25]. The success of the therapeutic strategy therefore relies on the total amount of radioligand that accumulates within tumor cells, which among other things depends on the receptor affinity and rate of internalization of ligand and receptor. The physical characteristics of radioactivity accumulated within tumor cells

determines also the dosimetric dose on neighbouring cells. As stated above, ^{177}Lu emits β-particles with a maximum energy of 0.5 MeV and a high tissue penetration, with a maximum range of 2 mm. Assuming a cell diameter of 20 μm, this means, when internalized into the tumor cell, ^{177}Lu is able to potentially kill cells at approximately 12 cell diameters from a cell in which it is internalized, with a maximum cell-killing potential of approximately 50 cell diameters [26]. This extra cell killing potential is also called a radiological bystander effect [27] and can be an additional advantage in the PRRT of tumors with a heterogeneous expression of receptors with affinity for the radiolabeled peptide.

In Table I and in Figure 2 the tumor growth control by ^{177}Lu-DOTA-tate is presented. Tumor growth in controls was excessive, 21 days post inoculation of the tumor cells, more than 100 tumor colonies were counted in the livers and, in addition, more than 50% of the liver was affected. The liver weight doubled ($p < 0.001$) *vs*. the 2 PRRT-treated groups of rats (Fig. 2). We reported recently that PRRT with ^{111}In-DTPA-octreotide had no effects on basic liver functions [28]. The effect of PRRT was also reflected in the survival curve: rats treated with 185 or 370 MBq ^{177}Lu- DOTA-tate had significantly lower tumor colonies present at Day 21 (Fig. 2). Two of 6 survived for 150 days, which is the generally accepted equivalent of 5 human years. In the PRRT-treated rats a higher survival was found in the rats treated with the lower dose. The amounts of injected radioactivity in these 2 groups were 185 and 370 MBq, and the concordant amount of injected ligand: 1.9 μg and 3.8 μg, respectively. This increase in amount of injected ligand reduces the uptake in the SSR-positive targets: the uptake herein is a function of the injected mass [24, 25]. The uptake in SSR-positive tumor cells in rats injected with 1.9 μg is approximately 70% of the optimal uptake, and in the other group injected with 3.8 μg is 40%, resulting in no significant increase in radioactivity in the targets. So although the radioactive dose was doubled, the uptake of radioactivity in these SSR-positive targets was not increased, and as a result, neither was the dosimetric dose (in contrast to SSR-negative kidney and bone marrow). These organs are critical organs for PRRT with radiolabeled somatostatin analogs [3], and by definition determine the maximal tolerated dose hereof. Because the radiation dose has doubled, the dosimetric dose for these organs has doubled. Lewis *et al*. [29] reported recently, however, no toxicity for ^{177}Lu-DOTA-tate, even up to doses of 4 GBq per kg, and up to 42 days post injection.

A major advantage of PRRT using radiolabeled peptides is that radiation can be delivered selectively, not only to (large) primary tumors, but also to tumors and metastases that are too small to be imaged and thereby treated by, for example, surgery or external beam radiotherapy. Even tumors of less than 1 g are not able to absorb all electron energy emitted by 90Y in their cells [10, 15, 18]. Therefore, patients bearing tumors of different sizes might be treated by a combination of radionuclides, *e.g*., the high-energy β-emitter ^{90}Y for large tumors (>1 g) and low-energy β-emitter, such as ^{177}Lu, or an Auger electron emitter, such as ^{111}In for smaller (<1 g) tumors and metastases. Preclinical and clinical PRRT experiments of SSR-positive tumors are ongoing.

CONCLUSION

^{177}Lu-DOTA-tate showed anti-tumor effects in an isolated SSR-positive tumor cell model *in vitro* and in a rat liver SSR-positive micrometastic model setting, making it a very promising new treatment modality for SSR-positive disseminated disease.

ACKNOWLEDGEMENTS

A. van Gameren and E. de Blois are acknowledged for technical assistance.

REFERENCES

1. Reubi JC, Laissue J, Krenning E, Lamberts SW. Somatostatin receptors in human cancer: incidence, characteristics, functional correlates and clinical implications. *J Steroid Biochem Mol Biol* 1992;43:27-35.
2. Kubota A, Yamada Y, Kagimoto S, Shimatsu A, Imamura M, Tsuda K, Imura H, Seino S, Seino Y. Identification of somatostatin receptor subtypes and an implication for the efficacy of somatostatin analogue SMS 201-995 in treatment of human endocrine tumors. *J Clin Invest* 1994;93:1321-1325.
3. Breeman WA, de Jong M, Kwekkeboom DJ, Valkema R, Bakker WH, Kooij PP, Visser TJ, Krenning EP. Somatostatin receptor-mediated imaging and therapy: basic science, current knowledge, limitations and future perspectives. *Eur J Nucl Med* 2001;28:1421-1429.
4. Reubi JC, Waser B, Schaer JC, Laissue JA. Somatostatin receptor sst1-sst5 expression in normal and neoplastic human tissues using receptor autoradiography with subtype-selective ligands. *Eur J Nucl Med* 2001;28:836-846.
5. Slooter GD, Breeman WA, Marquet RL, Krenning EP, van Eijck CH. Anti-proliferative effect of radiolabelled octreotide in a metastases model in rat liver. *Int J Cancer* 1999;81:767-771.
6. Krenning EP, Valkema R, Kooij PP, Breeman WA, Bakker WH, de Herder WW, van Eijck CH, Kwekkeboom DJ, de Jong M, Jamar F, Pauwels S. The role of radioactive somatostatin and its analogues in the control of tumor growth. *Recent Results Cancer Res* 2000;153:1-13.
7. McCarthy KE, Woltering EA, Espenan GD, Cronin M, Maloney TJ, Anthony LB. In situ radiotherapy with 111In-pentetreotide: initial observations and future directions. *Cancer J Sci Am* 1998;4:94-102.
8. Meyers MO, Anthony LB, McCarthy KE, Drouant G, Maloney TJ, Espanan GD, Woltering EA. High-dose indium 111In pentetreotide radiotherapy for metastatic atypical carcinoid tumor. *South Med J* 2000;93:809-811.
9. Caplin ME, Mielcarek W, Buscombe JR, Jones AL, Croasdale PL, Cooper MS, Burroughs AK, Hilson AW. Toxicity of high-activity 111In-Octreotide therapy in patients with disseminated neuroendocrine tumours. *Nucl Med Commun* 2000;21:97-102.
10. Bernhardt P, Benjegard SA, Kolby L, Johanson V, Nilsson O, Ahlman H, Forssell-Aronsson E. Dosimetric comparison of radionuclides for therapy of somatostatin receptor-expressing tumors. *Int J Radiat Oncol Biol Phys* 2001;51:514-524.
11. Cremonesi M, Ferrari M, Zoboli S, Chinol M, Stabin MG, Orsi F, Maecke HR, Jermann E, Robertson C, Fiorenza M, Tosi G, Paganelli G. Biokinetics and dosimetry in patients administered with (111)In-DOTA- Tyr(3)-octreotide: implications for internal radiotherapy with (90)Y- DOTATOC. *Eur J Nucl Med* 1999;26:877-886.
12. Otte A, Jermann E, Behe M, Goetze M, Bucher HC, Roser HW, Heppeler A, Mueller-Brand J, Maecke HR. DOTATOC: a powerful new tool for receptor-mediated radionuclide therapy. *Eur J Nucl Med* 1997;24:792-795.
13. Paganelli G, Zoboli S, Cremonesi M, Bodei L, Ferrari M, Grana C, Bartolomei M, Orsi F, De Cicco C, Macke HR, Chinol M, de Braud F. Receptor-mediated radiotherapy with 90Y-DOTA-D-Phe1-Tyr3-octreotide. *Eur J Nucl Med* 2001;28:426-434.
14. Kwekkeboom DJ, Bakker WH, Kooij PP, Konijnenberg MW, Srinivasan A, Erion JL, Schmidt MA, Bugaj JL, de Jong M, Krenning EP. [177Lu-DOTAOTyr3]octreotate: comparison with [111In-DTPAo]octreotide in patients. *Eur J Nucl Med* 2001;28:1319-1325.

15. O'Donoghue JA, Bardies M, Wheldon TE. Relationships between tumor size and curability for uniformly targeted therapy with beta-emitting radionuclides [see comments]. *J Nucl Med* 1995;36:1902-1909.
16. Bernard BF, Krenning E, Breeman WA, Visser TJ, Bakker WH, Srinivasan A, de Jong M. Use of the rat pancreatic CA20948 cell line for the comparison of radiolabelled peptides for receptor-targeted scintigraphy and radionuclide therapy. *Nucl Med Commun* 2000;21:1079-1085.
17. de Jong M, Breeman WA, Bernard BF, Bakker WH, Schaar M, van Gameren A, Bugaj JE, Erion J, Schmidt M, Srinivasan A, Krenning EP. [177Lu-DOTA(0),Tyr3] octreotate for somatostatin receptor-targeted radionuclide therapy. *Int J Cancer* 2001;92:628-633.
18. de Jong M, Breeman WA, Bernard BF, Bakker WH, Visser TJ, Kooij PP, van Gameren A, Krenning EP. Tumor response after [(90)Y-DOTA(0),Tyr(3)]octreotide radionuclide therapy in a transplantable rat tumor model is dependent on tumor size. *J Nucl Med* 2001;42:1841-1846.
19. Marquet RL, Westbroek DL, Jeekel J. Interferon treatment of a transplantable rat colon adenocarcinoma: importance of tumor site. *Int J Cancer* 1984;33:689-692.
20. Erion JL, Bugaj JE, Schmidt MA, Wilhelm RR, Srinivasan A. High radiotherapeutic efficacy of [Lu-177]-DOTA-Y3-octreotate in a rat tumor model. *J Nucl Med* 1999;40:223p.
21. de Jong M, Breeman WA, Bakker WH, Kooij PP, Bernard BF, Hofland LJ, Visser TJ, Srinivasan A, Schmidt MA, Erion JL, Bugaj JE, Macke HR, Krenning EP. Comparison of (111)In-labeled somatostatin analogues for tumor scintigraphy and radionuclide therapy. *Cancer Res* 1998;58:437-441.
22. De Jong M, Bernard BF, De Bruin E, Van Gameren A, Bakker WH, Visser TJ, Macke HR, Krenning EP. Internalization of radiolabelled [DTPA0]octreotide and [DOTA0,Tyr3]octreotide: peptides for somatostatin receptor-targeted scintigraphy and radionuclide therapy. *Nucl Med Commun* 1998;19:283-288.
23. Andersson P, Forssell-Aronsson E, Johanson V, Wangberg B, Nilsson O, Fjalling M, Ahlman H. Internalization of indium-111 into human neuroendocrine tumor cells after incubation with indium-111-DTPA-D-Phe1-octreotide. *J Nucl Med* 1996;37:2002-2006.
24. Breeman WA, Kwekkeboom DJ, Kooij PP, Bakker WH, Hofland LJ, Visser TJ, Ensing GJ, Lamberts SW, Krenning EP. Effect of dose and specific activity on tissue distribution of indium- 111-pentetreotide in rats. *J Nucl Med* 1995;36:623-627.
25. de Jong M, Breeman WA, Bernard BF, van Gameren A, de Bruin E, Bakker WH, van der Pluijm ME, Visser TJ, Macke HR, Krenning EP. Tumour uptake of the radiolabelled somatostatin analogue [DOTA0, TYR3]octreotide is dependent on the peptide amount. *Eur J Nucl Med* 1999;26:693-698.
26. Schlom J, Siler K, Milenic DE, Eggensperger D, Colcher D, Miller LS, Houchens D, Cheng R, Kaplan D, Goeckeler W. Monoclonal antibody-based therapy of a human tumor xenograft with a 177lutetium-labeled immunoconjugate. *Cancer Res* 1991;51:2889-2896.
27. Mairs RJ. Neuroblastoma therapy using radiolabelled [131I]meta-iodobenzylguanidine ([131I]MIBG) in combination with other agents. *Eur J Cancer* 1999;35:1171-1173.
28. Slooter GD, Aalbers AG, Breeman WA, Hiemstra CA, Marquet RL, Krenning EP, van Eijck CH. The inhibitory effect of (111)In-DTPA(0)-octreotide on intrahepatic tumor growth after partial hepatectomy. *J Nucl Med* 2002;43:1681-1687.

29. Lewis JS, Wang M, Laforest R, Wang F, Erion JL, Bugaj JE, Srinivasan A, Anderson CJ. Toxicity and dosimetry of (177)Lu-DOTA-Y3-octreotate in a rat model. *Int J Cancer* 2001;94:873-877.

CHAPTER 5

COMBINATION THERAPY; RGD-OCTREOTATE

5.1 Radiolabeled RGD-DTPA-Tyr^3-octreotate for receptor-targeted radionuclide therapy

Bert Bernard, Astrid Capello, Martin van Hagen, Wout Breeman, Anath Srinivasan, Michelle Schmidt, Jack Erion, Arthur van Gameren, Eric Krenning and Marion de Jong.

Cancer Biotherapy and Radiopharmaceuticals, 2004, 19 (2):173-180.

ABSTRACT

The aim of this study was to develop and investigate a radiopeptide for treatment of cancers which overexpress cell surface somatostatin receptors. The new radiopharmaceutical is composed of a somatostatin receptor-targeting peptide, a chelator (DTPA) to enable radiolabeling, and an apoptosis inducing RGD (arginine-glycine-aspartate) peptide moiety. The receptor-targeting peptide portion of the molecule, Tyr^3-octreotate, is specific for the somatostatin subtype-2 cell surface receptor (sst_2), which is overexpressed on many tumor cells. Because of the rapid endocytosis of the somatostatin receptor the entire molecule can thus be internalized, allowing the RGD portion to activate intracellular caspases, which in turn promotes apoptosis. In this paper, we present the synthesis and the in vitro and in vivo tumor binding and internalization characteristics of this hybrid peptide. In vitro internalization into sst_2-positive tumor cells of the radiolabeled hybrid peptide appeared to be a rapid process and could be blocked by an excess of unlabeled octreotide, indicating an sst_2-specific process. Tumor uptake in vivo in rats of radiolabeled RGD-DTPA-Tyr^3-octreotate was in agreement with the in vitro data and similar to that of radiolabeled DOTA-Tyr^3-octreotate. The combined molecule is expected to significantly enhance the therapeutic efficacy of the somatostatin-based agent.

INTRODUCTION

The number of somatostatin receptors may be greatly up-regulated in the cells of a variety of tumors, particularly those of neuroendocrine origin. Included are carcinoids, gastrinomas, paragangliomas, small-cell lung cancer, and insulinomas. Increased expression of somatostatin receptors has also been found in breast, and ovarian cancer [1]. Octreotide is an eight-amino-acid cyclic peptide that preserves a four-amino-acid motif (Phe-Trp-Lys-Thr) that is critical for the biological activity of somatostatin. It has a substantially longer serum half-life than endogenous somatostatin. ^{111}In-labeled octreotide has proven to be particularly useful in the diagnosis of neuroendocrine tumors (most of which overexpress somatostatin receptors) [2].

In general, somatostatin receptor-positive neuroendocrine tumors are unresponsive to standard therapy regimens, including adjuvant chemotherapy and, in many cases, external beam radiation therapy. The lack of an effective response to therapy for these tumors represents a serious unmet medical need. To that end, a variety of somatostatin radiolabeled derivatives have been prepared and are in various stages of preclinical and clinical investigation. These new agents are directed at the receptor-targeted radiation therapy of these tumors. For example, OctreoTher is a modified peptide derivative of OctreoScan, radiolabeled with the high-energy beta-emitting radionuclide, yttrium-90 [3]. This agent is currently in phase 1 and 2 clinical studies. In comparison, ^{177}Lu-DOTA-Tyr^3-octreotate (Fig. 1) provides further improvements as a targeted radiotherapeutic by having greater uptake and retention in tumor tissue [3-6]. While the results of these studies are very promising, the radioresistance of a number of tumor types is thought to significantly diminish the potential efficacy of these targeted agents.

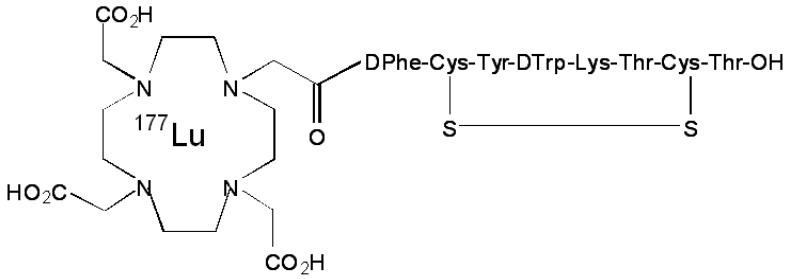

FIGURE 1. *Structure of DOTA-Tyr^3-octreotate*

We hypothesize that the synergistic effects of an apoptosis-inducing factor, such as arginine-glycine-aspartic acid (RGD) peptides, can increase the radiotherapeutic efficacy of these peptides.

A large number of RGD peptide derivatives have been synthesized because of the broad interest on the biochemical function of integrins. These receptors mediate the adhesion and migration of cells and are key factors in the spatial organization of cells through their interaction with extracellular matrix (ECM) proteins. A common amino-acid motif shared by these ECM proteins is an RGD sequence that mediates their interaction with specific integrins. The feasibility of designing small molecules/peptides that have a high affinity for

specific integrin receptors has been demonstrated by several laboratories [7-9]. These studies have shown that small peptides, bearing the RGD motif, can have high affinity and selectivity for even closely related integrin receptors. In addition to the RGD-binding sites found on integrins, it has been shown that two members of the procaspase family, caspase-1 and caspase-3, also contain potential RGD-binding motifs. Caspases are a small group of specific cysteine proteases that are key factors in programmed cell death. These intracellular factors exist as latent zymogens that when activated by apoptotic signals attack crucial protein targets to induce orderly death. Buckley et al.[10] demonstrated that RGD peptides are able to directly activate caspase-3 and induce apoptosis in cells by a mechanism that is completely independent of their association with integrin receptors. Since caspase-3 is one of the key executioner proteases in the apoptosis pathway, it seems likely that this enzyme will be an important site of action for targeted therapeutics that are designed to induce cell death selectively.

The aim of these studies was to develop and characterize a radiopeptide for the treatment of neuroendocrine cancer and other types of cancer which overexpress the cell surface somatostatin receptor subtype-2 (sst_2). The new radiopharmaceutical (Fig. 2) is composed of the somatostatin receptor-targeting peptide Tyr^3-octreotate, the chelator DTPA to enable radiolabeling, and an apoptosis inducing RGD (arginine-glycine-aspartate) peptide moiety. The use of such targeted peptides for therapy allows them to be used in conjunction with diagnostic imaging agents. The diagnostic agent uses the identical target molecule, but is labeled with a gamma emitting radionuclide that permits imaging with a gamma camera, thereby allowing for the selection of patients that will most likely respond to treatment.

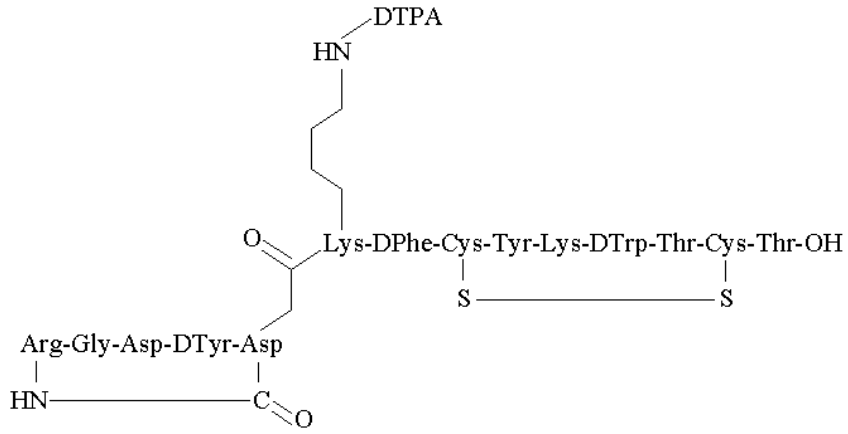

FIGURE 2. *Structure of RGD-DTPA-Tyr^3-octreotate*

MATERIALS AND METHODS

Peptides

Solid phase peptide synthesis (SPPS) of RGD-DTPA-Tyr^3-octreotate was performed using an Applied Biosystems "Pioneer" synthesizer employing Fmoc strategy. The target peptide was prepared on a 0.1 mmol scale using Fmoc-Thr(OtBu)-PEG-PS (Applied Biosystems, St. Louis, MO, 0.24 mmol/g loading) as the starting resin. Fmoc-protected amino acids (0.4 mmol) were activated with *N*- [(dimethylamino)-1H-1,2,3-triazolo[4,5-b]pyridin-1-ylmethylene]-*N*-methylmethan-aminium hexaflurophosphate *N*-oxide (HATU). Upon completion of the linear peptide, Arg(Pbf)-Gly-Asp(PtBu)-D-Tyr(tBu)Asp(OtBu)-Lys(Mtt)-Phe-Cys(Acm)-Tyr(tBu)-D-Trp(Boc)-Lys(Boc)-Thr(OtBu)-Cys(Acm)-Thr(OtBu)-OH)-OAl, on-board cyclization to form the lactam was achieved using the "Allyl Deblock" protocol followed by PyAOP activation. The resin containing the protected, mono-cyclized peptide was then removed from the instrument, and the disulfide formation was accomplished manually by the addition of thallium(III) trifluoracetate in Dimethylformamide. The Mtt protecting group of the lysine was removed next by treatment with 4% TFA/5% triisopropylsilane/91% dichloromethane. The resin was washed with dichloromethane and THF before resuspending in DMF (5 mL) containing DIEA (70 µl, 0.4 mmol). In a separate vessel, tri-t-butyl DTPA (224 mg, 0.4 mmol) was dissolved in DMF containing HBTU/HOBt (0.4 mmol, 2.0 mL of a 0.2 mmol/mL solution) and DIEA (70 µl, 0.4 mmol) to give a 10-mL solution. After agitating for one hour, the activated DTPA derivative was added to the previously suspended resin. The reaction was permitted to continue overnight before washing the resin with DMF and THF. Cleavage of the peptide from the resin with concomitant deprotection of the side chain protecting groups was finally completed using 85% TFA/5% thioanisole/5% phenol/5% water (overnight). The crude peptide was isolated by precipitation with t-butyl methyl ether (Sigma) and purified by reverse-phase HPLC. Molecular weight determination was accomplished by mass spectrometry, operating in the electrospray mode (ESI) (calc. 2139.9; found 1071.3, $(M + 2H)^+/2$).

Synthesis of DTPA-RGD, (c(Arg-Gly-Asp-DTyr-Lys)-ε-DTPA,) and DOTA-Tyr^3-octreotate (DOTA-c(DPhe-Cys-Tyr-DTrp-Lys-Thr-Cys-Thr),) were performed as described [6,8]. RGD c(Arg-Gly-Asp-DPhe-Val) was obtained from Bachem (Bern, Switzerland). Octreotide was supplied by Novartis (Basel, Switzerland).

Radiolabeling

$^{111}InCl_3$ was obtained from Mallinckrodt Medical BV (Petten, The Netherlands). RGD-DTPA-Tyr^3-octreotate and DOTA-Tyr^3-octreotate were labeled with $^{111}InCl_3$ as described previously[6].

Cell culture

CA20948 cells were cultured from the solid CA20948 rat pancreatic tumor and were grown in DMEM (Life Technologies, Breda, The Netherlands) supplemented with 10% heat-inactivated fetal bovine serum, 2 mM glutamine, 1 mM sodium pyruvate, fungizone (0.1 mg/L) and 50 IU/mL penicillin/streptomycin [11]. Rat pancreatic tumor AR42J cells (obtained from CAMR,

Wiltshire, UK) were grown in RPMI-1640 (Life Technologies, Breda, The Netherlands) supplemented with 10% heat-inactivated fetal bovine serum, 2 mM glutamine, 1 mM sodium pyruvate, fungizone (0.1 mg/L) and 50 IU/mL penicillin/streptomycin. CA20948 cells and AR42J cells express both sst_2 and integrins. Twenty-four (24) hours before the uptake and internalization-experiments, cells from subconfluent cell cultures were plated in 6-well plates at 10^6 cells/well.

Uptake and internalization

Uptake and internalization of radiolabeled RGD-DTPA-Tyr^3-octreotate in the cells was studied as described previously [12]. In short, cells were washed with phosphate-buffered saline (PBS). Incubation was started by addition of 1 mL of an incubation medium (RPMI, supplemented with 20 mM Hepes and 1% bovine serum albumin) containing 50 kBq of radioligand. Cells were incubated for the indicated periods of time at 37°C or 4°C. To determine receptor-specific versus nonspecific uptake, cells were incubated with either 0.1 nM of a radiolabeled peptide or with 0.1 nM of a radiolabeled peptide plus an excess of unlabeled octreotide (1 μM) or unlabeled RGD (1 μM). Cellular uptake was stopped by removing medium from the cells and washing twice with 2 ml ice cold PBS. To discriminate between internalized and noninternalized (surface-bound) radiolabeled peptide, intact cells were incubated with 1 ml 20 mM sodium acetate (pH 5.0) in PBS. Cells were lysed with 0.1 M NaOH. Internalized and surface-bound radioactivity was determined by measuring the different fractions in an LKB-1282-Compugammasystem. Cellular protein was determined using a commercially available kit (BioRad, Veenendaal, The Netherlands). Data are presented as the mean ± SD for at least triplicate incubations.

Biodistribution studies

All animal studies were conducted in compliance with the Animal Welfare Committee requirements of our institution and with generally accepted guidelines governing such work. The rat pancreatic CA20948 and rat pancreatic AR42J tumors were grown in the flank of Lewis rats (Harlan, The Netherlands; 80-120 g). Male Lewis rats were injected subcutaneously in the right flank with 10^6 CA20948 cells (from crude tumor tissue or cell culture) and in the left flank with 10^6 AR42J cells (from crude tumor tissue or cell culture). About 15 days after inoculation, experiments were started. For biodistribution studies rats were injected with 3 MBq (0.5 μg) RGD-^{111}In-DTPA-Tyr^3-octreotate into the dorsal vein of the penis. In order to determine the nonspecific binding of the radiopharmaceutical, separate groups of rats were co-injected intravenously with an excess of 500 μg octreotide. Tumor scintigraphy was performed using a gamma camera at 24 hours post-injection of RGD-^{111}In-DTPA-Tyr^3-octreotate. To study possible reduction of kidney uptake, a group of rats was simultaneously injected with RGD-^{111}In-DTPA-Tyr^3-octreotate and 400 mg/kg D-lysine. At 1, 4, 24 and 48 hours post-injection, rats were sacrificed. Organs, tumor and blood were counted in a LKB-1282-Compugammasystem (Perkin Elmer Life Sciences, Groningen, The Netherlands). For all groups: $n \geq 4$, data are expressed as mean ± SD.

Autoradiography

The presence of radioactivity in tumor and normal tissues obtained from the biodistribution studies was investigated by *ex vivo* autoradiography. Tumor and normal organs were isolated 24 hours post-injection, embedded in TissueTek (Sakura, Zoeterwoude, The Netherlands), and processed for cryosectioning. Tissue sections (10 μm) were mounted on glass slides and stored at –20ºC for at least 1 day to improve the adhesion of the tissue to the slide. The sections were exposed to phosphor imaging screens (Packard Instruments Co., Meriden, CT) for 1 day in X-ray cassettes. The screens were analyzed using a Cyclone phosphor imager and a computer-assisted OptiQuant 03.00 image processing system (Packard Instruments Co, Groningen, The Netherlands).

RESULTS

Figure 3A and 3B show, respectively, the time-dependent uptake and rapid internalization of RGD-^{111}In-DTPA-Tyr^3-octreotate at 37°C in CA20948 cells *in vitro*. Uptake and internalization of radiolabeled RGD-DTPA-Tyr^3-octreotate could be decreased nearly completely with an excess of 10^{-6} M octreotide, but not with an excess of 10^{-6} M RGD. Figure 3C shows that the internalization of RGD-^{111}In-DTPA-Tyr^3-octreotate in CA20948 cells is temperature-dependent. No uptake was found at 4°C.

Biodistribution studies in rats showed that the receptor-specific uptake in sst_2-positive tissues and tumors of RGD-^{111}In-DTPA-Tyr^3-octreotate (Table 1) is high (see also Fig. 4) and comparable to uptake of ^{111}In-DOTA-Tyr^3-octreotate in sst_2-positive tissues and tumors (Table 2). A decreased uptake in sst_2-positive tissues and tumors after RGD-^{111}In-DTPA-Tyr^3-octreotate plus 500 μg octreotide was found. The kidney uptake of RGD-^{111}In-DTPA-Tyr^3-octreotate was higher than kidney uptake of ^{111}In-DOTA-Tyr^3-octreotate (Tables 1 and 2). After the co-injection of 400 mg/kg D-lysine, kidney uptake of RGD-^{111}In-DTPA-Tyr^3-octreotate was reduced by 40% of control.

We also investigated the retention of RGD-^{111}In-DTPA-Tyr^3-octreotate in tissues and tumor as function of time. Table 3 shows that there is a good retention of radioactivity in the tumor after RGD-^{111}In-DTPA-Tyr^3-octreotate injection, 48 hours post-injection tumor radioactivity is about 70% of that at 1 hour post injection.

Ex vivo autoradiography showed results in agreement with the biodistribution data. Rats coinjected with an excess of unlabeled octreotide plus RGD-^{111}In-DTPA-Tyr^3-octreotate had a decreased radioactivity level in sst_2 -positive tissues and tumors compared to rats injected with only RGD-^{111}In-DTPA-Tyr^3-octreotate (Fig. 5), indicating receptor-specific uptake.

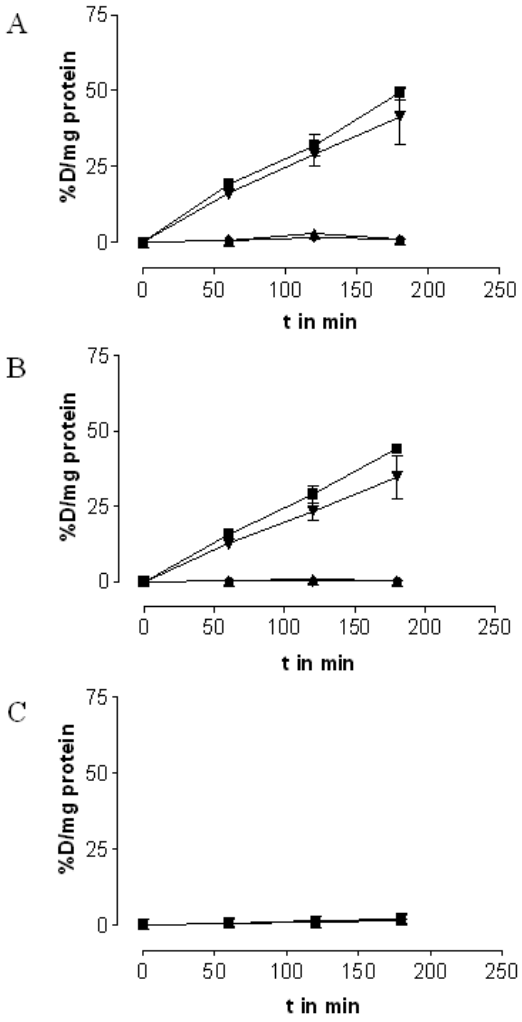

FIGURE 3. *(A) Uptake at 37°C in CA20948 cells of 0.1 nM RGD-^{111}In-DTPA-Tyr^{3}-octreotate (■), of 0.1 nM RGD-^{111}In-DTPA-Tyr^{3}-octreotate plus 10^{-6}M octreotide (▲), of 0.1 nM RGD-^{111}In-DTPA-Tyr^{3}-octreotate plus 10^{-6}M RGD (▼), or of 0.1 nM RGD-^{111}In-DTPA-Tyr^{3}-octreotate plus 10^{-6}M octreotide and 10^{-6}M RGD (◆). (B) Internalization at 37°C in CA20948 cells of 0.1 nM RGD-^{111}In-DTPA-Tyr^{3}-octreotate (■), of 0.1 nM RGD-^{111}In-DTPA-Tyr^{3}-octreotate plus 10^{-6}M octreotide (▲), of 0.1 nM RGD-^{111}In-DTPA-Tyr^{3}-octreotate plus 10^{-6}M RGD (▼), or of 0.1 nM RGD-^{111}In-DTPA-Tyr^{3}-octreotate plus 10^{-6}M octreotide and 10^{-6}M RGD (◆). (C) Internalization at 4°C in CA20948 cells of 0.1 nM RGD-^{111}In-DTPA-Tyr^{3}-octreotate (■), of 0.1 nM RGD-^{111}In-DTPA-Tyr^{3}-octreotate plus 10^{-6}M octreotide (▲), of 0.1 nM RGD-^{111}In-DTPA-Tyr^{3}-octreotate plus 10^{-6}M RGD (▼), or of 0.1 nM RGD-^{111}In-DTPA-Tyr^{3}-octreotate plus 10^{-6}M octreotide and 10^{-6}M RGD (◆).*

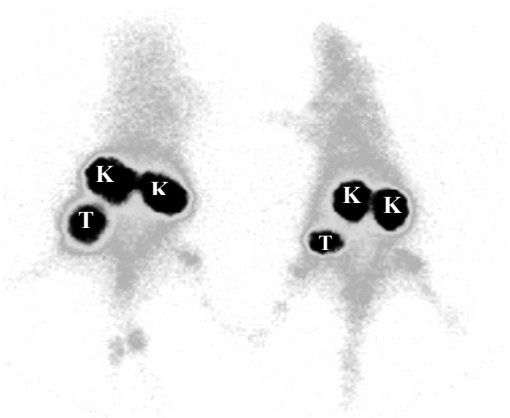

FIGURE 4. *Scan of two rats bearing a CA20948 tumor on their right hind leg, 24 hours post-injection of RGD-^{111}In-DTPA-Tyr^{3}-octreotate, K = kidney,T = tumor.*

TABLE 1. *Tissue/tumor uptake (expressed as %ID/g) of RGD-^{111}In-DTPA-Tyr^3-octreotate, with or without co-injection of 500 µg octreotide or 500 µg RGD, in Lewis rats, 24-hours post-injection (M ± SD, n=8 per group).*

	Control	+ 500 µg octreotide
Blood	0.004 ± 0.001	0.004 ± 0.001
Pancreas	1.55 ± 0.31	0.06 ± 0.01
Adrenals	2.22 ± 0.12	0.05 ± 0.00
Kidney	8.13 ± 0.71	10.31 ± 0.75
Pituitary	0.69 ± 0.01	0.02 ± 0.01
CA20948 tumor	1.91 ± 0.21	0.15 ± 0.01
AR42J tumor	1.63 ±0.14	0.05 ± 0.01

TABLE 2. *Tissue and tumor specific uptake (expressed as %ID/g) of ^{111}In-DOTA-Tyr^3-octreotate, with or without co-injection with 500 µg octreotide, in Lewis rats, 24-hours post injection (M ± SD, n=8 per group).*

	Control	+ 500 µg octreotide
Blood	0.002 ± 0.001	0.002 ± 0.001
Pancreas	2.22 ± 0.15	0.11 ± 0.02
Adrenals	4.25 ± 0.25	0.65 ± 0.03
Kidney	2.48 ± 0.37	2.61 ± 0.45
Pituitary	0.90 ± 0.24	0.08 ± 0.00
CA20948 tumor	2.19 ± 0.40	0.26 ± 0.09
AR42J tumor	1.82 ± 0.21	0.31 ± 0.10

TABLE 3. *Tissue and tumor uptake (expressed as %ID/g) of RGD-^{111}In-DTPA-Tyr^3-octreotate in Lewis rats, 1, 4, 24 and 48 hours post injection (p.i.). (M ± SD, n=4).*

	1 hour p.i.	4 hour p.i.	24 hour p.i.	48 hour p.i.
Blood	0.077 ± 0.019	0.011 ± 0.001	0.004 ± 0.001	0.002 ± 0.001
Spleen	0.77 ± 0.03	0.08 ± 0.01	0.06 ± 0.01	0.06 ± 0.02
Pancreas	2.86 ± 0.25	2.76 ± 0.33	1.55 ± 0.31	1.06 ± 0.15
Stomach	0.55 ± 0.11	0.43 ± 0.04	0.35 ± 0.04	0.22 ± 0.04
Pituitary	0.99 ± 0.19	0.80 ± 0.04	0.69 ± 0.01	0.46 ± 0.08
CA20948 tumor	2.11 ± 0.31	2.26 ± 0.44	1.91 ± 0.21	1.50 ± 0.18
AR42J tumor	1.43 ± 0.36	1.74 ± 0.29	1.63 ± 0.14	0.94 ± 0.41

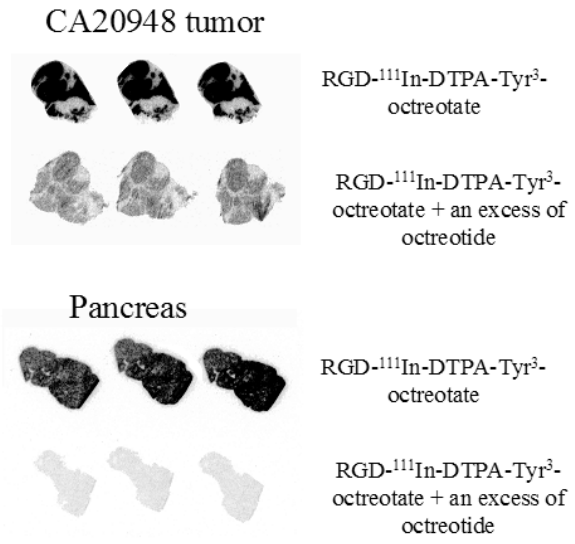

FIGURE 5. *Ex vivo autoradiography of CA20948 tumor and pancreas after RGD-^{111}In-DTPA-Tyr^3-octreotate injection in 2 different rats. Rat 1 injected with 3 MBq/0.5 µg RGD-^{111}In-DTPA-Tyr^3-octreotate, rat 2 with 3 MBq/0.5 µg RGD-^{111}In-DTPA-Tyr^3-octreotate plus 500 µg octreotide.*

DISCUSSION

Somatostatin analogs, like Tyr^3-octreotide and Tyr^3-octreotate, are being used successfully for the treatment of somatostatin receptor-positive tumors. [3-6] The important finding that RGD peptides are able to induce apoptosis in tissue and tumor by the activation of procaspase-3 warranted the pursuit of a hybrid peptide consisting of Tyr^3-octreotate and an RGD containing moiety, to increase the radiotherapeutic efficacy of the somatostatin analog.

RGD-^{111}In-DTPA-Tyr^3-octreotate showed high uptake and rapid time- and temperature-dependent internalization in the sst_2-positive rat pancreatic tumor CA20948 cell line. There was a nearly complete reduction of the internalization of RGD-^{111}In-DTPA-Tyr^3-octreotate by an excess of unlabeled octreotide—but not by an excess of unlabeled RGD—most probably because of the higher affinity of octreotate for its receptor than that of RGD for $\alpha_v\beta_3$ [4,8]. The *in vitro* and *in vivo* studies are consistent with the fact that this hybrid peptide RGD-DTPA-Tyr^3-octreotate, still has a good affinity for the sst_2 and internalized *in vivo* and *in vitro* into tumor cells mostly via the sst_2. The biodistribution studies showed that radioactivity retention in both tumors after RGD-^{111}In-DTPA-Tyr^3-octreotate injection is good.

A drawback of the new hybrid compound is the high renal uptake and retention of radioactivity, limiting the therapeutic dose that can be administered, as the kidneys are the first dose limiting organs in radionuclide therapy using somatostatin analogs. D-lysine injection resulted in 40% reduction of renal uptake. Currently, we are synthesizing and investigating various new RGD-containing somatostatin analogs to solve this problem and, also, the therapeutic effects of unlabeled hybrid peptide, with and without chelator, to change the route of elimination from the body, are being investigated.

To test if the RGD moiety applied in this peptide is still able to promote apoptosis, we performed *in vitro* cell-killing assays using the ^{111}In-labeled hybrid peptide in compared to the two ^{111}In-labeled monopeptides. Preliminary data showed a significantly increased apoptosis induction and cell death *in vitro* caused by RGD-^{111}In-DTPA-Tyr^3-octreotate in compared to ^{111}In-Tyr^3-octreotate or ^{111}In-RGD ^{13}, indicating the great therapeutic potential of this compound. Unlabeled hybrid peptide may be of interest in the treatment of tumors, neovascularization as well as an immunosuppressive agent in autoimmune diseases.

CONCLUSIONS

In conclusion, the hybrid peptide RGD-DTPA-Tyr^3-octreotate has retained a good sst_2 affinity and tumor uptake of RGD-^{111}In-DTPA-Tyr^3-octreotate, mainly occurring via sst_2 targeting, which was high and comparable to that of Tyr^3-octreotate. The hybrid molecule can, therefore, significantly enhance the therapeutic efficacy of the somatostatin-based agent.

REFERENCES

1. Reubi JC, Laissue J, Krenning EP, Lamberts SWJ. Somatostatin receptors in human cancer: incidence, characterics, functional correlates and clinical implications. *J.Steroid Biochem Mol Biol.* 1992; 43: 27-35.
2. Krenning EP, Kwekkeboom DJ, Bakker WH, Breeman WAP, Kooij PP, Oei HY, van Hagen PM, Postema PT, de Jong M, Reubi JC, et al. Somatostatin Receptor Scintigraphy with [^{111}In-DTPA-D-Phe^{1}]- and [^{123}I-Tyr^{3}]octreotide: The Rotterdam Experience with More than 1000 Patients. *Eur J Nucl Med* 1993; 20: 716-731.
3. De Jong M, Kwekkeboom D, Valkema R, Krenning EP. Radiolabelled peptides for tumour therapy: current status and future directions. Plenary lecture at the EANM 2002. *Eur J Nucl Med Mol Imaging 2003*; 30:463-469.
4. De Jong M, Breeman WA, Bakker WH, Kooij PP, Bernard BF, Hofland LJ, Visser TJ, Srinivasan A, Schmidt MA, Erion JL, Bugaj JE, Macke HR, Krenning EP. Comparison of (111)In-labeled somatostatin analogs for tumor scintigraphy and radionuclide therapy. *Cancer Res*. 1998; 58: 437-441.
5. Kwekkeboom DJ, Bakker WH, Kooij PP, Konijnenberg MW,Srinivasan A, Erion JL, Schmidt MA, Bugaj JL, de Jong M, Krenning EP. [^{177}Lu-DOTA,Tyr^{3}]octreotate: comparison with [^{111}In-DTPA^{0}]octreotide in patients. *Eur.J Nucl Med* 2001; 28: 1319-1325.
6. De Jong M, Breeman WA, Bernard BF, Bakker WH, Schaar M, van Gameren A, Bugaj JE, Erion JL, Schmidt MA, Srinivasan A, Krenning EP. [177Lu-DOTA0,Tyr3]octreotate for somatostatin receptor targeted radionuclide therapy. *Int J Cancer* 2001; 12: 355-361.
7. Haubner R, Wester HJ, Burkhart F, Senekowitsch-Schmidtke R, Weber W, Goodman SL, Kessler H and Schwaiger M. Glycosylated RGD-Containing Peptides: Tracer for Tumor Targeting and Angiogenesis Imaging with Improved Biokinetics. *J Nucl Med* 2001; 42:326-336.
8. Van Hagen PM, Breeman WAP, Bernard BF, Schaar M, Mooij CM, Srinivasan A, Schmidt MA, Krenning EP, De Jong M. Evaluation of a radiolabeled cyclic DTPA-RGD analog for tumor imaging and radionuclide therapy. *Int J Cancer* 2000; 90: 186-198.
9. Janssen ML, Oyen WJ, Dijkgraaf I, et al. Tumor targeting with radiolabeled alpha(v)beta(3) integrin binding peptides in a nude mouse model. *Cancer Res* 2002; 62: 6146-6151.
10. Buckley CD, Pilling D, Henriquez NV, Parsonage G, Threlfall K, Scheel-Toellner D, Simmons DL, Akbar AN, Lord JM, Salmon M. RGD-peptides induce apoptosis by direct caspase-3 activation. *Nature* 1999; 397: 534-539.
11. Bernard BF, Krenning EP, Breeman WAP, Visser TJ et al. Use of the rat pancreatic CA20948 cell line for the comparison of radiolabeled peptides for receptor-targeted scintigraphy and radionuclide therapy. *Nucl Med Comm*. 2000; 21: 1079-1085.
12. De Jong M, Bernard BF, de Bruin E, van Gameren A, Bakker WH, Visser TJ, Macke HR, Krenning EP. Internalization of radiolabelled [DTPA^{0}]octreotide and [DOTA^{0},Tyr^{3}]octreotide: peptides for somatostatin receptor-targeted scintigraphy and radionuclide therapy. *Nucl Med Comm*. 1998; 19:283-288.
13. Capello A, Breeman, WAP, Bernard BF, van Hagen PM, Srinivasan A, Krenning EP, de Jong M. RGD-DTPA-octreotate for radionuclide therapy of somatostatin receptor-positive tumours. *Eur J Nucl Med* 2002; 29:119: 265.

CHAPTER 5

COMBINATION THERAPY; RGD-OCTREOTATE

5.2 Increased cell death after therapy with an Arg-Gly-Asp-linked somatostatin analog

Astrid Capello, Eric Krenning, Bert Bernard, Wout Breeman, Martin van Hagen and Marion de Jong.

Journal of Nuclear Medicine, 2004, 45 (10): 1716-1720.

ABSTRACT

Receptor-targeted scintigraphy and radionuclide therapy with radiolabeled somatostatin analogs are successfully applied for somatostatin receptor-positive tumors. The synergistic effects of an apoptosis-inducing factor, for example, the Arg-Gly-Asp (RGD) motif, can increase the radiotherapeutic efficacy of these peptides. Hence, tumoricidal effects of the hybrid peptide RGD-diethylaminetriaminepentaacetic acid (DTPA)-Tyr^3-octreotate [c(Arg-Gly-Asp-D-Tyr-Asp)-Lys(DTPA)-D-Phe-c(Cys-Tyr-D-Trp-Lys-Thr-Cys)-Thr], hereafter referred to as RGD-DTPA-octreotate, were evaluated in comparison with those of RGD (c(Arg-Gly-Asp-D-Tyr-Asp)) and Tyr^3-octreotate (D-Phe-c(Cys-Tyr-D-Trp-Lys-Thr-Cys)-Thr). **Methods:** The therapeutic effects of RGD-^{111}In-DTPA-octreotate, ^{111}In-DTPA-RGD and ^{111}In-DTPA-Tyr^3-octreotate were investigated with various cell lines by use of a colony-forming assay, and caspase-3 activity was also determined. **Results:** Tumoricidal effects were found with ^{111}In-DTPA-RGD, ^{111}In-DTPA-Tyr^3-octreotate, and RGD-^{111}In-DTPA-octreotate, in order from least effective to most effective. Also, the largest increase in caspase-3 levels was found with RGD-^{111}In-DTPA-octreotate. **Conclusions:** RGD-^{111}In-DTPA-octreotate has more pronounced tumoricidal effects than ^{111}In-DTPA-RGD and ^{111}In-DTPA-Tyr^3-octreotate, because of increased apoptosis as indicated by increased caspase-3 activity.

INTRODUCTION

The ^{111}In-labeled somatostatin analog octreotide has proven to be particularly useful in the diagnosis of neuroendocrine tumors that overexpress somatostatin receptors [1]. Somatostatin receptor-positive neuroendocrine tumors are in general unresponsive to standard therapy regimes [2]. Therefore, a variety of radiolabeled somatostatin derivatives have been prepared for radionuclide therapy purposes and are in various stages of preclinical and clinical investigation; these include ^{90}Y-labeled 1,4,7,10-tetraazacyclododecane-*N,N',N'',N'''*-tetraacetic acid (DOTA)-Tyr^3-octreotide and ^{177}Lu-labeled DOTA-Tyr^3-octreotate.

Although the results of these studies are very promising, we hypothesize that the synergistic effects of an apoptosis-inducing factor, such as the Arg-Gly-Asp (RGD) motif, can increase the radiotherapeutic efficacy of these peptides. The RGD sequence is well known as a major integrin-binding site, such as the $\alpha_v\beta_3$-receptor. In addition, Buckley et al. [3] demonstrated that RGD peptides are able to directly activate caspase-3 and induce apoptosis. Other work has shown that molecules specific for GPIIb/IIIa integrins can also stimulate caspase-3 activity [4]. Since caspase-3 is one of the key executioners proteases [5] in the apoptosis pathway, it seems likely that this enzyme will be an important site of action for targeted therapeutics that are designed to selectively induce cell death.

To combine these characteristics in one compound a new peptide, RGD-diethylaminetriaminepentaacetic acid (DTPA)-octreotate (cyclic[c](Arg-Gly-Asp-D-Tyr-Asp)-Lys(DTPA)-D-Phe-c(Cys-Tyr-D-Trp-Lys-Thr-Cys)-Thr) (Fig. 1) was synthesized. This radiopharmaceutical consists of a somatostatin receptor-targeting peptide, Tyr^3-octreotate, the chelator DTPA to enable radiolabeling with for example, ^{111}In, and an RGD peptide moiety. Recently Bernard et al. reported the synthesis and characterization of this hybrid peptide in vitro and in vivo [6]. RGD-DTPA-octreotate enables rapid and high-specific-activity labeling with ^{111}In. The hybrid peptide retains affinity for 2 receptors; octreotate binds with high affinity to the somatostatin receptor subtype 2 (sst_2-receptor), and RGD binds to the $\alpha_v\beta_3$-receptor.

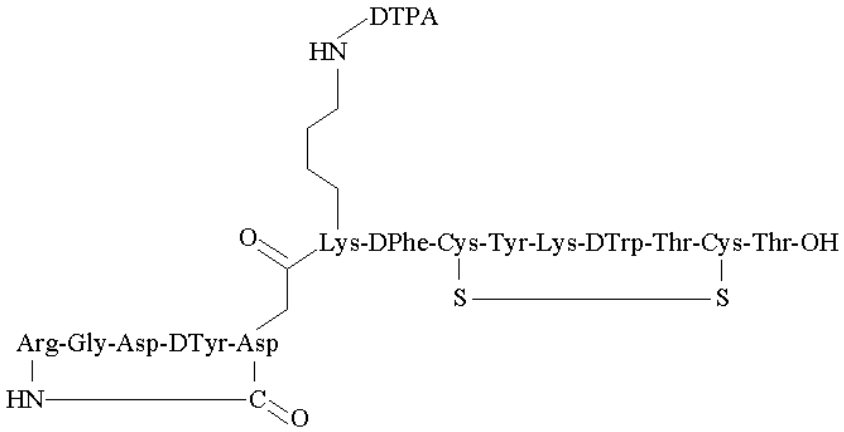

FIGURE 1. *Structure of RGD-DTPA-octreotate.*

In this study, we investigated the therapeutic effects of the ^{111}In-labeled hybrid peptide in comparison with those of ^{111}In labeled RGD (c(Arg-Gly-Asp-D-Tyr-Asp)) and Tyr^3-octreotate (D-Phe-c(Cys-Tyr-D-Trp-Lys-Thr-Cys)-Thr) by using an in vitro model [7]. We also determined caspase-3 activity after incubation with the 3 peptides for several cell lines.

MATERIALS AND METHODS

Peptides

RGD (c(Arg-Gly-Asp-D-Phe-Val)) was obtained from Bachem (Bern, Switzerland). RGD-DTPA-octreotate (Fig. 1), obtained from A. Srinivasan (Mallinckrodt) was synthesized as described previously [6]. DTPA-RGD (c(Arg-Gly-Asp-D-Tyr-Lys)-ε-DTPA) and DTPA-Tyr^3-octreotate, (DTPA-D-Phe-c(Cys-Tyr-D-Trp-Lys-Thr-Cys)-Thr), were synthesized as described previously [8, 9].

Radiochemistral analysis

$^{111}InCl_3$ was obtained from Mallinckrodt Medical BV. RGD-DTPA-octreotate, DTPA-Tyr^3-octreotate and DTPA-RGD were labeled as described previously [10], with $^{111}InCl_3$ at a specific activity of 130 MBq per microgram of peptide. Peptides with more than 99% labeling efficiency and more than 90% radiochemical purity were used.

Cell culture

CA20948 cells were grown in Dulbecco's modified Eagle's medium (Gibco BRL). The medium was supplemented with 10% heat-inactivated fetal bovine serum, glutamine at 2 mM, sodium pyruvate at 1 mM, amphotericin B (Fungizone; Gibco, Invitrogen) at 0.1 mg/L and penicillin-streptomycin at 50 IU/mL. Chinese Hamster Ovary (CHO) cells transfected with the sst_2-receptor (provided by J.E. Bugaj) were grown in RPMI-1640 medium (Life Technologies) supplemented with 5% heat-inactivated fetal bovine serum, glutamine at 2 mM, sodium pyruvate at 1 mM, amphotericin B at 0.1 mg/L and penicillin-streptomycin at 50 IU/mL, and 1:1000 (v/v) gentamicin (Gibco BRL).

Peptide receptor radionuclide therapy *in vitro*

One day before the start of the experiment, cells were transferred to 6-well plates at a density of 200 or 400 cells per well. Cells were washed with phosphate-buffered saline at 37°C and incubated for 1 h in internalization medium─RPMI-1640 medium without fetal bovine serum but with 1% bovine serum albumin and 20 mM of *N*-(2-hydroxyethyl)piperazine-*N*'-(2-ethanesulfonic acid)─containing increasing concentrations of RGD-^{111}In-DTPA-octreotate, ^{111}In-DTPA-RGD or ^{111}In-DTPA-Tyr^3-octreotate. In additional experiments performed with CA20948 cells RGD-^{111}In-DTPA-octreotate and ^{111}In-DTPA-Tyr^3-octreotate were co-

incubated with an excess (10^{-6} M) of unlabeled RGD. Control cells received only internalization medium for 1 h. Thereafter, cells were thoroughly washed with phosphate-buffered saline and allowed to form colonies during 12 d in medium. The medium was refreshed once after 3 days.

After 12 d the cells were fixed with methanol:glacial acetic acid (3:1) and stained with haematoxylin. Colonies that contained more than 50 cells were visually scored as survivors. Experiments were performed in triplicate for each cell density.

Caspase-3 assay

Cell extracts were prepared and caspase-3 activity was determined according to the package insert in the CASPASE-3 Cellular Activity Kit of BIOMOL QuantiZyme™ Assay System (SanverTECH).

Cells were treated with 18.5 MBq RGD-^{111}In-DTPA-octreotate, ^{111}In-DTPA-octreotate or ^{111}In-DTPA-RGD for 3 h. Caspase-3 activity was determined either directly after the incubation period or after 24 h recovery. For preparation of the cell extracts, cells were harvested by trypsin treatment and then lysed with the lysis buffer provided in the kit. The assay is based on the cleavage of the substrate Asp-Glu-Val-Asp (DEVD) bound to the chromophore *p*-nitroanilide, which is measured by reading the absorbance of the samples at a wavelength of 405 nm (microplate reader; Bio-Rad).

Statistical analysis

Statistical analysis was performed for the clonogenic survival data. Multiple-comparison analysis was performed for each concentration group by use of ANOVA and the Bonferroni correction.

RESULTS

Figure 2 shows the clonogenic survival after peptide receptor radionuclide therapy studies in vitro. CA20948 cells (Fig. 2A) and CHO cells transfected with the sst_2-receptor (Fig. 2B) were incubated for 1 h with the 3 different peptides─the hybrid peptide RGD-^{111}In-DTPA-octreotate and the monopeptides ^{111}In-DTPA-octreotate and ^{111}In-DTPA-RGD. Survival values are shown as percentage of survival of treated cells compared with control cells. Experiments were performed with 200 or 400 cells per well, but because both cell densities showed the same results, only the results obtained with 200 cells per well are shown. Figure 2 clearly shows for both cell lines that increasing concentrations of ^{111}In-DTPA-RGD had no effect on tumor cell survival, that ^{111}In-DTPA-Tyr^3-octreotate had a greater tumoricidal effect, but the most pronounced tumoricidal effect was achieved with the hybrid peptide RGD-^{111}In-DTPA-octreotate. As is also shown in Figure 2, a radioactivity dose dependence was seen for

RGD-^{111}In-DTPA-octreotate; the higher the administered dose, the lower the tumor cell survival. For the two highest concentrations (3.70 and 9.25 MBq), the effects of the hybrid peptide were significantly different from those of two monopeptides ($p < 0.01$ and $p < 0.05$ for CA20948 and sst_2 receptor-positive CHO cells, respectively).

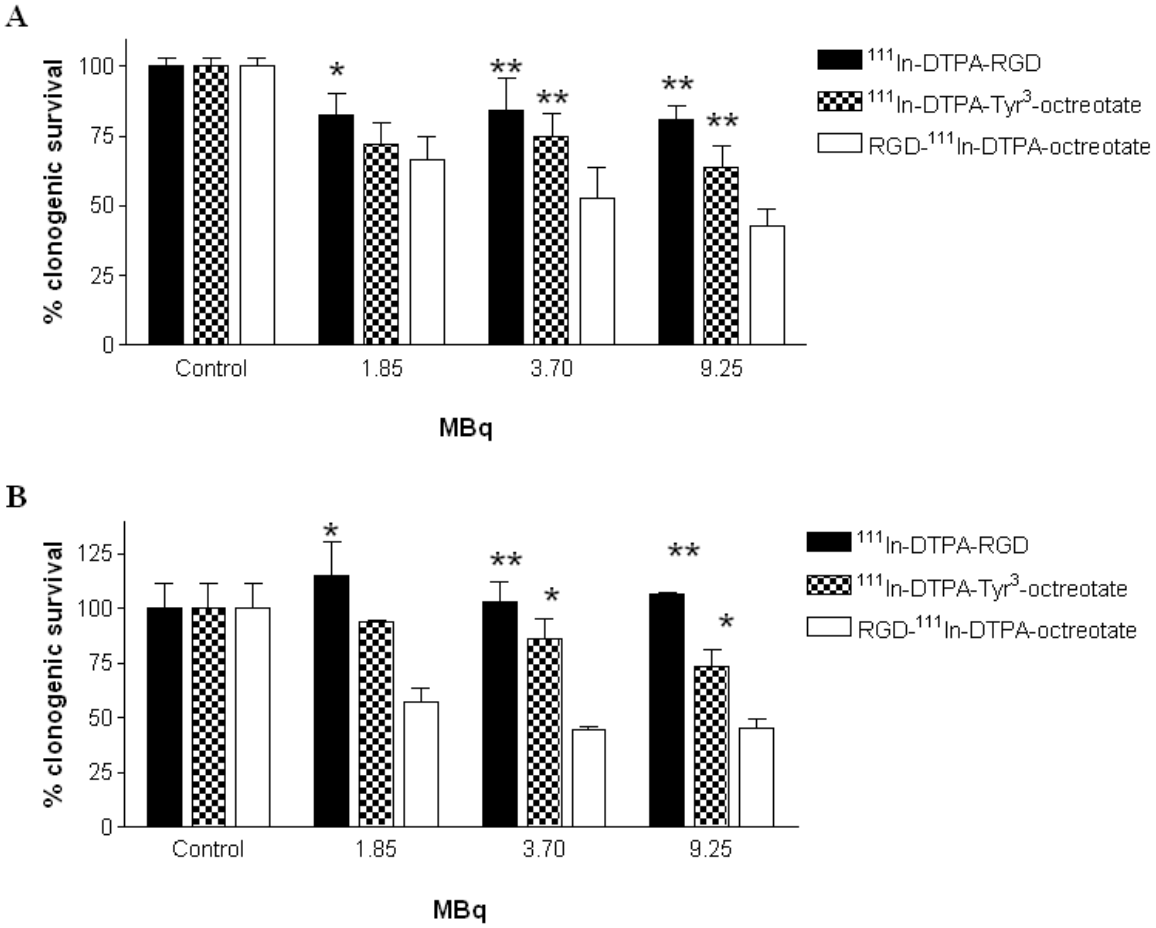

FIGURE 2. *Clonogenic tumoricidal effect of the ^{111}In-labelled compounds RGD, octreotate and RGD-DTPA-octreotate in rat pancreatic cell line CA20948 (A) and the sst_2 receptor-positive CHO cells (B). Cells were incubated for 1 h with increasing concentrations of the 3 peptides. Experiments were performed 2-4 times in triplicates; bars represent mean ± SEM, single and double asterisks indicate p values of <0.05 and <0.01 for comparisons with RGD-^{111}In-DTPA-octreotate within a concentration group.*

When the cells were co-incubated with an excess of unlabeled RGD (10^{-6} M), tumor cell survival decreased further (Fig. 3). This effect was seen when the cells were incubated with ^{111}In-DTPA-Tyr^3-octreotate, but also when the cell were incubated with RGD-^{111}In-DTPA-octreotate. The effects of the hybrid peptide were significantly different from those of ^{111}In-DTPA-Tyr^3-octreotate ($p < 0.05$), and the effects of the hybrid peptide with an excess of unlabeled RGD were significantly different from those of ^{111}In-DTPA-Tyr^3-octreotate with an excess of unlabeled RGD ($p < 0.05$).

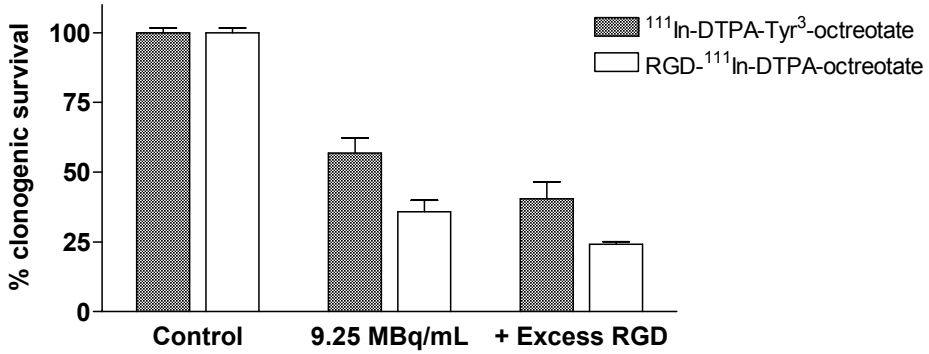

FIGURE 3. *Clonogenic tumor cell survival after 1 h incubation of the cell line CA20948 with no addition (control), with ^{111}In-DTPA-Tyr^3-octreotate or RGD-^{111}In-DTPA-octreotate at 9.25 MBq/mL, or with either those peptides with or without excess unlabelled RGD (10^{-6} M). Experiments were performed 2 times in triplicates; bars represent mean ± SEM, results for all peptides were significantly different from those for control.*

To investigate the mechanism of action of the hybrid peptide, we investigated possible caspase-3 activation. Figure 4 shows the caspase-3 activity after treatment with ^{111}In-DTPA-RGD, ^{111}In-DTPA-Tyr^3-octreotate and RGD-^{111}In-DTPA-octreotate. Figure 4A shows the caspase-3 activity measured directly after the incubation period, and Figure 4B shows the caspase-3 activity after 24 h. The highest caspase-3 activity was seen for the hybrid peptide RGD-^{111}In-DTPA-octreotate, and the lowest was seen for ^{111}In-DTPA-RGD. The caspase-3 activity measured after 24 h was higher (Fig. 4B) than that measured directly after incubation (Fig. 4A). When the cells were incubated with the caspase-3 inhibitor *N*-acetyl (Ac)-DEVD-CHO (aldehyde), the caspase-3 levels remained at control levels.

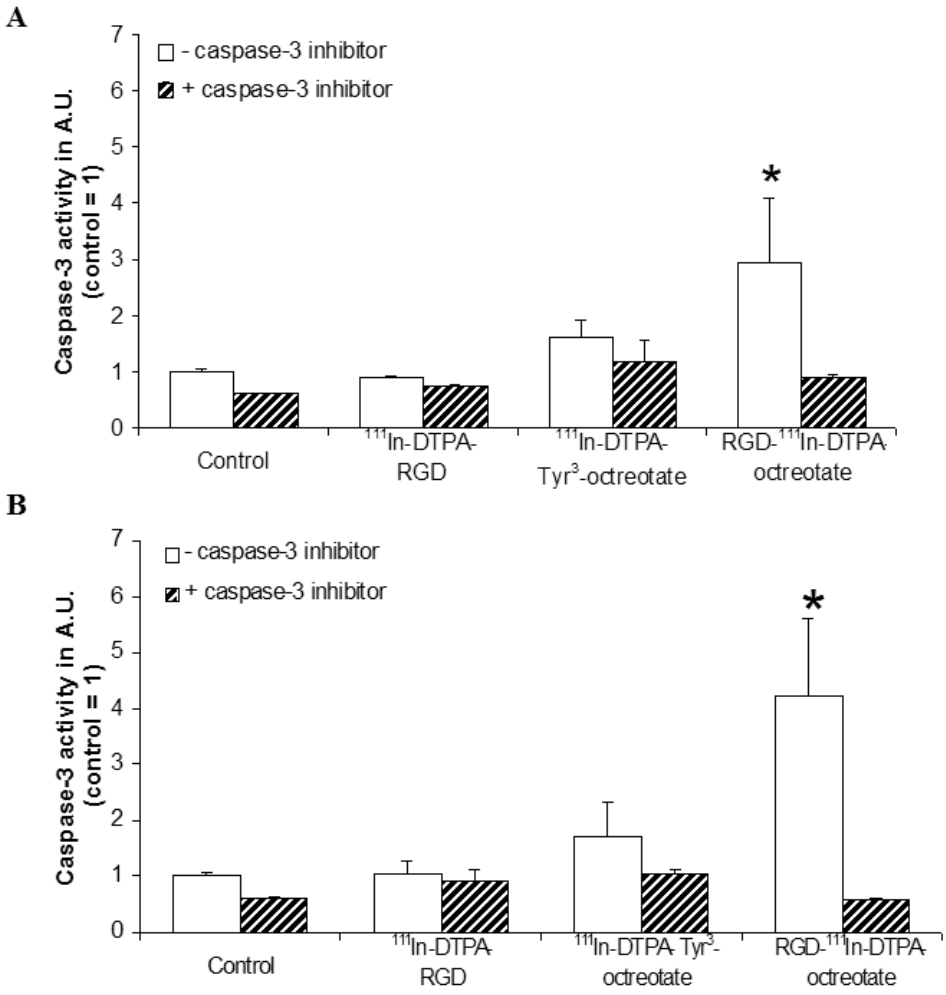

FIGURE 4. *Caspase-3 activity after 3 h incubation with ^{111}In-labelled RGD, Tyr^3-octreotate or RGD-DTPA-octreotate in the CA20948 cell line. Caspase-3 activity was measured directly after incubation (A) and after 24 h (B), and was expressed as a fraction of activity in control cells. (A.U., arbitrary units). Treatment with a known inhibitor of caspase-3 (Ac-DEVD-CHO) was used to determine assay specificity. Experiments were performed in triplicate; bars represent mean ± SEM. An asterisk indicates a p value of <0.05 for comparisons with controls.*

DISCUSSION

We examined the therapeutic potential of a ^{111}In-labeled hybrid peptide; an RGD peptide coupled to the somatostatin analog Tyr^3-octreotate (RGD-^{111}In-DTPA-octreotate). In a previous study [6], it was shown that this hybrid peptide exhibited high uptake and rapid, receptor-specific time- and temperature-dependent internalization in sst_2 receptor-positive CA20948 rat pancreatic tumor cells. Uptake and internalization of RGD-^{111}In-DTPA-Tyr^3-octreotate could be decreased almost completely with an excess of octreotide (10^{-6} M) but not with an excess of RGD (10^{-6} M). Therefore, internalization occurred mainly via sst_2 receptor

[6]. These findings might be explained by the somewhat higher affinity of Tyr^3-octreotate for its receptor than that of RGD for the $\alpha_v\beta_3$-integrin receptor. Another explanation, however, could be the difference in the rates of internalization of the receptors, on the basis of the differences in the biological roles of the integrin receptors and the somatostatin receptors. Furthermore, a difference in receptor densities could contribute to these findings. Biodistribution studies with rats revealed high tumor uptake of RGD-^{111}In-DTPA-octreotate in tumor-bearing rats. The level of retention of radioactivity for RGD-^{111}In-DTPA-octreotate was at least as high as that for Tyr^3-octreotate. From these in vitro and in vivo studies, it can be concluded that octreotate can serve as a carrier for RGD internalization [6].

In this study, it was shown that for both cell lines, the greatest tumoricidal effect was reached when the cells were incubated with the hybrid peptide RGD-^{111}In-DTPA-octreotate. Also, a clear dose response was observed with the hybrid peptide, whereas the ^{111}In-DTPA-RGD alone had almost no effect on the clonogenic tumor cell survival and ^{111}In-DTPA-Tyr^3-octreotate had a less pronounced tumoricidal effect.

An excess of unlabeled RGD (10^{-6} M) could further decrease the tumor cell survival when the cells were incubated with ^{111}In-DTPA-Tyr^3-octreotate or RGD-^{111}In-DTPA-octreotate. However, the tumoricidal effect of RGD-^{111}In-DTPA-octreotate alone was still greater than that of ^{111}In-DTPA-octreotate with an excess of unlabeled RGD. The further decrease in tumor cell survival seen with unlabeled RGD could be explained by the fact that RGD itself is also internalized [9]. Because a much higher concentration of the unlabeled peptide than that of the other radiotracers was used, RGD itself could have activated caspase-3 and thereby inducing apoptosis, leading to more tumor killing.

According to Buckley et al. [3], RGD peptides are able to activate caspase-3 inside cells. Because caspase-3 is an important executioner caspase in the apoptosis pathway, this enzyme will be an important site of action for targeted therapeutics to selectively induce cell death. We therefore investigated whether RGD-^{111}In-DTPA-octreotate indeed activated caspase-3.

Buckley et al. [3] showed a clear increase in caspase-3 levels after incubation periods of 2-24 h, we therefore incubated cells in the caspase assay for 3 h instead of 1 h used in the colony-forming assay. Because a much larger cell number (>10^6 cells) was used for the caspase-3 assay than for the clonogenic assay (200-400 cells), we doubled the amount of the peptide and the radioactivity administered. The same trend was found with 9.25 MBq per well. In this study, the effects on caspase-3 activity were studied with the CA20948 cell line. ^{111}In-DTPA-RGD and ^{111}In-DTPA-Tyr^3-octreotate induced no significant increase in caspase-3 levels, in contrast to the hybrid peptide RGD-^{111}In-DTPA-octreotate ($p < 0.05$). Samples treated with a caspase-3 inhibitor showed no increase in caspase-3 levels, a result that indicated the specificity of the assay. These findings are consistent with the results obtained in the colony-forming assay, as described above. The effects were reached with concentrations of RGD peptide lower than those used by Buckley et al. [3]; they demonstrated that caspase-3 induction could be achieved with peptide concentrations between 0.1 and 1 mM. Our results

at lower peptide concentration can be explained by the fact that cyclic derivatives of RGD peptides inhibit cell adhesion to vitronectin more than 100-fold more effectively than the linear variants [11]. In this study, we used cyclic peptides; Buckley et al. used linear peptides [3]. Furthermore, internalization studies showed that approximately 0.9% of ^{111}In-DTPA-RGD [9] and 15.7% of RGD-DTPA-octreotate [6] were internalized after 60 min in the CA20948 cell line. Biodistribution studies in vivo showed that the uptake of ^{111}In-DTPA-RGD after 60 min in the CA20948 tumor in rats was 0.18% [9]. The uptake of RGD-^{111}In-DTPA-octreotate was 1.9%, comparable to the uptake of ^{111}In-Tyr^3-octreotate [6].

From this study, we conclude that RGD-^{111}In-DTPA-octreotate promotes apoptosis via an increase in caspase-3 levels. The ^{111}In-labeled hybrid peptide can therefore significantly enhance the therapeutic efficacy of somatostatin-based agents.

Also very interesting is the possible use of the unlabeled hybrid peptide RGD-DTPA-octreotate for adjuvant therapy. Preliminary data showed that the unlabeled compound RGD-DTPA-octreotate also induced an increase in caspase-3 levels. The largest increase (5.3 times higher than that in the control) in caspase-3 levels with the unlabeled peptide RGD-DTPA-octreotate (10^{-6} M) was found after 24 h incubation. RGD and Tyr^3-octreotate induced no increase in caspase-3 levels (A. Capello, unpublished data, 2004).

RGD compounds have been shown to inhibit angiogenesis because of upregulation of $\alpha_v\beta_3$. Preclinical studies found that several RGD peptidomimetic agents and a monoclonal antibody to $\alpha_v\beta_3$ can inhibit tumor growth by blocking tumor angiogenesis [12]. Neovascular endothelium expresses both sst_2 and $\alpha_v\beta_3$-integrin receptors; these data make RGD-octreotate a candidate for the treatment of neovascular disease.

Another promising application is the coupling of RGD analogs to other peptides, for instance, bombesin, neurotensin, and cholecystokinin/gastrin, to increase the therapeutic effects of the peptides. Bombesin is a neuropeptide with high affinity for the gastrin-releasing peptide receptor; this receptor is expressed on a variety of tumors, including prostate and breast cancer [13, 14]. Neurotensin receptors, on the other hand, are overexpressed in exocrine pancreatic cancer and Ewing's sarcoma [15]. Cholecystokinin B receptors are frequently expressed on medullary thyroid carcinomas, small-cell lung cancers, astrocytomas, stromal ovarian tumors, and some gastroenteropancreatic tumors [16, 17].

CONCLUSION

Coupling RGD-peptides to somatostatin analogs can increase the therapeutic potential of these peptides.

ACKNOWLEDEGMENT

We thank Dr. A. Srinivasan for his expertise and kindly providing the hybrid peptide RGD-octreotate.

REFERENCES

1. Krenning EP, Kwekkeboom DJ, Bakker WH, Breeman WA, Kooij PP, Oei HY, van Hagen M, Postema PT, de Jong M, Reubi JC, et al. Somatostatin receptor scintigraphy with [111In-DTPA-D-Phe1]- and [123I- Tyr3]-octreotide: the Rotterdam experience with more than 1000 patients. *Eur J Nucl Med* 1993;20:716-731.
2. Oberg K. State of the art and future prospects in the management of neuroendocrine tumors. *Q J Nucl Med* 2000;44:3-12.
3. Buckley CD, Pilling D, Henriquez NV, Parsonage G, Threlfall K, Scheel-Toellner D, Simmons DL, Akbar AN, Lord JM, Salmon M. RGD peptides induce apoptosis by direct caspase-3 activation. *Nature* 1999;397:534-539.
4. Adderley SR, Fitzgerald DJ. Glycoprotein IIb/IIIa antagonists induce apoptosis in rat cardiomyocytes by caspase-3 activation. *J Biol Chem* 2000;275:5760-5766.
5. Wolf BB, Green DR. Suicidal tendencies: apoptotic cell death by caspase family proteinases. *J Biol Chem* 1999;274:20049-20052.
6. Bernard BF, Capello A, van Hagen PM, Breeman WA, Srinivasan A, Schmidt MA, Erion JL, van Gameren A, Krenning EP, de Jong M. Radiolabeled RGD-DTPA-Tyr^3-octreotate for receptor-targeted radionuclide therapy. *Cancer Biother Radiopharm* 2004;19:273-280.
7. Capello A, Krenning EP, Breeman WA, Bernard BF, de Jong M. Peptide receptor radionuclide therapy in vitro using [111In- DTPA0]octreotide. *J Nucl Med* 2003;44:98-104.
8. de Jong M, Breeman WA, Bakker WH, Kooij PP, Bernard BF, Hofland LJ, Visser TJ, Srinivasan A, Schmidt MA, Erion JL, Bugaj JE, Macke HR, Krenning EP. Comparison of (111)In-labeled somatostatin analogues for tumor scintigraphy and radionuclide therapy. *Cancer Res* 1998;58:437-441.
9. van Hagen PM, Breeman WA, Bernard HF, Schaar M, Mooij CM, Srinivasan A, Schmidt MA, Krenning EP, de Jong M. Evaluation of a radiolabelled cyclic DTPA-RGD analogue for tumour imaging and radionuclide therapy. *Int J Cancer* 2000;90:186-198.
10. Bakker WH, Krenning EP, Reubi JC, Breeman WA, Setyono-Han B, de Jong M, Kooij PP, Bruns C, van Hagen PM, Marbach P, et al. In vivo application of [111In-DTPA-D-Phe1]-octreotide for detection of somatostatin receptor-positive tumors in rats. *Life Sci* 1991;49:1593-1601.
11. Aumailley M, Gurrath M, Muller G, Calvete J, Timpl R, Kessler H. Arg-Gly-Asp constrained within cyclic pentapeptides. Strong and selective inhibitors of cell adhesion to vitronectin and laminin fragment P1. *FEBS Lett* 1991;291:50-54.
12. Westlin WF. Integrins as targets of angiogenesis inhibition. *Cancer J* 2001;7 Suppl 3:S139-143.
13. Markwalder R, Reubi JC. Gastrin-releasing peptide receptors in the human prostate: relation to neoplastic transformation. *Cancer Res* 1999;59:1152-1159.
14. Breeman WA, de Jong M, Erion JL, Bugaj JE, Srinivasan A, Bernard BF, Kwekkeboom DJ, Visser TJ, Krenning EP. Preclinical comparison of (111)In-labeled DTPA- or DOTA-bombesin analogs for receptor-targeted scintigraphy and radionuclide therapy. *J Nucl Med* 2002;43:1650-1656.

15. Reubi JC, Waser B, Friess H, Buchler M, Laissue J. Neurotensin receptors: a new marker for human ductal pancreatic adenocarcinoma. *Gut* 1998;42:546-550.
16. Reubi JC, Schaer JC, Waser B. Cholecystokinin(CCK)-A and CCK-B/gastrin receptors in human tumors. *Cancer Res* 1997;57:1377-1386.
17. de Jong M, Bakker WH, Bernard BF, Valkema R, Kwekkeboom DJ, Reubi JC, Srinivasan A, Schmidt M, Krenning EP. Preclinical and initial clinical evaluation of 111In-labeled nonsulfated CCK8 analog: a peptide for CCK-B receptor-targeted scintigraphy and radionuclide therapy. *J Nucl Med* 1999;40:2081-2087.

CHAPTER 5

COMBINATION THERAPY: RGD-OCTREOTATE

5.3 Anti-cancer activity of targeted pro-apoptotic peptides

Astrid Capello, Eric Krenning, Bert Bernard, Wout Breeman, Jack Erion and Marion de Jong

Submitted for publication

ABSTRACT

Tumor induced angiogenesis can be targeted by RGD (Arg-Gly-Asp) peptides, which bind to $\alpha_v\beta_3$-receptors upregulated on angiogenic endothelial cells. RGD containing peptides are capable of inducing apoptosis through direct activation of procaspase-3 to caspase-3 in the cell. On the other hand, tumor cells overexpressing somatostatin receptors can be targeted by somatostatin analogs. Radiolabeled somatostatin analogs are successfully used to image and treat those tumors via receptor-targeted scintigraphy and therapy.

We combined these two peptides, RGD and somatostatin, into a new compound by synthesizing a hybrid peptide, RGD-DTPA-octreotate (c(Arg-Gly-Asp-D-Tyr-Asp)-Lys(DTPA)-D-Phe-c(Cys-Tyr-D-Trp-Lys-Thr-Cys)-Thr). An earlier study in tumor-bearing rats showed a high receptor-specific uptake in somatostatin receptor subtype 2 (sst_2)-positive tissues and tumors of RGD-^{111}In-DTPA-octreotate. Furthermore RGD-^{111}In-DTPA-octreotate showed a pronounced tumoricidal effect, which is probably the result of increased apoptosis, as is shown by an increased caspase-3 activity after incubation with ^{111}In-labeled RGD-DTPA-octreotate in comparison with the two monopeptides ^{111}In-DTPA-RGD and ^{111}In-DTPA-Tyr^3-octreotate. In this study we evaluated the biodistributions of RGD-^{111}In-DTPA-octreotate and ^{125}I-RGD-octreotate, and investigated the caspase-3 activation of the unlabeled compound RGD-DTPA-octreotate in vitro.

Methods. Biodistribution studies in tumor-bearing rats were performed with RGD-^{111}In-DTPA-octreotate and ^{125}I-RGD-octreotate. The apoptotic activity, by activation of caspase-3, of RGD-DTPA-octreotate and RGD-octreotate was examined using a colorimetric assay and immunocytochemistry.

Results. In rats the radiolabeled compound RGD-^{111}In-DTPA-octreotate showed a high uptake in the CA20948 tumor and good tumor retention. A major drawback was the high renal uptake. In vitro the unlabeled peptide RGD-DTPA-octreotate induced a significant increase in caspase-3 levels in various cell lines in comparison with RGD and Tyr^3-octreotate ($p < 0.01$). Caspase-3 activity was time-dependent. To alter the elimination route we examined the biodistribution of radioiodinated RGD-octreotate without DTPA [c(Arg-Gly-Asp-D-Tyr-Asp)-D-Phe-c(Cys-Tyr-D-Trp-Lys-Thr-Cys)-Thr], as a model of unlabeled RGD-octreotate, in tumor-bearing rats. ^{125}I-RGD-octreotate showed a much lower renal uptake in comparison with RGD-^{111}In-DTPA-octreotate. Furthermore, the affinity of RGD-octreotate increased in comparison with RGD-DTPA-octreotate (IC_{50} values of 1.4×10^{-8}M vs. 9.4×10^{-8}M respectively). Finally, RGD-octreotate was still able to activate caspase-3 as was indicated with immunocytochemistry.

Conclusions. Due to the high renal uptake RGD-^{111}In-DTPA-octreotate is unsuitable for radionuclide therapy. The unlabeled peptide however, RGD-DTPA-octreotate and RGD-octreotate also induced an increase in caspase-3 levels, indicating the therapeutical potential of this compound. So, the development of hybrid molecules can become a new approach in the treatment of cancer.

INTRODUCTION

Cell matrix interactions are of fundamental importance to tumor invasion and formation of metastases as well as to tumor-induced angiogenesis. Integrins, heterodimeric transmembrane glycoproteins, composed of an α- and β-subunit, play a key role in these interactions. The main recognition site of integrins that bind to the extracellular matrix is the tripeptide sequence, Arg-Gly-Asp (RGD). The sequence was first identified in fibronectin and has since been shown to be a recognition sequence in intracellular matrix proteins such as vitronectin and fibrinogen [1, 2]. The vitronectin receptor, $\alpha_v\beta_3$ receptor, has been studied extensively because of its role in a number of biological processes, such as angiogenesis. This receptor is expressed on various malignant human tumors and upregulated in proliferating endothelial cells.

Several compounds have been designed, based on the RGD sequence, as $\alpha_v\beta_3$ antagonists. In previous studies it has been shown that these antagonists can regulate cell viability by inhibiting integrin binding. Apoptosis was induced by disruption of the interactions between normal epithelial cells and extracellular matrix, named anoikis [3-8]. In addition, recent studies show that RGD-containing peptides may induce apoptosis independent of the association with integrin receptors by directly activating caspase-3 inside the cell [9, 10]. These results suggest that effective and selective biological effects on tumor tissue can be achieved using RGD peptides.

On the other hand, somatostatin receptors are highly expressed on a variety of tumors, particularly those of neuroendocrine origin. Octreotide is an 8 amino acid cyclic peptide that preserves the four- amino acid motif (Phe-Trp-Lys-Thr) that is critical for the biological activity of somatostatin. It has a substantially longer serum half-life than endogenous somatostatin. Radiolabeled somatostatin analogs are successfully applied for the localization and staging of somatostatin receptor-positive tumors. Other somatostatin analogs, with a higher receptor affinity for the somatostatin receptor subtype 2 (sst_2), are Tyr^3-octreotide and Tyr^3-octreotate, wherein the latter the alcohol Thr(ol) at the C-terminus in octreotide is replaced with the natural amino acid Thr [11]. Peptide Receptor Radionuclide Therapy (PRRT) can be performed using these peptide analogs radiolabeled with therapeutic radionuclides, such as the Auger electron emitter ^{111}In, and the β-emitters ^{90}Y and ^{177}Lu. Promising results with regard to tumor growth inhibition were shown in pre-clinical studies and in patient studies using ^{111}In-DTPA-octreotide [12-16], ^{90}Y-DOTA-Tyr^3-octreotide [17-22], and ^{177}Lu-DOTA-Tyr^3-octreotate [23, 24].

Most peptide hormones are internalized after binding to specific surface receptors via invagination of the plasma membrane [25]. The efficient internalization of the receptor-ligand complex into sst-positive cells forms the basis for the concept of targeted sst-mediated chemo- and/or radiotherapy of somatostatin receptor-positive tumors. Internalization brings the somatostatin analog closer to the nucleus of the cell, resulting in a prolonged cellular retention and exposure to the radioactivity and/or cytotoxic agent [26-29]. We therefore synthesized a new peptide, RGD-DTPA-octreotate [c(Arg-Gly-Asp-D-Tyr-Asp)-Lys(DTPA)-D-Phe-c(Cys-Tyr-D-Trp-Lys-Thr-Cys)-Thr]. This hybrid peptide consists of a somatostatin receptor targeting peptide, Tyr^3-octreotate [D-Phe-c(Cys-Tyr-D-Trp-Lys-Thr-Cys)-Thr], the

chelator DTPA to enable radiolabeling, and RGD as apoptosis inducing peptide moiety. Recently we reported the synthesis and characterization of this hybrid peptide in vitro and in vivo [30]. RGD-DTPA-octreotate showed a rapid and high specific activity labeling with ^{111}In. The hybrid peptide had retained affinity for both receptors; the Tyr^3-octreotate part bounds with high affinity to the sst_2-receptor and the RGD part bounds to the $\alpha_v\beta_3$-receptor. Furthermore, the ^{111}In-labeled compound had a pronounced tumoricidal effect in vitro, which was better than that of the two monomers. The superior tumoricidal effect was probably the result of increased apoptosis, as shown by increased caspase-3 activity after incubation with RGD-DTPA-octreotate [31].

In this study we evaluated the biodistribution of RGD-^{111}In-DTPA-octreotate in more detail for the use of PRRT in rats bearing the CA20948 tumor. Unfortunately, the biodistribution showed a very high renal uptake, limiting the therapeutic dose that can be administered, as the kidneys are critical organs in therapy using radiolabeled somatostatin analogs. The aim of the study was to study the therapeutic effects of the unlabeled hybrid peptide in vitro in CA20948 cells, AR42J cells and CHO cells transfected with sst_2. Subsequently, the hybrid peptide RGD-octreotate, without the chelator present, was investigated in order to change the elimination route from the body (from renal clearance to more hepatic clearance). The affinity of both compounds RGD-octreotate and RGD-DTPA-octreotate to the sst_2-receptor was determined. Finally the induction of caspase-3 by RGD-octreotate was investigated.

MATERIALS AND METHODS

Peptides

The solid phase synthesis of cyclic RGD peptides linked to the somatostatin analog Tyr^3-octreotate with or without the DTPA chelator was carried out using methods similar to those described by van Hagen et al. [32] for DTPA linked cyclic RGD peptides. Synthesis was performed using an Applied Biosystems (Foster City, CA) Pioneer synthesizer and standard Fmoc solid phase peptide synthesis methods [33]. All Fmoc protected amino acids were purchased from Novabiochem (San Diego, CA). Other peptide synthesis reagents were obtained from Applied Biosystems except as noted. Peptides were prepared on a 0.1 mmol scale with Fmoc-Thr(Otbu)-PEG-PS (0.16 mmol/g loading) as the starting resin. Fmoc-protected amino acids (0.4 mmol) were activated with an equivalent amount of N-[(dimethylamino)-1H-1,2,3-triazolo[4,5-b]pyridine-1-ylmethylene]-N-methylmethan-aminium-hexaflurophosphate N-oxide (HATU) in DIEA/DMF. Prior to cyclization, the allyl protecting group on the carbonyl of the aspartic acid residue at position 5 was deblocked using 4 equivalents of $Pd(PPH_3)_4$ (Sigma-Aldrich) in $CHCl_3$/AcOH/NMM (37:2:1), followed by deblocking of the N-terminal Fmoc. Cyclization was carried out by activation of the free carbonyl on Asp-5 with 7-azabenzotriazol-1-yloxytris(pyrrolidino) phosphonium hexafluorophosphate (PyAOP) in DIEA/DMF. When preparing peptides coupled with DTPA, the resin containing the protected, cyclized peptide was removed from the instrument, and the

4-methyltrityl (Mtt) protecting group on the ε-amino group of lysine-6 was removed by treatment with 5% TFA/5% triisopropylsilane/90% dichloromethane (2x30 minutes). The resin was washed with dichloromethane and tetrahydrofuran (THF) before suspending in DMF (5 mL) containing 0.4 mmol DIEA. In a separate vessel, tri-t-butyl DTPA was dissolved in DMF containing HATU (0.4 mmol in 2.0 ml). After mixing for 1 hr, the activated DTPA derivative was added to the suspended resin. The reaction was continued overnight before washing the resin with DMF and THF. Cleavage and deprotection were finally accomplished using 85% TFA/5% thioanisole/5% phenol/5% water (4-6 hrs). The crude peptide was isolated by precipitation with t-butyl methyl ether (Sigma-Aldrich, St Louis, MO), lyophilized, and purified by reverse phase HPLC on a Vydac C-18 column using an acetonitrile/water gradient containing 0.1% TFA (Solvent A: 0.1% TFA in water; Solvent B, 0.1% TFA/90%CH_3CN in water). After loading the peptide, column flow (10mls/min) was isocratic at 95% A/5% B for 2.0 min before ramping to 30% A/70% B over 15 min. Molecular weight determination was accomplished by mass spectrometry using electrospray mode.

RGD (c(Arg-Gly-Asp-D-Phe-Val)) was obtained from Bachem (Berne, Switzerland). Synthesis of DTPA-RGD, (c(Arg-Gly-Asp-D-Tyr-Lys)-ε-DTPA) and DTPA-Tyr^3-octreotate, (DTPA-c-(D-Phe-Cys-Tyr-D-Trp-Lys-Thr-Cys-Thr)), was performed as described previously [11, 32]. Octreotide was supplied by Novartis (Basel, Switzerland).

Radiolabeling

$^{111}InCl_3$ was obtained from Mallinckrodt Medical BV (Petten, The Netherlands). RGD-DTPA-Tyr^3-octreotate and DOTA-Tyr^3-octreotate were labeled with $^{111}InCl_3$ as described previously [34]. Peptides with more than 99% labeling efficiency and more than 90% radiochemical purity were used. ^{125}I was obtained from Pharmacia (Roosendaal, The Netherlands). RGD-octreotate was labeled with ^{125}I according as described [35].

Cell culture

CA20948 cells were grown in Dulbecco's modified Eagle's medium (DMEM) (Gibco BRL, Grand Island, NY). Medium was supplemented with 10% fetal bovine serum, 2mM glutamine, 1mM sodium pyruvate, 0.1mg/L fungizone and 50 IU/mL penicillin/streptomycin. Rat AR42J cells were routinely maintained in F12K media (Herndon, VA USA) supplemented with 10% fetal calf serum, 50 µg/ml gentamycin, and 2 mM L-glutamine. CHO cells (Chinese Hamster Ovary cells) transfected with sst_2 (donated by dr. J.E. Bugaj, St. Louis, USA) were grown in RPMI-1640 (Gibco BRL, Grand Island, NY) supplemented with 5% fetal bovine serum, 2 mM glutamine, 1 mM sodium pyruvate, fungizone (0.1 mg/L), 50 IU/mL penicillin/streptomycin and 1/1000 (v/v) gentamicin (Gibco BRL, Grand Island, NY). All cell lines were cultured at 37°C in 5% CO_2.

Biodistribution studies

All animal studies were conducted in compliance with the Animal Welfare Committee requirements of our institution and with generally accepted guidelines governing such work. The rat pancreatic CA20948 tumor was grown in the flank of Lewis rats (Harlan, The Netherlands; 80-120 g). Male Lewis rats were injected subcutaneously in the right flank with 10^6 CA20948 cells (from crude tumor tissue or cell culture). About 15 days after inoculation, experiments were started. For biodistribution studies rats were injected with 3 MBq (0.5 μg) RGD-^{111}In-DTPA-octreotate into the dorsal vein of the penis. In order to determine non-specific binding of the radiopharmaceutical, some rats were co-injected intravenously with an excess of 500 μg octreotide, RGD or octreotide plus RGD. At 1, 4, 24, 48, 72 and 96 h post injection, rats were sacrificed. Organs, tumor and blood were counted in an LKB-1282-Compugammasystem. For all groups: $n \geq 3$, data are expressed as mean ± SD.

For the biodistribution study using ^{125}I-labeled RGD-octreotate (without DTPA), rats were injected with 0.25 MBq (0.5 μg) ^{125}I-RGD-octreotate into the dorsal vein of the penis. There were 2 separate groups of rats, one group of rats was injected with the first peak and the other group of rats was injected with the second peak of the HPLC purified product (see Results). At 1 and 2 h post injection, rats were sacrificed. Organs, tumor and blood were counted in an LKB-1282-Compugammasystem. For all groups: $n \geq 3$, data are expressed as mean ± SD.

Caspase-3 assay

Preparation of cell extracts and the determination of caspase-3 were performed according to the insert in the CASPASE-3 Cellular Activity Kit of BIOMOL QuantiZyme™ Assay System. The assay is based on the cleavage of the substrate DEVD bound to the chromophore p-nitroanilide (pNA), which is measured by reading the absorbance (at 405-nm wavelength, Bio-rad, microplate reader) of the samples.

Cells were treated with RGD, Tyr^3-octreotate or RGD-(DTPA-)octreotate for 3-48 hours, after exposure to trypsin cells were harvested, and then lysed with lysis buffer provided in the kit.

Immunocytochemistry. For apoptosis activation studies AR42J cells were plated into 24 well plates (Corning USA) at approximately 0.5 x 10^6 cells/well. Cells were cultured for 18h before use. Before treatments, cells were washed with phosphate buffered saline (PBS), treated with 0.25 ml media containing indicated peptides and subsequently fixed for 30 min at room temperature with 0.25 ml 2% formalin in PBS. Wells were washed 3 times for 5 min with PBS, and then permeabalized in 0.25 ml 1% triton X-100 for 10 min at room temperature. Following a blocking treatment with 0.25 ml of 3% BSA in PBS, cells were incubated overnight with gentle agitation with primary antibodies using a 3% BSA/PBS solution containing a 1/200 dilution of rabbit anti-cleaved caspase-3 (Cell Signaling Technologies Inc., Beverly, MA USA), and a 1/300 dilution of mouse anti β-tubulin. Cells were subsequently washed three times with PBS and then reacted for 1 hour with a 3% BSA/PBS solution containing a 1/1000 dilution of Alexa fluor-594 goat anti-rabbit and a

1/750 dilution of Alexa fluor-488 goat anti-mouse antibody (Molecular Probes Inc., Eugene, OR USA). Cells were washed 3 times with PBS. Fluorescence was visualized using a Nikon Diaphot inverted microscope equipped with epi-fluorescence illumination and appropriate filters. Digital images were captured using an S1pro Fuji digital camera, and composite images were prepared using Adobe Photoshop 5.0.

Autoradiography

The receptor affinity of RGD-DTPA-octreotate and RGD-octreotate was determined using autoradiography on brain (sst_2-positive tissue) sections. Brain tissue was embedded in TissueTek (Saqura, Zoeterwoude, The Netherlands) and processed for cryosectioning. Tissue sections (10 μm) were mounted on glass slides and stored at –20 °C for at least 1 day to improve adhesion of the tissue to the slide. Sections were air-dried, pre-incubated in 170 mM Tris-HCl buffer, pH 7.6, for 10 min at room temperature (RT) and then incubated for 60 min at RT with 10^{-10}M ^{111}In-DOTA-Tyr^3-octreotate. Displacement experiments were performed in adjacent sections by means of increasing concentrations of Tyr^3-octreotate, RGD-DTPA-octreotate and RGD-octreotate (range 10^{-10}-10^{-6}M). The incubation solution was 170 mM Tris-HCl buffer, pH 7.6, containing 1% (w/v) BSA, 1 mg bacitricin and 5 mM $MgCl_2$. After incubation, the sections were washed twice for 5 min in cold incubation buffer including 0.25% BSA, in buffer alone and with cold MilliQ. Finally the sections were dried quickly. The sections were exposed to phosphor imaging screens (Packard Instruments Co., Meriden, USA) in X-ray cassettes. The screens were analyzed using a Cyclone phosphor imager and a computer-assisted OptiQuant 03.00 image processing system (Packard Instruments Co, Groningen, The Netherlands). IC_{50} values were calculated from competitive binding curves using GraphPad Prism (GraphPad Prism Software, San Diego, CA).

Statistical analysis

Statistical analysis was performed, multiple comparison analysis was made within each group using ANOVA and the Bonferroni correction (GraphPad Prism Software, San Diego, CA).

RESULTS

RGD-DTPA-octreotide.

Biodistribution. Table 1 shows the biodistribution of RGD-^{111}In-DTPA-octreotate (c(Arg-Gly-Asp-D-Tyr-Asp)-Lys(^{111}In-DTPA)-D-Phe-c(Cys-Tyr-D-Trp-Lys-Thr-Cys)-Thr) at 24 post injection in tumor-bearing rats, a receptor-specific uptake of RGD-^{111}In-DTPA-octreotate in sst_2-positive tissues, e.g. pancreas and adrenals, and in the tumor was found (Table 1). As decreased uptake was found when RGD-^{111}In-DTPA-octreotate was co-injected with 500 μg octreotide ($p < 0.05$). In the liver ($p < 0.001$) and tumor, a decreased uptake was found when RGD-^{111}In-DTPA-octreotate was co-injected with 500 μg RGD, indicating a receptor-specific

uptake in these $\alpha_v\beta_3$-positive organs, although less pronounced when compared with the sst_2-positive tissues. When RGD-^{111}In-DTPA-octreotate was co-injected with an excess of octreotide plus RGD, a clear reduction ($p < 0.05$) was seen in both sst_2- and $\alpha_v\beta_3$-positive tissues and in the tumor.

We also investigated the retention in tissues and tumor as function of time. Table 2 shows that there is a good retention of the radioactivity in the tumor after RGD-^{111}In-DTPA-octreotate injection. Because of the high renal uptake we further investigated the therapeutic effects of the unlabeled hybrid peptide.

TABLE 1. *Tissue/tumor uptake (expressed as %ID/g) of RGD-^{111}In-DTPA-octreotate, with or without co-injection of 500 μg octreotide or RGD or octreotide plus RGD, in Lewis rats, 24 hour post injection (M ± SD, n≥3 per group).*

	Control	**+ Octreotide**	**+ RGD**	**+ Octreotide and RGD**
Blood	0.01 ± 0.00	0.01 ± 0.00	0.01 ± 0.00	0.01 ± 0.00
Spleen	0.08 ± 0.00	0.08 ± 0.01	0.05 ± 0.00	0.05 ± 0.01
Pancreas	1.41 ± 0.31	0.11 ± 0.01	1.33 ± 0.18	0.14 ± 0.01
Adrenals	2.29 ± 0.20	0.10 ± 0.02	1.75 ± 0.17	0.12 ± 0.01
Liver	0.06 ± 0.01	0.06 ± 0.01	0.03 ± 0.00	0.04 ± 0.00
Stomach	0.37 ± 0.02	0.07 ± 0.00	0.44 ± 0.04	0.04 ± 0.00
Femur	0.10 ± 0.00	0.04 ± 0.00	0.10 ± 0.00	0.03 ± 0.00
CA20948	1.65 ± 0.36	0.20 ± 0.06	1.13 ± 0.72	0.24 ± 0.09

TABLE 2. *Tissue/tumor uptake of RGD-^{111}In-DTPA-octreotate (0.5 μg/3 MBq) in Lewis rats, 4, 24, 48, 72 and 96 hour post injection (M ± SD, n≥ 3 per group). 24h expressed as %ID/g, other time points are expressed as % of 24h p.i..*

	4h % of 24h	**24h** set as 100%	**48h** % of 24h	**72h** % of 24h	**96h** % of 24h
Blood	271 ± 22	0.01 ± 0.00	59 ± 22	42 ± 7	33 ± 4
Spleen	117 ± 11	0.07 ± 0.01	83 ± 6	94 ± 4	97 ± 4
Pancreas	177 ± 21	1.41 ± 0.26	68 ± 10	64 ± 5	54 ± 3
Adrenals	85 ± 6	2.27 ± 0.20	73 ± 8	77 ± 5	69 ± 2
Kidney	115 ± 9	12.5 ± 1.43	83 ± 4	79 ± 5	66 ± 3
Liver	95 ± 5	0.07 ± 0.01	63 ± 6	67 ± 7	68 ± 2
Stomach	125 ± 8	0.36 ± 0.02	84 ± 8	66 ± 3	48 ± 2
Muscle	131 ± 22	0.01 ± 0.00	63 ± 9	68 ± 4	68 ± 12
Femur	111 ± 26	0.10 ± 0.01	66 ± 14	73 ± 2	72 ± 2
CA20948	107 ± 21	1.75 ± 0.43	71 ± 9	57 ± 4	47 ± 7

Caspase-3 activity. Figure 1 shows caspase-3 activity in CA20948 cells after 48 h incubation with the peptides RGD, Tyr^3-octreotate and RGD-DTPA-octreotate in a concentration of 10^{-6}M. Here is shown that the highest caspase-3 activity was seen after incubation with RGD-DTPA-octreotate ($p < 0.01$). As control, the 2 mono-peptides; RGD and Tyr^3-octreotate, induced almost no caspase-3 activation. Figure 2 shows a time-dependent response of caspase-3 activation, cells were incubated for various time intervals with RGD-DTPA-octreotate. The highest caspase-3 activity was seen after 24h ($p < 0.001$ vs. control).

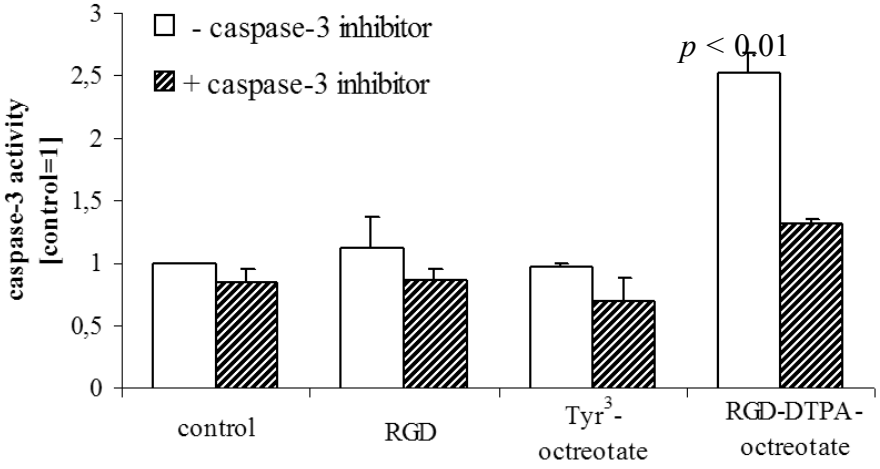

FIGURE 1. *Caspase-3 activity after 48h incubation with 10^{-6}M RGD, Tyr^3-octreotate or RGD-DTPA-octreotate [c(Arg-Gly-Asp-D-Tyr-Asp)-Lys(DTPA)-D-Phe-c(Cys-Tyr-D-Trp-Lys-Thr-Cys)-Thr] in the CA20948 cell line. Control received only incubation medium. The caspase-3 activity was measured directly after the 48h incubation period. The hatched bars are treated with an inhibitor of caspase-3 (Ac-DEVD-CHO). Experiments were performed in triplicate and each sample was measured in triplicate, bars represent mean ± SEM.*

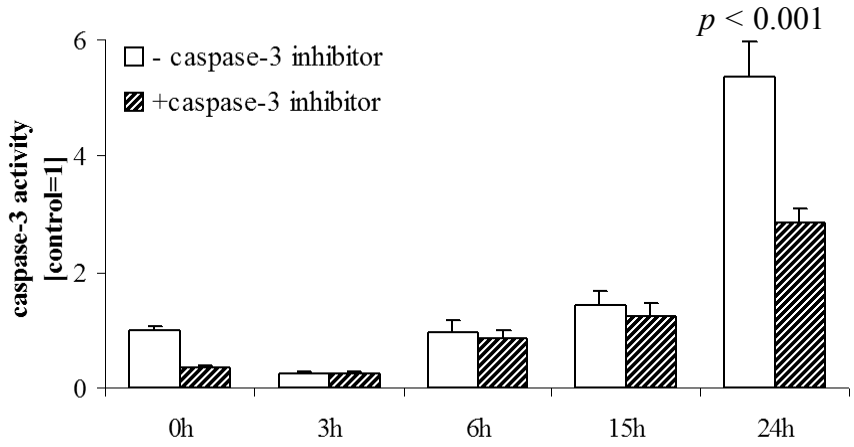

FIGURE 2. *Caspase-3 activity after various incubation periods (0-24h) with RGD-DTPA-octreotate [c(Arg-Gly-Asp-D-Tyr-Asp)-Lys(DTPA)-D-Phe-c(Cys-Tyr-D-Trp-Lys-Thr-Cys)-Thr] in the CA20948 cell line. Control received only incubation medium. Caspase-3 activity was measured directly after each incubation period. The hatched bars are treated with an inhibitor of caspase-3 (Ac-DEVD-CHO). Experiments were performed in triplicate and each sample was measured in triplicate, bars represent mean ± SEM.*

We further investigated if this phenomenon was also found in other cell lines. We therefore studied the caspase-3 activity after an incubation of 6 and 24h with the peptide RGD-DTPA-octreotate in the sst_2-positive cell line AR42J and the CHO cell line transfected with the sst_2. As is shown in Figure 3 both cell lines have a significant increase in caspase-3 activity after 24h incubation with 10^{-6}M RGD-DTPA-octreotate (AR42J $p < 0.01$ and CHO sst_2+ $p < 0.001$), after 6h incubation the caspase-3 activity was at the same level as the control.

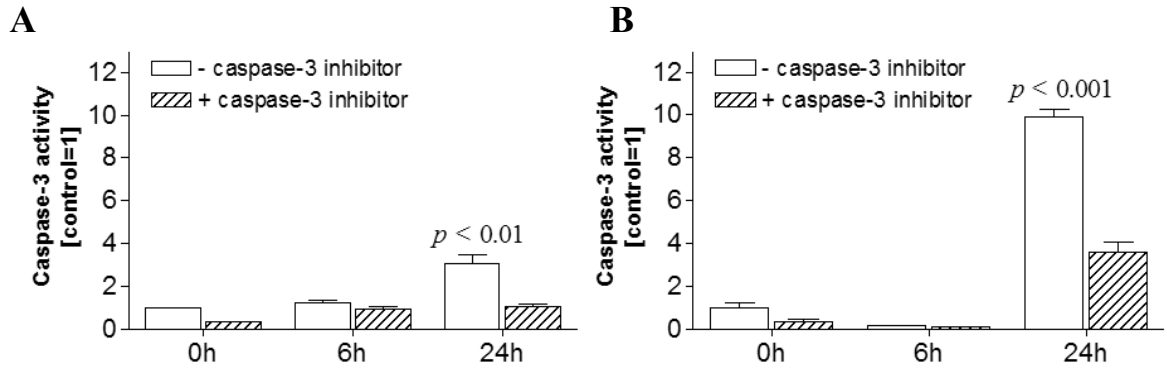

FIGURE 3. *Caspase-3 activity in other cell lines after treatment with 10^{-6}M RGD-DTPA-octreotate [c(Arg-Gly-Asp-D-Tyr-Asp)-Lys(DTPA)-D-Phe-c(Cys-Tyr-D-Trp-Lys-Thr-Cys)-Thr] for various time points; in AR42J cells (A) and in CHO sst_2 receptor-positive cells (B). Caspase-3 activity was measured directly after each incubation period. The hatched bars are treated with an inhibitor of caspase-3 (Ac-DEVD-CHO). Experiments were performed in triplicate and each sample was measured in triplicate, bars represent mean ± SEM.*

RGD-octreotate.

Because of the great apoptosis inducing potential of RGD-DTPA-octreotate in in vitro experiments and due to high renal uptake of RGD-^{111}In-DTPA-octreotate we synthesized RGD-octreotate (c(Arg-Gly-Asp-D-Tyr-Asp)-Lys-D-Phe-c(Cys-Tyr-D-Trp-Lys-Thr-Cys)-Thr), without the chelator DTPA present, to reduce the renal uptake of this hybrid peptide. We first determined the affinity to the sst_2 by autoradiography displacement experiments performed using brain sections.

The IC50 value of Tyr^3-octreotate was 8.5×10^{-9}M as calculated from data shown in Figure 4. The affinity of RGD-DTPA-octreotate and RGD-octreotate to the sst_2 were somewhat lower compared to that of Tyr^3-octreotate itself, although the affinity of RGD-octreotate, $IC_{50} = 1.4\times10^{-8}$M, to the sst_2 was higher compared to that of RGD-DTPA-octreotate, 9.4×10^{-8}M.

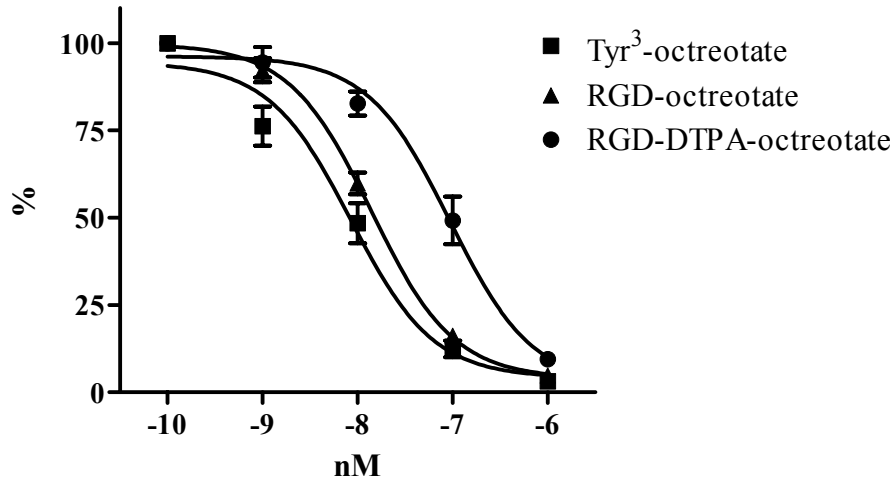

FIGURE 4. *Displacement curves of ^{111}In-DOTA-Tyr^3-octreotate in rat brain sections. The sections were incubated with ^{111}In-DOTA-Tyr^3-octreotate (10^{-10}M) analog and increasing concentrations of unlabeled Tyr^3-octreotate (■), RGD-octreotate (▲) or RGD-DTPA-octreotate (●). Each point represents the mean of three experiments with n=4 each. Binding of 10^{-10}M In-111 labeled Tyr^3-octreotate was considered as 100%.*

Biodistribution studies. In order to get an idea of the biodistribution of RGD-octreotate, without the chelator (DTPA) present, we radioiodinated RGD-octreotate. HPLC analysis showed two peaks (Figure 5), since there are two tyrosine residues in this molecule present. Biodistribution studies were performed in tumor-bearing rats using both peaks together (data not shown) and with the separated peaks. The results of these biodistribution studies were comparable (Table 3). The renal uptake of ^{125}I-RGD-octreotate had a maximum of 4.2 %ID/g at 1h p.i., which is significantly lower ($p < 0.001$) compared to the uptake of RGD-^{111}In-DTPA-octreotate (Table 2). In contrast, the liver uptake p.i. of ^{125}I-RGD-octreotate increased somewhat in comparison with RGD-^{111}In-DTPA-octreotate ($p < 0.05$).

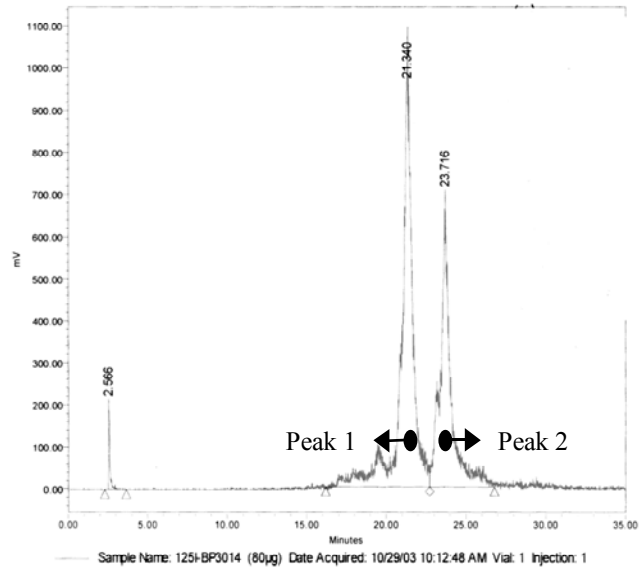

FIGURE 5. *HPLC-analysis of ^{125}I-RGD-octreotate.*

TABLE 3. *Tissue and tumor uptake of ^{125}I-RGD-octreotate (peak 1 and 2) in Lewis rats, 1 and 2 hours post injection (p.i.). Expressed as %ID/g, mean ± sd, n=3.*

	Peak 1		Peak 2	
	1h p.i.	2h p.i.	1h p.i.	2h p.i.
Blood	0.18 ± 0.03	0.08 ± 0.01	0.31 ± 0.03	0.15 ± 0.01
Kidney	3.92 ± 0.23	2.70 ± 0.27	4.22 ± 0.19	1.99 ± 0.21
Liver	0.22 ± 0.01	0.10 ± 0.01	0.31 ± 0.03	0.12 ± 0.01
Femur	0.17 ± 0.02	0.14 ± 0.02	0.18 ± 0.02	0.11 ± 0.01
Tumor	2.48 ± 0.24	1.14 ± 0.21	3.04 ± 0.11	1.91 ± 0.20

Caspase-3. In the AR42J cells we visualized the activation of caspase-3 by RGD-octreotate using immunocytochemistry (Figure 6). Figure 6A (top left) shows untreated AR42J cells, 6B (top right) shows AR42J cells treated with 0.002 mM RGD-octreotate and 6C (bottom right) AR42J cells treated with 0.1mM RGD-octreotate. Figure 6C (0.1 mM RGD-octreotate) shows an increase in caspase-3 cleavage (red fluorescence, indicated with an arrow) compared to untreated cells. When the cells were treated with 0.002 mM RGD-octreotate (6B) an increase in red fluorescence is seen compared with the control. So, also RGD-octreotate is able to activate caspase-3 in the cell, thereby inducing apoptosis.

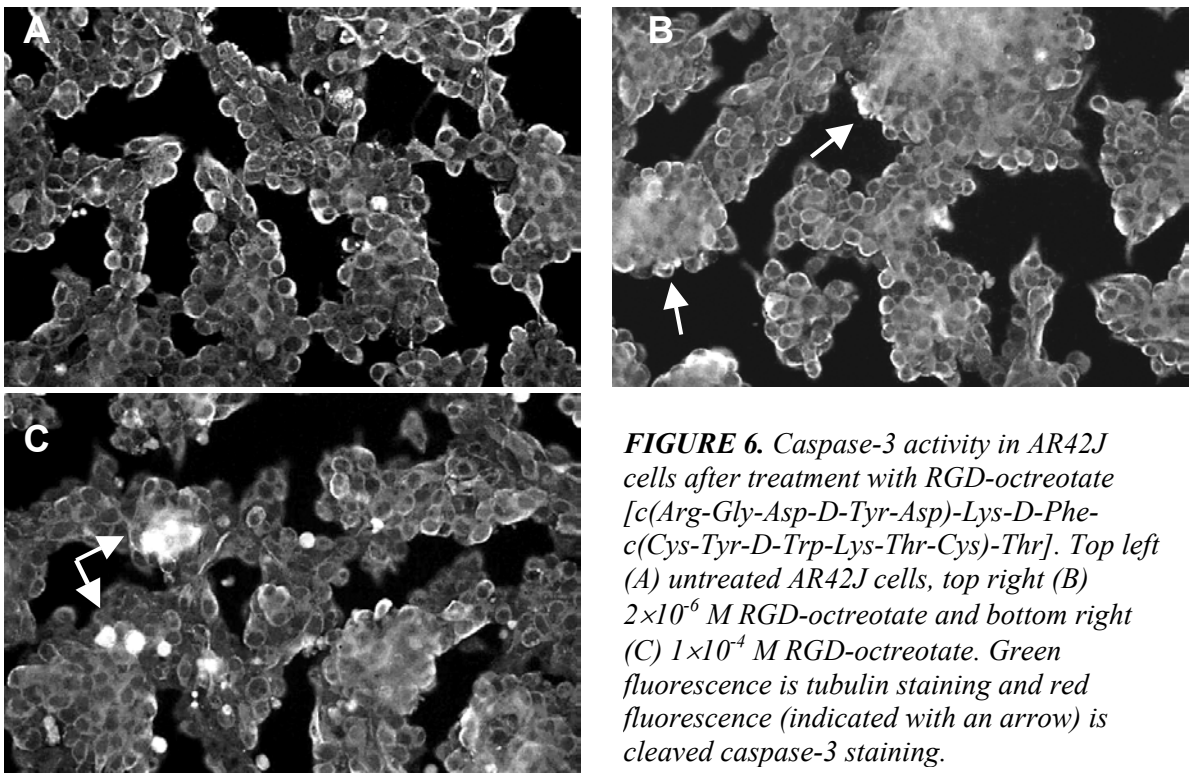

FIGURE 6. *Caspase-3 activity in AR42J cells after treatment with RGD-octreotate [c(Arg-Gly-Asp-D-Tyr-Asp)-Lys-D-Phe-c(Cys-Tyr-D-Trp-Lys-Thr-Cys)-Thr]. Top left (A) untreated AR42J cells, top right (B) 2×10^{-6} M RGD-octreotate and bottom right (C) 1×10^{-4} M RGD-octreotate. Green fluorescence is tubulin staining and red fluorescence (indicated with an arrow) is cleaved caspase-3 staining.*

DISCUSSION

Angiogenesis, or the formation of new blood vessels from pre-existing vessels, is a complex process that normally occurs in adults only under specific conditions such as wound healing and inflammation [1]. However, angiogenesis is also essential for the growth of tumors. The integrin $\alpha_v\beta_3$ receptor has a well-characterized involvement in angiogenesis [36, 37] and tumor invasiveness [36, 38], which was demonstrated by using $\alpha_v\beta_3$-specific antagonists, such as monoclonal antibodies and RGD peptides [3, 4]. Another important finding is that soluble RGD peptides are able to induce apoptosis by activation of procaspase-3 in the cytoplasm of the cell [10]. So, activation of caspases could be an explanation for the apoptotic activity of RGD peptides. We synthesized a hybrid peptide consisting of the somatostatin analog Tyr^3-octreotate and an RGD-containing moiety.

Radiolabeled somatostatin analogs are used for the localization and treatment of somatostatin receptor-positive tumors, mostly of neuroendocrine origin. A large variety of radiolabeled somatostatin derivatives have been prepared for radionuclide therapy and visualization of these tumors and metastases, and are in various stages of preclinical and clinical investigation. OctreoTher® (^{90}Y-DOTA-Tyr^3-octreotide) is an example of a somatostatin analog radiolabeled with the high-energy beta emitter yttrium-90. More recent is ^{177}Lu-DOTA-Tyr^3-octreotate, which provides further improvement as a targeted radiopharmaceutical by having higher uptake and retention in sst_2-positive tumors [23, 24, 39]. By creating a hybrid peptide the radiotherapeutic efficacy of the somatostatin analog could be increased through the induction of apoptosis via the RGD-peptide.

In a previous study [30] it was shown that this hybrid peptide had a high uptake in sst_2-positive and $\alpha_v\beta_3$-positive rat pancreatic CA20948 tumor cells. Internalization occurred mainly via sst_2-receptors. Biodistribution studies in rats showed high tumor uptake and good tumor radioactivity retention of RGD-^{111}In-DTPA-octreotate in tumor-bearing rats [30]. From these *in vitro* and *in vivo* studies it can be concluded that Tyr^3-octreotate can serve as a carrier for RGD internalization. *In vitro* studies [31] showed that RGD-^{111}In-DTPA-octreotate had a more pronounced tumoricidal effect than ^{111}In-DTPA-RGD and ^{111}In-DTPA-Tyr^3-octreotate in a colony-forming assay. The superior tumoricidal effect was probably the result of increased apoptosis, as shown by increased caspase-3 activity after incubation with RGD-octreotate [31].

The biodistribution studies in rats showed high specific tumor uptake and good tumor radioactivity retention of RGD-^{111}In-DTPA-octreotate in tumor-bearing rats (Tables 1 and 2). When an excess of octreotide, RGD or RGD plus octreotide was co-injected, a significant reduction in uptake in various sst_2- and $\alpha_v\beta_3$-receptor positive organs was seen. The reduction in e.g. the tumor was most pronounced when both peptides were co-injected ($p < 0.05$). The uptake of RGD-^{111}In-DTPA-octreotate occurred via both receptors but probably mainly via the sst_2 receptor. Unfortunately RGD-^{111}In-DTPA-octreotate has a very high renal uptake, limiting the therapeutic dose that can be administered, as the kidneys are the critical organs in PRRT using radiolabeled somatostatin analogs. We therefore investigated also the therapeutic effects of the unlabeled hybrid peptide RGD-DTPA-octreotate.

The highest levels of caspase-3 activity were found in CA20948 cells after incubation with this hybrid peptide RGD-DTPA-octreotate in comparison with the 2 mono-peptides; RGD and Tyr^3-octreotate. Caspase-3 activity after incubation with RGD-DTPA-octreotate was time-dependent. The highest caspase-3 activity was found after an incubation period of 24h. The caspase-3 activity was lower after 48h compared to that after 24h (not shown). In two other cell lines (AR42J and CHO transfected with the sst_2) caspase-3 was also investigated after incubation with unlabeled RGD-DTPA-octreotate. Here also a significant increase in caspase-3 levels was seen and again after 24h the highest levels were found. The height of the caspase-3 levels was dependent on the cell line used, the highest levels were found in the CHO sst_2^+ cell line. In a recent study [40] in HUVEC (human umbilical vein endothelial cells) cells also an increase in caspase-3 activation was found after 24h incubation with a RGD peptide. Also an increase in caspase-8 and –9 levels was found already after 4h incubation [40], supporting the hypothesis that RGD-peptides might directly trigger the caspase cascade at an early level.

Because of the great apoptosis inducing potential of RGD-DTPA-octreotate in *in vitro* experiments and due to high renal uptake of RGD-^{111}In-DTPA-octreotate we synthesized RGD-octreotate, without the chelator DTPA present, to change the route of elimination from the body. In a previous study in rats it was shown that ^{125}I-Tyr^3-octreotide was rapidly cleared via the liver [41], while ^{111}In-DTPA-Tyr^3-octreotide favored renal excretion, due to the addition of the relatively large and very hydrophilic DTPA group. These findings were in accordance with the in vivo scintigraphic results of ^{123}I-Tyr^3-octreotide and ^{111}In-DTPA-octreotide [42]. So, by eliminating the DTPA-group of RGD-DTPA-octreotate the elimination route could change from a renal clearance to more a hepatic clearance.

In order to get an idea of the biodistribution of unlabeled RGD-octreotate, without the chelator (DTPA) present, RGD-octreotate was radioiodinated. On HPLC analysis two peaks were detected and isolated, since there are two tyrosine residues in this molecule present, one in the RGD part and one in the octreotate part, ^{125}I can label in various ways. Biodistribution studies were performed in tumor-bearing rats using both peaks together (data not shown) and with both separated peaks. The results of both biodistribution studies, using both peaks together or separated peaks, were comparable. The biodistribution of ^{125}I-RGD-octreotate (Table 3) showed indeed a much lower renal uptake and a somewhat higher liver uptake in comparison with RGD-^{111}In-DTPA-octreotate. With the radioiodinated RGD-octreotate shorter time intervals were taken due to a more rapid release from the cells of ^{125}I compared to the radiometal ^{111}In. Finally it was shown that RGD-octreotate was still able to activate caspase-3 as was indicated with immunocytochemistry.

In conclusion, due to the high renal uptake RGD-^{111}In-DTPA-octreotate is unsuitable for radionuclide therapy. The unlabeled peptide, RGD-(DTPA-)octreotate also showed an increase in caspase-3 levels, indicating the therapeutical potential of this compound. To further enhance radionuclide therapy with somatostatin analogs, unlabeled hybrid peptide can be administered after or during therapy without radiotoxicity to non-target tissues.

ACKNOWLEDGEMENTS

We thank Renate Okker and Magda Bijster for their technical assistance with the experiments.

REFERENCES

1. Varner JA. The role of vascular cell integrins alpha v beta 3 and alpha v beta 5 in angiogenesis. *Exs* 1997;79:361-390.
2. Ruoslahti E, Pierschbacher MD. New perspectives in cell adhesion: RGD and integrins. *Science* 1987;238:491-497.
3. Brooks PC, Montgomery AM, Rosenfeld M, Reisfeld RA, Hu T, Klier G, Cheresh DA. Integrin alpha v beta 3 antagonists promote tumor regression by inducing apoptosis of angiogenic blood vessels. *Cell* 1994;79:1157-1164.
4. Brooks PC, Stromblad S, Klemke R, Visscher D, Sarkar FH, Cheresh DA. Antiintegrin alpha v beta 3 blocks human breast cancer growth and angiogenesis in human skin. *J Clin Invest* 1995;96:1815-1822.
5. Frisch SM, Francis H. Disruption of epithelial cell-matrix interactions induces apoptosis. *J Cell Biol* 1994;124:619-626.
6. Chen Y, Xu X, Hong S, Chen J, Liu N, Underhill CB, Creswell K, Zhang L. RGD-Tachyplesin inhibits tumor growth. *Cancer Res* 2001;61:2434-2438.
7. Anuradha CD, Kanno S, Hirano S. RGD peptide-induced apoptosis in human leukemia HL-60 cells requires caspase-3 activation. *Cell Biol Toxicol* 2000;16:275-283.
8. Chatterjee S, Brite KH, Matsumura A. Induction of apoptosis of integrin-expressing human prostate cancer cells by cyclic Arg-Gly-Asp peptides. *Clin Cancer Res* 2001;7:3006-3011.
9. Adderley SR, Fitzgerald DJ. Glycoprotein IIb/IIIa antagonists induce apoptosis in rat cardiomyocytes by caspase-3 activation. *J Biol Chem* 2000;275:5760-5766.
10. Buckley CD, Pilling D, Henriquez NV, Parsonage G, Threlfall K, Scheel-Toellner D, Simmons DL, Akbar AN, Lord JM, Salmon M. RGD peptides induce apoptosis by direct caspase-3 activation. *Nature* 1999;397:534-539.
11. de Jong M, Breeman WA, Bakker WH, Kooij PP, Bernard BF, Hofland LJ, Visser TJ, Srinivasan A, Schmidt MA, Erion JL, Bugaj JE, Macke HR, Krenning EP. Comparison of (111)In-labeled somatostatin analogues for tumor scintigraphy and radionuclide therapy. *Cancer Res* 1998;58:437-441.
12. Krenning EP, Valkema R, Kooij PP, Breeman WA, Bakker WH, deHerder WW, vanEijck CH, Kwekkeboom DJ, deJong M, Pauwels S. Scintigraphy and radionuclide therapy with [indium-111-labelled-diethyl triamine penta-acetic acid-D-Phe1]-octreotide. *Ital J Gastroenterol Hepatol* 1999;31 Suppl 2:S219-223.
13. Krenning EP, Kooij PP, Bakker WH, Breeman WA, Postema PT, Kwekkeboom DJ, Oei HY, de Jong M, Visser TJ, Reijs AE, et al. Radiotherapy with a radiolabeled somatostatin analogue, [111In-DTPA-D- Phe1]-octreotide. A case history. *Ann N Y Acad Sci* 1994;733:496-506.
14. Slooter GD, Breeman WA, Marquet RL, Krenning EP, van Eijck CH. Anti-proliferative effect of radiolabelled octreotide in a metastases model in rat liver. *Int J Cancer* 1999;81:767-771.
15. Anthony LB, Woltering EA, Espenan GD, Cronin MD, Maloney TJ, McCarthy KE. Indium-111-pentetreotide prolongs survival in gastroenteropancreatic malignancies. *Semin Nucl Med* 2002;32:123-132.
16. Capello A, Krenning EP, Breeman WA, Bernard BF, de Jong M. Peptide receptor radionuclide therapy in vitro using [111In- DTPA0]octreotide. *J Nucl Med* 2003;44:98-104.
17. De Jong M, Breeman WA, Bernard HF, Kooij PP, Slooter GD, Van Eijck CH, Kwekkeboom DJ, Valkema R, Macke HR, Krenning EP. Therapy of neuroendocrine tumors with radiolabeled somatostatin- analogues. *Q J Nucl Med* 1999;43:356-366.
18. Otte A, Herrmann R, Heppeler A, Behe M, Jermann E, Powell P, Maecke HR, Muller J. Yttrium-90 DOTATOC: first clinical results. *Eur J Nucl Med* 1999;26:1439-1447.

19. Stolz B, Weckbecker G, Smith-Jones PM, Albert R, Raulf F, Bruns C. The somatostatin receptor-targeted radiotherapeutic [90Y-DOTA-DPhe1, Tyr3]octreotide (90Y-SMT 487) eradicates experimental rat pancreatic CA 20948 tumours. *Eur J Nucl Med* 1998;25:668-674.
20. Bodei L, Cremonesi M, Zoboli S, Grana C, Bartolomei M, Rocca P, Caracciolo M, Macke HR, Chinol M, Paganelli G. Receptor-mediated radionuclide therapy with 90Y-DOTATOC in association with amino acid infusion: a phase I study. *Eur J Nucl Med Mol Imaging* 2003;30:207-216.
21. Waldherr C, Pless M, Maecke HR, Haldemann A, Mueller-Brand J. The clinical value of [90Y-DOTA]-D-Phe1-Tyr3-octreotide (90Y-DOTATOC) in the treatment of neuroendocrine tumours: a clinical phase II study. *Ann Oncol* 2001;12:941-945.
22. Waldherr C, Pless M, Maecke HR, Schumacher T, Crazzolara A, Nitzsche EU, Haldemann A, Mueller-Brand J. Tumor response and clinical benefit in neuroendocrine tumors after 7.4 GBq (90)Y-DOTATOC. *J Nucl Med* 2002;43:610-616.
23. de Jong M, Breeman WA, Bernard BF, Bakker WH, Schaar M, van Gameren A, Bugaj JE, Erion J, Schmidt M, Srinivasan A, Krenning EP. [177Lu-DOTA(0),Tyr3] octreotate for somatostatin receptor-targeted radionuclide therapy. *Int J Cancer* 2001;92:628-633.
24. Kwekkeboom DJ, Bakker WH, Kam BL, Teunissen JJ, Kooij PP, De Herder WW, Feelders RA, Van Eijck CH, De Jong M, Srinivasan A, Erion JL, Krenning EP. Treatment of patients with gastro-entero-pancreatic (GEP) tumours with the novel radiolabelled somatostatin analogue [(177)Lu-DOTA(0),Tyr(3)]octreotate. *Eur J Nucl Med Mol Imaging* 2003;30:417-422.
25. Schwartz AL, Fridovich SE, Lodish HF. Kinetics of internalization and recycling of the asialoglycoprotein receptor in a hepatoma cell line. *J Biol Chem* 1982;257:4230-4237.
26. De Jong M, Bernard BF, De Bruin E, Van Gameren A, Bakker WH, Visser TJ, Macke HR, Krenning EP. Internalization of radiolabelled [DTPA0]octreotide and [DOTA0,Tyr3]octreotide: peptides for somatostatin receptor-targeted scintigraphy and radionuclide therapy. *Nucl Med Commun* 1998;19:283-288.
27. Duncan JR, Stephenson MT, Wu HP, Anderson CJ. Indium-111-diethylenetriaminepentaacetic acid-octreotide is delivered in vivo to pancreatic, tumor cell, renal, and hepatocyte lysosomes. *Cancer Res* 1997;57:659-671.
28. Hornick CA, Anthony CT, Hughey S, Gebhardt BM, Espenan GD, Woltering EA. Progressive nuclear translocation of somatostatin analogs. *J Nucl Med* 2000;41:1256-1263.
29. Schally AV, Nagy A. Cancer chemotherapy based on targeting of cytotoxic peptide conjugates to their receptors on tumors. *Eur J Endocrinol* 1999;141:1-14.
30. Bernard B, Capello A, van Hagen M, Breeman W, Srinivasan A, Schmidt M, Erion J, van Gameren A, Krenning E, de Jong M. Radiolabeled RGD-DTPA-Tyr3-octreotate for receptor-targeted radionuclide therapy. *Cancer Biother Radiopharm* 2004;19:173-180.
31. Capello A, Krenning EP, Bernard BF, Breeman WA, van Hagen MP, de Jong M. Increased cell death after therapy with an arg-gly-asp-linked somatostatin analog. *J Nucl Med* 2004;45:1716-1720.
32. van Hagen PM, Breeman WA, Bernard HF, Schaar M, Mooij CM, Srinivasan A, Schmidt MA, Krenning EP, de Jong M. Evaluation of a radiolabelled cyclic DTPA-RGD analogue for tumour imaging and radionuclide therapy. *Int J Cancer* 2000;90:186-198.
33. Chan WC, White PS. eds. Fmoc solid phase peptide synthesis: a practical approach. *Oxford University Press, Oxford England* 2000.
34. Bakker WH, Albert R, Bruns C, Breeman WA, Hofland LJ, Marbach P, Pless J, Pralet D, Stolz B, Koper JW, et al. [111In-DTPA-D-Phe1]-octreotide, a potential radiopharmaceutical for imaging of somatostatin receptor-positive tumors: synthesis, radiolabeling and in vitro validation. *Life Sci* 1991;49:1583-1591.
35. Bakker WH, Krenning EP, Breeman WA, Koper JW, Kooij PP, Reubi JC, Klijn JG, Visser TJ, Docter R, Lamberts SW. Receptor scintigraphy with a radioiodinated somatostatin analogue: radiolabeling, purification, biologic activity, and in vivo application in animals. *J Nucl Med* 1990;31:1501-1509.

36. Haubner R, Wester HJ, Burkhart F, Senekowitsch-Schmidtke R, Weber W, Goodman SL, Kessler H, Schwaiger M. Glycosylated RGD-containing peptides: tracer for tumor targeting and angiogenesis imaging with improved biokinetics. *J Nucl Med* 2001;42:326-336.
37. Stromblad S, Cheresh DA. Integrins, angiogenesis and vascular cell survival. *Chem Biol* 1996;3:881-885.
38. Felding-Habermann B, Mueller BM, Romerdahl CA, Cheresh DA. Involvement of integrin alpha V gene expression in human melanoma tumorigenicity. *J Clin Invest* 1992;89:2018-2022.
39. De Jong M, Kwekkeboom D, Valkema R, Krenning EP. Radiolabelled peptides for tumour therapy: current status and future directionsPlenary lecture at the EANM 2002. *Eur J Nucl Med Mol Imaging* 2003;30:463-469.
40. Aguzzi MS, Giampietri C, De Marchis F, Padula F, Gaeta R, Ragone G, Capogrossi MC, Facchiano A. RGDS peptide induces caspase 8 and caspase 9 activation in human endothelial cells. *Blood* 2004;103:4180-4187.
41. de Jong M, Bakker WH, Breeman WA, van der Pluijm ME, Kooij PP, Visser TJ, Docter R, Krenning EP. Hepatobiliary handling of iodine-125-Tyr3-octreotide and indium-111- DTPA-D-Phe1-octreotide by isolated perfused rat liver. *J Nucl Med* 1993;34:2025-2030.
42. Krenning EP, Kwekkeboom DJ, Bakker WH, Breeman WA, Kooij PP, Oei HY, van Hagen M, Postema PT, de Jong M, Reubi JC, et al. Somatostatin receptor scintigraphy with [111In-DTPA-D-Phe1]- and [123I- Tyr3]-octreotide: the Rotterdam experience with more than 1000 patients. *Eur J Nucl Med* 1993;20:716-731.

CHAPTER 5

COMBINATION THERAPY: RGD-OCTREOTATE

5.4 Induction of apoptosis with hybrids of RGD and anti-mitotic effects of hybrids of cytostatic drugs and peptides (radiolabeled and non-radiolabeled)

Leo Hofland, Astrid Capello, Eric Krenning, Marion de Jong and Martin van Hagen

Journal of Nuclear Medicine, 2005, 46: 191S-198S.

ABSTRACT

The presence of a high density of somatostatin receptors (SSR) on human tumors forms the basis for the successful visualization of primary tumors and their metastases using radiolabeled SS-analogs. In recent years SS-analogs coupled to beta-emitting radioisotopes have been successfully applied in the treatment of patients with metastatic SSR-positive neuroendocrine tumors. This concept of targeting SSR-expressing tumors using peptide receptor radionuclide therapy may also apply to the use of SS-analogs coupled to chemotherapeutic compounds. Evidence for the effectiveness of such cytotoxic SS-analogs as anti-tumor agents has been provided from a significant number of studies in experimental tumor models. In addition to cytotoxic SS-analogs, recently also SS-analogs coupled to RGD molecules (arginine (R), glycine (G), and aspartate (D)-containing peptides) and to paclitaxol have been synthesized. In this paper, the development of the different cytotoxic SS-analogs and their anti-tumor effects in vitro and in vivo in experimental models are discussed.

INTRODUCTION

Toxicity of chemotherapeutic drugs is one of the main restrictions in the adjuvant treatment of patients with advanced or metastatic cancers. The concept of reducing toxicity via targeted delivery of cytotoxic agents has been proposed already more than a decade ago. Schally et al. [1, 2] developed a series of targeted anti-tumor agents by linking various cytotoxic radicals to analogs of luteinizing hormone releasing hormone (LHRH), somatostatin (SS) and bombesin. Targeted delivery of chemotherapeutic compounds coupled to small peptide molecules requires the presence of specific receptors on the target cancer cells. Following binding of the peptide coupled with a cytotoxic compound to its receptor, the hybrid molecule requires to be internalized by the tumor cells, after which the cytotoxic agent may be uncoupled from its linker and can thus produce its lethal action (Fig. 1). The aim of targeted chemotherapy in oncology is to improve effectiveness via the selective delivery of cytotoxic compounds to primary tumors and their metastases and to reduce peripheral toxicity. In addition to chemotherapeutic compounds also other molecules capable of modulating (tumor) cell growth can be coupled to SS-analogs. One group of small molecules include so-called RGD molecules, that bind with high affinity to the integrin $\alpha_v\beta_3$, and have been shown to be inhibitors of cell adhesion, migration, growth and differentiation. Again, via targeted delivery of such RGD-SS molecules to tumor cells, as well as to neovascular endothelial cells, known to express a high density of $\alpha_v\beta_3$ receptors, these molecules may be potentially interesting anti-tumor agents. In the present paper the development and anti-tumor action of different cytotoxic SS-analogs, as well as the development and preliminary characterization of radiolabeled RDG-coupled SS-analogs is reviewed.

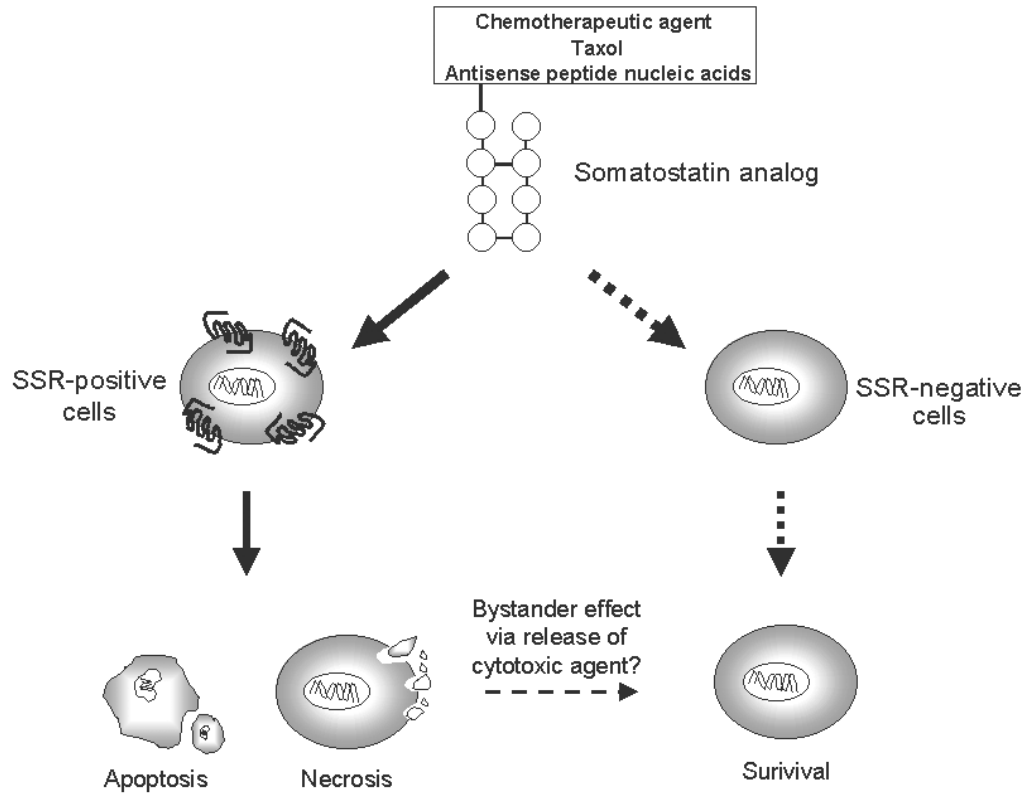

FIGURE 1. *Principle of SSR-targeted cytotoxic therapy.*

SOMATOSTATIN RECEPTOR SUBTYPE EXPRESSION IN TUMOR TISSUES

Neuroendocrine tumors, which often originate from SS-target tissues frequently express a high density of SS-receptors (SSR). Human tumors which express SSR are pituitary adenomas, islet cell tumors, carcinoids, paragangliomas, pheochromocytomas, small cell lung cancers and medullary thyroid carcinomas, as well as malignant lymphomas and breast-, prostate- and ovarian cancers [3]. The SSR subtype expression in different types of human cancers has been demonstrated at the mRNA level using in situ hybridization, RNAse protection assays, the reverse transcriptase polymerase chain reaction (RT-PCR), autoradiography, as well as by immunohistochemistry [3]. The majority of human SSR positive tumors simultaneously express multiple SSR subtypes, although there is a considerable variation in SSR subtype expression between the different tumor types and among tumors of the same type. SSR autoradiographic studies showed the absence of binding of the SSR subtype 2 (sst_2)- preferring analog ^{125}I-Tyr^3-octreotide in a small subgroup of human insulinomas, carcinoids, pituitary adenomas and meningiomas, in 50% of the medullary thyroid carcinomas (MTC), in prostate cancer and in all SSR-positive ovarian cancers, whereas in the same tumors binding sites for radioiodinated SS are present [3]. In such cases, targeting tumors with sst_2-preferring cytotoxic SS-analogs may not be successful. Apart from tumor cells also blood vessels, immune cells, stromal cells which are present in or surround, human tumors may express SSR subtypes [3]. When targeted therapy using SS-analogs coupled

to chemotherapeutic agents or -RGD is considered, it is important to realize that some tumors have a heterogeneous distribution of SSR. In particular, in more than 50% of the breast cancer specimens SSR expression displays a non-homogenous distribution, with regions of high density of SSR next to regions lacking the receptor [3]. Knowledge of the SSR subtype expression pattern, as well as non-homogeneity in the expression of SSR within tumors is very important for the development of the concept of SSR-targeted chemotherapy. As will be discussed below, SSR subtypes differ in their ability to internalize receptor-bound ligand [4], which is a crucial step to direct a SS-analog linked to a cytotoxic compound or RGD into the internal milieu of the tumor cell, where it can exert its cytotoxic action.

INTERNALIZATION OF SOMATOSTATIN RECEPTOR SUBTYPES

Since the cloning of the five SSR subtypes, the involvement of the individual human SSR subtypes in the process of receptor-mediated internalization of SS has been extensively investigated. As indicated, the ability of SSR to internalize the ligand-receptor complex following ligand binding, forms the basis for the concept of targeted chemotherapy using cytotoxic SS-analogs as well as for the use of radiolabeled RGD-SS analogs to selectively inhibit tumor growth. In general, the mechanism and route of internalization of SSR-agonist complexes follow those described for many other G-protein coupled receptors [5-8] and involve aggregation of the hormone receptor complex in specialized areas of the membrane, followed by internalization of the hormone-receptor complex via clathrin-coated, as well as -uncoated pits [5, 9]. Following internalization and pit formation, fusion of these vesicles with lysosomes occur, resulting in hormone degradation, or receptor recycling to the cell surface [7, 10, 11]. At this stage, the cytotoxic molecules are released and may exert their lethal action.

SSR subtypes differentially internalize SS and SS-analogs [12]. In CHO-K1 cells stably expressing one the five human SSR subtypes, sst_2, sst_3, sst_4 and sst_5 receptors displayed rapid (within minutes) agonist-dependent internalization of ^{125}I-LTT SS-28 ligand in a time- and temperature dependent manner [13]. Maximum internalization of the radioligand occurred within 60 minutes. Sst_3 and sst_5 expressing cells displayed the highest degree of internalization (78 and 66%, respectively), followed by sst_4 (29%) and sst_2 (20%). In contrast, the sst_1 subtype displayed only a very low amount (4%) of internalization. Another study using COS-7 cells transfected with the human sst_1 or sst_{2A} receptor subtypes [14] recently confirmed the low internalization rate of the sst_1 subtype. However, in this study, up to 75% of specifically bound fluorescent ligand was recovered inside sst_{2A}-expressing cells within 60 min. after agonist exposure, where it clustered into small endosome-like particles [14]. The capacity of internalization of SS via the sst_5 receptor was intermediate between sst_1 and sst_{2A} receptors [15].

A predominant importance of the sst_{2A} receptor, which is widely expressed in many human tumors, in determining the uptake of ^{111}In-DTPA-octreotide in vivo is further underlined by the observation that uptake of ^{111}In-DTPA-octreotide in SSR positive organs like the pituitary gland, adrenals and thymus, is reduced by more than 80% in sst_{2A} receptor

knock out mice, compared with the values of uptake in wild type mice carrying sst_{2A} receptors [16]. Moreover, a significant number of in vivo studies in experimental tumor models have shown that uptake of ^{111}In-DTPA-octreotide is blocked by the simultaneous administration of excess unlabeled octreotide [16-19]. Finally, relative uptake values of radioactivity in patients with carcinoid tumor or neuroblastoma correlate with tumoral sst_2 expression level [4]. In conclusion, the ability of SSR subtypes to undergo agonist-induced internalization is an important characteristic of these receptors for transporting radiolabeled and cytotoxic SS-analogs into the cell.

DEVELOPMENT AND IN VITRO CHARACTERIZATION CYTOTOXIC SOMATOSTATIN ANALOGS

The first cytotoxic SS-analog which has been described was methotrexate linked to the N-terminal of the octapeptide SS-analog RC-121 (D-Phe-Cys-Tyr-D-Trp-Lys-Val-Cys-Thr-NH_2). This compound was named AN-51 [20]. Binding studies of AN-51 to SS-R expressing tissues, e.g. rat brain cortex, Dunning rat tumor R3327H and MiaPaCa-2 pancreatic cancer cells showed that AN-51 has only slight reduced SSR-binding affinity (2- to 10-fold), compared to its parental molecule RC-121 [20]. In addition, a 27 day treatment of rats bearing MiaPaCa-2 pancreatic cancer xenografts with RC-121 (20 μg/day) and AN-51 (25 μg/day) resulted in a comparable suppression of serum GH levels, suggesting that both SSR binding- and biological activity is retained in the hybrid AN-51 molecule. More recently, Schally et al. developed a much more potent cytotoxic SS-analog, consisting of RC-121 coupled to 2-pyrrolino-doxorubicin (AN-201), which is a derivative of doxorubicin being 500-1000 more potent compared with doxorubicin. This novel molecule has been code-named AN-238 (Fig. 2) [21]. Compared with RC-121, the hybrid molecule AN-238 had a slightly reduced SSR binding affinity. Binding affinity, defined as IC_{50} value, the concentration of analog required to inhibit 50% of the specific binding of ^{125}I-RC-160 SS-analog to SSR-expressing rat pituitary membranes amounted 0.31 nM for RC-121 and 23.8 nM for AN-238, respectively. This binding affinity of AN-238 is comparable to the binding affinities of several DTPA- and DOTA- coupled SS-analogs to human sst_2 receptors [22]. In superfused rat anterior pituitary cell cultures, it was shown that AN-238 fully preserved the GH-release inhibitory potency of RC-121 [21]. Moreover, in vitro growth of gastric-, breast-, prostate- pancreatic and small cell lung cancer (SCLC) cell lines was inhibited by AN-238 in a dose-dependent fashion with IC_{50}-values ranging between 3.2 and 40 nM, which were comparable to values of inhibition of cell growth by the 2-pyrrolino-doxorubicin alone (between 1.8 and 24 nM). These data suggest that like AN-51, also AN-238 has retained the binding and functional properties of its parental molecules RC-121 and 2-pyrrolino-doxorubicin [21].

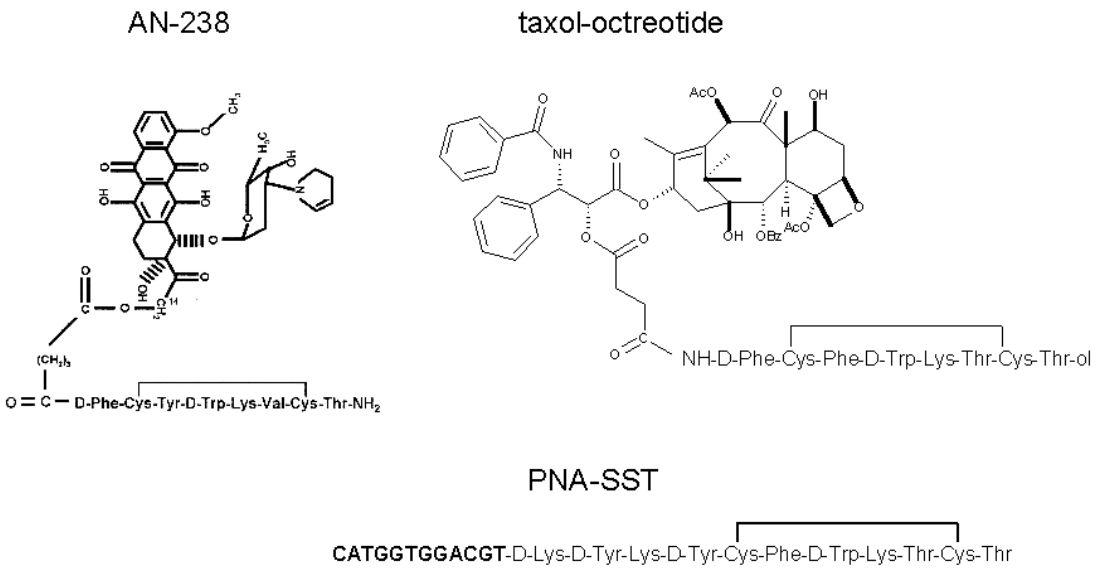

FIGURE 2. *Structure of three different cytotoxic SS-analogs. Reproduced with permission (copyright 1998 National Academy of Sciences [28]) and adapted from refs. [25, 29]. AN-238: SS-analog RC-121 coupled to 2-pyrrolino-doxorubicin; PNA-SST: SS-analog coupled to antisense peptide nucleic acid (PNA); taxol-octreotide: SS-analog octreotide conjugated to paclitaxel (taxol).*

Apart from cytotoxic SS-analogs containing methotrexate, doxorubicin or 2-pyrrolinodoxorubicin, other cytotoxic agents have been coupled to SS-analogs as well. Fuselier et al. [23], recently synthesized a series of SS-analogs coupled to the topoisomerase inhibitors camptothecin and combretastatin. Carbamates were used as linker, since they are known to be relative resistant in plasma, compared with for example ester-type linkages [24]. One of these compounds, named compound 2 [23], had a full retention of biological activity compared with native SS-14. Compound 2 inhibited GHRH-stimulated GH release by cultured rat pituitary cells with an IC_{50} value in the low nanomolar range (0.27 nM). In vitro cytotoxicity of this compound, as measured by a cell viability MTT assay was also in the nanomolar range (54.2 nM) and comparable to inhibitory values described for AN-238. Huang et al. [25], showed some degree of efficacy of octreotide conjugated to taxol in MCF-7 cells. Octreotide-taxol (Fig. 2) inhibited SSR positive MCF-7 cell viability with an IC_{50} value of 100nM, whereas SSR negative CHO cells showed a much lower sensitivity. Finally, a SS-analog conjugated to antisense peptide nucleic acids (PNA) targeting the n-*myc* oncogene showed retained functional activity in term of GH suppression in vitro, as well as enhanced cytotoxicity to human SSR expressing human IMR32 neuroblastoma cells, although with a relatively low efficacy in the micromolar range [26]. It should be mentioned that stability of these compounds in vitro may be very important. If the compounds are degraded while measuring its cytotoxic effect, it may be possible that in cytotoxic assays also the effects of the cytotoxic compounds alone is involved and thus the outcome of the vitro studies not necessarily reflects the potentials of the compounds to selectively target tumor cells in vivo.

IN VIVO ANTI-TUMOR ACTIVITY OF CYTOTOXIC SOMATOSTATIN ANALOGS

In this chapter, the pre-clinical studies demonstrating that cytotoxic SS-analogs inhibit tumor growth in experimental tumor models are discussed. In nude mice transplanted with the human MIA PaCa-2 pancreatic tumor, AN-51 significantly inhibited tumor growth, whereas the chemotherapeutic compound alone, methotrexate, or RC-121 alone, had no significant inhibitory effect [20], and with methotrexate alone displaying a much higher toxicity compared with AN-51. As far as known no other pre-clinical studies with AN-51 have been reported. This is probably due to the development of novel cytotoxic SS-analogs with enhanced cytotoxic activity. As indicated above, AN-238 has a very high cytotoxicity in SS-receptor positive cells in vitro [21]. In vivo, a large number of studies, mainly by Schally and co-workers, demonstrated that AN-238 has a very potent anti-tumor activity in proven SSR positive experimental tumor models. Although among the different studies some differences exist with respect to the dose and number of administrations of AN-238, all studies clearly show that compared with the cytotoxic parental molecule AN-201 (2-pyrrolinodoxorubicin), AN-238 displays a much higher anti-tumor activity and significant lower toxicity. Using AN-238, an effective tumor growth inhibition has been demonstrated in experimental rat and mouse models of human breast cancer [27], androgen-independent prostate cancer [28-31], ovarian cancer [32], small cell- and non small cell lung cancer [33, 34], pancreatic cancer [35, 36], renal cell cancer [37], glioblastoma [38], colon cancer [39], as well as gastric carcinomas [40]. In most studies, a much higher toxicity and lower or absent effectiveness on tumor growth was observed in animals treated with the cytotoxic radical AN-201 alone.

Since early degradation of cytotoxic SS-analogs in the circulation or in tissues may release the cytotoxic compound before it is able to reach its target, e.g. the SSR positive tumor cell, it is important to demonstrate specificity of the effects of targeted cytotoxic SS-analogs. A number of studies have addressed this issue and indeed provide evidence for specificity of the effects of AN-238: I. Compared with the effect of AN-238: I. Compared with the effect of AN-238, no or much lower anti-tumor activity is shown when the unlabeled SS-analog RC-121 and the cytotoxic compound are administered simultaneously [27, 29, 32, 34, 36]; II. In some studies no inhibitory effect of AN-238 could be demonstrated in SSR negative tumors, while in the same studies SSR positive tumor models showed an anti-tumor action of AN-238 [35, 36, 39]; III. Pretreatment of animals with the unconjugated SS-analogs RC-160 or RC-121, could partially or completely prevent the anti-tumor action by AN-238, suggesting that interaction with specific SSR is required for AN-238 to exerts its action [36, 38].

The mechanism via which AN-238 exerts its anti-tumor activity may include the induction of apoptosis and or necrosis. An increase in the number of apoptotic cells, alone or in combination with an increase in necrotic areas in AN-238 treated tumors has been shown in experimental human pancreatic tumors [36], gastric carcinomas [40], colon cancer [39], androgen-independent prostate cancer [31] and small cell- and non small cell lung cancer [33, 34].

In conclusion, SSR targeted chemotherapy is effective in pre-clinical tumor models and may therefore be a promising approach to treat SSR-positive tumors. Using SSR-targeted chemotherapy lower dosages of the chemotherapeutic compound may be used resulting in lower toxicity. Until now, however, no clinical trials have been reported using targeted LHRH-, bombesin- or SS-analogs. In addition, evidence will have to be provided that cytotoxic SS-analogs can be internalized by SSR positive tumor cells. As for the concept of SSR-targeted radiotherapy, the efficacy of SSR targeted chemotherapy will be determined by the SSR expression level on the tumor cells, the capability of the cytotoxic SS-analog to selectively bind with high affinity to these SSR, the stability of the compound in the circulation, as well as on the amount of internalization of the cytotoxic radicals by the tumor cells. Moreover, in contrast to the use of radiolabeled SS-analogs coupled with therapeutic radionuclides emitting β-particles with long particle range, such as ^{90}Y and ^{177}Lu, where radiation emitted form a receptor-positive tumor cells may kill receptor negative cells in tumors with heterogeneity [41], it is expected that targeted cytotoxic SS-analogs require a more homogenous SSR expression by the tumors to exert their action. However, it may hypothesized that following the induction of necrosis a local release of the cytotoxic radical may induce a "bystander effect" on adjacent SSR-negative cells (Fig. 1). In this respect it is important to notice that some human cancers, e.g. breast cancer, may have a non-homogenous intra-tumor SSR expression and that a number of experimental human tumor models express SSR, while studies in primary human tumors, e.g. non small cell lung cancer, colorectal cancer, or exocrine pancreatic cancer have shown a lack of SSR at the protein level [3].

SIDE-EFFECTS OF CYTOTOXIC SOMATOSTATIN ANALOGS

It is well known that SSR are widely expressed in various tissues, including rapidly proliferating cells in the gastro-intestinal tract. Therefore, some side-effects using cytotoxic SS-analogs may occur. At present, toxicity of cytoxic SS-analogs, in particular AN-238, has only been evaluated in rats and mice. These studies do not show specific toxicity of AN-238 to the gastro-intestinal tract, the pituitary or kidneys. No significant changes in pituitary function as measured by GH and LH levels have been observed in nude mice bearing human breast cancer xenografts treated with a single i.v. injection of 250nmol/kg AN-238 with a follow-up of 60 days [27]. While in the majority of in vivo studies in experimental tumor models a certain degree of toxicity of AN-238 treatment as measured by animal deaths, loss of body weight and leukopenia have been reported, all studies clearly show that toxicity of AN-201 in this respect was much greater than that of AN-238 treatment [1, 2]. An important factor determining toxicity of cytotoxic SS-analogs is their stability. The intact molecules should be able to reach their target tumor cells, bind to SSR, internalize and exert their cytotoxic action locally. AN-201 is linked to the RC-121 SS-analog by an ester bond. Therefore, deconjugation by non-specific esterases may occur. Differences between mice and rats with respect to toxicity of AN-201 and AN-238 have been reported and could be due to different esterase activities between the species [21]. The half-life of the ester bond in nude mice

is about 20 min, in rats 1 h and in human serum about 2 h [33, 42]. In addition, mice with suppressed esterase activity showed that up to 3 times higher doses of AN-238 than AN-201 were tolerated by the animals [2]. In this respect, the development of novel cytotoxic SS-analogs using carbamates as potential linker, which are known to be relative resistant in plasma, is of specific interest [23]. One of these compounds, the camptothecin conjugate 2 (see above), has a half-life in rat serum of 18 h.

RGD-SOMATOSTATIN ANALOGS

RGD. Integrins are a large family of heterodimeric glycoprotein cell surface receptors that regulate cell-cell and cell-matrix interactions. They are composed of two transmembrane glycoproteins, α and β subunit, each αβ combination has its own binding specificity. These integrin receptors mediate a variety of cell adhesion events and signal transduction processes, and are involved in an array of pathological events, such as tumor metastasis, angiogenesis, thrombosis and osteoporosis. One of these integrins, the $\alpha_v\beta_3$ receptor, is able to bind a number of extracellular matrix proteins via the sequence of three amino acids: arginine (R), glycine (G), and aspartate (D), commonly called RGD, after the single-letter codes assigned to these amino-acids [43]. The $\alpha_v\beta_3$ receptor is expressed on various malignant human tumors and is highly expressed in neovascular endothelial cells which are actively involved in angiogenesis [44]. Based on the RGD sequence a number of small, highly active peptides have been designed to antagonize the $\alpha_v\beta_3$ receptor. These are synthetic RGD molecules that bind with high affinity to this receptor and have been shown to be inhibitors of cell adhesion, migration, growth and differentiation [45-48]. These agents also inhibit growth of new blood vessels and induce tumor regression in animal models, presumably by restriction of the blood supply to the tumor [49-52].

In addition to the RGD binding sites found on integrins, it has been shown that several members of the procaspase family of apoptosis genes contain such binding motifs as well. Procaspase-1 and -3 contain potential RGD-binding motifs near the site necessary for activation of the procaspases [53]. Caspases are a small group of specific cysteine proteases that are key factors in programmed cell death [54]. These intracellular factors exist as latent zymogens that when activated induce orderly cell death. Buckley and coworkers [53] first demonstrated that RGD peptides are able to directly activate caspase-3 and induce apoptosis in cells by a mechanism that is completely independent of their association with integrin receptors. Further work by others has shown that molecules specific for GPIIb/IIIa integrins can also stimulate caspase-3 activity [55]. Since caspase-3 is one of the key executioner proteases [54] in the apoptosis pathway, it seems likely that this enzyme will be an important site of action for targeted therapeutics that are designed to selectively induce cell death. In a recent study [56] the effects of a RGD-containing peptide (RGDS, Arg-Gly-Asp-Ser) was investigated in human umbilical vein endothelial cells (HUVEC). It was shown that after 4h incubation both caspase-8 and caspase-9 was activated, caspase-3 was activated after 24h incubation with RGDS and thereby induces apoptosis. All together these findings support the hypothesis that RGD-peptides may directly trigger the caspase cascade at an early level.

Therefore the RGD direct interaction with caspases and their activation at different levels may represent a novel mechanism of apoptosis induction, in addition to the known death receptors- and mitochondria-mediated pathways.

Apart from cytotoxic RGD analogs, radionuclide coupled RGD have been designed for imaging and radiotreatment [57, 58]. These analogs have a high affinity to neovascular endothelium and tumors. In an animal model specific uptake and retention of radioactivity in the transplanted tumor has been described. These analogs are promising in the targeted radiotreatment of tumor vascularization. A new very interesting approach is the use of chimeric peptides. It has been shown that RGD-containing peptides can be used for homing to tumors via the $\alpha_v\beta_3$ receptor [59, 60], which are expressed on tumor vasculature. These peptides have the potential to allow targeting of tumor vasculature with toxins as pro-apoptotic peptides [52]. In a recent study [61] with a fusion protein containing the RGD sequence and the Fc fragment of mouse IgG (RGD/mFc) was designed to target the Fc portion of IgG to the tumor vasculature to elicit an anti-angiogenesis immune response. The Fc fragment can trigger phagocytosis by neutrophils or macrophages. Second, the Fc fragment is able to activate natural killer cells to lyse the cells bearing the Fc fragment. Third, they used the Fc fragment of IgG that triggers the cascade of the complement system. It was shown that the tumor angiogenesis and tumor growth can be indeed inhibited after treatment with RGD/mFc.

RGD-Somatostatin. Another fascinating approach is the use of RGD-peptides as an apoptosis-inducing agent. We synthesized via solid phase peptide synthesis (SPPS) using an Applied Biosystems "Pioneer" synthesizer employing Fmoc strategy a new peptide, RGD-DTPA-octreotate [c(Arg-Gly-Asp-D-Tyr-Asp)-Lys(DTPA)-Phe-c(Cys-Tyr-D-Trp-Lys-Thr-Cys)-Thr]. The action of this new radiopharmaceutical is based on the overexpression of the SSR subtype 2 (sst_2) on tumor cells. RGD-DTPA-octreotate is composed of the SSR targeting peptide Tyr^3-octreotate, the chelator DTPA to enable radiolabelling, and the apoptotic-inducing RGD sequence. We choose to create a cyclic RGD-derivative, since it was found that cyclic derivatives of RGD-peptides were to more than 100-fold better when compared to the linear variants [46].

It was shown that this hybrid peptide RGD-DTPA-octreotate had a high affinity for sst_2 and internalizes in vivo and in vitro into tumor cells mostly via sst_2, most probably because of the higher affinity of octreotate for sst_2 than that of RGD for the $\alpha_v\beta_3$-receptor [62]. Preliminary results showed that the ^{111}In-labeled compound had a pronounced tumoricidal effect in a clonogenic assay in comparison with the 2 mono-peptides RGD and Tyr^3-octreotate. Furthermore ^{111}In-labeled RGD-DTPA-octreotate showed a clear increase in caspase-3 levels [63], the highest levels were found after 24h incubation (Fig. 3). From these results it is clear that the ^{111}In-labeled peptide RGD-DTPA-octreotate is more powerful to promote apoptosis, in comparison with the two monopeptides RGD and octreotate. The radiolabeled hybrid peptide can therefore significantly enhance the therapeutic efficacy of SS-based agents. In order to investigate the contribution of the radionuclide, unlabeled RGD-DTPA-octreotate was tested as well. It was shown that the unlabeled compound RGD-DTPA-octreotate also gives an increase in caspase-3 levels after 24h incubation. This makes it interesting to use the unlabeled hybrid peptide RGD-octreotate as a treatment novelty as well.

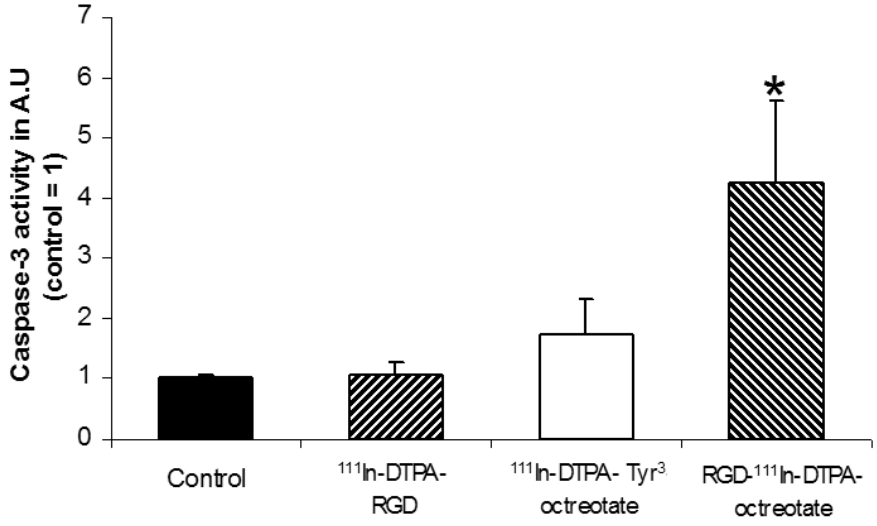

FIGURE 3. *Caspase-3 activity after incubation with ^{111}In-labeled RGD [c(Arg-Gly-Asp-D-Tyr-Asp)], octreotate or RGD-octreotate [c(Arg-Gly-Asp-D-Tyr-Asp)-Lys(DTPA)-Phe-c(Cys-Tyr-D-Trp-Lys-Thr-Cys)-Thr] in the CA20948 cell line. The caspase-3 activity was measured after 24h, expressed in arbitrary units (A.U.)., control set on 1. Experiments were performed in triplicate and each sample was measured in triplicate, bars represent mean ± SEM, $*p < 0.05$ versus control.*

The mechanism of action of this hybrid peptide RGD-DTPA-octreotate could be explained with the hypothesis that RGD-peptides may directly trigger the caspase cascade at an early level. Since a clear increase in caspase-3 levels is found after 24h it is possible that other caspases such as, caspase-8 and –9, could be activated first, as reported previously [56]. We cannot rule out the contribution of the chelator DTPA in the working mechanism of this hybrid peptide. It could play a role in for instance resistance to degradation, or DTPA can be a scavenger inside the cell. Besides the hypothesis that the RGD-sequence activated the caspase cascade, RGD-DTPA-octreotate could activate the known apoptotic pathway, the mitochondrial-mediated pathway, which also leads to an increase in caspase-3 levels (Fig. 4). Clearly more research has to be performed to understand the precise action of this new hybrid peptide RGD-DTPA-octreotate. The development of hybrid molecules that combine targeting and an effector function, such as apoptosis, can be a new approach in the treatment of cancer and inflammatory diseases.

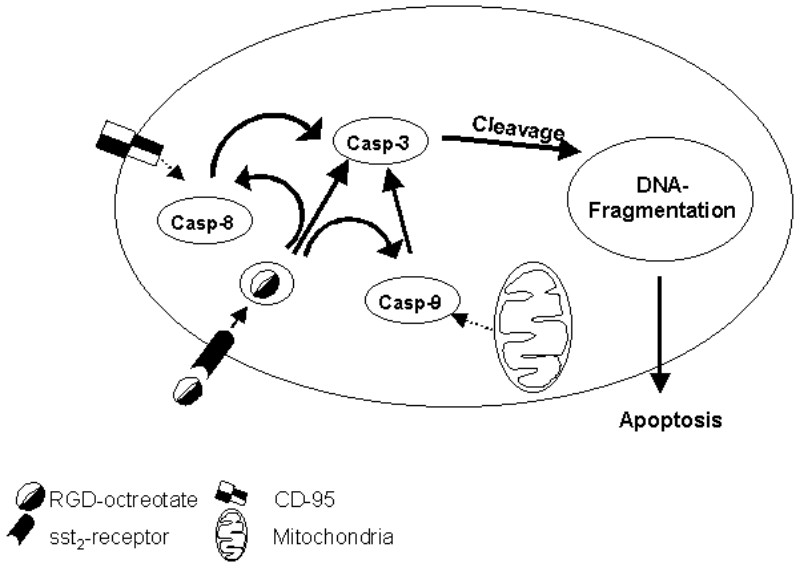

FIGURE 4. *Possible mechanism(s) of action of the hybrid peptide RGD-octreotate.*

CONCLUSIONS

In the past decade several cytotoxic SS-analogs have been developed, including analogs coupled to chemotherapeutic agents, taxol, antisense peptide nucleic acids, as well as RGD. Effectiveness as anti-tumor agents has been demonstrated in in vitro studies, as well as in in vivo experimental tumor models. The capability of such hybrid molecules to target SSR positive tumor cells in vivo will very much depend on their stability in the circulation, their SSR (subtype) binding affinity, as well as the capability of SSR positive tumor cells to internalize such hybrid molecules. Nevertheless, the current preclinical data clearly provide evidence for successful targeting of SSR positive tumors in vivo using SS-analogs coupled to chemotherapeutic agents, which have increased efficacy and considerable lower toxicity compared with the unconjugated cytotoxic radicals, as well as for the in vitro tumor cell targeting using taxol-, antisense oligo- and radiolabeled RGD-coupled SS-analogs.

REFERENCES

1. Schally AV, Nagy A. Cancer chemotherapy based on targeting of cytotoxic peptide conjugates to their receptors on tumors. *Eur J Endocrinol* 1999;141:1-14.
2. Schally AV, Nagy A. New approaches to treatment of various cancers based on cytotoxic analogs of LHRH, somatostatin and bombesin. *Life Sci* 2003;72:2305-2320.
3. Reubi JC. Peptide receptors as molecular targets for cancer diagnosis and therapy. *Endocr Rev* 2003;24:389-427.
4. Hofland LJ, Lamberts SW. The pathophysiological consequences of somatostatin receptor internalization and resistance. *Endocr Rev* 2003;24:28-47
5. Koenig JA, Edwardson JM. Endocytosis and recycling of G protein-coupled receptors. *Trends Pharmacol Sci* 1997;18:276-287.
6. Hausdorff WP, Caron MG, Lefkowitz RJ. Turning off the signal: desensitization of beta-adrenergic receptor function. *Faseb J* 1990;4:2881-2889.
7. Ferguson SS, Barak LS, Zhang J, Caron MG. G-protein-coupled receptor regulation: role of G-protein-coupled receptor kinases and arrestins. *Can J Physiol Pharmacol* 1996;74:1095-1110.
8. Yu SS, Lefkowitz RJ, Hausdorff WP. Beta-adrenergic receptor sequestration. A potential mechanism of receptor resensitization. *J Biol Chem* 1993;268:337-341
9. Roettger BF, Rentsch RU, Pinon D, Holicky E, Hadac E, Larkin JM, Miller LJ. Dual pathways of internalization of the cholecystokinin receptor. *J Cell Biol* 1995;128:1029-1041.
10. Brown MS, Goldstein JL. A receptor-mediated pathway for cholesterol homeostasis. *Science* 1986;232:34-47.
11. Steinman RM, Mellman IS, Muller WA, Cohn ZA. Endocytosis and the recycling of plasma membrane. *J Cell Biol* 1983;96:1-27.
12. Patel YC. Somatostatin and its receptor family. *Front Neuroendocrinol* 1999;20:157-198.
13. Hukovic N, Panetta R, Kumar U, Patel YC. Agonist-dependent regulation of cloned human somatostatin receptor types 1-5 (hSSTR1-5): subtype selective internalization or upregulation. *Endocrinology* 1996;137:4046-4049
14. Nouel D, Gaudriault G, Houle M, Reisine T, Vincent JP, Mazella J, Beaudet A. Differential internalization of somatostatin in COS-7 cells transfected with SST1 and SST2 receptor subtypes: a confocal microscopic study using novel fluorescent somatostatin derivatives. *Endocrinology* 1997;138:296-306.
15. Beaudet A, Nouel D, Stroh T, Vandenbulcke F, Dal-Farra C, Vincent JP. Fluorescent ligands for studying neuropeptide receptors by confocal microscopy. *Braz J Med Biol Res* 1998;31:1479-1489.
16. Hofland LJ, Lamberts SW, van Hagen PM, Reubi JC, Schaeffer J, Waaijers M, van Koetsveld PM, Srinivasan A, Krenning EP, Breeman WA. Crucial role for somatostatin receptor subtype 2 in determining the uptake of [111In-DTPA-D-Phe1]octreotide in somatostatin receptor-positive organs. *J Nucl Med* 2003;44:1315-1321.
17. Breeman WA, Kwekkeboom DJ, Kooij PP, Bakker WH, Hofland LJ, Visser TJ, Ensing GJ, Lamberts SW, Krenning EP. Effect of dose and specific activity on tissue distribution of indium-111-pentetreotide in rats. *J Nucl Med* 1995;36:623-627.
18. de Jong M, Breeman WA, Bakker WH, Kooij PP, Bernard BF, Hofland LJ, Visser TJ, Srinivasan A, Schmidt MA, Erion JL, Bugaj JE, Macke HR, Krenning EP. Comparison of

(111)In-labeled somatostatin analogues for tumor scintigraphy and radionuclide therapy. *Cancer Res* 1998;58:437-441.

19. Froidevaux S, Heppeler A, Eberle AN, Meier AM, Hausler M, Beglinger C, Behe M, Powell P, Macke HR. Preclinical comparison in AR4-2J tumor-bearing mice of four radiolabeled 1,4,7,10-tetraazacyclododecane-1,4,7,10-tetraacetic acid- somatostatin analogs for tumor diagnosis and internal radiotherapy. *Endocrinology* 2000;141:3304-3312.
20. Radulovic S, Nagy A, Szoke B, Schally AV. Cytotoxic analog of somatostatin containing methotrexate inhibits growth of MIA PaCa-2 human pancreatic cancer xenografts in nude mice. *Cancer Lett* 1992;62:263-271.
21. Nagy A, Schally AV, Halmos G, Armatis P, Cai RZ, Csernus V, Kovacs M, Koppan M, Szepeshazi K, Kahan Z. Synthesis and biological evaluation of cytotoxic analogs of somatostatin containing doxorubicin or its intensely potent derivative, 2-pyrrolinodoxorubicin. *Proc Natl Acad Sci U S A* 1998;95:1794-1799.
22. Reubi JC, Schar JC, Waser B, Wenger S, Heppeler A, Schmitt JS, Macke HR. Affinity profiles for human somatostatin receptor subtypes SST1-SST5 of somatostatin radiotracers selected for scintigraphic and radiotherapeutic use. *Eur J Nucl Med* 2000;27:273-282.
23. Fuselier JA, Sun L, Woltering SN, Murphy WA, Vasilevich N, Coy DH. An adjustable release rate linking strategy for cytotoxin-peptide conjugates. *Bioorg Med Chem Lett* 2003;13:799-803.
24. Hansen KT, Faarup P, Bundgaard H. Carbamate ester prodrugs of dopaminergic compounds: synthesis, stability, and bioconversion. *J Pharm Sci* 1991;80:793-798
25. Huang CM, Wu YT, Chen ST. Targeting delivery of paclitaxel into tumor cells via somatostatin receptor endocytosis. *Chem Biol* 2000;7:453-461.
26. Sun L, Fuselier JA, Murphy WA, Coy DH. Antisense peptide nucleic acids conjugated to somatostatin analogs and targeted at the n-myc oncogene display enhanced cytotoxity to human neuroblastoma IMR32 cells expressing somatostatin receptors. *Peptides* 2002;23:1557-1565.
27. Kahan Z, Nagy A, Schally AV, Hebert F, Sun B, Groot K, Halmos G. Inhibition of growth of MX-1, MCF-7-MIII and MDA-MB-231 human breast cancer xenografts after administration of a targeted cytotoxic analog of somatostatin, AN-238. *Int J Cancer* 1999;82:592-598.
28. Koppan M, Nagy A, Schally AV, Arencibia JM, Plonowski A, Halmos G. Targeted cytotoxic analogue of somatostatin AN-238 inhibits growth of androgen-independent Dunning R-3327-AT-1 prostate cancer in rats at nontoxic doses. *Cancer Res* 1998;58:4132-4137.
29. Plonowski A, Schally AV, Nagy A, Sun B, Halmos G. Effective treatment of experimental DU-145 prostate cancers with targeted cytotoxic somatostatin analog AN-238. *Int J Oncol* 2002;20:397-402.
30. Plonowski A, Schally AV, Nagy A, Sun B, Szepeshazi K. Inhibition of PC-3 human androgen-independent prostate cancer and its metastases by cytotoxic somatostatin analogue AN-238. *Cancer Res* 1999;59:1947-1953.
31. Letsch M, Schally AV, Szepeshazi K, Halmos G, Nagy A. Effective treatment of experimental androgen sensitive and androgen independent intraosseous prostate cancer with targeted cytotoxic somatostatin analogue AN-238. *J Urol* 2004;171:911-915.
32. Plonowski A, Schally AV, Koppan M, Nagy A, Arencibia JM, Csernus B, Halmos G. Inhibition of the UCI-107 human ovarian carcinoma cell line by a targeted cytotoxic analog of somatostatin, AN-238. *Cancer* 2001;92:1168-1176

33. Szereday Z, Schally AV, Szepeshazi K, Bajo AM, Hebert F, Halmos G, Nagy A. Effective treatment of H838 human non-small cell lung carcinoma with a targeted cytotoxic somatostatin analog, AN-238. *Int J Oncol* 2003;22:1141-1146.
34. Kiaris H, Schally AV, Nagy A, Szepeshazi K, Hebert F, Halmos G. A targeted cytotoxic somatostatin (SST) analogue, AN-238, inhibits the growth of H-69 small-cell lung carcinoma (SCLC) and H-157 non-SCLC in nude mice. *Eur J Cancer* 2001;37:620-628.
35. Benali N, Cordelier P, Calise D, Pages P, Rochaix P, Nagy A, Esteve JP, Pour PM, Schally AV, Vaysse N, Susini C, Buscail L. Inhibition of growth and metastatic progression of pancreatic carcinoma in hamster after somatostatin receptor subtype 2 (sst2) gene expression and administration of cytotoxic somatostatin analog AN-238. *Proc Natl Acad Sci U S A* 2000;97:9180-9185.
36. Szepeshazi K, Schally AV, Halmos G, Sun B, Hebert F, Csernus B, Nagy A. Targeting of cytotoxic somatostatin analog AN-238 to somatostatin receptor subtypes 5 and/or 3 in experimental pancreatic cancers. *Clin Cancer Res* 2001;7:2854-2861.
37. Plonowski A, Schally AV, Nagy A, Kiaris H, Hebert F, Halmos G. Inhibition of metastatic renal cell carcinomas expressing somatostatin receptors by a targeted cytotoxic analogue of somatostatin AN-238. *Cancer Res* 2000;60:2996-3001.
38. Kiaris H, Schally AV, Nagy A, Sun B, Szepeshazi K, Halmos G. Regression of U-87 MG human glioblastomas in nude mice after treatment with a cytotoxic somatostatin analog AN-238. *Clin Cancer Res* 2000;6:709-717.
39. Szepeshazi K, Schally AV, Halmos G, Armatis P, Hebert F, Sun B, Feil A, Kiaris H, Nagy A. Targeted cytotoxic somatostatin analogue AN-238 inhibits somatostatin receptor-positive experimental colon cancers independently of their p53 status. *Cancer Res* 2002;62:781-788.
40. Szepeshazi K, Schally AV, Nagy A, Wagner BW, Bajo AM, Halmos G. Preclinical evaluation of therapeutic effects of targeted cytotoxic analogs of somatostatin and bombesin on human gastric carcinomas. *Cancer* 2003;98:1401-1410.
41. Krenning EP, Kwekkeboom DJ, Valkema R, Pauwels S, Kvols LK, De Jong M. Peptide receptor radionuclide therapy. *Ann N Y Acad Sci* 2004;1014:234-245.
42. Nagy A, Plonowski A, Schally AV. Stability of cytotoxic luteinizing hormone-releasing hormone conjugate (AN-152) containing doxorubicin 14-O-hemiglutarate in mouse and human serum in vitro: implications for the design of preclinical studies. *Proc Natl Acad Sci U S A* 2000;97:829-834.
43. Varner JA. The role of vascular cell integrins alpha v beta 3 and alpha v beta 5 in angiogenesis. *Exs* 1997;79:361-390.
44. Brooks PC. Role of integrins in angiogenesis. *Eur J Cancer* 1996;32A:2423-2429
45. Ruoslahti E, Pierschbacher MD. Arg-Gly-Asp: a versatile cell recognition signal. *Cell* 1986;44:517-518.
46. Aumailley M, Gurrath M, Muller G, Calvete J, Timpl R, Kessler H. Arg-Gly-Asp constrained within cyclic pentapeptides. Strong and selective inhibitors of cell adhesion to vitronectin and laminin fragment P1. *FEBS Lett* 1991;291:50-54.
47. Pfaff M, Tangemann K, Muller B, Gurrath M, Muller G, Kessler H, Timpl R, Engel J. Selective recognition of cyclic RGD peptides of NMR defined conformation by alpha IIb beta 3, alpha V beta 3, and alpha 5 beta 1 integrins. *J Biol Chem* 1994;269:20233-20238.
48. Ruoslahti E. RGD and other recognition sequences for integrins. *Annu Rev Cell Dev Biol* 1996;12:697-715.

49. Brooks PC, Stromblad S, Klemke R, Visscher D, Sarkar FH, Cheresh DA. Antiintegrin alpha v beta 3 blocks human breast cancer growth and angiogenesis in human skin. *J Clin Invest* 1995;96:1815-1822.
50. Brooks PC, Montgomery AM, Rosenfeld M, Reisfeld RA, Hu T, Klier G, Cheresh DA. Integrin alpha v beta 3 antagonists promote tumor regression by inducing apoptosis of angiogenic blood vessels. *Cell* 1994;79:1157-1164.
51. Hammes HP, Brownlee M, Jonczyk A, Sutter A, Preissner KT. Subcutaneous injection of a cyclic peptide antagonist of vitronectin receptor-type integrins inhibits retinal neovascularization. *Nat Med* 1996;2:529-533.
52. Ellerby HM, Arap W, Ellerby LM, Kain R, Andrusiak R, Rio GD, Krajewski S, Lombardo CR, Rao R, Ruoslahti E, Bredesen DE, Pasqualini R. Anti-cancer activity of targeted pro-apoptotic peptides. *Nat Med* 1999;5:1032-1038.
53. Buckley CD, Pilling D, Henriquez NV, Parsonage G, Threlfall K, Scheel-Toellner D, Simmons DL, Akbar AN, Lord JM, Salmon M. RGD peptides induce apoptosis by direct caspase-3 activation. *Nature* 1999;397:534-539.
54. Wolf BB, Green DR. Suicidal tendencies: apoptotic cell death by caspase family proteinases. *J Biol Chem* 1999;274:20049-20052.
55. Adderley SR, Fitzgerald DJ. Glycoprotein IIb/IIIa antagonists induce apoptosis in rat cardiomyocytes by caspase-3 activation. *J Biol Chem* 2000;275:5760-5766.
56. Aguzzi MS, Giampietri C, De Marchis F, Padula F, Gaeta R, Ragone G, Capogrossi MC, Facchiano A. RGDS peptide induces caspase 8 and caspase 9 activation in human endothelial cells. *Blood* 2004;103:4180-4187.
57. Haubner R, Wester HJ, Reuning U, Senekowitsch-Schmidtke R, Diefenbach B, Kessler H, Stocklin G, Schwaiger M. Radiolabeled alpha(v)beta3 integrin antagonists: a new class of tracers for tumor targeting. *J Nucl Med* 1999;40:1061-1071.
58. van Hagen PM, Breeman WA, Bernard HF, Schaar M, Mooij CM, Srinivasan A, Schmidt MA, Krenning EP, de Jong M. Evaluation of a radiolabelled cyclic DTPA-RGD analogue for tumour imaging and radionuclide therapy. *Int J Cancer* 2000;90:186-198.
59. Pasqualini R, Koivunen E, Ruoslahti E. Alpha v integrins as receptors for tumor targeting by circulating ligands. *Nat Biotechnol* 1997;15:542-546.
60. Assa-Munt N, Jia X, Laakkonen P, Ruoslahti E. Solution structures and integrin binding activities of an RGD peptide with two isomers. *Biochemistry* 2001;40:2373-2378.
61. Li J, Ji J, Holmes LM, Burgin KE, Barton LB, Yu X, Wagner TE, Wei Y. Fusion protein from RGD peptide and Fc fragment of mouse immunoglobulin G inhibits angiogenesis in tumor. *Cancer Gene Ther* 2004;11:363-370.
62. Bernard BF, Capello A, van Hagen PM, Breeman WA, Srinivasan A, Schmidt MA, Erion JL, van Gameren A, Krenning EP, de Jong M. Radiolabeled RGD-DTPA-Tyr^3-octreotate for receptor-targeted radionuclide therapy. *Cancer Biother Radiopharm* 2004;19:273-280.
63. Capello A, Krenning EP, Bernard BF, Breeman WA, van Hagen MP, de Jong M. Increased cell death after therapy with an arg-gly-asp-linked somatostatin analog. *J Nucl Med* 2004;45:1716-1720.

CHAPTER 6

SUMMARY AND CONCLUSIONS

Summary and conclusions

Astrid Capello

SUMMARY AND CONCLUSIONS

There has been an exponential growth in the development of radiolabeled peptides for diagnosis and therapeutic applications in oncology. Peptides radiolabeled with γ-emitters can be used to visualize receptor-positive cells in vivo. In 1994 ^{111}In-DTPA-octreotide (OctreoScan®) received FDA approval as the first product of its kind, and to this day remains the "Gold Standard" in somatostatin receptor scintigraphy. Research continued in this area by introducing peptide receptor radionuclide therapy (PRRT) using Auger electron (^{111}In) and β particle (^{90}Y and ^{177}Lu) emitting radionculides.

The aim of this thesis was firstly to receive further insight in the therapeutic potential of somatostatin labeled analogs in vitro and in vivo. Secondly, we wanted to improve the potential of PRRT with somatostatin analogs by introducing the combination with an apoptosis-inducing factor.

Since the response of tumor cells to PRRT is dependent on their radiosensitivity we determined the radiosensitivity of CA20948 tumor cells, rat pancreatic tumor cells expressing the somatostatin receptor (sst), by using clonogenic survival assays after high-dose-rate external-beam radiotherapy (XRT) in vitro. It could be expected however that results of high-dose-rate XRT are not representative for those after low-dose-rate radionuclide therapy (RT), such as PRRT. Therefore, we compared clonogenic survival in vitro in CA20948 tumor cells after increasing doses of XRT or RT, the latter using ^{131}I (**Chapter 2**).

We observed a dose-dependent reduction in tumor-cell survival, which, at low doses, was similar for XRT and RT. For high-dose-rate XRT, the quadratic over linear component ratio (α/β) for CA20948 was 8.3 Gy, whereas that ratio for low-dose-rate RT was calculated to be 86.5 Gy. So, despite the huge differences in dose rate, RT tumor cell-killing effects were approximately as effective as those of XRT at doses of 1 and 2 Gy, the latter being the common daily dose given in fractionated external-beam therapies. At higher doses, RT was less effective than XRT.

In **chapter 3** the therapeutic potential of ^{111}In-DTPA-octreotide was evaluated. Since ^{111}In emits not only gamma-rays, but also therapeutic Auger and internal conversion electrons with a medium to short tissue penetration (0.02-10 μm, 200-550 μm, respectively), ^{111}In-DTPA-octreotide is also being used for PRRT.

First (Chapter 3.1), the therapeutic effects of ^{111}In-DTPA-octreotide in a single-cell model were investigated. In this single-cell model we discriminated between the effects of the Auger electrons and internal conversion electrons in PRRT. In this in vitro system ^{111}In-DTPA-octreotide could completely control tumor growth. The effects were dependent on incubation time, radiation dose, and specific activity used. Similar concentrations of ^{111}In-DTPA, which is not internalized into somatostatin-positive tumor cells, did not influence tumor survival. Excess unlabeled octreotide (10^{-6} mol/L) could decrease tumor cell survival to 60% of control; the addition of the radiolabeled peptide ^{111}In-DTPA-octreotide (10^{-9} mol/L) plus an excess of unlabeled (10^{-6} mol/L) octreotide, did not further decrease survival. So,

these in vitro studies show that the therapeutic effect of ^{111}In is dependent on internalization, enabling the Auger electrons with their very short particle range to reach the nucleus. Our results also indicate that the PRRT-effects were receptor-mediated.

Subsequently, we investigated the radiotherapeutic effect of different doses of ^{111}In-DTPA-octreotide in vivo in Lewis rats bearing small (≤ 1 cm2) or larger (≥ 8 cm2) somatostatin receptor-positive rat pancreatic CA20948 tumors. In addition, we investigated the somatostatin receptor density on the tumors before and after radionuclide therapy (Chapter 3.2).

The results showed impressive radiotherapeutic effects of ^{111}In-labeled octreotide in this rat tumor model. Cure (up to 50%) was found in the animals bearing small tumors after at least three injections of 111 MBq or a single injection of 370 MBq ^{111}In-DTPA-octreotide, leading to a dose of 6.3 – 7.8 mGy/MBq (1 – 10 g tumor). In the rats bearing the larger tumors the effects were much less pronounced and only partial responses were reached in these groups. A possible explanation for the various responses found is the increase of somatostatin receptor-negative cells, due to the lack of crossfire. We therefore investigated the somatostatin receptor expression before and after radionuclide therapy with an In-111 labeled somatostatin analog. In this study we found a clear somatostatin receptor subtype 2 (sst_2) expression both in the control and in the tumors treated with ^{111}In. A significantly higher tumor receptor density was found when the tumor re-grew after an initial decline in size after low dose PRRT in comparison with untreated tumors.

We concluded that radionuclide-therapy with ^{111}In-labeled somatostatin analogs is feasible but should preferably start as early as possible during tumor development. One might also consider the use of radiolabeled somatostatin analogs in an adjuvant setting after surgery of somatostatin receptor-positive tumors to eradicate occult metastases. Finally we showed that PRRT led to a significant increase in somatostatin receptor density, when the tumors re-grew after an initial decline in size after PRRT. The increase in the somatostatin receptor density will lead to a higher uptake of the radiolabeled peptides in therapeutic applications, making repeated injections of radiolabeled peptides more effective.

In **chapter 4** the therapeutic effects of the somatostatin analogs Tyr^3-octreotide and Tyr^3-octreotate radiolabeled with the β^- particle emitters ^{177}Lu or ^{90}Y were evaluated in an in vitro colony-forming assay using the rat pancreatic tumor cell line CA20948 (Chapter 4.1). ^{177}Lu-DOTA-Tyr^3-octreotate could reduce tumor growth with 100% and effects were dependent on radiation dose, incubation time, and specific activity used. Similar concentrations of ^{177}Lu-DOTA, which does not bind to the tumor cells, had a less pronounced effect on tumor cell survival. Both Tyr^3-octreotide and Tyr^3-octreotate labeled with either ^{177}Lu or ^{90}Y, using DOTA as chelator, were able to control tumor growth in a dose-dependent manner. In all concentrations used radiolabeled Tyr^3-octreotate showed a higher percentage tumor cell kill compared to radiolabeled Tyr^3-octreotide, labeled with ^{177}Lu or ^{90}Y. This is in accordance with the higher affinity of Tyr^3-octreotate for the sst_2-receptor compared to Tyr^3-octreotide, leading to a higher amount of cell-associated radioactivity, resulting in a significantly higher tumor radiation dose. So, Tyr^3-octreotate labeled with ^{177}Lu or ^{90}Y is the most promising

analog for PRRT. Subsequently, the anti-tumor effects of ^{177}Lu-DOTA-Tyr^3-octreotate on sst receptor positive CA20948 micrometastases in the liver were investigated (Chapter 4.2). Rats treated with ^{177}Lu-DOTA-Tyr^3-octreotate showed a significantly better survival in a rat liver micrometastic model setting, making it a very promising new treatment modality for sst receptor positive disseminated disease.

In **chapter 5** a study is described that aimed to develop and evaluate a new radiopharmaceutical for the treatment of cancers that overexpress sst_2. The new radiopharmaceutical is composed of a somatostatin receptor-targeting peptide, a chelator (DTPA) to enable radiolabeling, and an apoptosis inducing RGD (arginine-glycine-aspartate) peptide moiety. Biodistribution studies showed that the receptor-targeting peptide portion of the molecule, Tyr^3-octreotate, binds specifically to the sst_2. Because of the rapid endocytosis of the somatostatin receptor the entire molecule can thus be internalized, allowing the RGD portion to activate intracellular caspases, which in turn promotes apoptosis. Internalization experiments in vitro into sst_2-positive tumor cells of the radiolabeled hybrid peptide appeared to be a rapid process and could be blocked by an excess of unlabeled octreotide, indicating an sst_2-specific process. Tumor uptake of radiolabeled RGD-DTPA-octreotate in vivo in rats was in agreement with the in vitro data and comparable to that of radiolabeled Tyr^3-octreotate. A drawback of the new hybrid compound was high renal uptake and retention of radioactivity, limiting the therapeutic dose that can be administered, as the kidneys are critical organs in radionuclide therapy using somatostatin analogs labeled with beta particle emitting radionuclides (Chapter 5.1).

Tumoricidal effects of the hybrid peptide RGD-DTPA-octreotate were evaluated in comparison with those of RGD and Tyr^3-octreotate in an in vitro colony-forming assay, the compounds were all radiolabeled to ^{111}In. Subsequently caspase-3 activation was determined (Chapter 5.2). Tumoricidal effects were found for ^{111}In-DTPA-RGD < ^{111}In-DTPA-Tyr^3-octreotate < RGD-^{111}In-DTPA-octreotate. Also, the highest increase in caspase-3 levels was found with RGD-^{111}In-DTPA-octreotate. Concluding, RGD-^{111}In-DTPA-octreotate has a more pronounced tumoricidal effect than ^{111}In-DTPA-RGD and ^{111}In-DTPA-Tyr^3-octreotate, because of increased apoptosis as indicated by increased caspase-3 activity.

In chapter 5.3 we further evaluated the biodistribution of RGD-^{111}In-DTPA-octreotate and ^{125}I-RGD-octreotate, and investigated the tumoricidal effect of the unlabeled compound RGD-DTPA-octreotate in vitro. Since the biodistribution showed a very high renal uptake we studied the therapeutic effects of the unlabeled hybrid peptide, RGD-DTPA-octreotate, in vitro in the CA20948, AR42J and the CHO cell line transfected with sst_2, which showed that RGD-DTPA-octreotate induced a significant increase in caspase-3 levels in comparison with RGD and Tyr^3-octreotate in all cell lines. Subsequently, we examined the biodistribution of iodinated RGD-octreotate, without the presence of the chelator DTPA, in order to change the elimination route from the body (from renal clearance to more hepatic clearance). ^{125}I-RGD-octreotate showed indeed a much lower renal uptake in comparison with RGD-^{111}In-DTPA-octreotate. Furthermore, the affinity of RGD-octreotate increased in comparison with RGD-DTPA-octreotate (IC_{50} values of 1.4×10^{-8}M vs 9.4×10^{-8}M respectively). Finally, RGD-

octreotate, without the chelator DTPA, was also able to activate caspase-3 as was indicated with immunocytochemistry.

So, this concept of targeting somatostatin receptor-expressing tumors using peptide receptor radionuclide therapy might also apply for the use of somatostatin analogs coupled to chemotherapeutic compounds, which is further described in Chapter 5.4. The development of hybrid molecules that combine targeting and an effector function, such as apoptosis, can be a new approach in the treatment of cancer.

SAMENVATTING EN CONCLUSIES

SAMENVATTING EN CONCLUSIES

Somatostatine is een hormoon dat de afgifte van groeihormoon en een aantal andere hormonen (o.a. insuline, glucagon en schildklierhormonen) remt. Het peptide somatostatine bindt specifiek aan receptoren op de cel (sleutel-slot principe), en oefent na internalisatie vervolgens in de cel zijn remmende werking uit. Somatostatine wordt gevormd in de alvleesklier (= pancreas), hypothalamus en in de wand van maag en darm. Veel endocriene tumoren brengen de somatostatinereceptor tot expressie en worden dus in hun hormoon afgifte geremd door somatostatine. Deze remmende werking heeft ertoe geleid om patiënten met ziekten veroorzaakt door te hard werkende klieren of tumoren met somatostatine-receptoren te behandelen met somatostatine. Somatostatine is zelf echter niet geschikt voor therapie doordat het snel wordt afgebroken in het lichaam. Vandaar dat er soortgelijke peptiden (analogen) zijn gemaakt die veel stabieler zijn, een voorbeeld hiervan is octreotide. Vervolgens is octreotide radioactief gemaakt om receptorpositieve tumoren zichtbaar te maken in het lichaam met behulp van een gammacamera. In 1994 werd ^{111}In-DTPA-octreotide (OctreoScan®) goedgekeurd door de "U.S. Food and Drug Administration" (FDA) voor diagnostisch gebruik op patiënten met neuroendocriene tumoren. Tot op de dag van vandaag is OctreoScan® de "Gouden Standaard" voor de visualisatie van neuroeendocriene tumoren. Verder onderzoek op dit gebied heeft geleid tot de introductie van Peptide Receptor Radionuclide Therapie (PRRT), door gebruik te maken van radionucliden met bètastraling (^{90}Y en ^{177}Lu), die gekoppeld worden aan deze somatostatine analoga.

Het doel van dit proefschrift was in eerste instantie om meer inzicht te krijgen in de therapeutische mogelijkheden van gelabelde somatostatine analogen in vitro en in vivo. Vervolgens wilden we de radionucliden therapie met somatostatine analogen verbeteren door dit te combineren met een factor waarvan bekend is dat het celdood initieert in de cel.

Aangezien de respons van tumorcellen op PRRT afhankelijk is van de stralingsgevoeligheid van deze cellen hebben we de stralingsgevoeligheid van CA20948 tumorcellen, dit is een rattenpancreas tumorcellijn welke de somatostatinereceptor subtype 2 (sst_2) tot expressie brengt, in vitro bepaald met behulp van een kolonievormende assay na bestraling met externe radiotherapie (XRT). Het is echter te verwachten dat de resultaten van bestraling met een hoog dosistempo, XRT, niet representatief is voor bestraling met een laag dosistempo, radionucliden therapie (RT), bestraling. Daarom hebben we de overleving van CA20948 tumorcellen in vitro na een toenemende dosis van XRT of RT met elkaar vergeleken (**Hoofdstuk 2**).

We hebben een dosisafhankelijke reductie in tumorceloverleving waargenomen, welke, bij lage doses, dezelfde was voor XRT als RT. Dus, ondanks de enorme verschillen in dosistempo, zijn de tumorceldodende effecten van RT ongeveer even effectief als die van XRT bij doses van 1 en 2 Gy, de laatste is de dagelijks toegediende dosis bij gefractioneerde externe radiotherapie bestraling. Bij hogere doses was RT minder effectief dan XRT. Voor XRT, de kwadratische ten opzichte van de lineaire component ratio (α/β) voor de CA20948 cellijn was 8.3 Gy, terwijl deze ratio voor RT uitgerekend werd op 86.5 Gy.

In **hoofdstuk 3** is de therapeutische potentie van ^{111}In-DTPA-octreotide geëvalueerd. Aangezien ^{111}In, naast gammastraling, ook therapeutische Auger en interne conversie elektronen, met een middel tot korte dracht (0.02-10 µm, 200-550 µm, respectievelijk), uitzendt, wordt ^{111}In-DTPA-octreotide ook gebruikt voor PRRT.

Als eerste (Hoofdstuk 3.1) zijn de therapeutische effecten van ^{111}In-DTPA-octreotide in een kolonievormend model onderzocht. In dit model hebben we gediscrimineerd tussen the effecten van de Auger elektronen en interne conversie elektronen bij PRRT. ^{111}In-DTPA-octreotide kon de tumorgroei in dit model volledig remmen. De effecten waren afhankelijk van de incubatietijd, de hoeveelheid straling en de gebruikte specifieke activiteit. Dezelfde concentraties van ^{111}In-DTPA, welke niet kan internaliseren in somatostatine receptorpositieve tumorcellen, hadden geen effect op de tumorgroei. Een overmaat aan ongelabeld octreotide (10^{-6} M) kon de tumorgroei remmen tot 60% van de controlegroei; de toevoeging van gelabeld peptide ^{111}In-DTPA-octreotide (10^{-9} M) met een overmaat aan ongelabeld octreotide (10^{-6} M) kon de tumorgroei niet verder remmen. Deze in vitro experimenten laten zien dat the therapeutische effecten van ^{111}In afhankelijk zijn van internalisatie, hierdoor kunnen de Auger elektronen men hun korte dracht de kern bereiken. Onze resultaten geven verder weer dat de PRRT-resultaten receptorgemedieerd zijn.

Vervolgens hebben we de radiotherapeutische effecten van verschillende doses ^{111}In-DTPA-octreotide in vivo in Lewis ratten, die een kleine ($\leq$ 1 cm^2) of een grote ($\geq$ 8 cm^2) somatostatine receptorpositieve CA20948 tumor hadden, onderzocht. Bovendien hebben we de somatostatine receptordensiteit op de tumor voor en na behandeling met radionuclide therapie onderzocht (Hoofdstuk 3.2)

De resultaten laten fantastische radiotherapeutische effecten zien van ^{111}In-gelabeld octreotide in dit rattenmodel. Genezing (tot 50%) werd gevonden in de dieren met een kleine tumor na ten minste drie injecties met 111 MBq of één injectie met 370 MBq ^{111}In-DTPA-octreotide, wat leidde tot een dosis van 6.3 – 7.8 mGy/MBq (1 – 10 g tumor). In de groep ratten met een grote tumor waren de effecten minder duidelijk, hier werd alleen een partiele respons gevonden. Een mogelijke verklaring voor de verschillende effecten na ^{111}In therapie in grote versus kleine tumoren kan zijn dat er een toename is in de groei van somatostatine receptornegatieve cellen door een gebrek aan crossfire. We hebben daarom de expressie van de somatostatine receptor onderzocht voor en na radionuclide therapie met een In-111 gelabeld somatostatine analoog. In dit onderzoek hebben we een duidelijke expressie gevonden van de somatostatine receptor subtype 2 (sst_2) in zowel de controle tumoren als in de tumoren die behandeld zijn met ^{111}In. Een significant hogere receptordensiteit werd er gevonden op de tumoren die na een tumorverkleining door PRRT weer zijn gaan groeien in vergelijking met de onbehandelde tumoren.

We hebben hieruit geconcludeerd dat de behandeling van tumoren met radionuclide therapie met ^{111}In-gelabelde somatostatin analogen zo vroeg mogelijk gestart moet worden. Ook interessant is, bij somatostatine receptorpositieve tumoren, dat radioactief gelabelde somatostatine analogen te gebruiken na chirurgie om eventuele metastasen te behandelen.

Ten slotte hebben we laten zien dat de somatostatine receptor nog steeds aanwezig is na PRRT en zelfs is toegenomen in densiteit bij tumoren die eerst kleiner zijn geworden en vervolgens weer zijn gaan groeien. De toename in de somatostatine receptordensiteit leidt tot een hogere opname van de radioactief gelabelde peptiden bij therapeutische toepassingen, wat herhaalde injecties met radioactief gelabelde peptiden effectiever maakt.

In **hoofdstuk 4** zijn de therapeutische effecten van de somatostatine analogen Tyr^3-octreotide en Tyr^3-octreotate, gelabeld met de bètastralers ^{177}Lu en ^{90}Y, onderzocht in de ratten tumorcellijn CA20948 met behulp van een kolonievormende assay (Hoofdstuk 4.1). ^{177}Lu-DOTA-Tyr^3-octreotate kon de tumorgroei volledig remmen, de effecten waren afhankelijk van de hoeveelheid straling, de incubatietijd en de gebruikte specifieke activiteit. Dezelfde concentratie van ^{177}Lu-DOTA, dit bindt niet aan de tumorcellen en kan dus niet internaliseren, had een duidelijk minder effect op de tumorceloverleving. De beide analogen Tyr^3-octreotide en Tyr^3-octreotate, gelabeld met ^{177}Lu of ^{90}Y, konden de tumorgroei op een dosisafhankelijke manier controleren. Bij alle gebruikte concentraties kon het radiogelabelde analoog Tyr^3-octreotate de tumorgroei beter remmen dan Tyr^3-octreotide. Dit komt overeen met het feit dat Tyr^3-octreotate een hoger affiniteit heeft voor de sst_2-receptor dan Tyr^3-octreotide, wat leidt tot een hogere concentratie aan celgebonden radioactiviteit en daardoor een hogere stralingsdosis op de tumorcellen. Tyr^3-octreotate gelabeld met ^{177}Lu of ^{90}Y is dus een veelbelovend analoog voor PRRT. Vervolgens zijn de therapeutische effecten van ^{177}Lu-DOTA-Tyr^3-octreotate onderzocht op somatostatine receptorpositieve CA20948 lever micrometastasen (Hoofdstuk 4.2). Ratten die behandeld zijn met ^{177}Lu-DOTA-Tyr^3-octreotate hadden een duidelijk betere overleving dan de controle dieren (onbehandeld), waardoor dit een veelbelovende nieuwe therapie is voor (uitzaaiingen van) somatostatine receptorpositieve tumoren.

In **hoofdstuk 5** is een studie beschreven die erop gericht is een nieuw radiofarmacon te ontwikkelen en te evalueren voor de behandeling van tumoren die sst_2 tot expressie brengen. Dit nieuwe radiofarmacon bestaat uit 2 peptiden (een hybride peptide); een somatostatine-receptor gericht peptide, octreotate; en een peptide dat celdood initieert, RGD (arginine-glycine-aspartaat). Tevens bevat dit nieuwe radiofarmacon een chelator (DTPA) zodat het makkelijk radioactief gelabeld kan worden met ^{111}In. Biodistributie studies lieten zien dat dit nieuwe radiofarmacon goed bindt aan de somatostatine receptor. Na binding aan de receptor wordt het radiofarmacon geïnternaliseerd in de cel en kan het RGD-peptide celdood initiëren. Internalisatie-experimenten in sst_2-positieve tumorcellen met het radiogelabelde hybride peptide (RGD-^{111}In-DTPA-octreotate) laten zien dat de internalisatie hiervan snel verloopt en dat deze geblokkeerd kan worden met een overmaat aan ongelabeld octreotide, hetgeen duidt op een sst_2-specifieke opname. De tumoropname van RGD-^{111}In-DTPA-octreotate in ratten kwam overeen met de in vitro data en was vergelijkbaar met die van het radioactief gelabeld Tyr^3-octreotate. Een minpunt van dit nieuwe hybride peptide was de hoge opname en retentie van de radioactiviteit in de nieren, dit limiteert namelijk de therapeutische dosis die gegeven

kan worden, aangezien de nieren kritieke organen zijn bij radionuclide therapie met somatostatine analogen die gelabeld zijn met β-emitters (Hoofdstuk 5.1).

Therapeutische effecten van het hybride peptide RGD-DTPA-octreotate zijn geëvalueerd in vergelijking met die van RGD en Tyr^3-octreotate in een in vitro kolonievormende assay, alle peptiden waren radioactief gelabeld met ^{111}In. Vervolgens is de caspase-3 activiteit bepaald (Hoofdstuk 5.2). De therapeutische effecten waren (in volgorde van het minst effectief naar het meest effectief) ^{111}In-DTPA-RGD < ^{111}In-DTPA-Tyr^3-octreotate < RGD-^{111}In-DTPA-octreotate. Ook de hoogste toename van caspase-3 activiteit werd gevonden na behandeling met RGD-DTPA-octreotate. RGD-^{111}In-DTPA-octreotate heeft dus een duidelijk beter therapeutisch effect dan ^{111}In-DTPA-RGD en ^{111}In-DTPA-Tyr^3-octreotate, waarschijnlijk door een toename in de initiatie van celdood veroorzaakt door een toename in caspase-3 activiteit.

In hoofdstuk 5.3 hebben we de biodistributie van RGD-^{111}In-DTPA-octreotate en ^{125}I-RGD-octreotate geëvalueerd, tevens hebben we het therapeutische effect van het ongelabelde peptide RGD-DTPA-octreotate in vitro onderzocht. Aangezien de biodistributie een hoge nieropname liet zien hebben we therapeutische effecten van het ongelabelde hybride peptide, RGD-DTPA-octreotate, in de volgende sst_2-positieve cellijnen onderzocht; CA20948, AR42J en chinese hamster ovary (CHO) cellijn. De resultaten hiervan lieten zien dat er een significante toename in caspase-3 was activiteit in vergelijking met RGD en Tyr^3-octreotate in alle cellijnen die gebruikt zijn. Vervolgens hebben we, om de nieropname te verlagen in het lichaam, de biodistributie van gejodeerd RGD-octreotate zonder de chelator DTPA onderzocht. ^{125}I-RGD-octreotate liet inderdaad een veel lagere nieropname zien in vergelijking met RGD-^{111}In-DTPA-octreotate. Bovendien was de affiniteit voor de somatostatine receptor van RGD-octreotate toegenomen ten opzichte van RGD-DTPA-octreotate (IC_{50} waarde van 1.4×10^{-8}M vs 9.4×10^{-8}M, respectievelijk). Ten slotte bleek dat RGD-octreotate, zonder de chelator DTPA, ook caspase-3 kan activeren.

Dus het concept om tumoren, die somatostatine receptoren tot expressie brengen, te behandelen kan ook toegepast worden met behulp van somatostatine analogen die gekoppeld zijn aan chemotherapeutische middelen, dit is verder beschreven in Hoofdstuk 5.4. De ontwikkeling van hybride moleculen kan een nieuwe methode zijn voor de strijd tegen kanker.

LIST OF ABBREVIATIONS

$\alpha_v\beta_3$	alpha-v-beta-3 integrin receptor
CPM	count per minute
CR	complete response
DLU	density light units
DOTA	1,4,7,10-tetraazacyclododecande-*N,N',N'',N'''*-tetraacetic acid
DTPA	diethyleetriaminepentaacetic acid
ECM	extracellular matrix
GBq	Gigabecquerel (10^{12} Bq)
GEP tumours	gastro-entero-pancreatic tumours
GRP	gastrin-releasing peptide
Gy	Gray
HE	haematoxylin-eosin
HPLC	high-performance liquid chromotography
IC50	inhibitory concentration at 50% saturation
ITLC	instant thin-layer chromotography
FDA	Food and Drug Administration
GH	growth hormone
LET	linear energy transfer
LHRH	luteinizing hormone-releasing hormone
LQ-MODEL	linear-quadratic model
MBq	Megabequerel (10^6 Bq)
MTC	medullary thyroid carcinomas
NR	no response
PBS	phosphate buffered saline
PNA	peptide nucleic acid
PR	partial response
PRRT	peptide receptor radionuclide therapy
PRS	peptide receptor scintigraphy
RBE	relative biological effectiveness
RGD	Arg-Gly-Asp - argine-glycine-aspartate
RIT	radioimmunotherapy
RT	radionuclide therapy
RT-PCR	reverse transcriptase polymerase chain reaction
SCLC	small cell lung cancer
SD	standard deviation
SEM	standard error of mean
SF2	surviving fraction at 2 Gy
SRB	sulforhodamine B assay
SS	somatostatin
SSR	somatostatin receptor

SST1-SST5	somatostatin receptor subtype 1-5
TETA	1,4,8,11-tetraazacyclotetradecane-*N,N',N'',N'''*-tetraacetic acid
µg	microgram
XRT	external-beam therapy

DANKWOORD

En dan tenslotte het dankwoord; dit proefschrift zou er niet zijn zonder de bijdrage en steun van vele anderen. Daarom wil ik op deze plek iedereen bedanken voor zijn of haar bijdrage. Een aantal van hen wil ik in het bijzonder noemen.

Allereerst wil ik mijn promotor prof.dr. E.P. Krenning bedanken voor de gelegenheid die hij mij heeft geboden om op de afdeling Nucleaire Geneeskunde mijn promotieonderzoek uit te voeren. Met name uw enthousiasme voor onderzoek was fantastisch, ook de mogelijkheid die ik kreeg om congressen te bezoeken en het onderzoek te presenteren heb ik zeer gewaardeerd.

Veel heb ik te danken aan mijn copromotor dr.ir. M. de Jong. Marion, jij was de grote initiator achter dit onderzoek. Bedankt voor de vele ideeën die je hebt aangedragen en de vele discussies die we hebben gehad over mijn onderzoek. Jouw enthousiasme en optimisme hebben mij gestimuleerd om tot een goed einde te komen. Ook bij het schrijven van publicaties en het presenteren van de resultaten heb ik veel van je geleerd. Bedankt!

De leden van de kleine commissie Prof.dr.ir. T.J. Visser, prof.dr. S. Pauwels en prof.dr. P.C. Levendag wil ik bedanken voor de snelle beoordeling van mijn manuscript en het zitting nemen in de promotiecommissie.

Mijn collega's van de prekliniek. Bert Bernard met wie ik al die tijd een kamer heb gedeeld, we hebben vele ideeën uitgewisseld en discussies gevoerd, bedankt. Magda Bijster, Ria van den Berg, Marleen Melis, Monique de Visser, Suzanne Verwijnen en in het begin ook Arthur van Gameren wil ik bedanken voor de fijne werksfeer en hulp bij de verschillende experimenten. Suzanne, ik stel het zeer op prijs dat je mijn paranimf wil zijn. Magda en mijn stagiaire Renate Okker wil ik bedanken voor het werk wat ze voor mij hebben gedaan.

Enkele medewerkers van Nucleaire Geneeskunde; Wout Breeman, Erik de Blois, Linda de Jong, Gre van der Wagt en Willem Bakker wil ik met name bedanken voor de vele labelingen die nodig waren voor de verschillende experimenten. Wout, bedankt voor je ideeën en de discussies die we hebben gehad. Roelf Valkema, Peter Kooij en Ambroos Reijs wil ik bedanken voor hun bijdrage. Dais van der Wal wil ik bedanken voor de nodige ontspanning met de boekjes van de onderwatersport.

I would like to thank Jack Erion for his contribution and especially for synthesizing the various peptides needed for this research.

Furthermore I would like to thank dr. E.A.Woltering and dr. C. Anthony to let me spent several weeks on the lab at the Louisiana State University Health Sciences Center in New Orleans. Eugene, thank you for letting me stay at your home during those weeks, I had a wonderful time and you have shown me a lot in New Orleans. I hope that the tulips are still standing and that they bloom this year again. Cathy, thanks for showing me around the lab and teaching me the technique.

Mijn ouders, mijn broer en Jolanda, familie en vrienden bedanken voor hun steun en belangstelling. Mijn ouders, die me altijd hebben gestimuleerd en gesteund in mijn keuzes en een luisteren oor hadden. Marc, mijn broer, bedankt voor je vriendschap en steun. Jolanda, voor de wekelijkse ontspanning met squashen, ik vind het leuk dat je mijn paranimf wilt zijn.

Tenslotte, Jeroen, wil ik jou bedanken. Ook al sta je als laatste in de rij, je bent wel de belangrijkste. Bedankt voor jouw onvoorwaardelijke steun en de duwtjes in de rug die ik zo nu en dan nodig had. Het proefschrift is af!

CURRICULUM VITAE

Astrid Capello werd geboren op 8 november 1975 te Gouda. In 1995 behaalde zij het VWO diploma aan het St. Antoniuscollege te Gouda. In datzelfde jaar begon zij haar studie Biologie aan de Universiteit Utrecht en behaalde in 1996 haar propedeuse. Zij vervolgde haar studie Fundamentele BioMedische Wetenschappen aan de Universiteit Utrecht. Tijdens de doctoraalfase werden 2 stages gevolgd. De eerste liep zij gedurende 9 maanden bij de afdeling Moleculaire Celbiologie van de Universiteit Utrecht (dr. R. de Wit). De tweede stage van tevens 9 maanden werd gevolgd op de afdeling Interne Oncologie, Experimentele Chemotherapie, Josephine Nefkens Instituut van het Erasmus Medisch Centrum (dr. H. Burger). Het doctoraal examen werd behaald in november 1999. In februari 2000 trad zij als Assistent in Opleiding in dienst bij de afdeling Nucleaire Geneeskunde van het Erasmus Medisch Centrum te Rotterdam. Onder begeleiding van dr. ir. M. de Jong en Prof. dr. E.P. Krenning werd het promotieonderzoek uitgevoerd dat in dit proefschrift beschreven staat.